

YEAST GENOME-WIDE TELOMERE SCREENS AND INSIGHTS INTO CANCER

Joana Cristina Pedro Rodrigues

Thesis submitted for the degree of Doctor of Philosophy

July 2017



Institute for Cell & Molecular Biosciences, Medical School,
Newcastle University

Abstract

Telomeres are the very ends of linear eukaryotic chromosomes and when too short or dysfunctional they can trigger senescence (ageing). If the cell can bypass senescence, it can lead to genetic instability or cancer. Telomere capping proteins such as the CST (Cdc13, Stn1 and Ten1) complex and Yku70 are essential for the telomeres not to be recognised as double strand breaks.

In this thesis I have used published yeast genome-wide screens to identify genes that are relevant to cancer and telomere biology. Overall 14 out of 19 genetic interactions identified by genome-wide screens could be confirmed by small scale experiments. This work mainly focuses on the telomeric roles of *VPS74* and the PAF1 complex.

Here, I show that the Golgi gene *VPS74*, whose human orthologue, *GOLPH3*, is an oncogene, genetically interacts with telomere capping genes and DNA damage response genes. I demonstrate that Vps74 is important for cell fitness of *yku70Δ* cells and that the low fitness of Vps74 depleted cells is dependent on the presence of DNA damage checkpoint proteins.

I have also systematically investigated the roles of PAF1 complex (Cdc73, Paf1, Ctr9, Leo1 and Rtf1, in yeast) components on telomere biology. The conserved PAF1 complex affects RNA abundance in eukaryotes. I demonstrate that individual PAF1 complex components perform different functions at telomeres. I show that loss of Cdc73 improves fitness of telomere defective yeast cells, while loss of other PAF1 components has the opposite effect. Moreover, I show that Paf1 and Ctr9 strongly reduce telomeric repeat-containing non-coding RNA (TERRA), while Cdc73, Leo1 and Rtf1 have little effect. Paf1 and Ctr9 function independently of Sir4 to regulate TERRA and this is because they stimulate TERRA decay, as well as decay of other RNAs. Additionally, I found that Paf1 and Ctr9 decrease *TEN1* and *STN1* mRNA levels. I suggest that the PAF1 complex plays a specialized role at telomeres, with Paf1 and Ctr9 maintaining telomere integrity and Cdc73 decreasing the fitness of telomere defective cells.

Acknowledgements

I would like to thank everyone that somehow helped me throughout my PhD. First of all, I thank my supervisor David Lydall for giving me the opportunity and support to conduct my research in his laboratory. I appreciate all the freedom I was given, which I believe allowed me to grow as a scientist. I am also very grateful that he always found the time to discuss any questions I might have.

Second, I want to thank all the members that were part of the David's laboratory during the past 3 years. A special acknowledgement to Marion Dubarry, who taught me most of the techniques in the lab. I am also grateful to Marta Markiewicz and Victoria Torrance for all the productive discussions related and unrelated to science.

Finally, I would like to thank Professor Akihiko Nakano for providing me the plasmids with the Golgi markers. Also, Professor Manolis Papamichos-Chronakis for providing me the Anchor-Away strain.

None of this would have been possible without funding, therefore I thank the European Union's Seventh Framework Programme (CodeAge | FP7 Marie Curie Initial Training Network).

Table of contents

Abstract	i
Acknowledgements	ii
Table of contents	iii
List of Figures	ix
List of Tables	xii
Yeast Nomenclature	xiii
List of Abbreviations	xiv
1. Introduction	16
1.1. Telomeres, double-strand breaks and the DNA damage response	16
1.1.1. Human telomeres	17
1.1.2. Yeast telomeres	19
1.1.3. Alternative ways of maintaining telomere length	23
1.1.4. Telomere silencing	24
1.1.5. Telomeric repeat containing RNA (TERRA)	24
1.2. DNA damage response to double-strand breaks	26
1.2.1. Resection	27
1.2.2. Checkpoint activation	30
1.3. Telomeres, senescence and cancer	32
1.4. Yeast as a cellular model	33
1.4.1. <i>yku70Δ</i> mutants	33
1.4.2. <i>cdc13-1</i> mutants	34
1.4.3. Genome-wide screens	34
1.5. Aims	35
2. Materials and Methods	36
2.1. Yeast strains	36
2.2. Media composition	36
2.2.1. Yeast Extract, Peptone, Dextrose (YEPD)	36
2.2.2. 5-Fluoroorotic Acid Media (5-FOA)	36
2.2.3. Complete Synthetic Media (CSM)	36
2.2.4. Selective media	37

2.2.5.	Sporulation media	37
2.2.6.	Lysogeny Broth (LB)	37
2.2.7.	Super Optimal broth with Catabolite repression (SOC)	37
2.3.	Methods	38
2.3.1.	Yeast cell maintenance and culture	38
2.3.2.	Sporulation of diploids	38
2.3.3.	Primer design	38
2.3.4.	Gene deletion	39
2.3.5.	Lithium acetate (LiAC) transformation	39
2.3.6.	Transformation of plasmids into yeast	40
2.3.7.	<i>E.coli</i> transformation	40
2.3.8.	Plasmid recovery from <i>S. cerevisiae</i>	40
2.3.9.	DNA isolation from yeast (Yale quick method)	41
2.3.10.	DNA isolation (using phenol)	41
2.3.11.	RNA isolation (using phenol)	42
2.3.12.	RNA isolation (using RNeasy Mini Kit)	43
2.3.13.	<i>In vivo</i> cloning	44
2.3.14.	<i>In vitro</i> cloning	44
2.3.15.	Spot test	44
2.3.16.	Southern blot	45
2.3.17.	Passage test	45
2.3.18.	Genomic/Plasmid PCR	45
2.3.19.	Colony PCR	46
2.3.20.	qPCR	46
2.3.21.	RT-qPCR	46
2.3.22.	In-gel assay	47
2.3.23.	Yeast cell imaging	47
2.3.24.	RNA half-life	48
2.3.25.	ImageJ quantification of images	48
3.	Yeast telomere screens and cancer	50
3.1.	Introduction	50
3.2.	Results	52
3.2.1.	Small scale experiments validated the majority of the high-throughput data	62

3.2.2.	Cdc73 and Vps74 have a strong role in telomere biology	63
3.2.3.	<i>DYN1</i> and <i>UFD2</i> , but not <i>BAS1</i> , <i>DOA1</i> , <i>FYV10</i> , <i>SKI2</i> , <i>MON1</i> , <i>SUB1</i> or <i>INP52</i> , strongly interact with <i>CDC13</i>	65
3.2.4.	<i>SKI2</i> , but not <i>BAS1</i> , <i>FYV10</i> , <i>DYN1</i> , <i>UFD2</i> or <i>INP52</i> , strongly interacts with <i>YKU70</i>	68
3.2.5.	Ski2 represses telomeric ssDNA formation in <i>cdc13-1</i> cells	71
3.2.6.	The Ski complex suppress <i>cdc13-1</i> fitness defects.....	73
3.2.7.	Ski2 does not affect CST mRNA levels	77
3.2.8.	<i>ski2Δ exo1Δ rad24Δ cdc13-1</i> cells are viable at non-permissive temperatures.....	77
3.2.9.	<i>ski2Δ rad24Δ exo1Δ cdc13-1</i> strains are respiration defective	83
3.2.10.	Deletion of <i>SKI2</i> causes a high fitness variability in a <i>cdc13-1</i> background	87
3.3.	Discussion/Conclusion.....	90
3.3.1.	<i>DYN1</i>	91
3.3.2.	<i>UFD2</i>	92
3.3.3.	<i>BAS1</i> , <i>MON1</i> , <i>DOA1</i> and <i>FYV10</i>	92
3.3.4.	<i>SUB1</i>	93
3.3.5.	<i>SKI2</i>	93
3.4.	Future work.....	95
3.4.1.	<i>DYN1</i>	95
3.4.2.	<i>UDF2</i>	95
3.4.3.	<i>SUB1</i>	95
3.4.4.	<i>SKI2</i>	96
4.	Vps74 as a bridge between the Golgi apparatus and the DDR.....	97
4.1.	Introduction	97
4.1.1.	Inositol signalling and telomeres.....	99
4.1.2.	Golgi and the DNA damage response	99
4.2.	Results.....	102
4.2.1.	Golgi structure changes upon DNA damage	102
4.2.2.	Exo1 and Rad24 decrease, whereas Mre11 increases, <i>vps74Δ</i> cell fitness	104
4.2.3.	Exo1, but not Sae2, contribute to fitness defects of <i>yku70Δ vps74Δ</i> cells.....	108

4.2.4.	Vps74 slightly increases telomeric ssDNA of <i>cdc13-1</i> cells and decreases the ssDNA of <i>yku70Δ</i> cells	110
4.2.5.	Rad27 contributes to the fitness of <i>vps74Δ</i> cells	112
4.2.6.	Mec1 decreases the fitness of <i>vps74Δ</i> and <i>yku70Δ vps74Δ</i> cells	113
4.2.7.	Sgs1 has no effect on the fitness of <i>vps74Δ</i> cells and Rad53 and Chk1 decrease the fitness of <i>yku70Δ vps74Δ</i> cells	115
4.2.8.	Vps74 contributes to genome stability	119
4.2.9.	Vps74 is potentially phosphorylated by Rad53	120
4.2.10.	Vps74 and Sac1 contribute to cell fitness through independent pathways	122
4.2.11.	Deletion of <i>SAC1</i> affects tryptophan intake	124
4.3.	Discussion/Conclusion	128
4.4.	Future work	131
5.	Adjacent gene effect reveals synthetic genetic interactions between the PAF1 complex and the ESCRT machinery.....	133
5.1.	Introduction	133
5.1.1.	The PAF1 complex and transcription regulation	133
5.1.2.	The PAF1 complex and cancer.....	135
5.1.3.	Different roles for different PAF1 complex components.....	135
5.1.4.	<i>CDC73</i> and its adjacent gene, <i>VPS36</i>	136
5.2.	Results	137
5.2.1.	The PAF1 complex affects telomere defective strains	137
5.2.2.	Members of the PAF1 complex interact differently with <i>cdc13-1</i>	137
5.2.3.	<i>Cdc73</i> , <i>Paf1</i> and <i>Ctr9</i> induce <i>TLC1</i> RNA.....	140
5.2.4.	<i>TEN1</i> mRNA is increased in <i>paf1Δ</i> and <i>ctr9Δ</i> strains	142
5.2.5.	Synthetic sickness and neighbouring gene effect between <i>CDC73</i> and adjacent gene <i>VPS36</i>	145
5.2.6.	Expression of <i>VPS36</i> on a plasmid decreases <i>cdc73Δ cdc13-1</i> fitness	148
5.2.7.	ESCRT-II complex does not affect telomere length in W303.....	149
5.2.8.	The PAF1 complex regulates <i>VPS36</i> transcription	151
5.2.9.	<i>vps36Δ</i> is synthetically lethal with <i>paf1Δ</i> or <i>ctr9Δ</i> but not with <i>cdc73Δ</i> , <i>rtf1Δ</i> or <i>leo1Δ</i>	151

5.2.10.	<i>paf1Δ</i> and <i>ctr9Δ</i> are synthetically lethal with deletions of ESCRT-I, ESCRT-II and ESCRT-III components	156
5.3.	Discussion	158
5.4.	Future work.....	162
6.	PAF1 complex components regulate TERRA and telomere function...	163
6.1.	Introduction	163
6.1.1.	The PAF1 complex and RNA metabolism	163
6.1.2.	Different functions for different PAF1c components	164
6.2.	Results.....	165
6.2.1.	PAF1 complex components affect fitness in different ways	165
6.2.2.	Loss of <i>CDC73</i> in telomere defective strains leads to telomere rearrangements	165
6.2.3.	<i>cdc73Δ cdc13-1</i> cells recover from fitness defects faster than <i>paf1Δ cdc13-1</i> or <i>ctr9Δ cdc13-1</i>	167
6.2.4.	Paf1 and Ctr9, but not Cdc73, reduce TERRA levels.....	170
6.2.5.	Telomere length is not a main regulator of TERRA expression in PAF1 complex mutants.....	175
6.2.6.	<i>RNH1</i> overexpression does not affect <i>paf1Δ cdc13-1</i> fitness	178
6.2.7.	Paf1 and Ctr9 repress TERRA independently of the Sir complex	180
6.2.8.	Paf1, Ctr9 and Cdc73 have distinct roles in telomere silencing	183
6.2.9.	Paf1 and Ctr9 repress TERRA transcription more than other telomeric transcripts	185
6.2.10.	The PAF1 complex does not regulate mating locus silencing	188
6.2.11.	Paf1 promotes RNA, especially TERRA, degradation.....	188
6.2.12.	Nmd2 and Ski2 do not strongly affect TERRA levels	193
6.3.	Discussion	195
6.4.	Future work.....	199
7.	Overall Perspectives.....	200
7.1.	<i>VPS74</i>	200
7.2.	PAF1 complex	202
	Appendix A.....	205
	Appendix B.....	216
	Appendix C.....	222

Appendix D223
Appendix E225
References238

List of Figures

Figure 1-1 Telomere structure in yeast and humans.	18
Figure 1-2 Secondary structure of human telomeres.	20
Figure 1-3 Changes in yeast telomeres.	25
Figure 1-4 DNA damage checkpoint in <i>S. cerevisiae</i>	28
Figure 1-5 Model for bidirectional processing of DSBs by Mre11 and Exo1.	29
Figure 3-1 <i>cdc73Δ</i> and <i>vps74Δ</i> suppress <i>cdc13-1</i> and enhance <i>yku70Δ</i> fitness defects.	64
Figure 3-2 <i>ufd2Δ</i> , <i>bas1Δ</i> , <i>doa1Δ</i> , <i>fyv10Δ</i> , <i>ski2Δ</i> , <i>mon1Δ</i> , <i>sub1Δ</i> and <i>dyn1Δ</i> genetically interact with <i>cdc13-1</i> , while <i>inp52Δ</i> does not.	67
Figure 3-3 <i>MON1</i> , <i>SUB1</i> and <i>DOA1</i> deletions do not significantly affect fitness of <i>cdc13-1</i> cells.	69
Figure 3-4 <i>ski2Δ</i> enhances <i>yku70Δ</i> fitness defects.	70
Figure 3-5 Ski2 helps telomere resection in <i>cdc13-1</i> cells.	72
Figure 3-6 <i>ski2Δ</i> suppresses <i>cdc13-1</i>	74
Figure 3-7 <i>ski7Δ</i> and <i>ski8Δ</i> are weaker <i>cdc13-1</i> suppressors than <i>ski2Δ</i>	76
Figure 3-8 Ski2 does not affect mRNA levels of CST complex components.	78
Figure 3-9 Evidence that <i>ski2Δ</i> strongly suppresses <i>rad24Δ</i> <i>exo1Δ</i> <i>cdc13-1</i> fitness defects.	80
Figure 3-10 <i>ski2Δ</i> <i>rad24Δ</i> <i>exo1Δ</i> <i>cdc13-1</i> cells that can grow at 36°C have the wild-type <i>CDC13</i>	82
Figure 3-11 Evidence that prions are not responsible for <i>ski2Δ</i> <i>rad24Δ</i> <i>exo1Δ</i> <i>cdc13-1</i> colony red colour.	84
Figure 3-12 <i>ski2Δ</i> <i>rad24Δ</i> <i>exo1Δ</i> <i>cdc13-1</i> cells cannot use glycerol as a carbon source.	86
Figure 3-13 <i>ski2Δ</i> <i>cdc13-1</i> strain fitness is highly variable and independent of the respiration capacity.	89
Figure 4-1 Phosphoinositide signalling in yeast.	98
Figure 4-2 Mammalian Golgi <i>versus</i> yeast Golgi.	101
Figure 4-3 Yeast presents Golgi structural changes upon DNA damage.	103
Figure 4-4 <i>vps74Δ</i> fitness defects are suppressed by <i>exo1Δ</i> and <i>rad24Δ</i> but not <i>rad17Δ</i> or <i>rad9Δ</i> , and are enhanced by <i>mre11Δ</i>	107
Figure 4-5 <i>vps74Δ</i> <i>yku70Δ</i> fitness defects are suppressed by <i>exo1Δ</i> but not <i>sae2Δ</i>	109

Figure 4-6 <i>vps74Δ</i> decreased telomeric ssDNA of <i>cdc13-1</i> cells and increased <i>yku70Δ</i> ssDNA.	111
Figure 4-7 <i>rad27Δ</i> enhances <i>vps74Δ</i> and <i>yku70Δ</i> fitness defects.	114
Figure 4-8 <i>mec1Δ sml1Δ</i> suppresses <i>vps74Δ</i> and <i>yku70Δ vps74Δ</i> fitness defects.	116
Figure 4-9 <i>rad53Δ</i> and <i>chk1Δ</i> suppress <i>yku70Δ vps74Δ</i> fitness defects.	118
Figure 4-10 <i>vps74Δ</i> and <i>sac1Δ</i> are synthetically sick.	123
Figure 4-11 <i>sac1Δ</i> fitness defects are strongly suppressed by <i>sae2Δ</i>	125
Figure 4-12 <i>SAC1</i> deletion affects the cell capacity to uptake tryptophan from the medium.	127
Figure 4-13 Model for a role of Vps74 in the DDR.	130
Figure 5-1 The PAF1 complex is conserved between yeast and humans and is involved in the Wnt pathway.	134
Figure 5-2 The <i>PAF1</i> complex affects telomere defective strains.	138
Figure 5-3 PAF1 complex genes interact differently with <i>cdc13-1</i>	139
Figure 5-4 PAF1 complex increases <i>TLC1</i> RNA levels in W303.	141
Figure 5-5 <i>PAF1</i> and <i>CTR9</i> regulate <i>TEN1</i> mRNA.	144
Figure 5-6 <i>CDC73</i> and its adjacent gene <i>VPS36</i> interact.	147
Figure 5-7 Expression of <i>CDC73</i> adjacent genes in plasmids suggests that <i>VPS36</i> might be affected in <i>cdc73Δ</i> strains.	150
Figure 5-8 ESCRT-II complex components do not regulate W303 telomere length.	152
Figure 5-9 PAF1 complex controls <i>VPS36</i> expression.	153
Figure 5-10 <i>vps36Δ</i> is synthetically lethal with <i>paf1Δ</i> or <i>ctr9Δ</i> but not with <i>rtf1Δ</i> or <i>leo1Δ</i>	155
Figure 5-11 <i>paf1Δ</i> and <i>ctr9Δ</i> are synthetically lethal with deletions of many ESCRT components.	157
Figure 5-12 Cartoon for the regulation of cell viability by the PAF1 complex.	161
Figure 6-1 Paf1 and Ctr9, but not Cdc73, are needed for fitness of telomere defective cells.	166
Figure 6-2 <i>cdc73Δ</i> induces telomere rearrangements in telomere defective cells.	169
Figure 6-3 <i>cdc73Δ cdc13-1</i> do not show fitness defects while <i>paf1Δ cdc13-1</i> recover from severe fitness defects by passage 3.	171
Figure 6-4 Paf1 and Ctr9, but not Cdc73, repress TERRA expression.	174
Figure 6-5 Telomere length in strains with PAF1 components deleted.	177

Figure 6-6 <i>RNH1</i> overexpression does not affect <i>paf1Δ cdc13-1</i> fitness.	179
Figure 6-7 Paf1 and Ctr9 repress TERRA expression independently of the Sir complex.	181
Figure 6-8 <i>sir4Δ</i> shortens <i>paf1Δ</i> and <i>ctr9Δ</i> telomeres.	182
Figure 6-9 Paf1, Ctr9 and Rtf1, but not Cdc73 and Leo1, affect telomere silencing.	184
Figure 6-10 Paf1 and Ctr9 repression of telomeric transcript does not perfectly correlate with TERRA repression.	187
Figure 6-11 Deletion of PAF1 components in <i>MATα</i> cells does not affect a1 mRNA levels.	189
Figure 6-12 Paf1 promotes RNA degradation.	192
Figure 6-13 Nmd2 weakly represses TERRA and Ski2 does not affect TERRA.	194
Figure 6-14 The role the PAF1 complex components in telomere function.	196
Figure 7-1 Model for the many roles of the different PAF1 complex components at telomeres.	204

List of Tables

Table 3-1 Yeast genes with a potential role at telomeres.	53
Table 3-2 Genetic interactions between the candidate genes and <i>cdc13-1</i> or <i>yku70Δ</i> in high-throughput versus low-throughput screens.	63
Table 3-3 Progeny of a <i>ski2Δ rad24Δ exo1Δ cdc13-1</i> heterozygous diploid randomly loses mitochondria integrity.....	87
Table 4-1 Genetic interactions between <i>vps74Δ</i> or <i>vps74Δ yku70Δ</i> and members of the DDR.	120
Table 4-2 Vps74 potential phosphorylation sites.....	121
Table 6-1 RNA half-life.	190

Yeast Nomenclature

<i>YFG</i>	Wild type gene
<i>yfg</i> Δ	Gene deletion
<i>yfg-1</i>	Mutant allele
Yfg	Protein encoded by the wild type gene

List of Abbreviations

BIR	Break-induced replication
bp	Base pair
BSA	Bovine serum albumin
C57, 1a	Cross 57, spore 1a (number of cross and spore varies)
cDNA	Complementary DNA
clonNAT	Nourseothricin
DDR	DNA damage response
DIG	Digoxigenin
DNA	Deoxyribonucleic acid
dNTPs	Deoxyribonucleotide triphosphate
DSB	DNA double strand break
DSBR	Double strand break resection
dsDNA	Double-stranded DNA
GC	Content Percentage Guanine and Cytosine content of DNA
G418	Geneticin
HR	Homologous recombination
HU	Hydroxyurea
kbp	Kilo base pair
LB	Lysogeny broth
min	Minute
MMS	Methyl methanesulfonate
MQ Water	Milli-q water
ms	Milliseconds
mtDNA	Mitochondrial DNA
NHEJ	Non-homologous end joining
OD	Optical density
ORF	Open reading frame
PCR	Polymerase chain reaction
PEG	Polyethylene glycol
qPCR	Quantitative PCR
rDNA	Ribosomal DNA
RFLP	Restriction fragment length polymorphism

rpm	Revolutions per minute
RT-qPCR	Quantitative reverse transcription PCR
SDS	Sodium dodecyl sulphate
sec	Second
SGD	Saccharomyces genome database
SSC	Saline sodium citrate
ssDNA	Single-stranded DNA
TAE	Tris-acetic acid-edta
TBE	Tris-boric acid-edta
TE	Tris-EDTA
T _m	Melting Temperature (of DNA)
ts	Temperature sensitivity

1. Introduction

1.1. Telomeres, double-strand breaks and the DNA damage response

Telomeres are the protein/nucleic acid structures at the ends of chromosomes that help confer stability to linear chromosomes (Muller 1938). In most human somatic cells, telomeric DNA gets shorter every cell division due to the end-replication problem (Olovnikov 1973; Harley et al. 1990). Telomerase facilitates telomere elongation in stem and cancer cell types (or yeast cells) but is less active in most somatic human cells (Shukla et al. 2010; Zvereva et al. 2010).

Loss of telomere protection and/or excessive telomere shortening causes genome instability leading to very drastic phenotypes like chromosome fusions, cell cycle arrest or apoptosis (Bekaert et al. 2005; Donate and Blasco 2011). Gross chromosome rearrangements such as chromosome fusions are often present in cancer cells, and are associated with uncontrolled cell division. On the other hand, cell cycle arrest and apoptosis are associated with ageing organisms. Therefore telomeres are attractive targets for both anti-cancer and anti-ageing therapies (Stewart and Weinberg 2006).

Notably, regardless of the strong similarity between telomeres and double-strand breaks, the cell reacts differently to these two types of DNA ends. While telomeres are maintained as DNA ends, double-strand breaks in more internal regions of the chromosome tend to be fixed by the cell. How the cell distinguishes telomeres and double-strand breaks is thought to be mainly related to the proteins that are present at each end. Telomeres have a particular and repetitive DNA sequence which is responsible to bind specific proteins that in turn protect the telomere against DNA damage response proteins (Webb et al. 2013). Human and mouse telomeric DNA is composed of TTAGGG repeats while *S. cerevisiae* telomeric repeats consist of TG(1-3) (de Lange 2005; Wellinger and Zakian 2012). Importantly, subtelomeric regions in both mammals and yeast are composed of silent chromatin, which permits telomere erosion without the danger of losing essential genetic information (Tham and Zakian 2002; Wood and Sinclair 2002). Thus, the telomeres have evolved to protect the chromosome, having the “power” to sacrifice the cell to preserve genome stability.

1.1.1. Human telomeres

Human telomeric DNA is associated with a protein complex called shelterin (de Lange 2005). TRF1, TRF2, TIN2, RAP1, TPP1 and POT1 are the six components of the human shelterin (Figure 1-1A) (de Lange 2005). All of them negatively regulate telomerase (Smogorzewska and de Lange 2004).

TRF1 and TRF2 (TTAGGG repeat-binding factors 1 and 2) bind to telomeric dsDNA, and other members of the shelterin but they do not interact with each other (Broccoli et al. 1997; Walker and Zhu 2012). TRF1 and TRF2 have in common the TRF homology (TRFH) domain and a C-terminal SANT/Myb DNA-binding domain (Palm and de Lange 2008). Additionally, TRF2 is important for the formation of the t-loop *in vitro* (further details on the t-loop can be found later on) (Stansel et al. 2001). TIN2 (TRF1 interacting nuclear protein 2) is able to interact with TRF1, TRF2 and TPP1 (Palm and de Lange 2008). TIN2 does not interact directly with DNA but can interact with both TRF1 and TRF2 simultaneously being considered as an important bridge between the two (Ye et al. 2004a; Palm and de Lange 2008; Hadjiladis and Sletten 2009). RAP1 (repressor activator protein 1) lacks the capacity to bind DNA, is directly involved in telomere length regulation and its telomeric localisation depends on an interaction with TRF2 (Li et al. 2000; Palm and de Lange 2008; Duong and Sahin 2013). TPP1 does not directly interact with telomeric DNA but keeps POT1 and TIN2 together and has the ability to interact with telomerase, being an important intermediate between shelterin and telomerase (Cristofari et al. 2007). POT1 is the shelterin member able to bind to the telomeric ssDNA and TPP1 simultaneously, inhibiting telomerase action. Importantly, the TPP1-POT1 interaction is necessary to the localisation of POT1 at the 3' overhang (Ye et al. 2004b). Finally, at the end of the double stranded DNA, the Ku heterodimer is essential to maintain telomere integrity (Indiviglio and Bertuch 2009). Ku, composed of Ku70/Ku86, is a part of NHEJ (non-homologous end joining) response, however it is thought that its loss is lethal due to its role at telomeres instead of NHEJ (Wang et al. 2009). One characteristic of human telomeres is the presence of the t-loop (Griffith et al. 1999). The t-loop is a secondary DNA structure and its function is to protect the chromosome ends (de Lange 2002). It is formed by the folding of the 3' overhang in such way that the extremity replaces the G-rich strand, base pairing with the C-rich

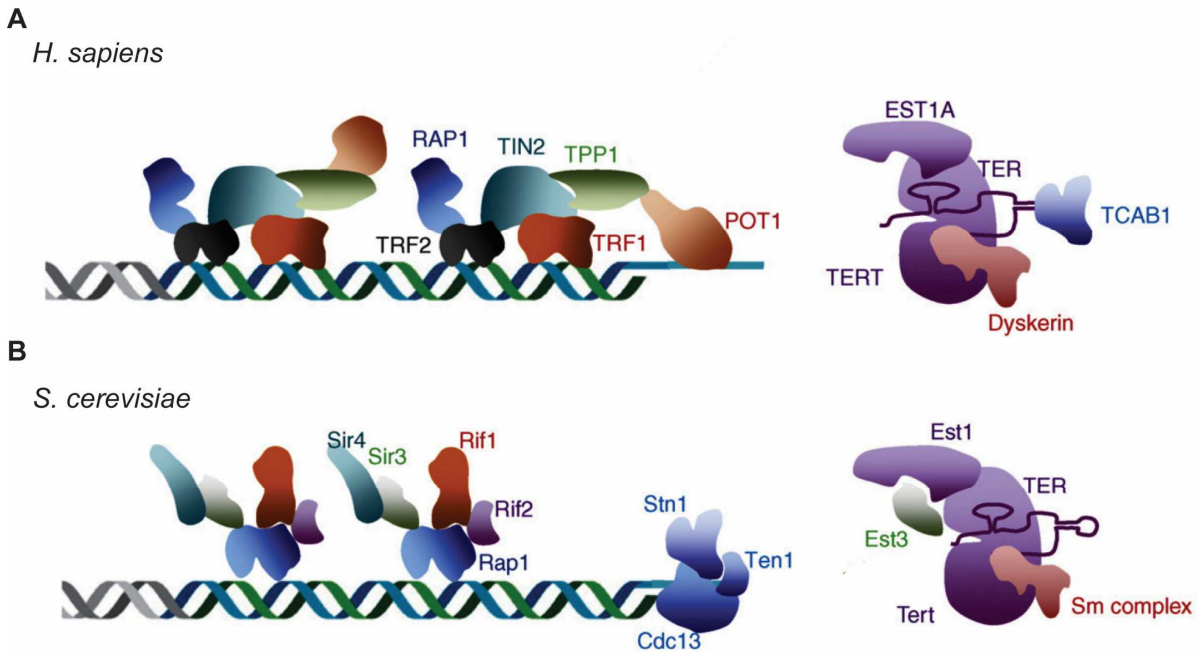


Figure 1-1 Telomere structure in yeast and humans. A) In humans, the telomeric dsDNA is bound by TRF1 and TRF2 (held together by TIN2) and TRF2 recruits RAP1 to telomeres. The telomeric ssDNA is bound by POT1 which is linked to TRF1–TRF2–TIN2 by TPP1. Human telomerase consists of EST1A, TER, and TERT subunits. Human TPP1 and yeast Est3 have structural similarities but appear to perform different roles (Lee et al. 2008). **B)** In budding yeast, the telomeric dsDNA is bound by Rap1, which recruits the accessory factors Rif1, Rif2, Sir3 and Sir4. Cdc13 binds the telomeric ssDNA and recruits Stn1 and Ten1 to form the CST complex. Yeast telomerase consists of Est1, Tert (Est2), Est3 and TER (*TLC1*, Telomerase RNA). Figure taken from (Lue 2010).

strand (the unpaired DNA strand forms a D-loop) (Figure 1-2) (Palm and de Lange 2008). The loop sizes are variable, and because of that it appears not to be functional (de Lange 2002). Also there are subtelomeric regions with (TTAGGG)_n-like sequences (which are present along the genome, but enriched close to the telomeres) and duplicons (Riethman 2008).

1.1.2. Yeast telomeres

Yeast telomeres have many similarities with human telomeres (Figure 1-1). The yeast single stranded G tail is usually very short (around 300 bp against the more than 10kb of mammals) and is bound by Cdc13, which forms a complex with Stn1 and Ten1 (the CST complex) (Price et al. 2010; Wellinger and Zakian 2012; Webb et al. 2013). Yeast possesses well-defined subtelomeric regions (Figure 1-3A, B) or TAS elements (telomeric associated sequences), the X and Y' elements (Chan and Tye 1983) that contain autonomously replicating sequences (ARS) (origins of replication) (Wellinger and Zakian 2012). The X element is closer to the centromere and is present in all the chromosomes while the Y' element is missing in about half of the chromosomes (Jager and Philippsen 1989; Wellinger and Zakian 2012). These subtelomeric regions (X and Y') are organized in nucleosomes, however the histone content in the core X region is lower than in the distal Y' (Wellinger and Zakian 2012). The X region is enriched in proteins responsible for DNA silencing such as Sir2, Rap1 (Zhu and Gustafsson 2009) and Sir3 (Takahashi et al. 2011b). The Y' region, on the other hand, does not bind these proteins and is much more similar to euchromatin (Zhu and Gustafsson 2009; Wellinger and Zakian 2012).

Rap1 (Repressor Activator Protein 1) is present in the double-stranded telomeric DNA repeats, where it binds with high affinity (Wellinger and Zakian 2012). Rap1 is able to interact with Sir2, Sir3 and Sir4 (transcription repressors, part of the Sir complex) and with Rif1 and Rif2 (Rap1 interacting factor proteins 1 and 2) (Moretti et al. 1994; Wotton and Shore 1997; Allison 2009). Together with Rif1/Rif2, Rap1 has an important role in telomere length maintenance and protection (Gallardo et al. 2011; Wellinger and Zakian 2012). Regardless of its high telomere binding affinity, most of Rap1 is not associated to telomeres (Wellinger and Zakian 2012).

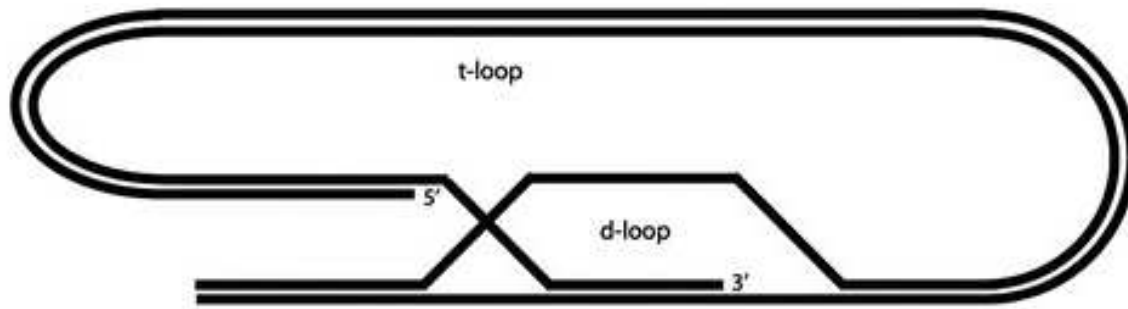


Figure 1-2 Secondary structure of human telomeres. Telomere repeats at chromosome ends fold back to form a lariat structure (t-loop). The 3' telomeric DNA overhang invades the double-stranded DNA region of telomeric repeats to form a displacement-loop (d-loop). Figure and legend taken from (Tamakawa et al. 2013)

Another complex that is involved in telomere maintenance is RPA (Replication Protein A). RPA is a heterotrimeric complex (composed of Rfa1, Rfa2 and Rfa3) that binds ssDNA (Braun et al. 1997). RPA does not specifically bind to telomeric ssDNA but mutations in *RFA2* decrease telomere length (Schramke et al. 2004). Since *RFA2* mutations decreased the binding of Est1 to telomeres during S-phase, it was suggested that RPA recruits telomerase to telomeres (Schramke et al. 2004). Throughout the genome, RPA plays an essential role in the DNA damage repair and stimulates the DNA damage response (Marechal and Zou 2015). For instance, RPA helps to load the 9-1-1 complex to lesion sites and is phosphorylated by checkpoint kinases in response to DNA damage (Mec1) (Brush et al. 1996; Majka et al. 2006). The replacement of RPA by Rad51 is essential for HR (homologous recombination) and the presence of RPA at lesion sites is essential to dismantle DNA secondary structures that could interfere with Rad51 action (Krejci et al. 2012). Additionally, RPA stimulates the Sgs1 helicase, promoting Dna2-dependent resection and formation of ssDNA (that stimulates the DNA damage response) (Krejci et al. 2012).

The conserved Ku complex binds the double-stranded telomeric DNA. The yKu complex is composed of Yku70 and Yku80 (Gallardo et al. 2011; Wellinger and Zakian 2012). This complex protects the telomeres against Exo1 (Exonuclease 1) degradation (Maringele and Lydall 2002; Bertuch and Lundblad 2004) and it is thought to recruit telomerase to the telomeres through its ability to interact with the telomerase RNA (Peterson et al. 2001). The Ku complex has also an important role regulating NHEJ and in the repair of double stranded breaks (DSBs), having the potential to modulate checkpoint activation (Balestrini et al. 2013). Chromatin immunoprecipitation studies showed that Yku80 preferentially binds to regions of repressed chromatin (at telomeres) in a Sir4-dependent manner (Martin et al. 1999). Interestingly, upon exposure to bleomycin (DNA damaging agent), Yku80 was shown to relocate from the telomere to a more centromeric position in a manner dependent on the Rad9 checkpoint protein (Martin et al. 1999). Finally, the yKu complex was also shown to be important for proper telomere silencing (Martin et al. 1999).

Telomerase is the reverse transcriptase responsible for maintaining the telomere length by adding the G rich repetitive DNA sequences to the telomere end (Taggart and Zakian 2003; Churikov et al. 2013). In yeast, telomerase is composed of Est1, Est2, Est3 and *TLC1* (RNA molecule used as template for the 3' extension of telomere) (Taggart and Zakian 2003). The lack of any member of the telomerase

complex causes the same growth defects and decreased telomere length (Lendvay et al. 1996). Both Est1 and Est2 directly bind *TLC1* and Est3 is recruited by the Est2-*TLC1* complex (Gallardo and Chartrand 2008). Est2 has the catalytic site of the reverse transcriptase enzyme (Wellinger and Zakian 2012). Est1 abundance varies throughout the cell cycle having a peak during S/G2 (Taggart et al. 2002). In late S/G2 phase, an Est1-*TLC1* interaction is required for Est1 binding to telomeres which in turn promotes Est2 binding to telomeres (Chan et al. 2008). Est3 is dependent on Est1 and Est2 for its association to the telomerase complex. *TLC1* RNA exists in both polyadenylated and non polyadenylated forms and only the latter is used by telomerase as template (Wellinger and Zakian 2012; Webb et al. 2013).

Finally, the CST (Cdc13-Stn1-Ten1) complex is essential to yeast cell survival as the lack of any of its components leads to death (Wellinger and Zakian 2012). This complex shares some functional and structural properties with RPA (Wellinger and Zakian 2012). Cdc13 is able to specifically bind to the G-rich single stranded telomeric overhang and is the only CST subunit with the capacity to bind DNA directly *in vivo* (Lin and Zakian 1996; Qi and Zakian 2000). Thus, Cdc13 is the CST component responsible to keep the whole complex at telomeres where it exerts its capping function, protecting the telomere (Giraud-Panis et al. 2010). Importantly, both Stn1 and Ten1 show DNA binding activity *in vitro* with preference to telomeric DNA and can act apart from Cdc13 as chromosome caps (Petreaca et al. 2006; Gao et al. 2007; Holstein et al. 2014). Together with a capping role, the CST complex also plays an important role in telomere replication. For instance, Cdc13 interacts with Est1, promoting the recruitment of telomerase to telomeres (Grandin et al. 2000; Wu and Zakian 2011). To counteract telomerase recruitment by Cdc13, Stn1 competes with Est1 to bind Cdc13, repressing telomerase (Grandin et al. 2000; Chandra et al. 2001). Cdc13 phosphorylation by Cdk1 promotes the Stn1-Cdc13 interaction in a cell-cycle dependent manner and Cdk1 inhibition stalls the *de novo* addition of telomere repeats possibly by disrupting the timing of telomere elongation (Frank et al. 2006; Liu et al. 2014). Additionally, SUMOylation of the Cdc13 Stn1-binding domain increases Cdc13-Stn1 affinity leading to repression of telomerase action (Hang et al. 2011). In yeast, a role for Ten1 in telomerase recruitment has not been described and Ten1 was shown to enhance the DNA-binding activity of Cdc13 (Qian et al. 2009b). Interestingly, CST complex proteins show no direct orthology to any of the mammalian shelterin members (Price et al. 2010). Instead, the human CST complex

(CTC1, STN1 and TEN1) independently contributes to telomere maintenance by interacting with the ssDNA overhang of the human telomeres (Rice and Skordalakes 2016).

1.1.3. Alternative ways of maintaining telomere length

When telomerase is not active, there are other ways that cells use in order to preserve their telomeres. This mechanism was first described in yeast by Lundblad and Blackburn in 1993, and in human cells in 1995 by Bryan et al., who gave it the name of ALT (alternative lengthening of telomeres) (Lundblad and Blackburn 1993; Bryan et al. 1995; Bryan and Reddel 1997). The ALT mechanism is important in some types of cancer development and maintenance (Grach 2011). APBs (ALT-associated promyelocytic leukaemia (PML) bodies) are very common in cells that use ALT and contain telomeric DNA, DNA repair proteins and recombination proteins (Grach 2011).

ALT- positive cells are dependent on DNA recombination, and consequently on recombination proteins like Rad52 (present in both humans and yeast) (Teng and Zakian 1999). In yeast, Rad52 has an extremely important role in DNA recombination and repair while in humans its role is more modest, sharing functions with other proteins (BRCA2 for example) (Mortensen et al. 2009). The yeast Rad52 is expressed throughout the cell cycle, showing an increase during meiosis and in response to DNA damage (Cole et al. 1987; Cole et al. 1989). This protein is also recruited to (lesion) sites coated with RPA and can interact with Rad51 (Mortensen et al. 2009). Yeast cells that bypass senescence using ALT mechanisms can be divided into two major groups: type I survivors and type II survivors (Wellinger and Zakian 2012) (Figure 1-3). Type I survivors are mostly characterized by the amplification of the Y' regions, while the ends of the telomeres are maintained more or less stable with the repetitive dsDNA and the ssDNA overhang (Figure 1-3C) (Wellinger and Zakian 2012). The genes described as being involved in the formation of these survivors are: *RAD52*, *POL32*, *RAD54*, *RAD57* and *RAD55* (Le et al. 1999; Chen et al. 2001). In contrast, type II survivors show amplifications in the telomeric repeats which are very heterogeneous (Figure 1-3D, E) (Wellinger and Zakian 2012). Indeed, the telomere length of type II survivors can vary from very short to the very long telomeres with more than 10kb that are very unstable (Wellinger and Zakian 2012). In the formation of type II survivors, the Rad50/Mre11/Xrs2 pathway is involved as

well as Rad52, Rad59, Srs2, Sgs1 and Tid1 (Chen et al. 2001; Signon et al. 2001). Maringele and Lydall described an important role for *EXO1* in the formation of both type I and type II survivors in *yku70Δ mre11Δ* and *tlc1Δ* backgrounds (Maringele and Lydall 2004).

1.1.4. Telomere silencing

Transcription from telomeres happens at low rates and in an intermittent manner, a phenomenon described as telomere silencing (Gottschling et al. 1990). Telomere silencing is promoted mainly by the Sir complex and Rap1 (Cockell et al. 1995; Strahl-Bolsinger et al. 1997). The Sir complex is composed of Sir2, Sir3 and Sir4 and promotes histone deacetylation (Hoppe et al. 2002). Hyperacetylation is associated with transcriptional activity, therefore, histone deacetylases like the Sir complex inhibit transcription (Shahbazian and Grunstein 2007). Rap1 binds the DNA, with a strong affinity to telomeric DNA, and its interaction with Sir3 and Sir4 positions the Sir complex at telomeres (Moretti et al. 1994). The Sir complex is also essential for the silencing at the mating type loci (Rine and Herskowitz 1987; Kueng et al. 2013).

1.1.5. Telomeric repeat containing RNA (TERRA)

Regardless of the strong transcriptional repression observed at telomeres, some residual transcription still occurs, for example, to generate the non-coding RNA, TERRA (telomeric repeat containing RNA) (Azzalin et al. 2007). TERRA is transcribed mainly by RNA polymerase II, from subtelomeric regions towards the chromosome end (Azzalin and Lingner 2015). In yeast, Rif1/Rif2 and the Sir complex were shown to repress TERRA expression (mainly in X telomeres) and Rat1 actively degrades TERRA (X and Y' telomeres) (Iglesias et al. 2011). Almost all TERRA is polyadenylated, and loss of TERRA polyadenylation has been suggested to destabilize it (Azzalin and Lingner 2015). In *S. pombe*, polyadenylated TERRA was shown to diffuse and interact with the catalytic subunit of telomerase (Moravec et al. 2016). TERRA also has the capacity to interact with *TLC1 in vitro* (Cusanelli et al. 2013). In humans, not all TERRA is polyadenylated and only the non-polyadenylated TERRA is bound to chromatin (Porro et al. 2010).

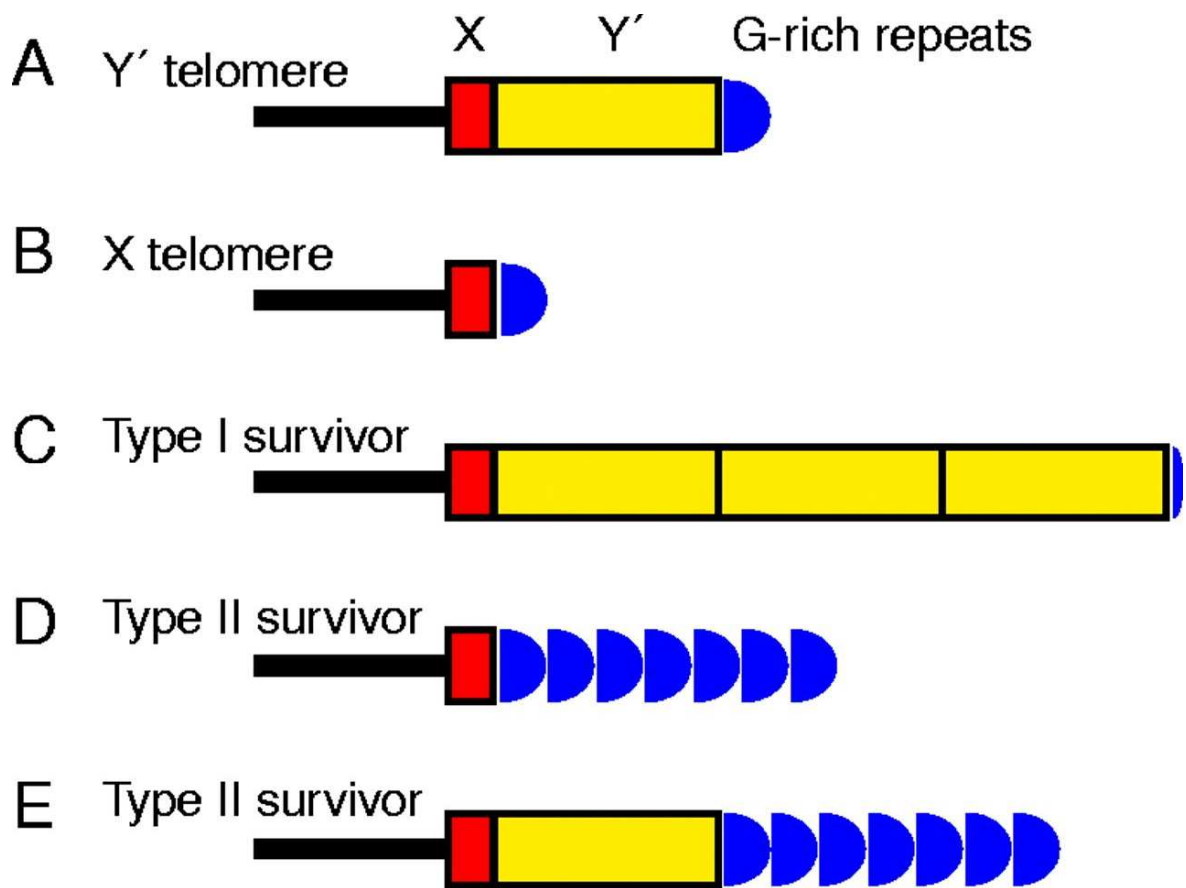


Figure 1-3 Changes in yeast telomeres. A-B) Yeast telomeres can be subdivided into Y' telomeres or X telomeres. **C)** Type I survivors amplify the Y' elements. **D-E)** Type II survivors amplify G-rich sequences. Taken from (Lydall 2003).

The exact functions of TERRA at telomeres (and perhaps elsewhere) are still being addressed, however a role in telomere length regulation and recombination facilitation was shown (Balk et al. 2013). Interestingly, telomere shortening was shown to induce TERRA expression (Cusanelli et al. 2013) and TERRA overexpression (by the insertion of an artificial promoter in subtelomeric regions) led to telomere shortening and senescence (Maicher et al. 2012; Pfeiffer and Lingner 2012). However, a more recent study in *S. pombe*, showed that induction of TERRA expression caused telomere elongation in *cis*, instead of shortening (Moravec et al. 2016). Due to the nature of TERRA (complementary to telomeric DNA) it has the capacity to form RNA:DNA hybrids at the telomeres (Balk et al. 2013). The RNA molecule of a RNA:DNA hybrid is hydrolysed by Ribonucleases H. The two main yeast Ribonucleases H are RNase H1 (encoded by *RNH1*) and RNase H2 (whose catalytic subunit is encoded by *RNH201*) (Cerritelli and Crouch 2009). RNA:DNA hybrids are suggested to promote recombination, since one DNA strand of the RNA:DNA hybrids stays single-stranded stimulating HR events (Balk et al. 2013). Indeed, ALT cells were shown to have high TERRA levels and overexpression of RNase H1 decreased telomere recombination in both human tumour cells and yeast (Balk et al. 2013; Arora et al. 2014).

1.2. DNA damage response to double-strand breaks

Double stranded breaks (DSBs), like telomeres, contain the end of a DNA molecule. However the way the cell perceives each of these DNA termini is different. While DSBs need to be eliminated/repared mainly by homologous recombination (HR) or non-homologous end joining (NHEJ), telomeres need to be maintained and protected from the repair mechanisms that act on DSBs (Karran 2000). DNA lesion repair by HR is dependent on resection at the break, which creates single stranded overhangs that can search for regions of homology in the genome. After finding homology, the “healthy” region is used as a template for error-free repair. During NHEJ the break is simply aligned and ligated, thus this pathway can introduce errors (Marcomini and Gasser 2015).

During the cell cycle there are many checkpoints that can be activated upon DNA damage. When the DNA damage checkpoint is activated, there is typically cell cycle arrest that can be temporary or permanent. During this pause in the cell cycle, the DNA repair machinery is activated in order to repair the damage and restore

normality (Zhou and Elledge 2000). DNA damage sensors are the first to respond to DNA damage sites, followed by the action of the transduction and effector proteins (Longhese et al. 1998). The initial steps of the DNA damage response is dependent on the presence of blunt ends or ssDNA and is initiated by ATM (Tel1 in yeast) and/or ATR (Mec1) (Hurley and Bunz 2007). ATM/Tel1 is more prone to respond to dsDNA while ATR/Mec1 is activated by the presence of ssDNA (Jazayeri et al. 2006; Gravel et al. 2008; Shiotani and Zou 2009). Figure 1-4 shows the DNA damage checkpoint activation upon DNA damage.

1.2.1. Resection

The first step to resolve double-strand breaks consists of DNA resection and initially involves the MRX complex (Mre11, Rad50 and Xrs2) and the endonuclease Sae2 (Chapman et al. 2012; Cannavo and Cejka 2014). MRX (MRN in mammals) and Sae2 (CtIP in mammals) are responsible for the generation of short ssDNA at DSB. Sae2 is suggested to promote 50-100 bp long cuts in the 5' strand and Mre11 mediates the nuclease activity of the MRX complex, having both 3'-5' exonuclease activity and an endonuclease activity (Trujillo and Sung 2001; Mimitou and Symington 2008; Garcia et al. 2011) (Figure 1-5). The MRX complex is important for DSB repair through HR and NHEJ pathways (Symington 2002; Zhang and Paull 2005). Importantly, Sae2 is thought to limit the MRX checkpoint activation since in *sae2Δ* cells Mre11 stays longer at DSB (Clerici et al. 2006). At telomeres, Mre11 is dispensable for ssDNA generation (Maringele and Lydall 2002), but MRX appears to be important for telomere maintenance, as *mrx* mutants have short telomeres (Wilson et al. 1999; Ritchie and Petes 2000; Tsubouchi and Ogawa 2000).

After initial MRX/Sae2 resection, Exo1 together with Sgs1-Dna2 are responsible for more extensive resection (Tsubouchi and Ogawa 2000; Llorente and Symington 2004; Zhu et al. 2008; Shiotani and Zou 2009) (Figure 1-5). Exo1 (EXO1 in mammals) is a 5'-3' flap endonuclease (can cut branched DNA) and was shown to be important for the ssDNA regulation of uncapped telomeres (Maringele and Lydall 2002). Exo1 plays a major role in DNA repair and mismatch repair throughout the genome (Amin et al. 2001; Tran et al. 2004). Sgs1 (BLM in mammals), a helicase, acts together with Dna2 (DNA2 in mammals), a nuclease (with helicase function), to promote both initial and extensive resection (Mimitou and Symington 2008; Zhu et al. 2008; Bonetti et al. 2009). Sgs1 was shown to associate with recombination proteins

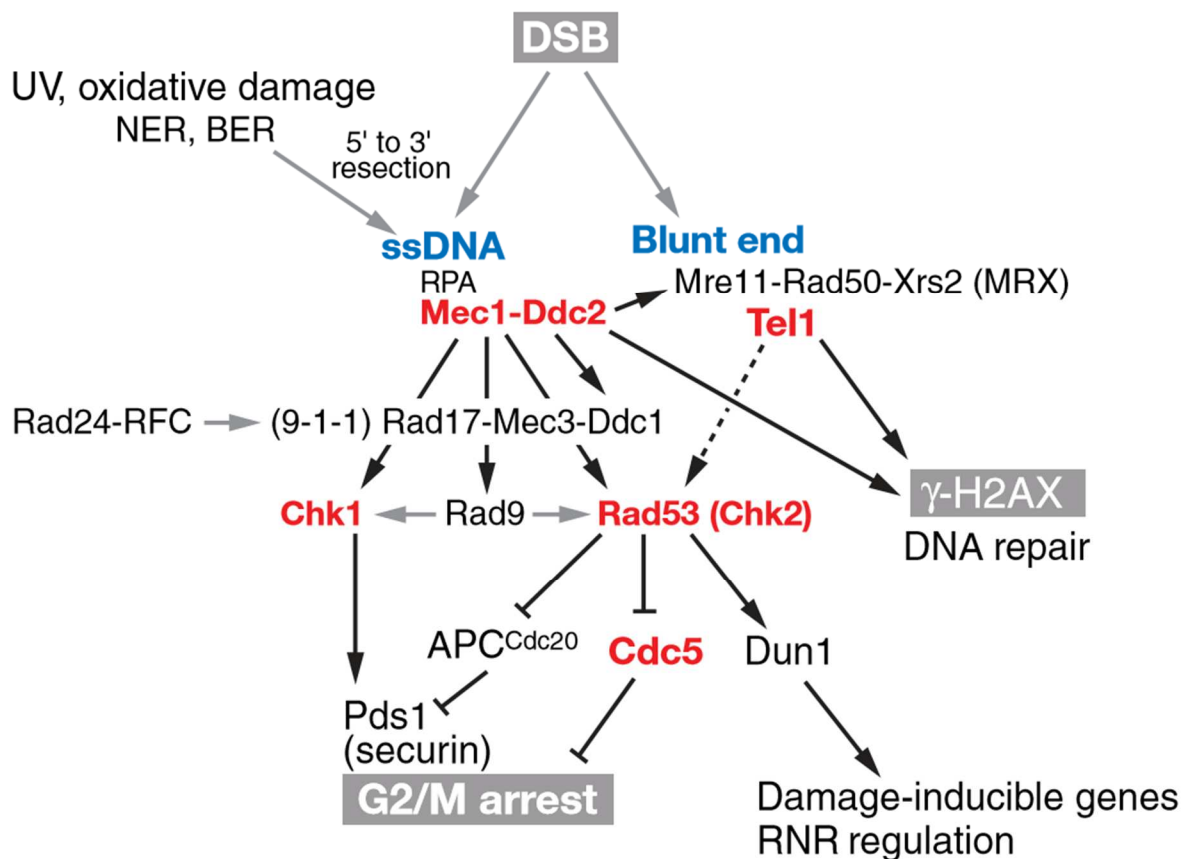


Figure 1-4 DNA damage checkpoint in *S. cerevisiae*. Resection of the DSB end yields long 3'-ended ssDNA tails that trigger the Mec1-Ddc2-dependent DNA damage checkpoint kinase cascade. Mec1 is also activated by ssDNA gaps arising by nucleotide excision repair (NER) or base excision repair (BER). Unresected, blunt-ended DNA also activates a DNA damage response, primarily through the Tel1 protein kinase and its associated MRX complex. Kinases in the cascade are indicated in red. Under some circumstances where Mec1 is absent, Tel1 can activate the S-phase checkpoint involving Rad53 and other kinases, as indicated by a dotted line. There are three important outputs of DNA damage signalling: phosphorylation of histone H2AX (γ -H2AX) and associated increases in some DSB repair events; arrest of the cell cycle prior to anaphase (G2/M arrest); and induction of damage-inducible genes as well as posttranslational regulation of ribonucleotide reductase (RNR). Black arrows indicate protein kinase phosphorylation of several target proteins that activate downstream events, whereas a black line terminated in a bar indicates an inhibitory modification. Gray arrows protein interactions that facilitate checkpoint activation. Figure and legend taken from (Harrison and Haber 2006).

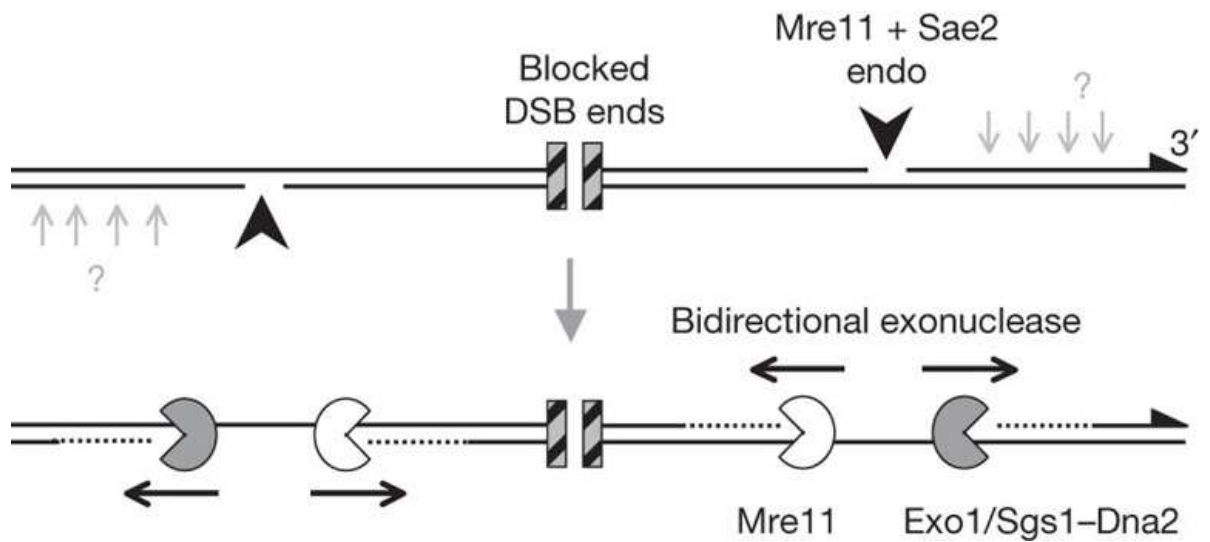


Figure 1-5 Model for bidirectional processing of DSBs by Mre11 and Exo1. After DSB formation with blocked ends (hatched squares), Mre11/Sae2-dependent nicks flanking the DSB ends create initiation sites for bidirectional resection by Exo1 and/or Sgs1–Dna2 away from the DSB, and by Mre11 towards the DSB end. Such terminal blocks could arise after base damage, trapping of a topoisomerase, or by avid binding of the NHEJ complex. 3' ends are marked with triangles. Mre11/Sae2 may make multiple nicks on the 5' strand (light grey arrows), facilitating resection. Figure and legend taken from (Garcia et al. 2011).

responsible for ALT and to play a role in G-quadruplex unwinding (Sun et al. 1999; Lu et al. 2010). An increase in mitotic hyperrecombination in *sgs1Δ* cells suggested that Sgs1 is important to maintain genomic stability (Watt et al. 1996).

Finally, *in vitro* studies showed that FEN1, a 5' to 3' flap endonuclease (the human orthologue of the yeast Rad27) is able to process DNA substrates similar to those observed during NHEJ (Tseng and Tomkinson 2004). In yeast, *rad27Δ* cells are viable but require the HR machinery to be present (Symington 1998; Debrauwere et al. 2001). Although Rad27 was implicated in DSB repair through NHEJ, its main role is in Okazaki fragment processing (Tseng and Tomkinson 2004; Rossi and Bambara 2006). While Rad27 is not thought to be an active part of the response to DSB, Rad27 depletion can lead to DSB and trigger HR events (due to non-cleaved DNA flap) (Lopes et al. 2006).

1.2.2. Checkpoint activation

After resection, RPA capped ssDNA recruits Mec1/Ddc2 (ATR-ATRIP in humans) to sites of DNA damage (Paciotti et al. 2000; Zou and Elledge 2003). Mec1 is an essential protein kinase and it phosphorylates a diversity of DNA damage response proteins, like Rad9, Rad55 and Chk1 (Emili 1998; Sanchez et al. 1999; Bashkirov et al. 2000). Signal amplification is achieved through Dpb11 phosphorylation by Mec1, which in turn increases the capacity of Dpb11 to activate Mec1 (Mordes et al. 2008). RPA-capped ssDNA recognition by Mec1/Ddc2 is essential for checkpoint activation (Paciotti et al. 2000). Mec1 has also been shown to associate with telomeres that carry structural abnormalities and to promote telomere silencing (Craven and Petes 2000; Takata et al. 2004).

In parallel to Mec1/Ddc2, the 9-1-1 complex (Rad17/Mec3/Ddc1) plays a non-essential but very important role in checkpoint activation (Lisby et al. 2004). The 9-1-1 complex was named after its mammalian orthologue, which is composed of Rad9-Hus1-Rad1. Rad24, a checkpoint “clamp loader”, loads the 9-1-1 complex to the DNA where the latter aids DSB repair (Majka and Burgers 2003). The 9-1-1 complex can be loaded to short ssDNA overhangs (produced by MRX/Sae2), promoting the loading of Rad9 near DSBs where the latter inhibits resection (Mimitou and Symington 2008; Ngo and Lydall 2015). On the other hand, the 9-1-1 complex promotes the recruitment of Dna2-Sgs1 and Exo1 to DSBs, which places the 9-1-1

complex in a central position in the coordination of DNA resection, both inhibiting and stimulating resection (Ngo et al. 2014; Ngo and Lydall 2015). Deletion of 9-1-1 complex components leads to reduced phosphorylation of Rad9 and Rad53, indicating the importance of this complex to the DNA damage response (Emili 1998).

A second sensor kinase that can be activated in response to DSB is Tel1. Tel1 has an important role in DNA damage response and it is redundant to Mec1 (Morrow et al. 1995). Tel1 loss does not increase sensitivity to DNA damaging agents, however when deleted in a Mec1 mutant background this sensitivity is significantly increased (Morrow et al. 1995). Importantly, Tel1 seems to act in the absence of ssDNA, when the MRX complex remains associated with the lesion site (Lisby et al. 2004). Additionally, the presence of Xrs2 (part of the MRX complex) seems to be important for Tel1 recruitment to DSB (Nakada et al. 2003). Tel1 promotes phosphorylation of Rad9 and Rad53 and does not rely on the 9-1-1 complex for such function (Giannattasio et al. 2002; Nakada et al. 2003).

The Rad9 checkpoint protein is part of a pathway that acts parallel to the Rad24 pathway (de la Torre-Ruiz et al. 1998). Rad9 is a mediator that promotes Rad53 and Chk1 phosphorylation by Mec1 after DNA damage (Blankley and Lydall 2004; Sweeney et al. 2005). Rad9 activation/phosphorylation can be performed by Mec1 and Tel1, promoting Rad9 oligomerization (Longhese et al. 1998; Vialard et al. 1998; Usui et al. 2009). Rad53 then binds to the phosphorylated/oligomerized Rad9, gets oligomerized and finally promotes its own phosphorylation/activation (Schwartz et al. 2002; Sweeney et al. 2005). Also, Rad9 inhibits ssDNA generation both dependent and independently of Mec1/Rad53 (Jia et al. 2004).

Finally, Rad53 and Chk1 are effector kinases whose activation is dependent on Rad9 and Mec1 (Blankley and Lydall 2004; Sweeney et al. 2005). Chk1 and Rad53 promote cell cycle arrest upon DNA damage by inducing Pds1 phosphorylation (Chk1-dependent) and repressing Pds1 degradation (Rad53-dependent) (Cohen-Fix and Koshland 1997; Sanchez et al. 1999; Agarwal et al. 2003). Pds1 is required for yeast cell cycle arrest in response to DNA damage (Cohen-Fix and Koshland 1997). Interestingly, Chk1 (and Rad9), but not Rad53, plays an important role in the cell cycle arrest of *yku70Δ* cells (Maringele and Lydall 2002). Rad53 also has the important function to inhibit Exo1 in order to avoid extensive DNA resection, which constitutes damage (Jia et al. 2004).

1.3. Telomeres, senescence and cancer

In 1961, Hayflick noticed that human fibroblasts cultivated for long periods of time (more than 50 passages) start to degenerate, i.e. they enter senescence (Hayflick and Moorhead 1961). Cellular senescence is related to telomere shortening (Lopez-Otin et al. 2013), however there are other factors involved as suggested by the senescence entry of some cells that are telomerase positive (Kiyono et al. 1998; Dickson et al. 2000). Importantly, the presence of only one (or few) short telomeres is able to trigger senescence (Hemann et al. 2001). Cells that become senescent cannot replicate and therefore senescence is believed to be an anti-cancer process (Lopez-Otin et al. 2013).

In 2007, Ruddon came up with the following definition: “Cancer is an abnormal growth of cells caused by multiple changes in gene expression leading to dysregulated balance of cell proliferation and cell death and ultimately evolving into a population of cells that can invade tissues and metastasize to distant sites, causing significant morbidity and, if untreated, death of the host” (Ruddon 2007). Thus, the ability to resist cell death, to evade growth suppressors, to sustain the proliferative signalling and induce angiogenesis, to enable replicative immortality and to activate invasion are all hallmarks of cancer (Hanahan and Weinberg 2011). Cancers present dysregulated cellular energetics (mitochondrial dysfunction) as well as a capacity to avoid immune destruction (Hanahan and Weinberg 2011). The causes for all of this to happen are vast, varied (each tumour is different) and not fully understood. However, genetic and epigenetic modifications are thought to be responsible for the development of the majority of these hallmarks (Hanahan and Weinberg 2011). Genomic instability is an extremely common characteristic in most cancers, however, whether it is the cause or the consequence of cancer is not yet defined (Negrini et al. 2010). One of the most common genes mutated in cancers is the tumour suppressor gene and DNA damage checkpoint TP53 (Negrini et al. 2010). Many other genes responsible for the DNA damage checkpoint/repair are often found to be mutated in cancers: ATM (which, like TP53, is inactivated during cancer), BRCA1, BRCA2, MRE11, RAD52, RAD51L3, etc. (Negrini et al. 2010; Salk et al. 2010). Epigenetic alterations are also an important way of repressing or stimulating gene expression (Esteller 2007; Jones and Baylin 2007; Berdasco and Esteller 2010). Consequently, DNA methylation patterns suffer great changes during cancer, with hypermethylation of some promoters and decreased methylation in some genes (Esteller 2007). At the

same time, histones also suffer modifications: deacetylation in some promoter-associated histones, and change in the methylation pattern (Esteller 2007; Jones and Baylin 2007).

Cancer is a serious threat to human health, with 8.2 million worldwide deaths related to cancer in 2012 (World Health Organization). Since telomere maintenance is a key feature of cancer cells, with telomerase being expressed in most cancer cells, the understanding of telomere regulation is extremely important (Shay and Wright 2011).

1.4. Yeast as a cellular model

S. cerevisiae, budding yeast or simply, yeast, has proven to be a very helpful organism regarding the study of many basic cellular functions (Botstein et al. 1997). *S. cerevisiae* belongs to the Fungi phylum and it was the first eukaryote to have its genome completely sequenced in 1996 (Goffeau et al. 1996; Hedges 2002). The main characteristics of this organism are its fast growth and ease of maintenance, the fact that it can be both cultivated as a diploid or haploid, the facility to perform genetic modifications and the possibility to cross strains with opposing mating types (Gomez et al. 2005). Yeast can enter the stationary phase when faced with lack of nutrients and it is able to go through meiosis (when in its diploid state). And perhaps the most important of all: it shows a high rate of conservation with human genes and cellular functions, which makes it very suitable to study new gene functions and interactions (Gomez et al. 2005). Thus, because of all these characteristics *S. cerevisiae* is often used in a first line of studies before the slower studies in human/mammalian cells or multicellular organisms like worms, rats and mice.

1.4.1. *yku70Δ* mutants

yku70Δ cells are both defective in their capacity to cap the telomere and in their capacity to repair double stranded breaks. *yku70Δ* cells are temperature sensitive presenting extensive fitness defects at 37°C, but not at 30°C (Feldmann and Winnacker 1993). Telomere defects are thought to be the main cause of the fitness defects in *yku70Δ* cells, since overexpression of telomerase subunits can partially suppress the fitness defects at higher temperatures (Nugent et al. 1998; Teo and Jackson 2001; Lewis et al. 2002). Additionally *yku70Δ* cells accumulate telomeric

ssDNA and deletion of *EXO1*, both decreases telomeric ssDNA and increases *yku70Δ* cell fitness (Maringele and Lydall 2002).

1.4.2. *cdc13-1* mutants

Cdc13 is an essential telomeric capping protein and the *cdc13-1* allele is a temperature sensitive version of the gene (the highest permissive temperature is 26°C) (Nugent et al. 1996). *cdc13-1* mutants, as well as *yku70Δ* mutants (which are also temperature sensitive), are very important to study genes that affect telomere maintenance (by affecting the temperature sensitivity of these strains) (Addinall et al. 2011).

1.4.3. Genome-wide screens

One of the advantages of yeast studies is the possibility of performing genome-wide screens, where one can evaluate the effect of a parameter in a considerable amount of genes and strains (Carpenter and Sabatini 2004). Synthetic genetic array (SGA), first described in 2001, is an example of a high-throughput study that can be performed in *S. cerevisiae*, which involves the cross of a mutated strain with a library of thousands of strains, each of them carrying one single mutation (Tong et al. 2001). Diploids are then sporulated and double mutants selected using antibiotic resistance. SGA relies on the use of an automated robotic system and allows the creation of a large number of double (or multiple) mutants in one single experiment (Tong et al. 2001). Importantly, this approach not only generates a large number of double mutants simultaneously but also allows the detection of synthetic lethality or synthetic sick interactions between the genes analysed.

In 2011, Addinall et al. used SGA followed by QFA (quantitative fitness analysis) in order to find a vast number of genetic interactions that affected cell fitness (Addinall et al. 2011). In this case the objective was to find genes that could affect telomere maintenance by crossing *cdc13-1* or *yku70Δ* strains against a mutant library (single deletions). QFA is an experimental and computational workflow that involves the analysis of a growth curve obtained from time course photography of cell cultures grown in solid agar plates (Addinall et al. 2011). The use of QFA allowed the authors to evaluate the differences between the growth of double mutants and single mutants to infer the existence of genetic interactions (Addinall et al. 2011). Genome-wide

screens are therefore an important tool to provide a large amount of genetic information that can be further studied in more detail in yeast or other organisms.

1.5. Aims

The aim of this thesis is to identify a small number of genetic interactions that occur in yeast and that can be relevant to both telomeres and cancer. This will be achieved by the analysis of previously published high-throughput screens. After the identification of candidate genes, I intend to confirm and understand their role at telomeres. If possible I will extrapolate my results to a human context and gain new insights about the role of the candidate genes in cancer development.

2. Materials and Methods

2.1. Yeast strains

S. cerevisiae strains used in this study are listed in Appendix A. Strains are in the W303 genetic background and are *RAD5*⁺.

2.2. Media composition

2.2.1. Yeast Extract, Peptone, Dextrose (YEPD)

1% (w/v) yeast extract, 2% Bactopeptone, 2% (w/v) dextrose, 0.0075% (w/v) adenine. For plates 2% (w/v) agar was added. For antibiotic selection either 0.2 mg/mL of G418 or 0.1 mg/mL of clonNAT or 0.3 mg/mL of hygromycin was added.

The media was autoclaved for 12 min at 121°C and cooled to 60°C. Antibiotics and sensitive chemical compounds were not autoclaved. Instead, antibiotic stock solutions were filtrated and added to the media after autoclaving.

2.2.2. 5-Fluoroorotic Acid Media (5-FOA)

0.13% (w/v) amino acid powder (lacking uracil), 0.67% (w/v) yeast nitrogen base, 0.005% (w/v) uracil, 0.1% (w/v) 5-FOA, 2% (w/v) dextrose.

2.2.3. Complete Synthetic Media (CSM)

Amino Acid Powder Recipe

Adenine	2.5 g
L-arginine (HCl)	1.2 g
L-aspartic acid	6.0 g
L-glutamic acid (monosodium salt)	6.0 g
L-histidine	1.2 g
L-leucine	3.6 g
L-lysine (mono-HCl)	1.8 g
L-methionine	1.2 g

L-phenylalanine	3.0 g
L-serine	22.5 g
L-threonine	12.0 g
L-tryptophan	2.4 g
L-tyrosine	1.8 g
L-valine	9.0 g
Uracil	1.2 g

The amino acids above were thoroughly mixed together and stored in a dry place. For the media: 0.13% (w/v) of amino acid powder, 0.17% (w/v) yeast nitrogen base, 0.5% (w/v) ammonium sulphate, 2% (w/v) dextrose.

2.2.4. Selective media

0.13% (w/v) of amino acid powder (lacking the appropriate amino acid), 0.17% (w/v) yeast nitrogen base, 0.5% (w/v) ammonium sulphate, 2% (w/v) dextrose.

2.2.5. Sporulation media

0.1% (w/v) yeast extract, 0.05% (w/v) dextrose, 1% (w/v) potassium acetate, pH 7.6.

2.2.6. Lysogeny Broth (LB)

0.5% (w/v) yeast extract, 1% (w/v) peptone, 1% (w/v) NaCl. For solid media 2% of agar added prior to autoclaving. When necessary, after autoclaving, ampicillin was added to a final concentration of 50 µg/mL.

2.2.7. Super Optimal broth with Catabolite repression (SOC)

0.5% (w/v) yeast extract, 2% (w/v) bactotryptone, 9.7 mM NaCl, 2.2 mM KCl, 0.36% (w/v) glucose, 10 mM MgCl₂, 10 mM MgSO₄.

2.3. Methods

2.3.1. Yeast cell maintenance and culture

Yeast strains were cultivated at 30°C or 23°C. Cultivation at 23°C was used for strains carrying the *cdc13-1* allele and experiments involving *paf1Δ* or *ctr9Δ* strains. Standard procedures for culture, mating and tetrad dissection were followed (Adams et al. 1997).

2.3.2. Sporulation of diploids

A single colony of diploid cells was inoculated in 2 mL of YEPD and grown overnight at 30°C. 500 μL of the saturated culture were washed twice with 4 mL of sterile water (1000 rpm for 3 min). The cell pellet was resuspended in 2 mL of sporulation media and incubated at 23°C for 2-5 days. In cases where the diploids carried a plasmid, cells were scraped from a fresh selective plate and resuspended directly in the sporulation media.

2.3.3. Primer design

Primer design was performed using the software ApE – A plasmid Editor by M. Wayne Davis (<http://biologylabs.utah.edu/jorgensen/wayned/ape/>). For gene deletions primers consisted of 40 bp of homology to the region immediately upstream (forward) or downstream (reverse) of the start or stop codons, followed by 20 bp with homology to a plasmid containing an antibiotic resistance or auxotrophy marker. For deletion confirmation, ~20 bp primers were designed to anneal roughly 500 bp upstream and downstream of the start and stop codons. A reverse primer recognising inside the deletion cassette was used together with a forward primer upstream of the coding region of the deleted gene. qPCR primers were designed using the Invitrogen Perfect Primer Design application (PCR detecting application) (Kim *et al.*, 2010). Primer specificity of all qPCR primers was verified (Kent). Primer efficiency was tested for all pairs of primers used in qPCR (and RT-qPCR). To calculate primer efficiency 16, 1.6, 0.16 and 0.016 ng of genomic DNA were used as template for the primers. A standard curve ($y=mx+b$) was obtained by plotting the Log₂ (DNA concentration) against the CTs. Primer efficiency was calculated using

the following equation: $\text{Efficiency} = (10^{(-1/m)} - 1) \times 100$. All primers used in this study had efficiencies between 85 and 115.

2.3.4. Gene deletion

All the genetic modifications were made according to Longtine et al. (Longtine et al. 1998). Shortly, specific plasmids carrying an antibiotic resistance cassette or a nutrient gene were amplified by PCR and then transformed into the appropriate strains by high efficiency lithium acetate (LiAc) transformation. The primers were designed as described in section 2.3.3.

2.3.5. Lithium acetate (LiAC) transformation

50 mL of exponentially-dividing cells ($\text{OD}_{600} = 0.5-1$) were harvested at 1500 rpm for 3 min, the medium was poured off, washed once in 25 mL sterile water and the cells were resuspended in 1 mL 0.1 M (1X) LiAc. Cells were transferred to an Eppendorf tube and spun down at 13000 rpm for 15 sec. LiAc was removed by aspiration. Cells were resuspended in a final volume of 500 μL by adding 400 μL of 0.1 M LiAc. 50 μL of the cell suspension were pelleted at 13 000 rpm for 15 sec and used for one transformation. The following reagents were then added to the pellet in the following order: 240 μL of PEG 4000 (50% w/v); 36 μL of 1 M (10X) LiAc; 50 μL of Salmon Sperm DNA (2 mg/mL, previously boiled and rapidly cooled in ice); and 50 μL of Transforming DNA in Water (0.1 – 10 μg). Samples were vortexed vigorously and incubated at 23°C for 30 min before being heat shocked at 42°C for 20 min. Cells were pelleted at 6000 rpm for 15 sec and transformation mix removed by aspiration. Cells were carefully resuspended in 200 μL sterile water then either plated onto selection plate to select for auxotrophy markers, or plated onto YEPD, incubated at 23°C (for *ts* strains) or 30°C overnight and then replica plated the next day onto plates containing antibiotics. Transformants were allowed to grow at 23°C for 4-5 days or at 30°C for 3-4 days. Single colonies were then picked and streaked for single colonies onto selective media. Transformants were verified by colony PCR.

2.3.6. Transformation of plasmids into yeast

Fresh cells were scraped from an agar plate using a yellow tip and resuspended in 100 μL of freshly prepared One-Step buffer (0.2 M LiAc, 40% (w/v) PEG, 100 mM DTT). 1 μL of plasmid (100-400 ng) and 5.3 μL salmon sperm DNA (10 mg/mL; boiled for 5 min then cooled rapidly in iced water) were added. Samples were vortexed and incubated at 45°C for 30 min. Cells were then plated onto the appropriate selective media and the grown colonies were streaked for single colonies and a single colony was picked for further experiments.

2.3.7. *E.coli* transformation

1-15 μL of plasmid DNA were added to 50 μL *E.coli* DH5 α competent cells. Cells and DNA were incubated on ice for 30 min and heat-shocked in a 42°C water bath for 90 sec. Cells were then incubated on ice for 2 min and 450 μL of pre-warmed (37°C) SOC medium was added to the cells. Cells were incubated in a rotating wheel for 1 hour at 37°C. 200 μL of the cell suspension were spread onto LB plates with 0.1 mg/mL of ampicillin and incubated overnight at 37°C. Single colonies were inoculated into 2 mL of LB with 0.1 mg/mL of ampicillin and incubated overnight at 37°C. Plasmid DNA was recovered using a QIAprep Spin Miniprep Kit (Qiagen).

2.3.8. Plasmid recovery from *S. cerevisiae*

Plasmid recovery from *S. cerevisiae* was made using QIAprep Spin Miniprep Kit (Qiagen). All buffers are provided by the kit and the compositions are confidential. Shortly, overnight cell cultures (grown at 36°C) were harvested by centrifugation for 5 min at 6500 rpm and the cell pellets were resuspended in 250 μL of Buffer P1 containing 0.1 mg/mL RNase A. 100 μL of acid-washed glass beads were added and samples were vortexed for 5 min. Supernatants were transferred to a new Eppendorf, 250 μL of buffer P2 were added and mixed by inversion. Samples were incubated at room temperature for 5 min and 350 μL of buffer N3 were added. After mixing by inversion, samples were spun for 10 min at 13000 rpm. Supernatant was transferred to a QIAprep Spin Column and spun for 30 sec at 13000 rpm. 750 μL of buffer PE were added and samples were centrifuged for 30 sec at 13000 rpm. An additional centrifugation at 13000 rpm for 1 min was performed. Finally, DNA was eluted in 25

μL of water. 10 μL were used to transform *E.coli* DH5 α competent cells (as described in section 2.3.7).

2.3.9. DNA isolation from yeast (Yale quick method)

Yeast strains were grown overnight to saturation on a wheel and spun at 13000 rpm. Pellet was resuspended in 0.1 M EDTA (pH 7.5), 1:1000 β -mercaptoethanol and 2.5 mg/ml zymolyase and incubated at 37°C until spheroplasted. A solution of 0.25 M EDTA pH 8.5, 0.5 M Tris Base, 2.5% (w/v) SDS was added to each tube and the mixture incubated at 65°C. After that, 5 M of KAc was added to the mixture followed by incubation on ice. Samples were spun again and the supernatants transferred to a new tube that was filled with 100% ethanol. Samples were spun again. The pellets were dried briefly before adding 100 μL of a solution of 10 mM Tris, 1 mM EDTA (pH 8) and RNase A. The mixture was incubated at 37°C, followed by precipitation with isopropanol. Samples were spun again, washed with 70% ethanol and the pellets resuspended in 40 μL of 10 mM Tris, 1 mM EDTA (pH 8) after a period of air drying. Isolation of DNA to amplify genes by PCR was performed using the YeaStar Genomic DNA Kit (Zymo Research).

2.3.10. DNA isolation (using phenol)

Between 7×10^7 to 1.5×10^9 (exponentially growing) yeast cells were spun at 1500 rpm for 5 min (4°C). Pellets were washed twice in ice-cold mQ H₂O, supernatants were completely removed and pellets were frozen at -80°C for at least 2 hours. Cell pellets were thawed on ice, resuspended in 400 μL of lysis buffer (2 % (v/v) Triton X-100, 1 % (w/v) SDS, 100 mM NaCl, 10 mM Tris-HCl, pH 8.0, 100 mM EDTA, pH 8.0) and added to screw-cap tubes (Sarstedt) containing 0.6 g glass beads. 400 μL of phenol:chloroform:isoamyl alcohol (25:24:1, v/v/v) were added and lysis was performed using a Precellys 24 ribolyser at 5.5 power setting for 20 sec (3 times, placing the samples on ice between cycles). 400 μL of TE (10 mM Tris-Cl, 1 mM EDTA, pH 8.0) were added and samples were spun at 13000 rpm for 5 min (4°C). The aqueous phase (top) was transferred to previously spun 2 mL tubes of phase lock gel, light. 750 μL of phenol:chloroform: isoamyl alcohol (25:24:1) were added and mixed by inversion. Samples were spun at 13000 rpm for 5 min. Aqueous phase was transferred to a 2 mL Eppendorf and 100% ethanol was added to fill the tube.

Tubes were incubated at room temperature for 5 min and then centrifuged at 13000 rpm for 3 min. Supernatant was completely removed and pellet was air dried for 5 min. Pellet was resuspended in 806 μL of TE/RNA (7.5 $\mu\text{g}/\text{mL}$ RNase) by incubation at 37°C for 30 min. 50 μL of 3 M NaAc, pH 5.2 were added together with 100% ethanol to fill the tube. After 15 min incubation at room temperature, samples were centrifuged at 13000 rpm for 5 min. Pellet was air-dried and resuspended in 40 μL of TE by incubation in a 37°C water bath. DNA yield and purity was determined using a Nanodrop 2000 (Thermo Scientific).

2.3.11. RNA isolation (using phenol)

25 mL of overnight exponentially growing yeast culture (e.g. 2×10^7 cells/mL) was spun for 2 min at 3,000 rpm at 4°C (culture was set by 2:10000 dilution of a saturated culture). Pellet was resuspended in 1 mL ice-cold DEPC-treated water (Sigma Aldrich) and transferred to two 1.5 mL Eppendorf tubes. Samples were spun for 30 sec at 13,000 rpm, and pellet washed again in 0.5 mL ice-cold DEPC water. Pellets were frozen at -80°C for at least 2 hours. Pellets were resuspended in 300 μL of ice-cold RNA buffer (0.5 M NaCl, 0.2 M Tris- HCl pH 7.5, 10 mM EDTA pH 8.0) and transferred to a 2 mL screw cap tube (Sarstedt) containing 200 μg of glass beads (ice cold). 300 μL of chilled phenol:chloroform:isoamyl alcohol (25:24:1 (v/v/v)) saturated with RNA buffer were added and lysis was performed in a Precellys 24 ribolyser (Bertin Technologies) using two cycles of 30 sec at 6500 rpm with a 15 sec pause between cycles. Samples were spun at 13,000 rpm for 1 min at 4°C. The upper phase was transferred to a new Eppendorf and 300 μL of chilled phenol:chloroform:isoamyl alcohol (25:24:1 (v/v/v)) saturated with RNA buffer were added. After brief vortexing samples were centrifuged for 1 min at 13,000 rpm at 4°C. Upper phase was transferred to a new Eppendorf and 900 μL of ice-cold 100% ethanol were added. Samples were incubated at -80°C for 2 hours and then centrifuged 2 min at 13,000 rpm at 4°C. Supernatant was completely removed and pellets were air-dried for 15 min. Finally, RNA was dissolved in 50 μL of RNase-free water. Samples were stored at -80°C. 100 μL of 1 $\mu\text{g}/\mu\text{L}$ RNA were purified using the RNA Cleanup in the RNeasy Mini Kit (Qiagen) and eluting the RNA in 30 μL of RNase free water. 5 μL of 1 $\mu\text{g}/\mu\text{L}$ RNA were then digested with 2 μL (2 units) of DNase I (Amplification grade, Invitrogen) and 1X DNase I buffer (Invitrogen) in a final volume of 19 μL . Reaction was stopped with 2 μL of 25 mM EDTA (Invitrogen) and

incubation at 65°C for 10 min. 40 µL of DEPC-treated water were added to each sample to get a concentration of 82 ng/µL. 2 µL of this RNA were used in One-Step RT-qPCR.

2.3.12. RNA isolation (using RNeasy Mini Kit)

All TERRA measurements were made using this protocol. RNA was extracted using the RNeasy Mini Kit (Qiagen) with 3 DNase treatments (RNase-Free DNase Set, Qiagen). All buffers are provided by the kit and the compositions are confidential. Pellets (5×10^7 to 20×10^7 cells) were collected, washed and frozen as described in section 2.3.11. Frozen pellets were resuspended in 600 µL of buffer RLT supplemented with β-mercaptoethanol (10 µL β-mercaptoethanol/1 mL RLT buffer) and lysed as described in section 2.3.11. 350 µL of the lysate were transferred to a new Eppendorf, centrifuged at full speed and the supernatant transferred to a new Eppendorf. 350 µL of 70% ethanol were added and the sample was transferred to an RNeasy mini column. Samples were centrifuged for 15 sec at 12,000 rpm and 350 µL of buffer RW1 were added. Samples were centrifuged for 15 sec at 12,000 rpm and 80 µL of DNase I incubation mix (10 µL DNase I stock solution to 70 µL Buffer RDD) was added. Samples were incubated for 15 min at 23°C, 350 µL of Buffer RW1 were added and samples were centrifuged for 15 sec at 12,000 rpm. Samples were washed twice with 500 µL of RPE buffer (first by centrifugation for 15 sec at 12,000 rpm and then for 2 min at 12,000 rpm). An extra centrifugation (1 min at max speed) was performed to get rid of residual buffer. RNA was eluted with RNase-free water in two centrifugation steps: first with 40 µL and then with 47.5 µL (1 min at 12,000 rpm). 10 µL of Buffer RDD and 2.5 µL of DNase I stock were added to each sample and incubated at 23°C for 10 min. 350 µL of Buffer RLT were added to each sample followed by 250 µL of 100% ethanol. Each sample was applied to the corresponding previously used RNeasy mini column. Samples were centrifuged for 15 sec at 12,000 rpm and 350 µL of buffer RW1 were added. A new on-column DNase I digestion and subsequent washing steps was performed as described above. RNA was eluted with RNase-free water in two centrifugation steps: first with 30 µL and then by reapplying the eluted sample to the column.

2.3.13. *In vivo* cloning

In vivo cloning was performed using the Lithium acetate transformation method (Section 2.3.5). The DNA to transform was created the following way: 0.6-1.5 µg of plasmid (vector) was cut with 15 units of the appropriate restriction enzyme (New England Biolabs) and the appropriate restriction enzyme buffer (New England Biolabs) in a 20 µL volume digest for 2 hours at the appropriate temperature. Insert DNA was created by PCR. Both vector and insert were purified using a Biomiga Gel Purification kit. The transformation was carried out with 15 µL of the vector and 20 µL of the insert. Transformations with the following controls were also performed: vector; insert; undigested vector; and TE. Plasmids were then removed from yeast using the method described in section 2.3.8.

2.3.14. *In vitro* cloning

2 µg plasmid vector DNA and plasmid DNA containing the required insert were cut with 15 units of the appropriate restriction enzyme (New England Biolabs) and the appropriate restriction enzyme buffer (New England Biolabs) in a 20 µL volume digest for 90 min at 37°C. Then, to the vector, 1 µL of 5X New England Biolabs Buffer 4 (CutSmart) and 1 µL of 2X CIP phosphatase (New England Biolabs) were added. After 30 min of incubation both vector and insert DNA were ran on a gel and purified using a Biomiga Gel Purification kit. Vector (2 µL) and insert (6 µL) were ligated together using T4 DNA ligase in 1X T4 DNA ligase buffer by overnight incubation at 16°C. 5 µL of the ligated DNA were transformed into 100 µL *E.coli* DH5α competent cells as described in section 2.3.7.

2.3.15. Spot test

A pool of colonies were grown until saturation overnight at 23°C in liquid YEPD (for spot tests containing sick strains saturation was only achieved after 2 days). 5, 10 or 20-fold serial dilutions in water were spotted onto the appropriate plates using a replica plating device. Plates were incubated for 2 (or 5) days at the appropriate temperatures. Pictures were taken using a SPimager.

2.3.16. Southern blot

Southern blot analysis was used to assess telomere length and performed as previously described (Dewar and Lydall 2010). Genomic DNA was extracted from 2 different strains for each genotype. 2.5 μL of equally concentrated DNA preparations were digested with 0.5 μL XhoI or Hind III (20 units/ μL), 2 μL 5x NEBuffer 4, 1 μL 10x BSA, 4 μL water for 3 hours at 37°C. Samples were run on a 1% agarose gel (0.5X TBE, SybrSafe) at 20 volts for ~17 hours. The gel was photographed using a Fuji LAS 4000 imager to determine loading. The gel was depurinated in 0.25 M HCl for 15 min, rinsed twice in sterile water then denatured in 0.5 M NaOH for 30 min. The gel was blotted to positively-charged nylon membrane (Roche) using a vacuum blotter (Model 785, BioRad) at 5 inches Hg in 10X SSC (87.6 g of NaCl, 44.1 g of sodium citrate, pH 7.0, in 1 litre) for 90 min. DNA was cross-linked to the wet membrane using auto UV cross-linking (Stratalinker). The membrane was rinsed briefly in sterile water and allowed to air-dry. The probe was hybridized to the membrane using the labelled probe and the DIG High Prime Labelling and Detection Starter Kit II (Roche). The probe was detected using the same kit and the membrane was imaged using a Fuji LAS 4000 imager for chemiluminescence, for 20-30 min.

2.3.17. Passage test

Single colonies (from the germination plates) were streaked on to a YEPD plate and let grow for 2 (30°C) or 4 (23°C) days. Pictures were taken using a SPimager and pooled colonies from this plate were used to streak on a new YEPD plate. Pictures were taken again and this procedure was repeated until no differences were observed between two subsequent passages.

2.3.18. Genomic/Plasmid PCR

PCR was used to amplify DNA fragments from genomic DNA or plasmids. Oligonucleotides used in this study are listed in Appendix B and a list of plasmids can be found in Appendix C. PCR was performed in a final volume of 20 μL containing: 0.3 μM of each primer, 0.5 units of ExTaq polymerase (TaKaRa Bio Inc.), 0.2 mM of dNTPs, 1X ExTaq buffer and 5-15 ng of genomic or plasmid DNA. PCR conditions used were: 1 cycle of 1 min at 95°C; 35 cycles of 30 sec at 94°C, 30 sec at 55°C and 1 min per kb DNA amplified at 68°C; 1 cycle of 10 min at 68°C. PCR product sizes

were verified by running samples on agarose gels made with 0.5X TBE and 1X SyBrSafe (1/10,000 dilution; Invitrogen). Gels were imaged using a FujiFilm LAS Image 4000.

2.3.19. Colony PCR

Colony PCR was used to confirm correct deletion of genes. PCR was performed in a final volume of 20 μ L containing: 0.3 μ M of each primer, 0.5 units of GoTaq HotStart polymerase (Promega), 0.2 mM of dNTPs, 2.5 mM of MgCl₂, 1x green GoTaq buffer and 2 μ L cell suspension in water. PCR product sizes were verified as described in section 2.3.18.

2.3.20. qPCR

Quantitative PCR was performed with 2 μ L of 0.08-80 ng/ μ L of DNA in 1X Platinum SYBR Green qPCR SuperMix-UDG with ROX (Invitrogen), 200 nM forward primer and 200 nM reverse primer. For each sample three replicates were measured and a no-template control was also analysed (with water instead of DNA). The qPCR program was 50°C for 2 min, 95°C for 2 min, followed by 40 cycles of 95°C for 15 sec and 60°C for 30 sec using an ABI Systems StepOnePlus thermal cycler. A melting curve was also analysed. *BUD6*, *ACT1* or 7S RNA were used as internal controls to normalize the DNA loaded. Fold changes were calculated using the formula: $2^{-(\text{SampleCT}-\text{ControlCT})}$. Data was then analysed relative to *WT* values (considering *WT* fold change to be 1).

2.3.21. RT-qPCR

Reverse transcriptase PCR was performed either by a One-Step or a Two-Step method. The One-Step method was made using the SuperScript® III Platinum® SYBR® Green One-Step qPCR Kit w/ROX (Invitrogen). The RT-qPCR was performed using 2 μ L of 80-82 ng/ μ L RNA in 1X SYBR® Green Reaction Mix, 200 nM of forward and reverse primers, 0.2 μ L of SuperScript® III Reverse Transcriptase and 0.2 μ L of Rox Reference Dye. The qPCR program was 50°C for 3 min, 95°C for 5 min, followed by 40 cycles of 95°C for 15 sec and 60°C for 30 sec and a final cycle of 1 min at 40°C using an ABI Systems StepOnePlus thermal cycler. Data was

analysed as described in section 2.3.20. In the Two-Step method cDNA was produced using SuperScript™ II Reverse Transcriptase (Invitrogen). 3.8 µL of 0.8 µg/µL RNA with 0.769 µM of dNTP mix, 2 µM of reverse primers (10 µM for CA-rich primer, m4104) in a final volume of 13 µL were incubated at 90 °C for 1 min followed by 1 min at 55°C. With the mix still at 55°C, 7 µL of the following mix were added to each sample: 4 µL of 5X First-Strand Buffer, 1 µL of DTT (0.1M), 1 µL SuperScript™ II RT and 1 µL of RNasin plus inhibitor (Promega). Samples were incubated for a further 60 min at 55°C followed by 15 min at 70°C. Samples were diluted 2.5 times in water and 2 µL of the cDNA was quantified by qPCR using the method described in section 2.3.20.

2.3.22. In-gel assay

In-gel assay was used to assess the amount of telomeric ssDNA. Telomeric DNA damage was induced by shifting the temperature of exponentially growing cultures (containing *cdc13-1* or *yku70Δ* cells) from 23°C to 36°C. Cells were collected after 4 hours and DNA extracted as described in section 2.3.10. 5-10 µg of DNA were digested overnight at 37°C in a 20 µL reaction containing: 2 units of XhoI, 1X NEB Buffer 4 and 0.1 µg/µL of BSA. Enzyme was inactivated by 20 min incubation at 65 °C. Samples were placed on ice and 1 µL of an AC-rich oligo labelled on the 5' end with IRDye800 (m3157, 500 nM) was added. Samples were incubated first 10 min at 37°C and then 30 min on ice. 4 µL of Orange G Loading Buffer (0.125 g Orange G, 0.75 g Ficoll Type 400, 12 mL 0.5 M EDTA, pH 8.0 water to 50 mL) was added to each sample, to blank samples (1X NEB Buffer 4, 0.1 µg/µL of BSA, 25 nM of IRDye 800 AC Oligo) and to DNA ladder (4 ng of DNA ladder, 1X NEB Buffer 4, 0.1 µg/µL of BSA, 25 nM of IRDye 800 AC Oligo). Samples, ladder and blanks were loaded onto a 1% (w/v) agarose gel (in 0.5X TBE) and ran at 5 V/cm for 90–120 min. Gel was imaged in a LI-COR Odyssey® Infrared Imaging System (channel 800 nm). The gel was then incubated in 200 mL of 0.5X TBE with SYBR Safe (1:10000) for 30 min. Gels were imaged using a FujiFilm LAS Image 4000 to get the loading control image.

2.3.23. Yeast cell imaging

Yeast live imaging was performed with filter-sterilized liquid YEPD. Saturated cultures were diluted (1:125) and grown overnight at 23°C, in a water bath with agitation (190

rpm). When the OD_{600} was between 0.4-0.5, the temperature was shifted to 36°C, cultures were subdivided and MMS (0.1% w/v) and HU (200 mM) were added. Addition of water was used as a control. Pictures were taken either before temperature change (and addition of the drugs) and after 180 min of exposure to temperature and the drugs. For microscopy, YEPD media was removed and cells were resuspended in CSM media. Cells were photographed under a fluorescence microscope (Nikon eclipse 50i), 500 ms exposure with the GFP filter (phase contrast pictures were taken for each field). For each culture/condition at least 8 different and randomly chosen fields were analysed. Images were analysed with the ImageJ software (Schneider et al. 2012). To all images (fluorescent and phase contrast) the following sequence of actions was performed in ImageJ: 1) Cut pictures in order to reproduce the size and position of a selection (Ctrl+Alt+E, in Windows); 2) subtract background (75 px); 3) LUT (green); 4) Split channels (Keep green).

2.3.24. RNA half-life

Anchors-Away strain background (*tor1-1 fpr1::NAT RPL13A-2*FKBP12::TRP1 Rpb1-FRB-KANMX6*) was used to stop RNA pol II-mediated transcription upon rapamycin addition. Cell cultures were grown overnight at 30°C until early exponential ($OD_{600} \sim 0.5$). A fraction of the culture was harvested (0 min time-point) and rapamycin was added (1 µg/mL final). Total RNA was isolated from cells harvested at 0, 10, 20, 40 and 60 min after rapamycin addition. RNA levels were measured for each time-point and normalized for the amount of 7S RNA. The fold change from the 0 min time point was obtained and the logged (LOG2) data was plotted as a function of time starting from the 10 min time-point. The slope (m) of a line that best represents the data was finally used to calculate RNA half-life: 0.693/m.

2.3.25. ImageJ quantification of images

Image quantifications were performed using the ImageJ software (<https://imagej.nih.gov/ij/>) as described in the website: <https://imagej.nih.gov/ij/docs/menus/analyze.html#gels>. Rectangular selection tool was used to surround the areas to quantify (pressing “1” to define the first lane and “2” to define any other lanes). By pressing “3” profile plots were generated. The straight line selection tool was used to draw a line in the base of each peak of

interest and the wand tool was used to quantify the area of each peak, by clicking inside the peak.

3. Yeast telomere screens and cancer

3.1. Introduction

A report by Kachroo and colleagues showed that close to half of the yeast essential genes can be replaced by their human orthologues (Kachroo et al. 2015). This high degree of conservation of function between basic processes in yeast and humans allows us to gain important insights into human biology by studying a simple unicellular organism like yeast. Hence, yeast genome-wide screens are a powerful tool to identify genetic interactions that might be relevant to human biology. For example, there are thousands of genes that are affected/mutated in cancer, but how those mutations influence cancer onset and progression is still not fully understood (Pon and Marra 2015). This is where the use of yeast genome-wide screens might help to speed up the process of further understanding cancer biology. For instance, the study of the orthologues of cancer-related genes in yeast might reveal which processes are affected by certain mutations in cancer.

Telomere maintenance is a priority for highly dividing cells, like cancer cells, or yeast (Dilley and Greenberg 2015). Therefore, the better understanding of telomere biology in yeast might help to understand the mechanisms involved in the maintenance of telomeres in cancer cells.

Published yeast genome wide-screens reported how the lack of a given gene affected the fitness of cells with telomere capping defects caused by *yku70Δ* or *cdc13-1* (Addinall et al. 2011). From these screens they identified various gene deletions that suppressed or enhanced *yku70Δ* or *cdc13-1* fitness defects (i. e, gene deletions that genetically interacted with *yku70Δ* and/or *cdc13-1*).

High-throughput screens generate an immense amount of data and consequently often contain errors. Therefore, it is essential to validate genetic interactions identified in those screens. Validation consists of repeating the result/genetic interaction in a small-scale experiment, preferentially in a different yeast genetic background. After the validation, small and focused experiments can be performed to understand the biological processes underneath the genetic interaction observed. Ultimately, the objective is to understand how genes interact in yeast and, if possible,

extrapolate from the results obtained to understand how similar genes interact in humans.

In this chapter I used the Addinall et al. screens to identify genes that are potentially relevant to both cancer and telomere biology. Some of the genes validated in this Chapter will be further studied in Chapters 4, 5 and 6.

3.2. Results

Around 700 strong enhancers or suppressors of *cdc13-1* fitness (Addinall et al. 2011) were analysed for cancer relevance by: orthology to human genes (only genes with human orthologues were considered); gene function; presence in cancer gene databases and frequency of gene mutations reported in cancers. Gene deletions affecting *yku70Δ* fitness and genes whose overexpression affected *cdc13-1* fitness were also analysed by the same criteria. Table 3-1 shows the top 91 genes identified, ranked by percentage of mutations that affect protein function, present in cancer samples (mutational score). Additionally, I added to the table the mutational score of well known tumour suppressor genes: TP53 (transcriptional activator) and BRCA1 (involved in homologous recombination). Importantly, BRCA1 is found mutated in 1.4% of the cancer samples, a value much lower than TP53 (32.2%), but similar to the genes on the top of Table 3-1.

From the 91 genes identified in Table 3-1, 12 (*DYN1*, *UFD2*, *SKI2*, *INP52*, *CDC73*, *BAS1*, *SLA2*, *MON1*, *DOA1*, *VPS74*, *FYV10* and *SUB1*) were further investigated. The 12 candidates were chosen not only by their mutational score (Table 3-1) but also by the relevance of the processes they are known to be involved in and the relevance of the most recent literature on those genes. For instance, genes involved in proteasome degradation, transcription, replication, DNA damage, etc. were preferred over genes involved in cell wall maintenance, nutrient/energy metabolism, etc. Additionally, genes that have been previously deleted and were already present in David Lydall's yeast library were not taken into account for further studies (highlighted in blue in Table 3-1).

Table 3-1 Yeast genes with a potential role at telomeres. Genes presented in this table were found to be either enhancers or suppressors of *cdc13-1* fitness defects on genome-wide screens (Addinall et al. 2011). Description for each gene function is exactly as it is found in the Saccharomyces Genome Database website (Cherry et al. 2012). In each case, human orthologues were found using the Ensembl online database (Herrero et al. 2016), and the Intogen (<http://www.intogen.org/search>) database provided information about the mutations of each gene in cancer (if mutations in that gene can originate the onset of cancer and how frequently mutations in the gene are found in cancers) (Gonzalez-Perez et al. 2013). Red indicates the genes deleted in this study. Blue indicates genes previously studied in David Lydall's laboratory. For comparison, TP53 and BRCA1, widely characterized cancer genes, are present in the table

GENE	Description (yeast) (Saccharomyces Genome Database)	Human orthologue (Ensembl)	Mutational cancer driver (Intogen)	% of mutated cancer samples (affecting protein) (Intogen)
		TP53	Yes	32.2
DYM1	Cytoplasmic heavy chain dynein; required for anaphase spindle elongation; involved in spindle assembly, chromosome movement, and spindle orientation during cell division.	DNAH5	No	7
		BRCA1	Yes	1.4
RAD9	DNA damage-dependent checkpoint protein; required for cell-cycle arrest in G1/S, intra-S, and G2/M, plays a role in postreplication repair (PRR) pathway; transmits checkpoint signal by activating Rad53p and Chk1p; hyperphosphorylated by Mec1p and Tel1p; multiple cyclin dependent kinase consensus sites and the C-terminal BRCT domain contribute to DNA damage checkpoint activation; Rad9p Chk1 Activating Domain (CAD) is phosphorylated at multiple sites by Cdc28p/Clb2p.	53BP1 (same protein family)	Yes	1.3
SIN3	Component of the Sin3p-Rpd3p histone deacetylase complex, involved in transcriptional repression and activation of diverse processes; involved in the maintenance of chromosomal integrity.	SIN3A	Yes	1
NMD2	Protein involved in the nonsense-mediated mRNA decay (NMD) pathway; interacts with Nam7p and Upf3p; involved in telomere maintenance.	UPF2	No	1
UFD2	Ubiquitin chain assembly factor (E4) that cooperates with a ubiquitin-activating enzyme (E1), a ubiquitin-conjugating enzyme (E2), and a ubiquitin protein ligase (E3) to conjugate ubiquitin to substrates; also functions as an E3.	UBE4B	No	0.9
DUN1	Cell-cycle checkpoint serine-threonine kinase required for DNA damage-induced transcription of certain target genes, phosphorylation of Rad55p and Sml1p, and transient G2/M arrest after DNA damage; also regulates postreplicative DNA repair.	CHEK2	Yes	0.8

INP52	Polyphosphatidylinositol phosphatase, dephosphorylates a number of phosphatidylinositols (PIs) to PI; involved in endocytosis; hyperosmotic stress causes translocation to actin patches.	OCRL	No	0.8
KEX2	Subtilisin-like protease (proprotein convertase); a calcium-dependent serine protease involved in the activation of proproteins of the secretory pathway.	PCSK2	No	0.8
SKI2	Ski complex component and putative RNA helicase; mediates 3'-5' RNA degradation by the cytoplasmic exosome; null mutants have superkiller phenotype of increased viral dsRNAs and are synthetic lethal with mutations in 5'-3' mRNA decay.	SKIV2L	No	0.8
NUP1	FG-nucleoporin component of central core of the nuclear pore complex (NPC); contributes directly to nucleocytoplasmic transport and maintenance of the NPC permeability barrier; possible karyopherin release factor that accelerates release of karyopherin-cargo complexes after transport across NPC.	NUP153	No	0.7
PMS1	ATP-binding protein required for mismatch repair in mitosis and meiosis; functions as a heterodimer with Mlh1p; binds double- and single-stranded DNA via its N-terminal domain, similar to <i>E.coli</i> MutL.	PMS1	No	0.7
EXO1	5'-3' exonuclease and flap-endonuclease; involved in recombination, double-strand break repair, MMS2 error-free branch of the post replication (PRR) pathway and DNA mismatch repair; role in telomere maintenance; member of the Rad2p nuclease family, with conserved N and I nuclease domains; relative distribution to the nucleus increases upon DNA replication stress; EXO1 has a paralog, DIN7, that arose from the whole genome duplication.	EXO1	No	0.6
NAM7	ATP-dependent RNA helicase of the SFI superfamily; involved in nonsense mediated mRNA decay; required for efficient translation termination at nonsense codons and targeting of NMD substrates to P-bodies; involved in telomere maintenance; forms cytoplasmic foci upon DNA replication stress.	UPF1	No	0.6
UBI4	Ubiquitin, becomes conjugated to proteins, marking them for selective degradation via the ubiquitin-26S proteasome system; essential for the cellular stress response.	UBC	No	0.6
CDC73	Component of the Paf1p complex; binds to and modulates the activity of RNA polymerases I and II; required for expression of certain genes, modification of some histones, and telomere maintenance; involved in transcription elongation as demonstrated by the G-less-based run-on (GLRO) assay; protein abundance increases in response to DNA replication stress.	CDC73/PARAFIB ROMIN	Yes	0.5
BAS1	Myb-related transcription factor involved in regulating basal and induced expression of genes of the purine and histidine biosynthesis pathways; also involved in regulation of meiotic recombination at specific genes.	MYBL2	No	0.5
DNA2	Serine/threonine kinase and DNA damage checkpoint effector; mediates cell cycle arrest via phosphorylation of Pds1p; phosphorylated by checkpoint signal transducer Mec1p; homolog of <i>S. pombe</i> and mammalian Chk1 checkpoint kinase.	DNA2	No	0.5
MRE11	Nuclease subunit of the MRX complex with Rad50p and Xrs2p; complex functions in repair of DNA double-strand breaks and in telomere stability; Mre11p associates with Ser/Thr-rich ORFs in premeiotic phase;	MRE11A	No	0.5

	nuclease activity required for MRX function; widely conserved; forms nuclear foci upon DNA replication stress.			
TKL1	Transketolase; catalyzes conversion of xylulose-5-phosphate and ribose-5-phosphate to sedoheptulose-7-phosphate and glyceraldehyde-3-phosphate in the pentose phosphate pathway; needed for synthesis of aromatic amino acids; TKL1 has a paralog, TKL2, that arose from the whole genome duplication.	TKTL1	No	0.5
YME1	Catalytic subunit of the mitochondrial inner membrane i-AAA protease complex, which is responsible for degradation of unfolded or misfolded mitochondrial gene products; also has a role in intermembrane space protein folding; mutation causes an elevated rate of mitochondrial turnover.	YME1L1	No	0.5
CKA2	Alpha' catalytic subunit of casein kinase 2 (CK2); CK2 is a Ser/Thr protein kinase with roles in cell growth and proliferation; CK2, comprised of CKA1, CKA2, CKB1 and CKB2, has many substrates including transcription factors and all RNA polymerases; protein abundance increases in response to DNA replication stress; regulates Fkh1p-mediated donor preference during mating-type switching.	CSNK2A1	Yes	0.4
STI1	Hsp90 cochaperone, interacts with the Ssa group of the cytosolic Hsp70 chaperones and activates Ssa1p ATPase activity; interacts with Hsp90 chaperones and inhibits their ATPase activity; homolog of mammalian Hop.	STIP1	Yes	0.4
ACS2	Acetyl-coA synthetase isoform which, along with Acs1p, is the nuclear source of acetyl-coA for histone acetylation; mutants affect global transcription; required for growth on glucose; expressed under anaerobic conditions.	ACSS1	No	0.4
CHK1	Serine/threonine kinase and DNA damage checkpoint effector; mediates cell cycle arrest via phosphorylation of Pds1p; phosphorylated by checkpoint signal transducer Mec1p; homolog of <i>S. pombe</i> and mammalian Chk1 checkpoint kinase.	CHEK1	No	0.4
EDE1	Endocytic protein; involved in a network of interactions with other endocytic proteins; binds membranes in a ubiquitin-dependent manner, may also bind ubiquitinated membrane-associated proteins; interacts with Cmk2 and functions upstream of CMK2 in regulating non-apoptotic cell death.	EPS15/ITSN2 (?)	No	0.4/1
FUM1	Fumarase, converts fumaric acid to L-malic acid in the TCA cycle; cytosolic and mitochondrial distribution determined by the N-terminal targeting sequence, protein conformation, and status of glyoxylate shunt; phosphorylated in mitochondria.	FH	No	0.4
FUS3	Mitogen-activated serine/threonine protein kinase involved in mating; phosphoactivated by Ste7p; substrates include Ste12p, Far1p, Bni1p, Sst2p; inhibits invasive growth during mating by phosphorylating Tec1p, promoting its degradation.	MAPK1	No	0.4
KRS1	Lysyl-tRNA synthetase.	KARS	No	0.4
MON1	Protein required for fusion of cvt-vesicles and autophagosomes with the vacuole; associates, as a complex with Ccz1p, with a perivacuolar compartment; potential Cdc28p substrate.	MON1A	No	0.4

RTF1	Subunit of RNAPII-associated chromatin remodeling Paf1 complex; regulates gene expression by directing cotranscriptional histone modification, influences transcription and chromatin structure through several independent functional domains; directly or indirectly regulates DNA-binding properties of Spt15p and relative activities of different TATA elements; involved in transcription elongation.	Rtf1	No	0.4
SLA2	Transmembrane actin-binding protein involved in membrane cytoskeleton assembly and cell polarization; adaptor protein that links actin to clathrin and endocytosis; present in the actin cortical patch of the emerging bud tip; dimer in vivo.	HIP1R	No	0.4
SSN3	Cyclin-dependent protein kinase, component of RNA polymerase II holoenzyme; involved in phosphorylation of the RNA polymerase II C-terminal domain; involved in glucose repression	CDK8	No	0.4
UBP3	Ubiquitin-specific protease involved in transport and osmotic response; interacts with Bre5p to co-regulate anterograde and retrograde transport between the ER and Golgi; involved in transcription elongation in response to osmotic stress through phosphorylation at Ser695 by Hog1p; inhibitor of gene silencing; cleaves ubiquitin fusions but not polyubiquitin; also has mRNA binding activity; protein abundance increases in response to DNA replication stress.	USP10	No	0.4
ALD6	Cytosolic aldehyde dehydrogenase, activated by Mg ²⁺ and utilizes NADP ⁺ as the preferred coenzyme; required for conversion of acetaldehyde to acetate; constitutively expressed; locates to the mitochondrial outer surface upon oxidative stress.	ALDH1A3	No	0.3
ALG1	Mannosyltransferase, involved in asparagine-linked glycosylation in the endoplasmic reticulum (ER); essential for viability, mutation is functionally complemented by human ortholog.	ALG1	No	0.3
ARP5	Nuclear actin-related protein involved in chromatin remodeling, component of chromatin-remodeling enzyme complexes.	ACTR5	No	0.3
ARP6	Actin-related protein that binds nucleosomes; a component of the SWR1 complex, which exchanges histone variant H2AZ (Htz1p) for chromatin-bound histone H2A.	ACTR6	No	0.3
CAC2	Subunit of chromatin assembly factor I (CAF-1), with Rif2p and Msi1p; chromatin assembly by CAF-1 is important for multiple processes including silencing at telomeres, mating type loci, and rDNA; maintenance of kinetochore structure, deactivation of the DNA damage checkpoint after DNA repair, and chromatin dynamics during transcription; relocates to the cytosol in response to hypoxia.	CHAF1B	No	0.3
CLB2	B-type cyclin involved in cell cycle progression; activates Cdc28p to promote the transition from G2 to M phase; accumulates during G2 and M, then targeted via a destruction box motif for ubiquitin-mediated degradation by the proteasome; CLB2 has a paralog, CLB1, that arose from the whole genome duplication.	ACTR6	No	0.3
CLB4	B-type cyclin involved in cell cycle progression; activates Cdc28p to promote the G2/M transition; may be involved in DNA replication and spindle assembly; accumulates during S phase and G2, then targeted for ubiquitin-mediated degradation.	CCNA2	No	0.3

DOA1	WD repeat protein required for ubiquitin-mediated protein degradation; forms a complex with Cdc48p; plays a role in controlling cellular ubiquitin concentration; also promotes efficient NHEJ in postdiapyc/stationary phase; facilitates N-terminus-dependent proteolysis of centromeric histone H3 (Cse4p) for faithful chromosome segregation; protein increases in abundance and relocalizes from nucleus to nuclear periphery upon DNA replication stress.	PLAA	No	0.3
ELO3	Elongase, involved in fatty acid and sphingolipid biosynthesis; synthesizes very long chain 20–26-carbon fatty acids from C18-CoA primers; involved in regulation of sphingolipid biosynthesis.	ELOVL4	No	0.3
GGA2	Protein that interacts with and regulates Arf1p and Arf2p in a GTP-dependent manner to facilitate traffic through the late Golgi; binds phosphatidylinositol 4-phosphate, which plays a role in TGN localisation; has homology to gamma-adaptin.	GGA1	No	0.3
LAT1	Dihydropyrimidine acetyltransferase component (E2) of pyruvate dehydrogenase complex, which catalyzes the oxidative decarboxylation of pyruvate to acetyl-CoA.	DLAT	No	0.3
LEO1	Component of the Paf1 complex; which associates with RNA polymerase II and is involved in histone methylation; plays a role in regulating Ty1 transposition; involved in transcription elongation as demonstrated by the G-less-based run-on (GLRO) assay.	LEO1	No	0.3
NAP1	Protein that interacts with mitotic cyclin Clb2p; required for the regulation of microtubule dynamics during mitosis; controls bud morphogenesis; involved in the transport of H2A and H2B histones to the nucleus; phosphorylated by CK2; protein abundance increases in response to DNA replication stress.	NAP1L1	No	0.3
PAC2	Microtubule effector required for tubulin heterodimer formation, binds alpha-tubulin, required for normal microtubule function, null mutant exhibits cold-sensitive microtubules and sensitivity to benomyl.	TBCE	No	0.3
PUF6	Pumilio-homology domain protein that binds the 3' UTR of ASH1 mRNA and represses its translation, resulting in proper asymmetric localisation of ASH1 mRNA; also co-sediments with the 60S ribosomal subunit and is required for its biogenesis.	KIAA0020	No	0.3
RAD24	Checkpoint protein; involved in the activation of the DNA damage and meiotic pachytene checkpoints; subunit of a clamp loader that loads Rad17p-Mec3p-Ddc1p onto DNA; homolog of human and <i>S. pombe</i> Rad17 protein.	RAD17	No	0.3
REI1	Cytoplasmic pre-60S factor; required for the correct recycling of shuttling factors Alb1, Arx1 and Tif6 at the end of the ribosomal large subunit biogenesis; involved in bud growth in the mitotic signaling network.	ZNF622	No	0.3
RPN10	Non-ATPase base subunit of the 19S regulatory particle (RP) of the 26S proteasome; N-terminus plays a role in maintaining the structural integrity of the RP; binds selectively to polyubiquitin chains; homolog of the mammalian S5a protein.	PSMD4	No	0.3
RRD1	Peptidyl-prolyl <i>cis/trans</i> -isomerase; activator of the phosphotyrosyl phosphatase activity of PP2A; involved in G1 phase progression, microtubule dynamics, bud morphogenesis and DNA repair; required for rapid	PPP2R4	No	0.3

	reduction of Sgs1p levels in response to rapamycin; subunit of the Tap42p-Sit4p-Rtd1p complex; protein increases in abundance and relative distribution to the nucleus increases upon DNA replication stress.			
VID30	Central component of GID Complex. involved in FBPAse degradation; interacts strongly with Gid8p to serve as a scaffold for other GID Complex subunits; contains SPRY domain and 3 domains that are also found in Gid8p - Lish, CTLH, and CRA; required for association of Vid vesicles and actin patches in vacuole import and degradation pathway. shifts the balance of nitrogen metabolism toward glutamate production; localizes to the nucleus and the cytoplasm.	SPRYD3	No	0.3
BAT1	Mitochondrial branched-chain amino acid (BCAA) aminotransferase, preferentially involved in BCAA biosynthesis; homolog of murine ECA39; highly expressed during logarithmic phase and repressed during stationary phase.	BCAT2	No	0.2
BMH1	14-3-3 protein, major isoform; controls proteome at post-transcriptional level, binds proteins and DNA, involved in regulation of many processes including exocytosis, vesicle transport, Ras/MAPK signaling, aggresome formation and rapamycin-sensitive signaling; protein increases in abundance and relative distribution to the nucleus increases upon DNA replication stress.	YWHAE	No	0.2
CMK2	Calmodulin-dependent protein kinase; may play a role in stress response, many CA ⁺⁺ /calmodulin dependent phosphorylation substrates demonstrated <i>in vitro</i> , amino acid sequence similar to Cmk1p and mammalian Cam Kinase II.	PSKH1	No	0.2
ERG1	Squalene epoxidase; catalyzes the epoxidation of squalene to 2,3-oxidosqualene; plays an essential role in the ergosterol-biosynthesis pathway and is the specific target of the antifungal drug terbinafine.	SQLE	No	0.2
FYV10	Subunit of GID complex; involved in proteasome-dependent catabolite inactivation of gluconeogenic enzymes FBPAse, PEPCK, and c-MDH; forms dimer with Rmd5p that is then recruited to GID Complex by Gid8p; contains a degenerate RING finger motif needed for GID complex ubiquitin ligase activity <i>in vivo</i> , as well as CTLH and CRA domains; plays role in anti-apoptosis; required for survival upon exposure to K1 killer toxin.	MAEA	No	0.2
GET3	Guanine nucleotide exchange factor for Gpa1p; amplifies G protein signaling; subunit of the GET complex, which is involved in Golgi to ER trafficking and insertion of proteins into the ER membrane; has low-level ATPase activity.	ASNA1	No	0.2
GTR1	Cytoplasmic GTPase; forms a heterodimer with Gtr2p to stimulate TORC1 in response to amino acids; component of GSE complex, which is required for sorting of Gap1p; involved in phosphate transport and telomeric silencing; similar to human RagA and RagB.	RRAGB	No	0.2
HAT1	Catalytic subunit of the Hat1p-Hat2p histone acetyltransferase complex that uses the cofactor acetyl coenzyme A, to acetylate free nuclear and cytoplasmic histone H4; involved in telomeric silencing and DNA double-strand break repair.	HAT1	No	0.2

HST2	Cytoplasmic member of the silencing information regulator 2 (Sir2) family of NAD(+)-dependent protein deacetylases; modulates nucleolar (rDNA) and telomeric silencing; possesses NAD(+)-dependent histone deacetylase activity <i>in vitro</i> .	SIRT2	No	0.2
HXT4	High-affinity glucose transporter of the major facilitator superfamily, expression is induced by low levels of glucose and repressed by high levels of glucose.	SLC2A6	No	0.2
MET18	Component of cytosolic iron-sulfur protein assembly (CIA) machinery; acts at a late step of Fe-S cluster assembly; forms the CIA targeting complex with Cia1p and Cia2p that directs Fe-S cluster incorporation into a subset of proteins involved in methionine biosynthesis, DNA replication and repair, transcription, and telomere maintenance; ortholog of human MMS19.	MMS19	No	0.2
PEP4	Vacuolar aspartyl protease (proteinase A), required for the posttranslational precursor maturation of vacuolar proteinases; important for protein turnover after oxidative damage; synthesized as a zymogen, self-activates.	CTSD	No	0.2
PEP8	Vacuolar protein component of the retromer; forms part of the multimeric membrane-associated retromer complex involved in vacuolar protein sorting along with Vps35p, Vps29p, Vps17p, and Vps5p; essential for endosome-to-Golgi retrograde protein transport; interacts with Ypt7p; protein abundance increases in response to DNA replication stress.	VPS26B	No	0.2
PHO23	Probable component of the Rpd3 histone deacetylase complex, involved in transcriptional regulation of PHO5; affects termination of snoRNAs and cryptic unstable transcripts (CUTs); C-terminus has similarity to human candidate tumor suppressor p33(ING1) and its isoform ING3.	ING4	No	0.2
RFC5	Subunit of heteropentameric Replication factor C (RF-C), which is a DNA binding protein and ATPase that acts as a clamp loader of the proliferating cell nuclear antigen (PCNA) processivity factor for DNA polymerases delta and epsilon.	RFC3	No	0.2
SIF2	WD40 repeat-containing subunit of the Set3C histone deacetylase complex, which represses early/middle sporulation genes; antagonizes telomeric silencing; binds specifically to the Sir4p N-terminus.	TBL1Y	No	0.2
UBP6	Ubiquitin-specific protease; situated in the base subcomplex of the 26S proteasome, releases free ubiquitin from branched polyubiquitin chains; negatively regulates degradation of ubiquitinated proteins by the proteasome; works in opposition to Hui5p polyubiquitin elongation activity; mutant has aneuploidy tolerance.	USP14	No	0.2
VPS74	Golgi phosphatidylinositol-4-kinase effector and PtdIns4P sensor; interacts with the cytosolic domains of <i>cis</i> and medial glycosyltransferases, and in the PtdIns4P-bound state mediates the targeting of these enzymes to the Golgi; interacts with the catalytic domain of Sac1p.	GOLPH3	No	0.2
YPT6	Rab family GTPase; Ras-like GTP binding protein involved in the secretory pathway, required for fusion of endosome-derived vesicles with the late Golgi, maturation of the vacuolar carboxypeptidase Y; has similarity to the human GTPase, Rab6.	RAB36	No	0.2

ACB1	Acyl-CoA-binding protein, transports newly synthesized acyl-CoA esters from fatty acid synthetase (Fas1p-Fas2p) to acyl-CoA-consuming processes; subject to starvation-induced, Grh1p-mediated unconventional secretion.	ACBD7	No	0.1
CDC21	Thymidylate synthase, required for <i>de novo</i> biosynthesis of pyrimidine deoxyribonucleotides; expression is induced at G1/S.	TYMS	No	0.1
DFR1	Dihydrofolate reductase, part of the dTTP biosynthetic pathway, involved in folate metabolism, possibly required for mitochondrial function.	DHFR	No	0.1
EIM5	Protein required for flavinylation of Sdh1p; binds to Sdh1p and promotes FAD cofactor attachment, which is necessary for succinate dehydrogenase (SDH) complex assembly and activity.	SDHAF2	No	0.1
FKH2	Forkhead family transcription factor; plays a major role in the expression of G2/M phase genes; positively regulates transcriptional elongation; negative role in chromatin silencing at HML and HMR; substrate of the Cdc28p/Clb5p kinase; FKH2 has a paralog, FKH1, that arose from the whole genome duplication.	FOXJ1	No	0.1
IMP3	Component of the SSU processome, which is required for pre-18S rRNA processing, essential protein that interacts with Mpp10p and mediates interactions of Imp4p and Mpp10p with U3 snoRNA.	IMP3	No	0.1
LEM3	Membrane protein of the plasma membrane and ER; interacts specifically <i>in vivo</i> with the phospholipid translocase (flippase) Dnf1p; involved in translocation of phospholipids and alkylphosphocholine drugs across the plasma membrane.	TMEM30A	No	0.1
LSM1	Lsm (Like Sm) protein; forms heteroheptameric complex (with Lsm2p, Lsm3p, Lsm4p, Lsm5p, Lsm6p, and Lsm7p) involved in degradation of cytoplasmic mRNAs; unlike most Sm-like proteins, Lsm1p requires both its SM-domain and C-terminal domain for RNA-binding; forms cytoplasmic foci upon DNA replication stress.	LSM1	No	0.1
MRT4	Protein involved in mRNA turnover and ribosome assembly, localizes to the nucleolus.	MRTO4	No	0.1
PHB2	Subunit of the prohibitin complex (Phb1p-Phb2p), a 1.2 MDa ring-shaped inner mitochondrial membrane chaperone that stabilizes newly synthesized proteins; determinant of replicative life span; involved in mitochondrial segregation.	PHB2	No	0.1
RPL16A	Ribosomal 60S subunit protein L16A; N-terminally acetylated, binds 5.8 S rRNA; transcriptionally regulated by Rap1p; homologous to mammalian ribosomal protein L13A and bacterial L13; RPL16A has a paralog, RPL16B, that arose from the whole genome duplication; protein abundance increases in response to DNA replication stress.	RPL13A	No	0.1
RPL37A	Ribosomal 60S subunit protein L37A; homologous to mammalian ribosomal protein L37, no bacterial homolog; RPL37A has a paralog, RPL37B, that arose from the whole genome duplication.	RPL37	No	0.1
RVS161	Amphiphysin-like lipid raft protein; interacts with Rvs167p and regulates polarization of the actin cytoskeleton, endocytosis, cell polarity, cell fusion and viability following starvation or osmotic stress.	BIN3	No	0.1

SHY1	Mitochondrial inner membrane protein required for assembly of cytochrome c oxidase (complex IV); associates with complex IV assembly intermediates and complex III/complex IV supercomplexes; similar to human SURF1 involved in Leigh Syndrome.	SURF1	No	0.1
SUB1	Transcriptional coactivator; facilitates elongation through factors that modify RNAP II; role in peroxide resistance involving Rad2p; role in nonhomologous end-joining (NHEJ); role in the hyperosmotic stress response through polymerase recruitment at RNAP II and RNAP III genes; protein abundance increases in response to DNA replication stress.	SUB1	No	0.1
TIP41	Protein that interacts with Tap42p, which regulates PP2A; component of the TOR (target of rapamycin) signaling pathway; protein abundance increases in response to DNA replication stress	TIPRL	No	0.1
UBC4	Ubiquitin-conjugating enzyme (E2); mediates degradation of abnormal or excess proteins, including calmodulin and histone H3; interacts with many SCF ubiquitin protein ligases; component of the cellular stress response; UBC4 has a paralog, UBC5, that arose from the whole genome duplication.	UBE2D4	No	0.1
UPS1	Phosphatidic acid transfer protein; plays a role in phospholipid metabolism by transporting phosphatidic acid from the outer to the inner mitochondrial membrane; localizes to the mitochondrial intermembrane space; null mutant has altered cardiolipin and phosphatidic acid levels; ortholog of human PRELI.	PRELID1	No	0.1

3.2.1. Small scale experiments validated the majority of the high-throughput data

In order to validate high-throughput data, 12 genes of interest highlighted in red in Table 3-1 were deleted in a *cdc13-1 rad9Δ* heterozygous diploid in the W303 genetic background (versus the S288C background used in the screens) (Addinall et al. 2011). *RAD9*, a checkpoint gene that responds to DNA damage, was used as a control for strong *cdc13-1* fitness defects suppression (Siede et al. 1993). *yfgΔ rad9Δ cdc13-1* heterozygous diploids were sporulated and tetrad dissection was carried out to obtain haploid cells with the relevant genotypes. Fitness of haploid cells was tested by spot test to detect genetic interactions between *yfgΔ*, *cdc13-1* and *rad9Δ* (Figure 3-1, Figure 3-2, Figure 3-3 and in sections 3.2.2 and 3.2.3). Additionally, some of the strains carrying a single deletion of the candidate genes were crossed to *yku70Δ* (and *yku80Δ*) cells (Figure 3-1 and Figure 3-4 in sections 3.2.2 and 3.2.4).

Table 3-2 summarises the effects that the deletion of the candidate genes had in low-throughput experiments versus high-throughput experiments. From the candidates deleted in the *cdc13-1* background, nine out of eleven, behaved as predicted by high-throughput data. Five, out of eight, genes deleted in the *yku70Δ* background behaved as predicted by high-throughput data. Importantly, many of the genetic interactions confirmed in low-throughput experiments appeared not to be as strong as suggested by the high-throughput screens (Table 3-2 and sections 3.2.2 and 3.2.4).

I conclude that the majority of the interactions described in Addinall et al. dataset could be confirmed by low-throughput experiments in W303. Nonetheless, the phenotypic changes representing those interactions were much milder in the low-throughput experiments here performed.

Table 3-2 Genetic interactions between the candidate genes and *cdc13-1* or *yku70Δ* in high-throughput versus low-throughput screens. High-throughput (HT) data was obtained from the Addinall et al. screen (Addinall et al. 2011), and low-throughput (LT) data was obtained from Figures 3-1 to 3-4 and Figure 3-6. Enhancers increase the fitness defects of *cdc13-1* or *yku70Δ*. Suppressors decrease the fitness defects of *cdc13-1* or *yku70Δ*. N.d., not determined.

Mutation	<i>cdc13-1</i>		<i>yku70Δ</i>	
	HT	LT	HT	LT
<i>dyn1Δ</i>	Enhancer	Enhancer	No effect	Enhancer (very weak)
<i>ufd2Δ</i>	Suppressor	Suppressor	Enhancer (very weak)	Enhancer (very weak)
<i>ski2Δ</i>	Suppressor	Suppressor	No effect	Enhancer
<i>inp52Δ</i>	Enhancer	No effect	Enhancer (very weak)	No effect
<i>cdc73Δ</i>	Enhancer	Suppressor	Enhancer (23°C)	Enhancer
<i>bas1Δ</i>	Suppressor	Suppressor (very weak)	No effect	No effect
<i>sla2Δ</i>	N.d.	No effect	N.d.	N.d.
<i>mon1Δ</i>	Suppressor	Suppressor (very weak)	No effect	N.d.
<i>doa1Δ</i>	Suppressor	Suppressor (very weak)	No effect	N.d.
<i>vps74Δ</i>	Suppressor (very weak)	Suppressor (very weak)	Enhancer	Enhancer
<i>fyv10Δ</i>	Suppressor	Suppressor (very weak)	No effect	No effect
<i>sub1Δ</i>	Suppressor	Suppressor (very weak)	Enhancer (very weak)	N.d.

3.2.2. Cdc73 and Vps74 have a strong role in telomere biology

From the gene list in Table 3-1, a telomere role of two very distinct genes was particularly exciting: *CDC73* and *VPS74*. First, human orthologues of both genes have been implicated in cancer onset, increasing the relevance of the study of these genes (Carpten et al. 2002; Ma et al. 2014; Zhang et al. 2014; Zhang et al. 2015). Additionally, the yeast *CDC73* was shown to regulate telomerase function (Mozdy et al. 2008), while the mammalian *VPS74* (*GOLPH3*) was shown to sense DNA damage (Farber-Katz et al. 2014).

In the Addinall et al. dataset, *CDC73* appears as an enhancer of *cdc13-1* fitness defects (Figure 3-1A) and due to its own fitness defects at 36°C an interaction with *YKU70* could not be measured in the screens (Figure 3-1A, B) (Addinall et al. 2011). *vps74Δ* weakly suppresses *cdc13-1* fitness defects (Figure 3-1A) and enhances *yku70Δ* fitness defects (Figure 3-1B) in high-throughput studies. Surprisingly and opposite to that observed in high-throughput studies, *cdc73Δ cdc13-1* cells grew better than *cdc13-1* at 27°C and 28°C (Figure 3-1A, C). Interestingly, *cdc73Δ rad9Δ cdc13-1* cells grow worse than *cdc73Δ cdc13-1* and *rad9Δ cdc13-1* at any

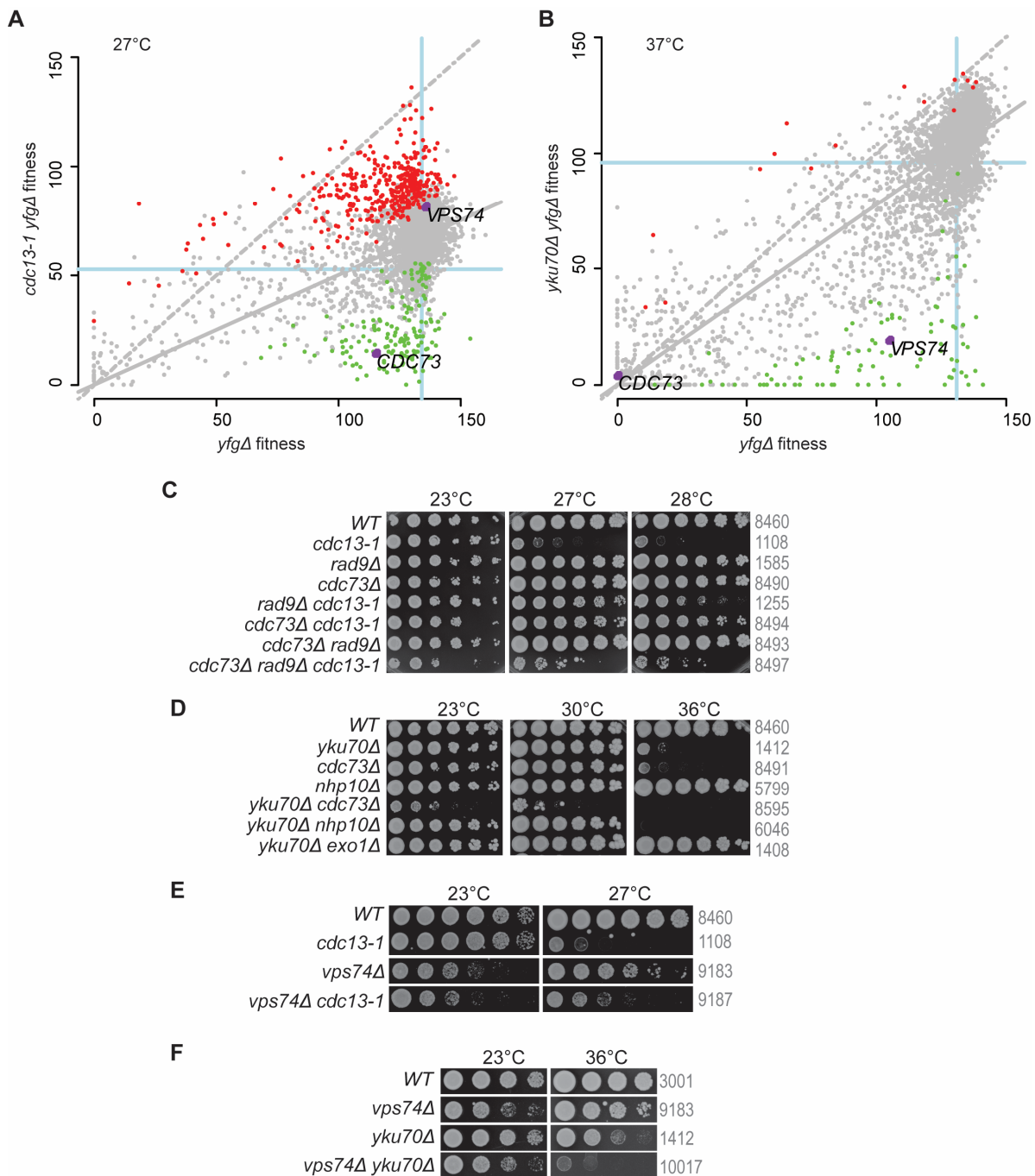


Figure 3-1 *cdc73Δ* and *vps74Δ* suppress *cdc13-1* and enhance *yku70Δ* fitness defects. **A and B**) The yeast genome knock out collection (~4200 strains) was crossed with *cdc13-1* (A), *yku70Δ* (B) or *ura3Δ* (A and B). Double mutants were then grown on solid agar plates and the fitness was measured at 27°C (A) or 37°C (B) (Addinall et al. 2011). Each dot indicates the effect of a gene deletion (*yfgΔ*) on the fitness of *cdc13-1* (A), *yku70Δ* (B) or *ura3Δ*. Represented by grey dots are all the deletions that did not significantly alter the fitness of *cdc13-1* (A) or *yku70Δ* (B). Green dots represent gene deletions that are enhancers of the *cdc13-1* (A) or *yku70Δ* (B), red dots are suppressors and the purple dots represent the fitness of *CDC73* and *VPS74* deletions. **C-F**) Saturated cultures of the genotypes indicated were serially diluted across YEPD agar plates and grown for 3 days at the temperatures indicated. One single rectangular plate was used for each temperature but have been cut and pasted to allow better comparisons.

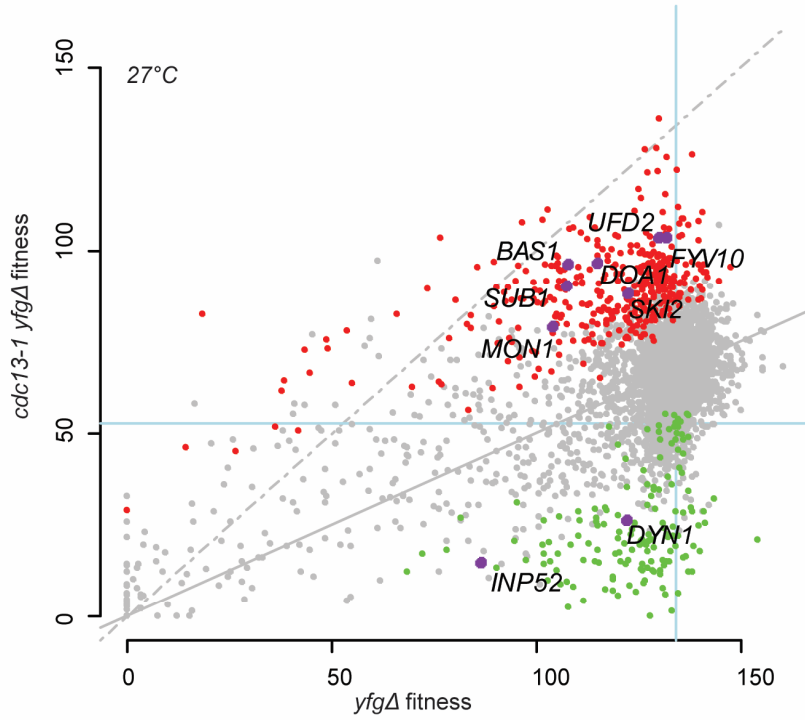
temperature tested. This suggests that Rad9 increases the fitness of *cdc73Δ cdc13-1* cells, which is the opposite to the described checkpoint role of Rad9 in *cdc13-1* cells. *cdc73Δ* cells have no fitness defects at these temperatures. As expected, *cdc73Δ yku70Δ* grow very poorly, even at 23°C, showing *cdc73Δ* as an enhancer of *yku70Δ* fitness defects (Figure 3-1D). Also, as previously reported *cdc73Δ* is temperature sensitive at 36°C (Betz et al. 2002). These data suggests that Cdc73 has an important role in telomere biology and this role will be studied in more detail in Chapters 5 and 6.

Figure 3-1E shows that *vps74Δ* is, as suggested by high-throughput data, a weak suppressor of *cdc13-1* fitness defects at 27°C (Addinall et al. 2011). Deletion of *VPS74* also causes fitness defects observable at both 23°C and 27°C. It was also confirmed that *vps74Δ* strongly enhances *yku70Δ* fitness defects at 36°C (Figure 3-1F). The high-throughput data was confirmed and the role of Vps74 in telomere biology will be addressed in Chapter 4 (Addinall et al. 2011).

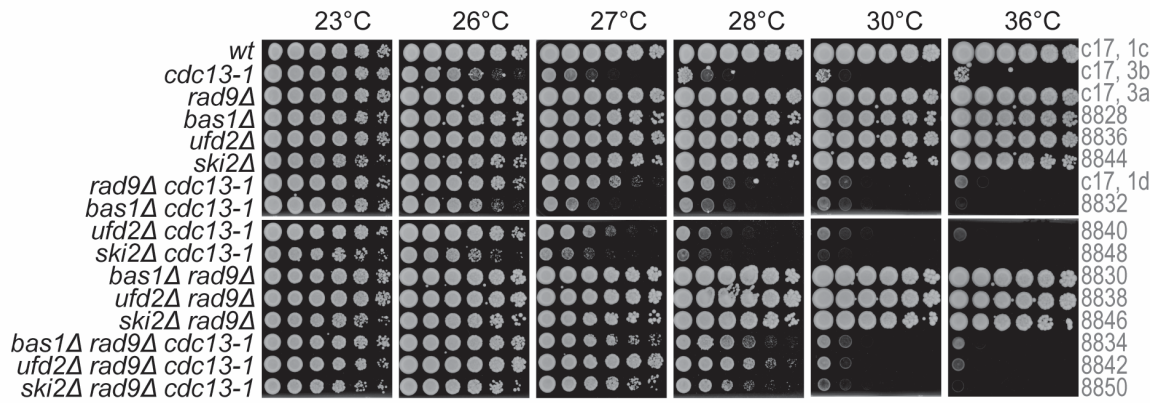
3.2.3. *DYN1* and *UFD2*, but not *BAS1*, *DOA1*, *FYV10*, *SKI2*, *MON1*, *SUB1* or *INP52*, strongly interact with *CDC13*

According to the high-throughput data, deletion of *UFD2*, *BAS1*, *DOA1*, *FYV10*, *SKI2*, *MON1* or *SUB1* suppresses *cdc13-1* fitness defects while *DYN1* and *INP52* deletions enhance *cdc13-1* fitness defects (Figure 3-2A) (Addinall et al. 2011). However, spot test assays in a different genetic background only confirmed *UFD2* and *DYN1* to (strongly) genetically interact with *CDC13* (Figure 3-2 and Figure 3-3). Figure 3-2B shows that *ufd2Δ* strongly suppresses *cdc13-1* fitness defects at 26°C, while *ski2Δ*, *bas1Δ* and *fyv10Δ* have a very mild suppressing effect. *inp52Δ* does not affect *cdc13-1* cell growth at any temperature while *dyn1Δ* was confirmed to enhance *cdc13-1* fitness defects at 26°C and 27°C. Interestingly, at 27°C and 28°C, *ufd2Δ* improves the fitness of *rad9Δ cdc13-1* cells, suggesting that Ufd2 might play a small role in the DNA damage response to telomere uncapping when Rad9 is missing. Deletion of *DYN1* enhances *cdc13-1* fitness defects at 26°C and 27°C, as suggested by the high-throughput data (Figure 3-2A). Single deletions of *BAS1*, *UFD2*, *SKI2*, *DYN1*, *INP52* or *FYV10* do not cause any visible fitness defect or temperature sensitivity.

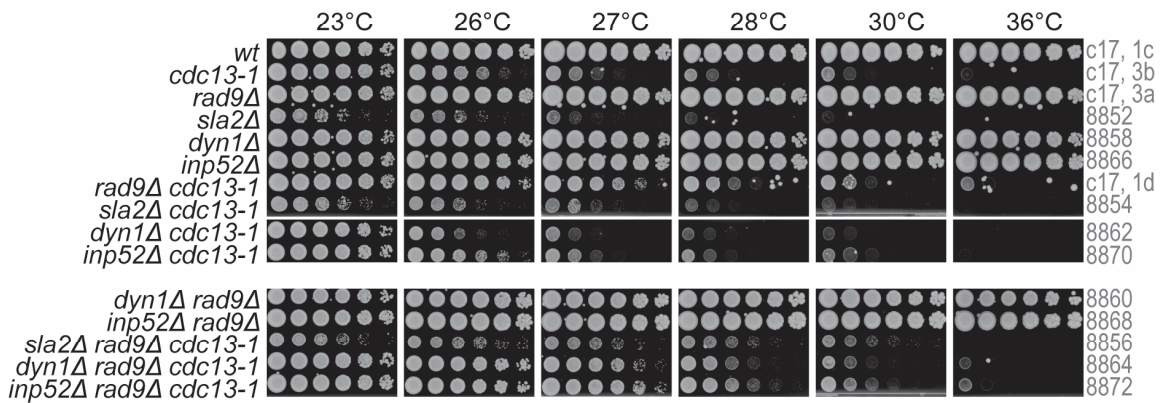
A



B



C



D

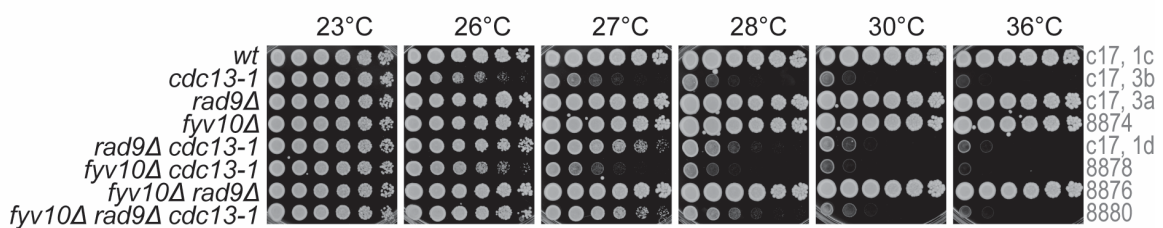


Figure 3-2 *ufd2Δ*, *bas1Δ*, *doa1Δ*, *fyv10Δ*, *ski2Δ*, *mon1Δ*, *sub1Δ* and *dyn1Δ* genetically interact with *cdc13-1*, while *inp52Δ* does not. **A)** Purple dots represent the fitness of *UFD2*, *BAS1*, *DOA1*, *FYV10*, *SKI2*, *MON1*, *SUB1*, *DYN1* and *INP52* deletions. High-throughput data was obtained as described in Figure 3-2A. **B-D)** Saturated cultures of the genotypes indicated were serially diluted across YEPD agar plates and grown for 3 days at the temperatures indicated. 3 independent spot tests are represented. One single rectangular plate was used for each temperature (images were cut and pasted for clarity). For each genotype 2 or 3 strains were tested by independent spot test assays and one representative strain is shown. When the strain number is not shown, the number of the spore and the cross is shown. These strains were not frozen, but the phenotype is representative of the genotype.

An unpublished screen by David Lydall's laboratory suggested that *SLA2* overexpression (under a GAL promoter) suppressed *cdc13-1* fitness defects. However, there was no data for this gene in the *cdc13-1* or *yku70Δ* deletion screens (Addinall et al. 2011). Deletion of *SLA2* did not affect the fitness of *cdc13-1* strains: *sla2Δ cdc13-1* cells are as sick as *sla2Δ* cells, therefore no genetic interaction is observed (Figure 3-2C). The poor growth of *sla2Δ* cells at any temperature is likely related to the role of Sla2 in cytoskeleton assembly (Holtzman et al. 1993).

Figure 3-3 shows that deletions of *MON1*, *SUB1* and *DOA1* just very weakly suppressed *cdc13-1* fitness defects at 26°C, with no effect at 27°C. *mon1Δ* also slightly suppresses *rad9Δ cdc13-1* fitness defects. Interestingly, *sub1Δ rad9Δ cdc13-1* cells barely grow at 20°C but are able to grow at 23°C. This fitness defect only happens when all the 3 genes are affected simultaneously and suggest that somehow *MON1*, *RAD9* and *CDC13* work in parallel to maintain the capacity of yeast to divide at low temperatures.

3.2.4. *SKI2*, but not *BAS1*, *FYV10*, *DYN1*, *UFD2* or *INP52*, strongly interacts with *YKU70*

The yKu complex is composed of Yku70 and Yku80 and forms a ring-like structure that binds to double stranded DNA close to telomere ends (Walker et al. 2001). Although a major function of the yKu complex is at telomeres, maintaining telomere stability and length, the complex is also known to re-localise to double-stranded break sites to promote repair through NHEJ (Bertuch and Lundblad 2003). To better understand the role of the selected genes (Table 3-1) in telomere protection, *bas1Δ*, *fyv10Δ*, *dyn1Δ*, *ski2Δ*, *ufd2Δ* and *inp52Δ* strains were crossed with a *yku70Δ* strain. The Addinall et al. screen showed *inp52Δ* and *ufd2Δ* as weak enhancers of *yku70Δ* fitness defects while *bas1Δ*, *fyv10Δ*, *dyn1Δ* and *ski2Δ* showed no effect on *yku70Δ* fitness (Figure 3-4A) (Addinall et al. 2011). The spot test assay in Figure 3-4B-D confirms that *BAS1*, *FYV10* and *DYN1* do not interact with *YKU70* while deletion of *UFD2* slightly enhances *yku70Δ* fitness defects at 36°C. Also, opposite to that expected for *inp52Δ*, it did not affect *yku70Δ* cell fitness at 36°C (Figure 3-4C).

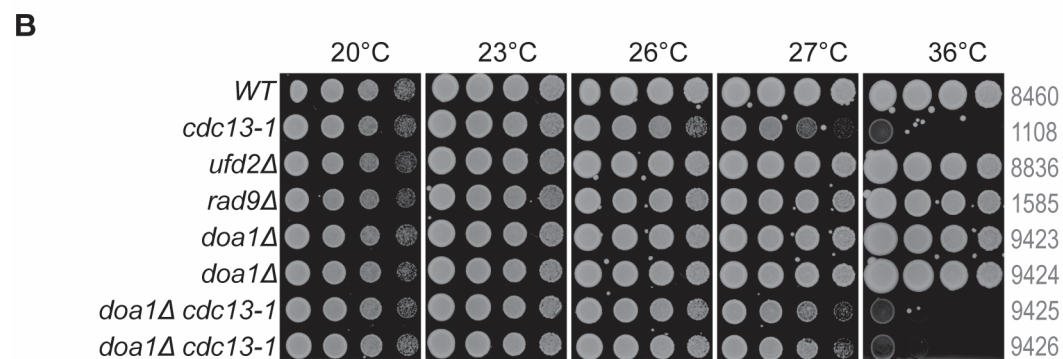
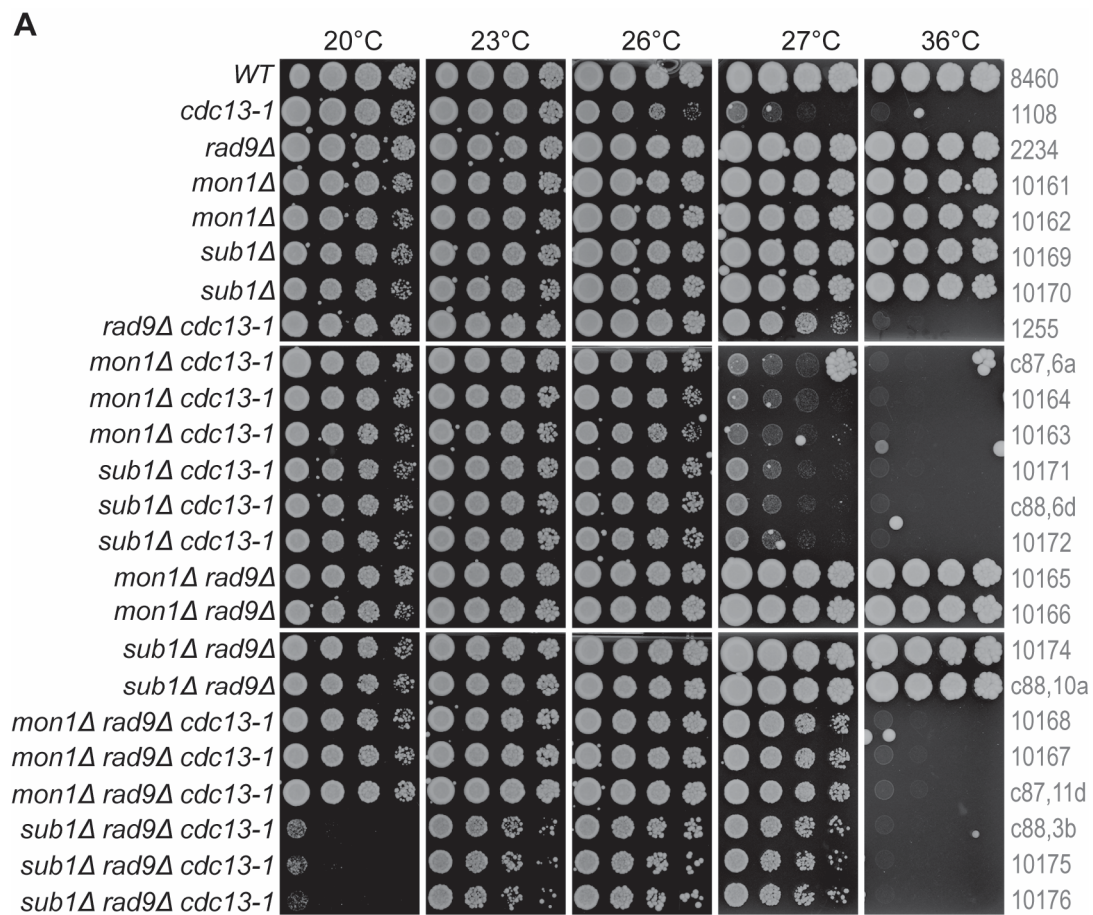


Figure 3-3 *MON1*, *SUB1* and *DOA1* deletions do not significantly affect fitness of *cdc13-1* cells. **A and B)** Saturated cultures of the genotypes indicated were serially diluted across YEPD agar plates and grown for 3 days at the temperatures indicated. One single rectangular plate was used for each temperature. Images were cut and pasted for clarity. When the strain number is not shown, the number of the spore and the cross is shown. These strains were not frozen, but the phenotype is representative of the genotype.

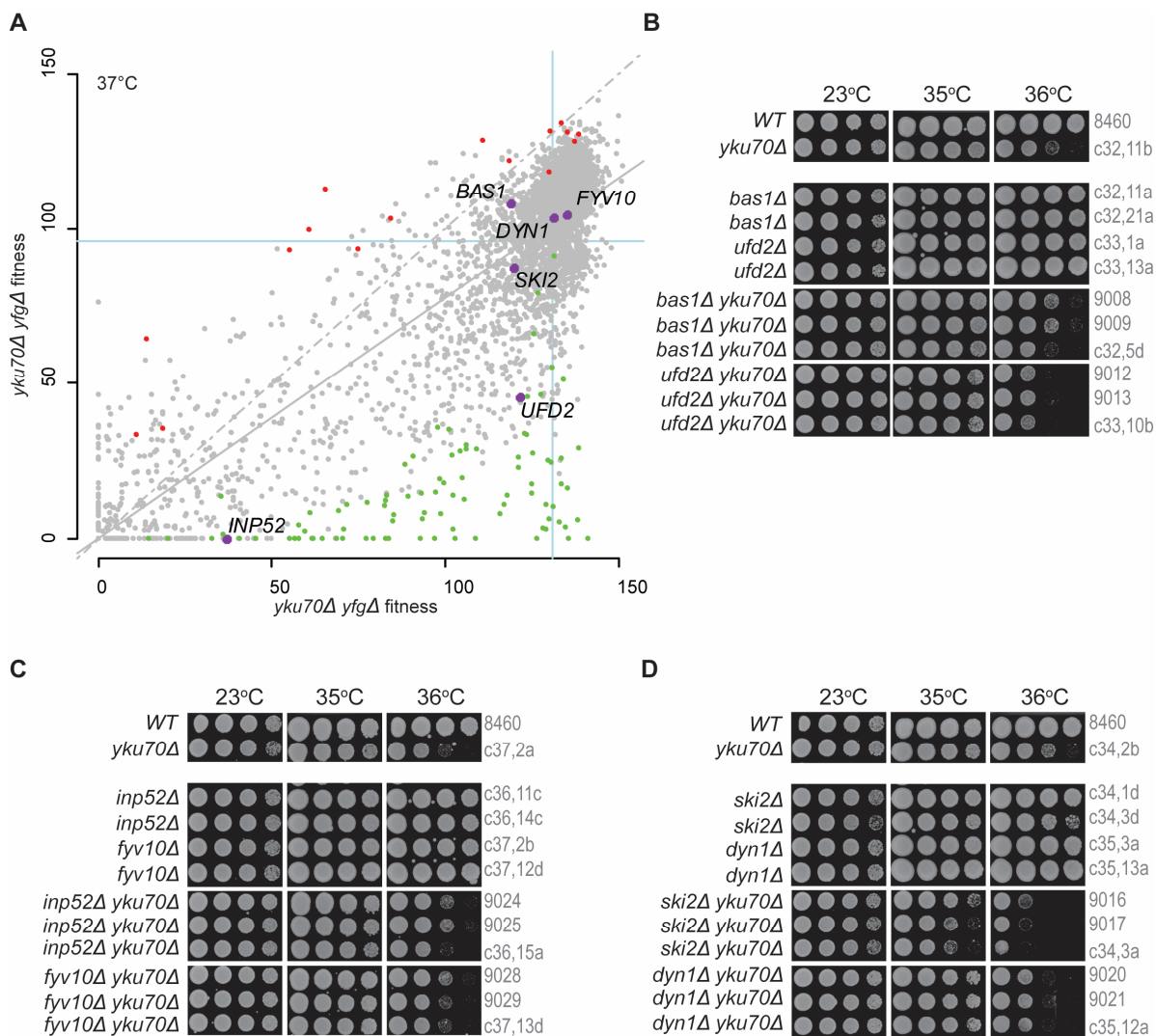


Figure 3-4 *ski2Δ* enhances *yku70Δ* fitness defects. **A)** The yeast genome knock out collection (~4200 strains) was crossed with *yku70Δ* or *ura3Δ*. Double mutants were then grown on solid agar plates and the fitness was measured at 37°C (Addinall et al. 2011). Each dot indicates the effect of a gene deletion (*yfgΔ*) on the fitness of *yku70Δ* or *ura3Δ*. Represented by grey dots are all the deletions that did not significantly alter the fitness of *yku70Δ*. Green dots represent gene deletions that are enhancers of the *yku70Δ*, red dots are suppressors and the purple dots represent the fitness of *UFD2*, *BAS1*, *FYV10*, *SKI2*, *DYN1* and *INP52* deletions. **B-D)** Saturated cultures of the genotypes indicated were serially diluted across YEPD agar plates and grown for 3 days at the temperatures indicated. One single rectangular plate was used for each temperature. When the strain number is not shown, the number of the spore and the cross is shown. These strains were not frozen, but the phenotype is representative of the genotype.

Different from what was suggested by high-throughput screens (Figure 3-4A), *ski2Δ* enhanced *yku70Δ* fitness defects at 35°C and 36°C (Figure 3-4D). Furthermore, the fitness of different *ski2Δ yku70Δ* strains showed some variability. This variability will be addressed in section 3.2.10.

I conclude that, although the majority of the gene deletions confirmed the high-throughput data (Table 3-2), the interactions are milder in W303 low-throughput experiments. This difference between high and low-throughput might be related to the fact that in high-throughput experiments colony growth is followed (photographed) very early after inoculation, making it easier to catch growth differences. In low-throughput experiments usually only one time-point is captured. Nevertheless, *SKI2* seems to clearly affect the fitness of telomere defective cells and a more careful study of this gene will be presented next.

3.2.5. Ski2 represses telomeric ssDNA formation in *cdc13-1* cells

The *cdc13-1* allele causes telomere uncapping at non-permissive temperatures (higher than 26°C) (Garvik et al. 1995). Uncapped telomeres are resected by nucleases such as Exo1. *EXO1* deletion improves the growth of *cdc13-1* cells at non-permissive temperatures by decreasing telomere resection (Zubko et al. 2004). To test if the deletion of *BAS1*, *SKI2*, *UFD2* and *VPS74* suppressed *cdc13-1* fitness defects by decreasing the levels of telomeric ssDNA in *cdc13-1* cells, single-stranded telomeric DNA was analysed by In-gel assay (a cartoon to aid the interpretation of a telomeric In-gel assay can be found in Appendix D).

Figure 3-5 shows that *cdc13-1* cells have, as expected, high levels of single-stranded DNA in TG repeats (arrows). Also, as previously reported, *yku70Δ* cells have short telomeres and high levels of telomeric ssDNA (last lane, bottom band) (Maringele and Lydall 2002). *bas1Δ*, *ski2Δ* and *ufd2Δ* single deletion do not cause any increase in telomeric ssDNA, while *vps74Δ* seems to cause an increase on telomeric ssDNA. From the analysis of double mutants, only *ski2Δ cdc13-1* have a decrease in telomeric ssDNA (with same length of that observed in *cdc13-1* cells). These data suggest that Ski2 facilitates telomere resection in *cdc13-1* cells.

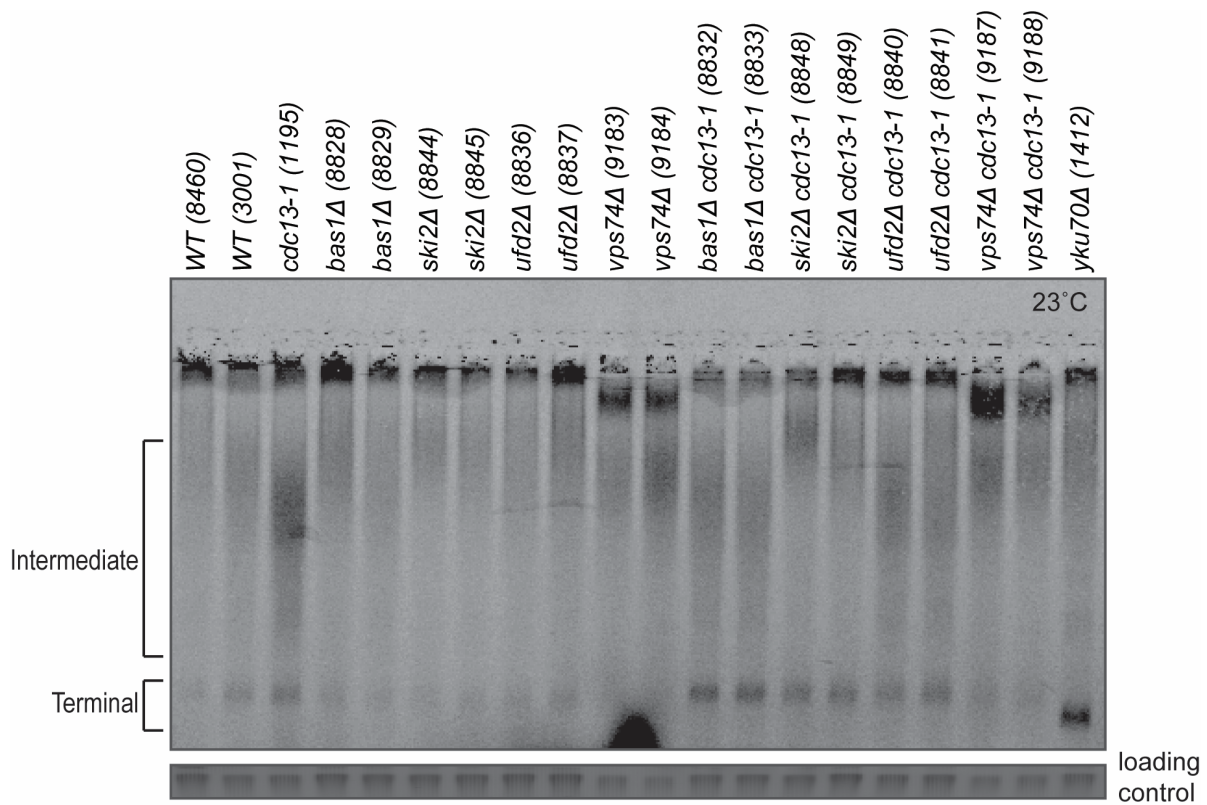


Figure 3-5 Ski2 helps telomere resection in *cdc13-1* cells. Cell cultures of the indicated genotypes were grown to saturation at 23°C. DNA was extracted and ssDNA in the TG repeats was measured by In-gel assay (Appendix D). The arrow indicates the signal corresponding to the telomeric ssDNA that is found to be increased in *cdc13-1* cells at 23°C. SYBR Safe staining was used as loading control.

3.2.6. The Ski complex suppress *cdc13-1* fitness defects

SKI2 deletion caused a strong enhancement of *yku70Δ* fitness defects (Figure 3-4D) and *ski2Δ* weakly suppressed of *cdc13-1* fitness defects (Figure 3-2). In both cases, strains with the same genotype showed slightly variable growth phenotypes. To understand the true effect of *ski2Δ* deletion on *cdc13-1* fitness defects, the fitness of 4 different *ski2Δ cdc13-1* strains was assessed by spot test.

Figure 3-6 shows that 3, out of 4, *ski2Δ cdc13-1* strains grow noticeable better than the *cdc13-1* strain (DLY1108) at both 26°C and 27°C. I conclude that overall Ski2 decreases the fitness of telomere uncapped cells.

Ski2, part of the Ski complex together with Ski3 and Ski8, is involved in 3'-5' RNA degradation (Brown et al. 2000; Araki et al. 2001). Together with Ski7 and the exosome, the Ski complex is responsible for the degradation of normal and dysfunctional RNAs in the cytoplasm (Anderson and Parker 1998; van Hoof et al. 2002; Mitchell and Tollervy 2003). A role in the degradation of viral dsRNAs is also well characterized and gave the name to the complex: Superkiller complex (Toh et al. 1978). To validate the role of the Ski complex at telomeres, *SKI8* was deleted in telomere defective cells (carrying the *cdc13-1* mutation) (Figure 3-7). *SKI7*, responsible for the link of the Ski complex to the exosome was also deleted to understand if the lack of interaction of the Ski complex to the exosome is responsible for the better fitness of *ski2Δ cdc13-1* when compared to *cdc13-1* cells (Figure 3-6).

Figure 3-7A shows that *ski8Δ* weakly suppresses *cdc13-1* fitness defects at 27°C. It is interesting to note that *ski2Δ* is a slightly stronger suppressor of *cdc13-1* fitness defects than *ski8Δ* (27°C, third dilution), even though Ski2 and Ski8 are part of the same complex. This difference suggests that Ski2 and Ski8 must play slightly different roles in the context of telomere biology (they have, perhaps, distinct interaction partners). This division of labour is not new, since Ski8 was found to play a distinct role in double-strand break formation during meiotic recombination, where it localises to the nucleus and promotes DSB by interacting with Spo11 (Arora et al. 2004). *ski2Δ ski8Δ cdc13-1* triple mutant cells have a variable phenotype, making it difficult to tell whether they grow better or worse than *cdc13-1* cells. Figure 3-7B shows that *ski7Δ* behaves very similarly to *ski8Δ* in a *cdc13-1* or *ski2Δ cdc13-1* background. Again, I observe high variability between strains with the same genotype.

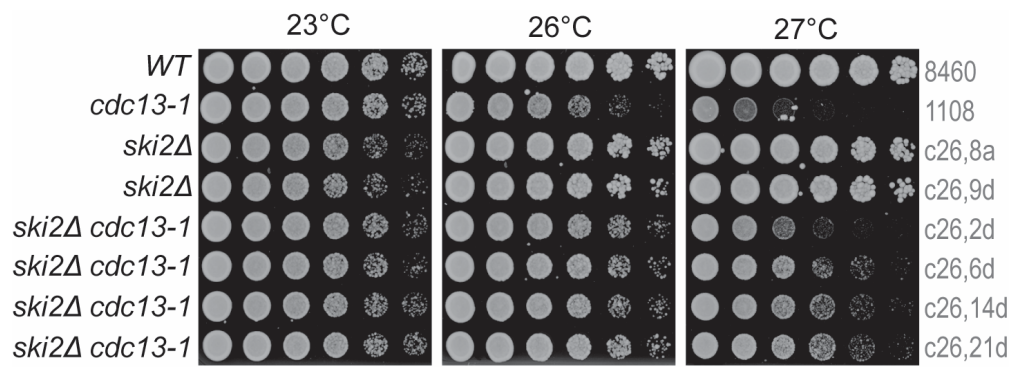


Figure 3-6 *ski2Δ* suppresses *cdc13-1*. Saturated cultures of the genotypes indicated were serially diluted across YEPD agar plates and grown for 3 days at the temperatures indicated. One single rectangular plate was used for each temperature. When the strain number is not shown, the number of the spore and the cross is shown. These strains were not frozen, but the phenotype is representative of the genotype.

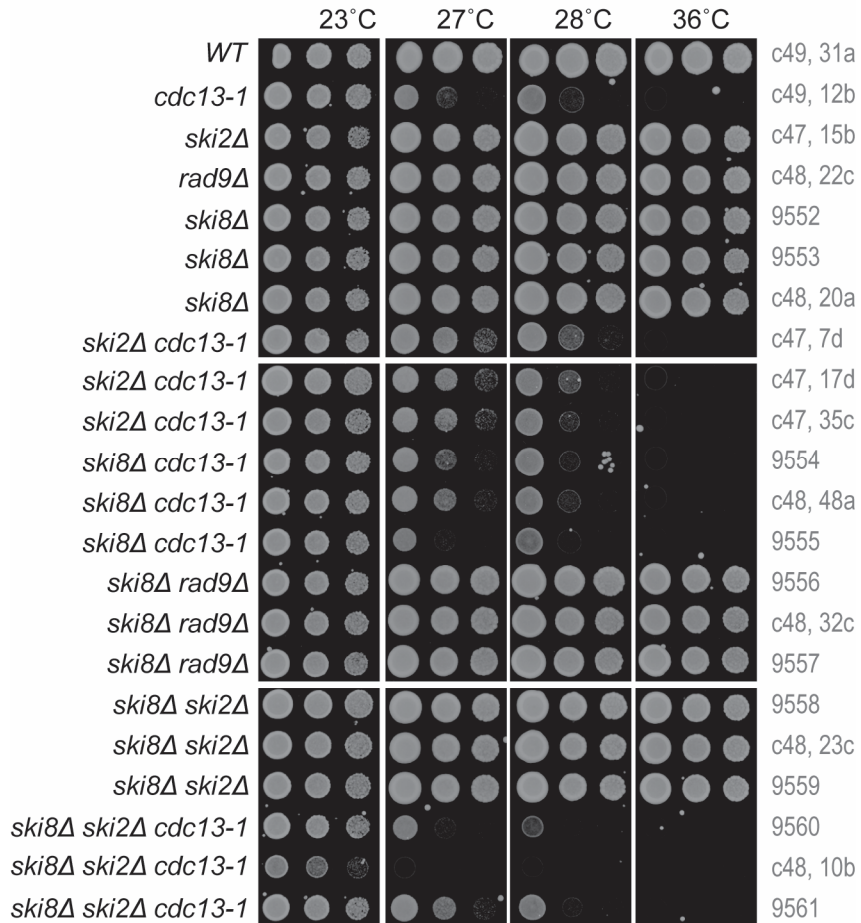
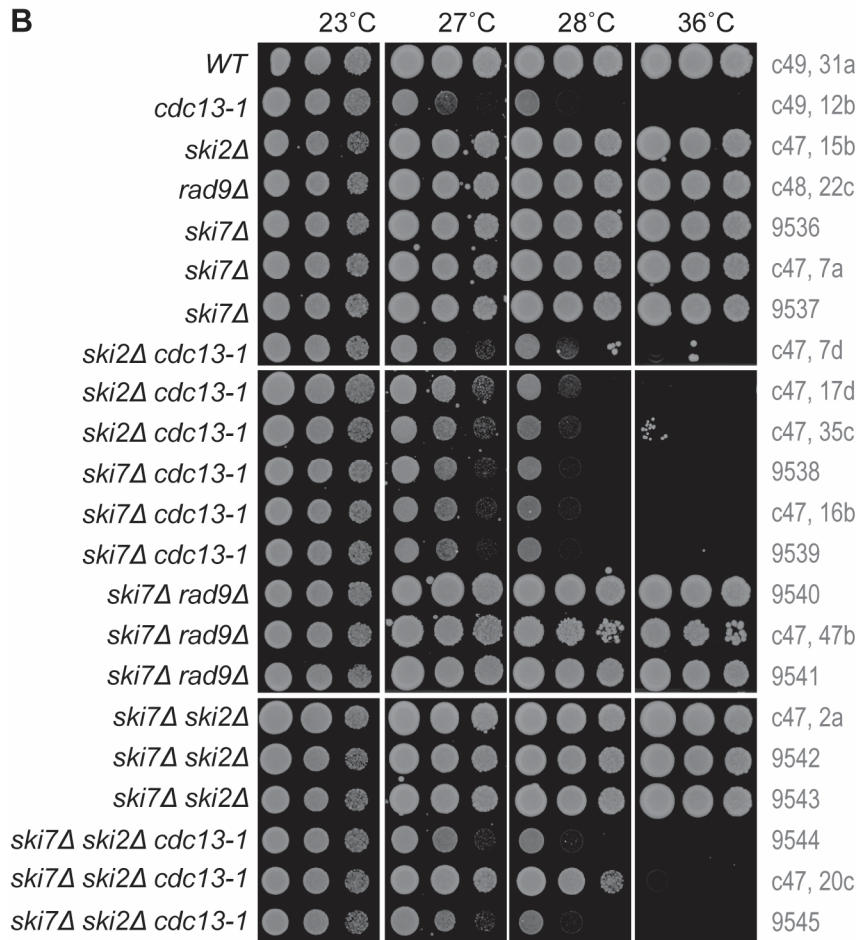
A**B**

Figure 3-7 *ski7* Δ and *ski8* Δ are weaker *cdc13-1* suppressors than *ski2* Δ . A and B) Saturated cultures of the genotypes indicated were serially diluted across YEPD agar plates and grown for 3 days at the temperatures indicated. One single rectangular plate was used for each temperature. When the strain number is not shown, the number of the spore and the cross is shown. These strains were not frozen, but the phenotype is representative of the genotype.

I conclude that *ski2Δ* is a stronger suppressor of *cdc13-1* fitness defects than *ski7Δ* or *ski8Δ*. This suggests that Ski2 plays a role at telomeres independent of the exosome RNA degradation functions.

3.2.7. Ski2 does not affect CST mRNA levels

The cytoplasmic Ski complex is involved in mRNA decay (Anderson and Parker 1998; van Hoof et al. 2002; Mitchell and Tollervey 2003). A role for another RNA decay pathway in telomere biology was previously shown for the NMD (Nonsense-mediated mRNA Decay) complex (Holstein et al. 2014). It was shown that the deletion of members of the NMD complex strongly suppresses *cdc13-1* fitness defects (Holstein et al. 2014). *NMD2* deletion (a member of NMD complex) leads to the increase of *STN1* mRNA by around 8-fold and *TEN1* mRNA by 3-fold, which might compensate for the less functional Cdc13-1 (Holstein et al. 2014). To test whether Ski2 has a similar role to Nmd2, reducing the levels of Ten1 and Stn1, *CDC13*, *TEN1* and *STN1* mRNA levels were measured in *ski2Δ* cells.

It is shown in Figure 3-8 that deletion of *SKI2* does not strongly affect the CST mRNA levels. As expected, *nmd2Δ* leads to high levels of both *TEN1* and *STN1* mRNA, while *CDC13* mRNA is unaffected (Holstein et al. 2014). Therefore, unlike the NMD complex, the Ski complex does not directly affect the levels of CST complex components.

3.2.8. *ski2Δ exo1Δ rad24Δ cdc13-1* cells are viable at non-permissive temperatures

It was previously shown that if *EXO1* and *RAD24* (both affecting the DNA damage response) were deleted with *NMD2*, *cdc13-1* cells could grow at 36°C (Holstein et al. 2014). Even more strikingly, simultaneous deletion of *EXO1*, *RAD24* and *NMD2* allows the deletion of *CDC13* (Holstein et al. 2014). To understand if the Ski complex inhibits the growth of *cdc13-1* cells similarly to the NMD complex, I assessed the growth of *ski2Δ rad24Δ exo1Δ cdc13-1* cells (Figure 3-9). To obtain these, *ski2Δ* was crossed to *rad24Δ exo1Δ cdc13-1*, the diploid was sporulated, and the haploid progeny tested by spot test. Figure 3-9A shows that *ski2Δ rad24Δ exo1Δ cdc13-1* cells are able to normally grow at 36°C, and are much fitter than *rad24Δ exo1Δ cdc13-1* cells, which do not grow at 36°C. *ski2Δ exo1Δ cdc13-1* strains were also

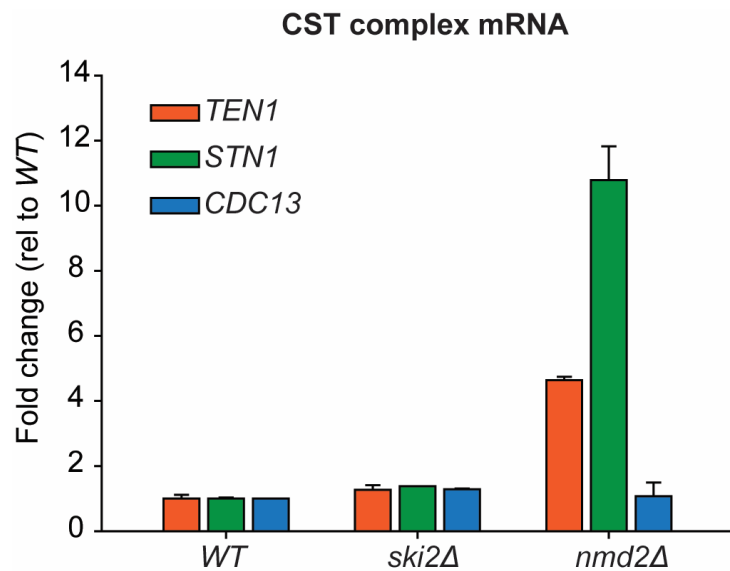
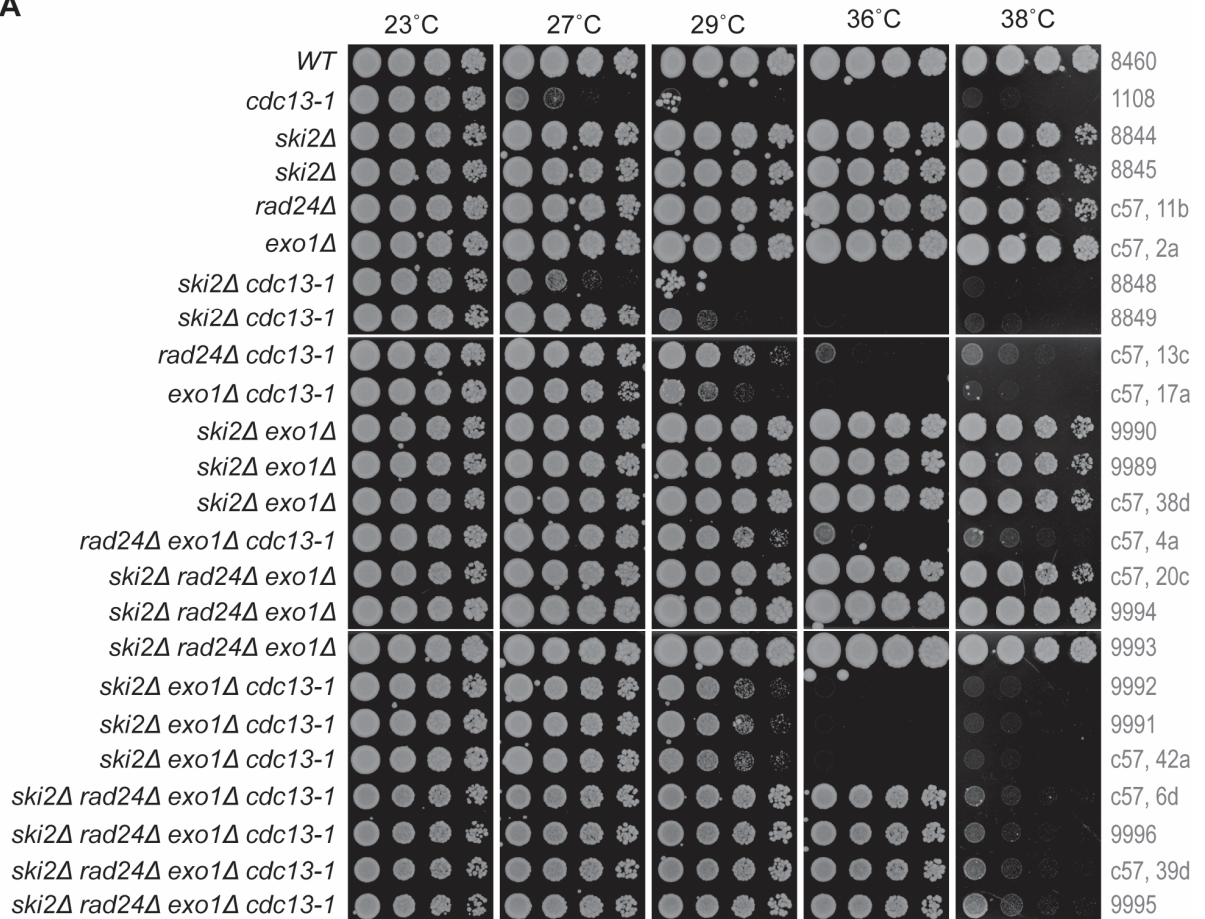


Figure 3-8 Ski2 does not affect mRNA levels of CST complex components. RT-qPCR analysis of *TEN1*, *STN1* and *CDC13* RNA expression levels in the strains indicated. Two independent strains of each genotype were analysed and each value was normalized to *BUD6* mRNA. The mean of the wild-types (*WT*) was set to 1. The other genotypes were expressed relative to the *WT*. *WT* strain numbers were 3001 and 8460; *ski2Δ* were 8844 and 8845; and *nmd2Δ* were 4528 and 4765. Error bars indicate the value of each individual strain.

A



B

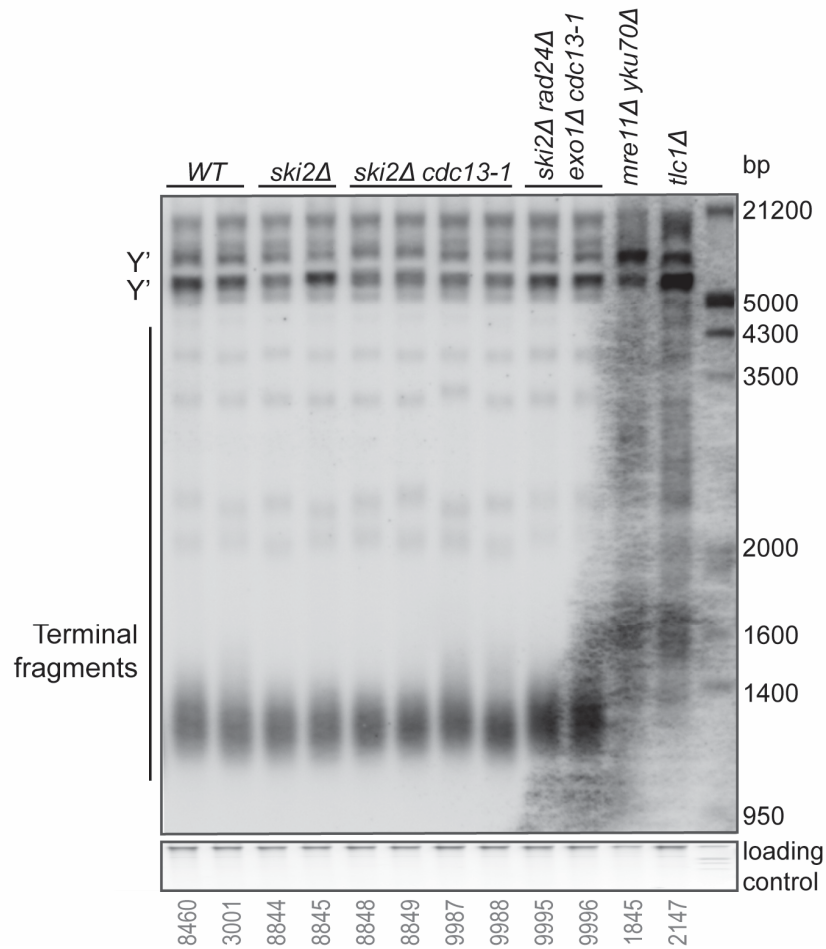


Figure 3-9 Evidence that *ski2Δ* strongly suppresses *rad24Δ* *exo1Δ* *cdc13-1* fitness defects. A) Saturated cultures of the genotypes indicated were serially diluted across YEPD agar plates and grown for 3 days at the temperatures indicated. One single rectangular plate was used for each temperature. When the strain number is not shown, the number of the spore and the cross is shown. These strains were not frozen, but the phenotype is representative of the genotype. **B)** Telomeric Southern blot was performed using a probe against the Y'+TG fragments. SYBR Safe staining was used as loading control.

fitter than *exo1Δ cdc13-1* (29°C). Intriguingly, no *ski2Δ rad24Δ cdc13-1* strains were obtained from this *ski2Δ rad24Δ exo1Δ cdc13-1* heterozygous diploid (for 56 tetrads dissected and 149 viable spores analysed).

At low rates, yeast telomere defective cells can escape senescence and generate “survivors” using recombination dependent mechanisms to rearrange their telomeres (Lundblad and Blackburn 1993). Since *ski2Δ rad24Δ exo1Δ cdc13-1* strains showed elevated fitness, I hypothesised that these strains had rearranged their telomeres to become survivors. To test this hypothesis I analysed the telomere length (and structure) of *ski2Δ rad24Δ exo1Δ cdc13-1* cells by Southern Blot using a probe to the Y' and TG repeats (Figure 3-9B). It was surprising to note that the *ski2Δ rad24Δ exo1Δ cdc13-1* cells that are able to grow at the non-permissive temperature of 36°C have telomere length similar to those of the wild-type cells. *ski2Δ* and *ski2Δ cdc13-1* also have normal telomere structure. These results suggested that Ski2, like NMD proteins, inhibits the growth of *cdc13-1* cells by a DDR-independent pathway.

The capacity of *ski2Δ rad24Δ exo1Δ cdc13-1* cells to growth at 36°C is a very strong and exciting result even more when those cells have normal telomere structure (Figure 3-9). *ski2Δ cdc13-1* cells showed some phenotypic variability (Figure 3-6), suggesting that those cells might be subject to genetic instability. It was therefore tested whether *ski2Δ rad24Δ exo1Δ cdc13-1* had acquired the wild-type *CDC13*. The distinction between *cdc13-1* and *CDC13* can be easily made by PCR followed by the use of an RFLP (Figure 3-10) (Zubko and Lydall 2006). Interestingly the *ski2Δ rad24Δ exo1Δ cdc13-1* strains tested had both *cdc13-1* and *CDC13* alleles. The presence of both *CDC13* and *cdc13-1* alleles might be because the cells are diploid or aneuploid. The possibility of those *ski2Δ rad24Δ exo1Δ cdc13-1* cells to be diploids is unlikely: 1) cells cannot grow at 38°C as it would be expected for diploid cells; 2) cells do not sporulate; 3) cells have respiration defects, unlike, their diploid parent (see next Section); 4) 2 out of the 4 *ski2Δ rad24Δ exo1Δ cdc13-1* strains were from a tetrad where all spores were viable and a 2:2 genetic segregation was observed to all genes scored. On the other hand, *ski2Δ rad24Δ exo1Δ cdc13-1* cells did not mate (two of the four strains were “crossed” to many haploid strains, and a diploid carrying markers from both parents was never obtained). I conclude that *ski2Δ rad24Δ exo1Δ cdc13-1* cells can grow at 36°C because they have the wild-type *CDC13*.

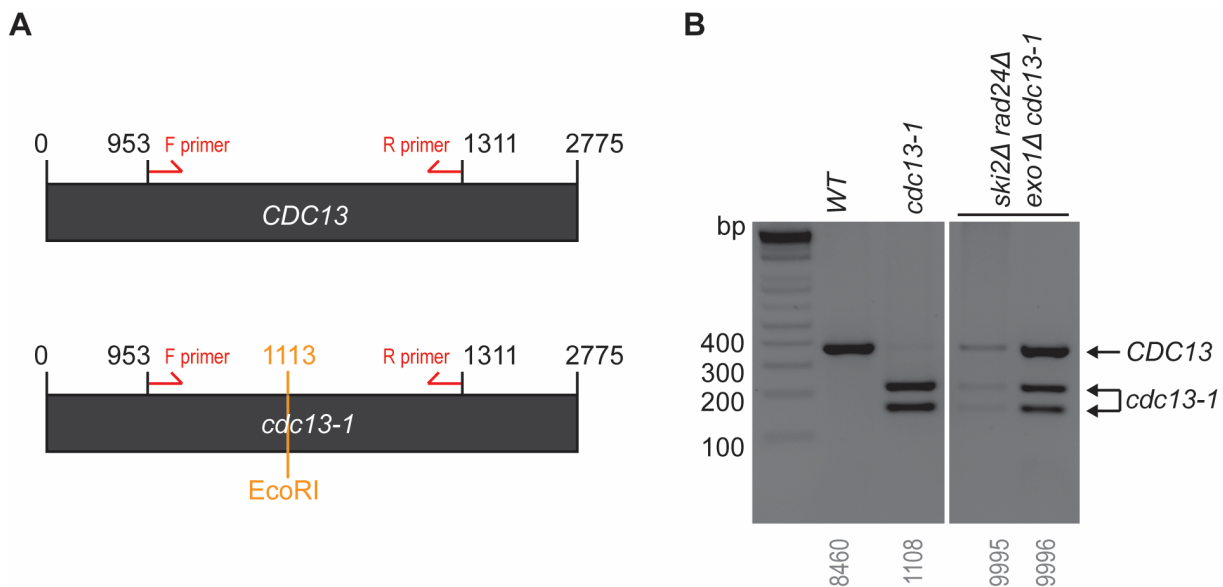
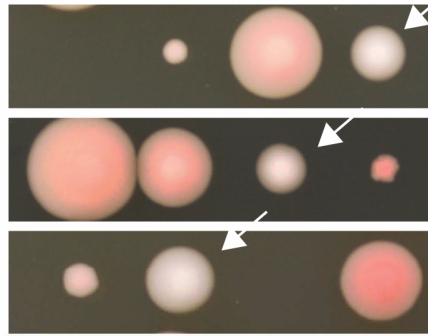
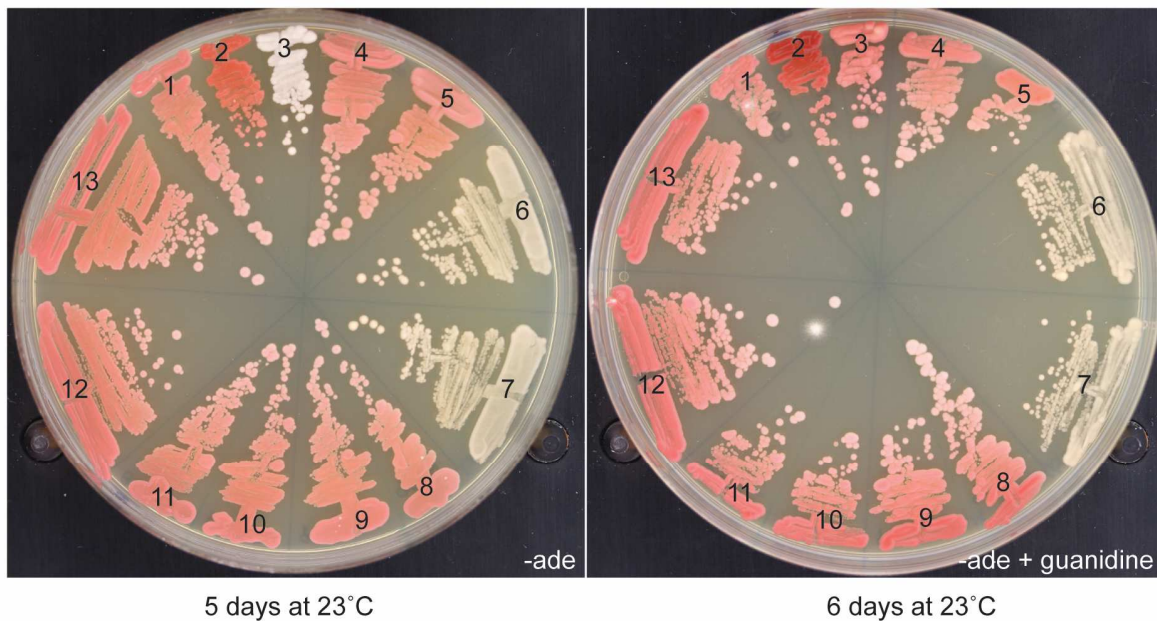


Figure 3-10 *ski2Δ rad24Δ exo1Δ cdc13-1* cells that can grow at 36°C have the wild-type *CDC13*. **A)** *cdc13-1*, but not *CDC13*, has an *EcoRI* cutting site introduced by the point mutation (Zubko and Lydall 2006). After PCR and *EcoRI* digestion, *CDC13* produces a single band of 358 bp (position 953 to 1311 of ORF), while *cdc13-1* produces two bands of 198 and 160 bp (*cdc13-1*/*EcoRI* site at position 1113 of ORF). **B)** Colony PCR (using primers m550 and m551) followed by *EcoRI* digestion was performed in colonies of the genotypes indicated. DNA products were then ran on an agarose gel. The presence of *cdc13-1* is detected as two bands in the gel while the wild-type *CDC13* DNA runs as a single band.

3.2.9. *ski2Δ rad24Δ exo1Δ cdc13-1* strains are respiration defective

During the manipulation of *ski2Δ rad24Δ exo1Δ cdc13-1* cells it was noticed that, when left on YEPD solid media, upon nutrient exhaustion, colonies never acquired a red colour, characteristic of old yeast colonies that carry the *ade2-1* mutation (Figure 3-11A). Yeast lab strains (W303) carry a mutation in the *ADE2* gene (*ade2-1*), which catalyses the sixth step of the purine biosynthetic pathway (Saffran et al. 1994). In the absence of adenine, *ADE2* mutants accumulate purine precursors that, upon oxidation, cause red pigmentation, observable in the colony colour (Aronson and Silveira 2009). The *ade2-1* allele introduces a premature stop codon, leading to a truncated, non-functional enzyme (Wilson et al. 2005). The presence of the prion-like structure *[PSI⁺]* was known to be able to bypass the *ade2-1* premature stop codon causing white colonies (True et al. 2004). The *[PSI⁺]* prion is a less functional version of the eRF3 protein, encoded by the *SUP35* gene (Uptain and Lindquist 2002). eRF3 is needed for efficient translation termination, hence, the prion version, leads to read-through of the *ade2-1* nonsense mutation, and to expression of *ADE2*. Therefore, the white colour of *ski2Δ rad24Δ exo1Δ cdc13-1* colonies in medium lacking adenine could be due to: 1) cells are able to bypass *ade2-1* mutation due to the presence of prions; 2) cells reverted the *ade2-1* mutation to the wild-type *ADE2* allele; 3) cells lack oxidative capacity to cause the red pigment.

First I tested if *ski2Δ rad24Δ exo1Δ cdc13-1* had acquired the *[PSI⁺]* prion. *[PSI⁺]* is “cured” by the overexpression of the Hsp104 chaperone which can be achieved by growth on medium containing guanidine hydrochloride (GdnHCl) (Liebman and Derkatch 1999; Ferreira et al. 2001). Therefore, a *ski2Δ rad24Δ exo1Δ cdc13-1* strain and its parental diploid were grown on YEPD media lacking adenine and supplemented with 3 mM of GdnHCl (Figure 3-11B). *[PSI⁺]* and *[PSI⁻]* strains were used as controls. The growth in the presence of GdnHCl totally reverted the white phenotype of the *[PSI⁺]* control colonies, while no change was observed in *ski2Δ rad24Δ exo1Δ cdc13-1* (Figure 3-11B). *ski2Δ*, *ski2Δ cdc13-1* and the parental *ski2Δ rad24Δ exo1Δ cdc13-1* heterozygous diploid did not show the white phenotype. This suggests that the *ski2Δ rad24Δ exo1Δ cdc13-1* cells tested do not carry the *[PSI⁺]* prion, or at least this is not the only reason why those cells cannot form red colonies.

A**B**

- 1 8460 (WT)
- 2 9895 (PSI⁻)
- 3 9894 (PSI⁺)
- 4 1108 (*cdc13-1*)
- 5 DDY 727 (*ski2Δ/SKI2 exo1Δ/EXO1 rad24Δ/RAD24 cdc13-1/CDC13*) ← Diploid
- 6 9996 (*ski2Δ rad24Δ exo1Δ cdc13-1*)
- 7 9995 (*ski2Δ rad24Δ exo1Δ cdc13-1*)
- 8 9988 (*ski2Δ cdc13-1*)
- 9 9987 (*ski2Δ cdc13-1*)
- 10 8849 (*ski2Δ cdc13-1*)
- 11 8848 (*ski2Δ cdc13-1*)
- 12 8845 (*ski2Δ*)
- 13 8844 (*ski2Δ*)

Figure 3-11 Evidence that prions are not responsible for *ski2Δ rad24Δ exo1Δ cdc13-1* colony red colour. A) A *ski2Δ rad24Δ exo1Δ cdc13-1* heterozygous diploid strain was sporulated and tetrad spores were dissected using standard techniques. Spores were germinated at 23°C for 8 days before photographing. Arrows indicate the strains with the *ski2Δ rad24Δ exo1Δ cdc13-1* genotype. **B)** Cells of the indicated genotypes were streaked onto a YEPD agar plate with no adenine supplementation (-ade) and allowed to grow for 5 days at 23°C. A pool of colonies was then transferred to a new YEPD (-ade) supplemented with 3mM of guanidine hydrochloride and allowed to grow for 6 days at 23°C.

As previously mentioned, the incapacity of yeast colonies to turn red over time, might be due to: 1) prions; 2) *ADE2* presence; 3) lack oxidative of capacity. Therefore, after the suggestion that the *[PSI+]* prion is not causing the white colony phenotype observed in Figure 3-11, the capacity of *ski2Δ rad24Δ exo1Δ cdc13-1* cells to grow on synthetic complete media lacking adenine and in media with glycerol as carbon source was tested (Figure 3-12). The ability of cells to growth without any adenine supplementation would mean that cells have a functional *ADE2* gene. Because glycerol is a non-fermentable carbon source, yeast rely on mitochondria and respiration to obtain energy from glycerol. Therefore, growth on glycerol indicates healthy mitochondria and the capacity to generate reactive oxygen species able to oxidize cellular metabolites.

Figure 3-12 shows that *ski2Δ rad24Δ exo1Δ cdc13-1* cells (and all the strains obtained from the same parental diploid) are unable to grow on synthetic complete media lacking adenine (SC-ade). This indicates that *ski2Δ rad24Δ exo1Δ cdc13-1* cells did not bypass the *ade2-1* mutation. Interestingly, *ski2Δ rad24Δ exo1Δ cdc13-1* cells were also unable to use glycerol as carbon source. Since glycerol can only be used as a precursor for oxidative respiration, I conclude that *ski2Δ rad24Δ exo1Δ cdc13-1* cells are respiration-defective (petite) and that this might be the reason for their whitish colony phenotype.

It was curious to notice that all *ski2Δ rad24Δ exo1Δ cdc13-1* cells tested were petite. It is not reported that a petite phenotype suppress the *cdc13-1* fitness defects, however, mitochondria have an important role in DDR. For example, iron-sulphur (Fe/S) clusters are important co-factors for DNA helicases and proteins involved in DNA replication and repair, such as Rad3 and Dna2 (Zhang 2014). Fe/S clusters biosynthesis is dependent on the mitochondria and defective synthesis of Fe/S clusters affects proteins of the respiratory chain (Lill and Muhlenhoff 2008; Stehling et al. 2009). To understand if the genotype of *ski2Δ rad24Δ exo1Δ cdc13-1* was associated with loss of respiratory chain function (petite phenotype), random spore analysis was performed to score the petite genotype (by incapacity to grow in glycerol containing media). It was observed that from the sporulation of a *ski2Δ rad24Δ exo1Δ cdc13-1* heterozygous diploid, 10% of the progeny was respiration deficient (Table 3-3). However, loss of respiration capacity seems to happen randomly, and is not associated with a particular genotype.

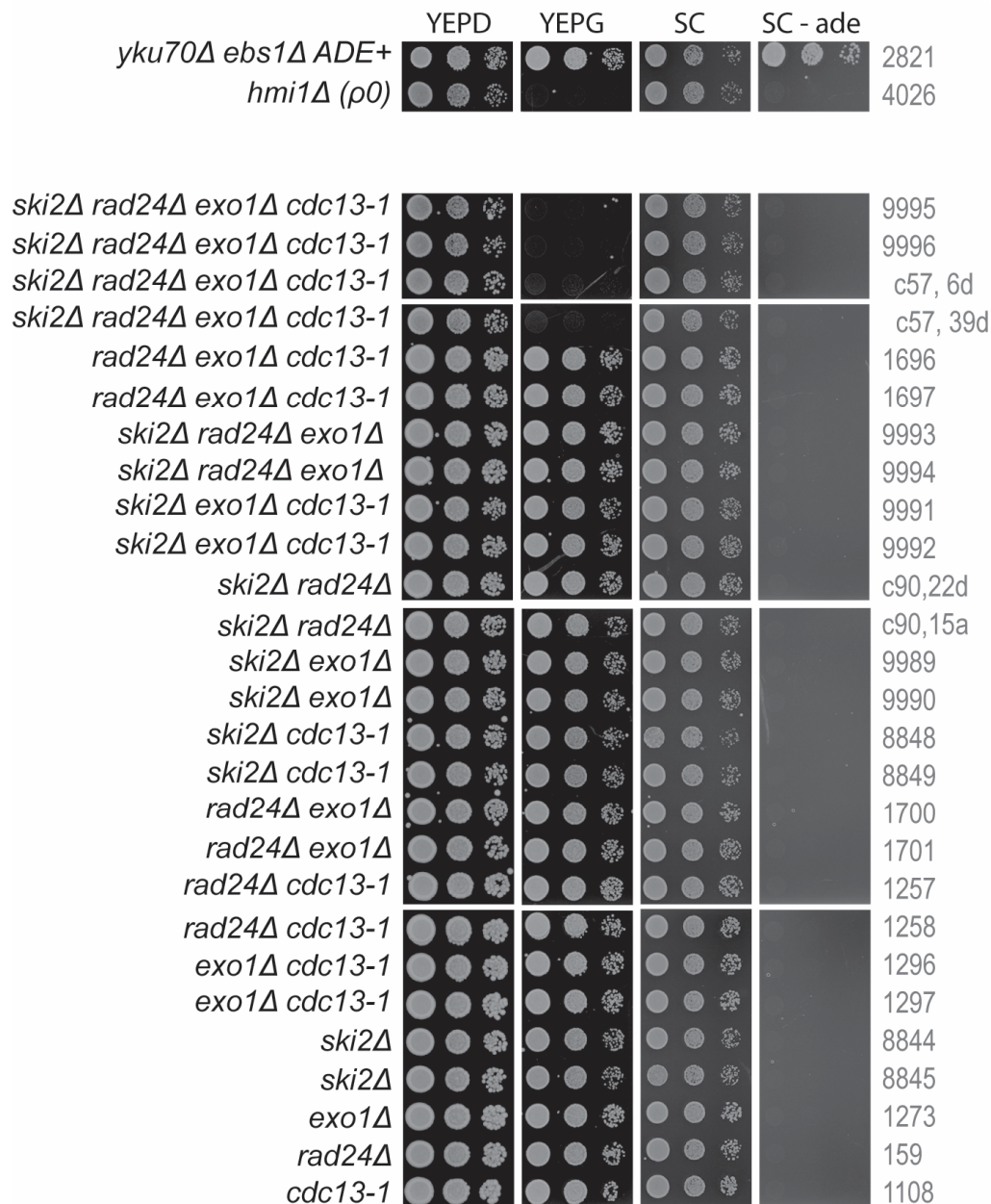


Figure 3-12 *ski2Δ rad24Δ exo1Δ cdc13-1* cells cannot use glycerol as a carbon source. Saturated cultures of the genotypes indicated were serially diluted across YEPD, YEPG (with glycerol instead of dextrose), synthetic complete (SC) and SC depleted of adenine (SC-ade) agar plates and grown for 3 days at 23°C. *p0*, or petite, are mitochondria defective cells (by loss of *HMI1*). One single rectangular plate was used for each temperature. When the strain number is not shown, the number of the spore and the cross is shown. These strains were not frozen, but the phenotype is representative of the genotype.

I conclude that some of the progeny of a *ski2Δ rad24Δ exo1Δ cdc13-1* heterozygous diploid loses respiration capacity in a manner that is independent of the genotype.

Table 3-3 Progeny of a *ski2Δ rad24Δ exo1Δ cdc13-1* heterozygous diploid randomly loses mitochondria integrity. Random spore analysis of *ski2Δ rad24Δ exo1Δ cdc13-1* heterozygous diploid. Numbers obtained per genotype are shown (number) as well as number of petite colonies per genotype (petite). Petite cells were defined by the incapacity to grow in glycerol containing plates.

Genotype	WT	<i>ski2Δ</i>	<i>exo1Δ</i>	<i>rad24Δ</i>	<i>cdc13-1</i>	<i>ski2Δ exo1Δ</i>	<i>ski2Δ rad24</i>	<i>ski2Δ cdc13-1</i>	<i>exo1Δ rad24Δ</i>	<i>exo1Δ cdc13-1</i>	<i>rad24Δ cdc13-1</i>	<i>ski2Δ exo1Δ rad24Δ</i>	<i>ski2Δ exo1Δ cdc13-1</i>	<i>ski2Δ rad24Δ cdc13-1</i>	<i>exo1Δ rad24Δ cdc13-1</i>	<i>ski2Δ exo1Δ rad24Δ cdc13-1</i>	EXPECTED	SPORES ANALYSED
Number	18	7	31	17	17	10	7	10	19	30	13	3	5	15	7	7	14	220
Petite	0	0	1	0	2	0	0	3	0	2	1	0	3	1	5	3	0?	21

3.2.10. Deletion of *SKI2* causes a high fitness variability in a *cdc13-1* background

The high phenotypic variability that was observed in strains with *SKI2* (and *SKI8*) deleted made it questionable if Ski2 (and Ski8) was directly involved in decreasing the fitness of *cdc13-1* cells. When *ski2Δ cdc13-1* cells grow well at non-permissive temperatures it might be the result of defects in pathways that have nothing to do with Ski2 directly, but are affected when mRNA surveillance pathways are affected. For example, a defective mRNA might be translated originating a defective checkpoint protein that can act as a dominant negative and suppress *cdc13-1* fitness defects. It could also happen that defective chromatin modifiers alter gene expression (maybe even giving raise to epigenetic changes), or defective chaperone proteins allow the accumulation of unfolded proteins. In all those cases, the degree of variability makes the process of understanding the connection of Ski2 to telomeres much harder. To understand the degree of variability caused by deletion of *SKI2* in *cdc13-1* cells, we assessed the fitness of *ski2Δ cdc13-1* progeny from 3 different crosses. Simultaneously, I tested if the petite phenotype had any effect on *cdc13-1*

cells fitness, since the *ski2Δ rad24Δ exo1Δ cdc13-1* cells tested in Figure 3-9, able to grow at 36°C without rearranging their telomeres, are petite.

Figure 3-13 shows that there is indeed a significant variability between the *ski2Δ cdc13-1* cells. Interestingly, the fittest strains are petite (although not all petite strains are very fit) suggesting that dysfunction in mitochondrial respiration might facilitate the bypass of *cdc13-1* telomere defects. *cdc13-1* petite cells might be fitter due to effects on the DDR proteins (that can happen if Fe/S cluster synthesis is affected in the petite cells). I conclude that deletion of *SKI2* causes high phenotypic instability in *cdc13-1* cells, making the study of a telomeric role for Ski2 difficult. It was therefore decided, at this stage, not to proceed further with the study of *SKI2* and to focus on *VPS74* and *CDC73*.

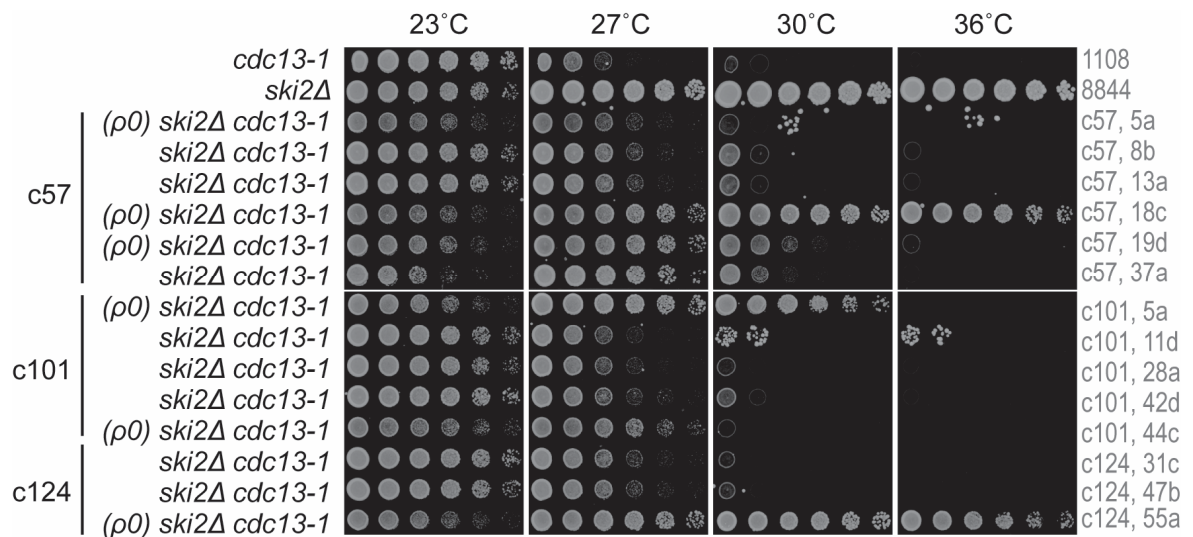


Figure 3-13 *ski2Δ cdc13-1* strain fitness is highly variable and independent of the respiration capacity. Saturated cultures of the genotypes indicated were serially diluted across YEPD agar plates and grown for 3 days at the temperatures indicated. Strains were obtained from the random spore analysis of 3 different crosses: Cross 57 (c57), originated from the mating of DLY8845 (*ski2Δ*) to DLY1697 (*exo1Δ rad24Δ cdc13-1*); Cross 101 (c101), originated from *SKI2* deletion in a diploid obtained by the backcross of DLY7752 (*nmd2Δ exo1Δ rad24Δ cdc13-1*); and Cross 124 (c124), originated from the mating of DLY10540 (*ski2Δ nmd2Δ*) to DLY1696 (*exo1Δ rad24Δ cdc13-1*). $\rho 0$ means that cells are respiration deficient, or petite, as tested by growth in glycerol containing plates. One single rectangular plate was used for each temperature. When the strain number is not shown, the number of the spore and the cross is shown. These strains were not frozen, but the phenotype is representative of the genotype.

3.3. Discussion/Conclusion

Yeast genome-wide screens have been used in the analysis and discovery of new gene interactions in various fields: acetic acid metabolism (Sousa et al. 2013), pesticide resistance (Gaytan et al. 2013), UV radiation sensitivity (Birrell et al. 2001), DNA damage responses (*S. pombe*) (Pan et al. 2012), telomere capping defects (Addinall et al. 2008), among others. In this study I have used Addinall et al. data, performed in the yeast S288C background, in order to find a group of genes that were relevant to cancer and telomere biology.

One of the main issues with high-throughput studies is that together with the large amount of valuable data it also comes plenty of false positives and false negatives. Therefore, data needs to be filtered and validated by more focused experiments before major conclusions are taken. In this work, the spot test assay was used to validate and follow the high-throughput data. An advantage of the spot test when compared to high-throughput assays is the capacity to analyse various dilutions of the same cell culture. This analysis of different cell densities allows us to distinguish growth differences that might be ignored when only one concentration is analysed. Furthermore, the spot tests were performed with strains newly generated by tetrad dissection and careful genotyping, as opposed to the screens, where the strains go through a very complex sequence of selection, which is more prone to contamination with diploid cells. On the other hand, in high-throughput assays, more replicates are analysed and unbiased mathematical models are used to detect fitness differences (as opposed to the human interpretation, whose judgement can be influenced by the expectations regarding the results). Consequently, one should critically compare the data from high and low-throughput assays and not assume that one is wrong when the data seems divergent.

DYN1, *UFD2*, *SKI2*, *INP52*, *CDC73*, *BAS1*, *SLA2*, *MON1*, *DOA1*, *VPS74*, *FYV10* and *SUB1* were all deleted in the W303 yeast genetic background to assess interactions with *cdc13-1* and/or *yku70Δ* telomere defective strains (Table 3-2). *INP52* deletion did not cause any fitness alterations in *cdc13-1* or *yku70Δ* cells and was one of the 2 cases where high-throughput data was not validated by small scale experiments. *CDC73* and *VPS74* showed strong interactions with both *cdc13-1* and *yku70Δ* and will be studied in the remaining Chapters of this thesis. The reason why *cdc73Δ cdc13-1* cells show opposite fitness phenotypes in low and high-throughput experiments will be discussed in Chapter 5.

It was shown in this Chapter how powerful genome-wide screens can be, since 9 of the 11 (*cdc13-1* screen) or 5 out of 8 (*yku70Δ* screen) genes analysed demonstrated the same phenotype as suggested by high-throughput studies (Table 3-2). However, overall the interactions observed in low-throughput experiments were weaker than those suggested by large-scale experiments. Many factors can influence the “strength” of the interactions measured in large- versus small-scale experiments. For example, the growth conditions: while in small scale experiments 96 well plates are used for fitness measurements, in large scale experiments 384 well plates allow smaller space for each strain to grow increasing competitiveness and exacerbating growth differences between healthy and sick strains. Also, as explained before, high-throughput experiments have the advantage of taking hundreds of pictures of each growing strain, allowing the creation of a growth curve, and the use of mathematical models that are sensitive to small differences in growth curves. The spot test assay used in small scale experiments is based on one (to three) pictures, or time-points, from where one can assess differences between strain fitness. Therefore, the spot test ignores what happens in all the other time-points, making it more prone to miss small fitness differences. Another important difference between the low and high-throughput experiments shown in this Chapter is the genetic background. While low-throughput experiments were performed in the W303 genetic background, the high-throughput data was obtained from S288c. Phenotypic differences amongst budding yeasts with different genetic backgrounds have been described and can be as extreme as some genes being essential in only one of the genetic backgrounds (Louis 2016). Thus, it is not surprising to see small differences in the strength of some genetic interactions when comparing S288c to W303. To assess the role of the strain background, low-throughput experiments should be repeated in the S288C background.

3.3.1. *DYN1*

DYN1 deletion enhanced the fitness defects of both *cdc13-1* and *yku70Δ* telomere defective strains (as suggested by the high-throughput data). *DYN1* encodes a cytoplasmic heavy chain dynein (Eshel et al. 1993). The human orthologue is *DNAH5* (and the paralogs *DNAH1*, *DNAH2*, *DNAH3*, *DNAH9*, *DNAH10*, etc.), which is also a dynein (Herrero et al. 2016). Dynein is important for cargo transport along microtubules and for the positioning of spindle microtubules, Golgi and mitochondria

(Sharp et al. 2000; Asai and Koonce 2001; Barr and Egerer 2005; Frederick and Shaw 2007). Interestingly, dynein was shown to be important for telomere clustering during meiosis and dynein defects cause chromosome segregation defects characteristic of cancer cells (Lee et al. 2015). Since this role in telomere clustering was only observed in meiotic division, it is not clear if it relates to the Dyn1 function increasing fitness of *cdc13-1* and *yku70Δ* cells. However, it was shown that DDR proteins, like Mre11 and ATM, co-precipitate with dynein and microtubules in human cell lines (Poruchynsky et al. 2015). Additionally, DNA damage is prolonged when dynein is affected (Poruchynsky et al. 2015). Since *mre11Δ* was shown to enhance the fitness defects of *cdc13-1* and *yku70Δ* cells, it is possible that *DYN1* deletion limits Mre11 access to the nucleus. For instance, lack of dynein would result in less Mre11 in the nucleus, leading to an enhancement of the telomere defects of *cdc13-1* and *yku70Δ* cells (due to prolonged DDR).

3.3.2. *UFD2*

UFD2 deletion suppressed *cdc13-1* fitness defects and weakly enhanced *yku70Δ* fitness defects. *UFD2* encodes an ubiquitin chain assembly factor (Johnson et al. 1995). Ubiquitination controls processes such as protein localisation, degradation and interactions (Pickart and Eddins 2004). The role of Ufd2 on telomere maintenance might be through an effect on DDR or checkpoints proteins, either by decreasing/increasing their stability or by affecting localisation and interaction partners. Changes in protein levels and stability, like apoptotic signalling proteins and DDR proteins, are among the reasons why loss of ubiquitination homeostasis can lead to cancer onset/propagation (Shen et al. 2013).

3.3.3. *BAS1*, *MON1*, *DOA1* and *FYV10*

BAS1, *MON1*, *DOA1*, *FYV10* all showed very weak genetic interactions with *cdc13-1*. Therefore, it would be hard to understand the basis of so subtle phenotypic differences.

3.3.4. ***SUB1***

SUB1 deletion in the *cdc13-1* background did not affect *cdc13-1* fitness defects at 27°C. However, it was observed that *sub1Δ rad9Δ cdc13-1* cells cannot grow at 20°C, unlike *rad9Δ cdc13-1*. This shows that Sub1 increases the fitness of *rad9Δ cdc13-1* cells at 20°C. Since at 27°C *sub1Δ rad9Δ cdc13-1* and *rad9Δ cdc13-1* cell fitness is similar, Sub1 does not seem to affect the temperature dependent telomere resection and the Rad9 checkpoint pathway. This is a puzzling result, nevertheless, it shows that Sub1, a transcriptional regulator, does play a role at telomeres and affect the DNA damage response to whichever defects *cdc13-1* cells have at 20°C.

Sub1 has been shown to stimulate basal transcription *in vitro* (Henry et al. 1996). ChIP experiments showed Sub1 primarily at RNA pol II and RNA pol III promoters (Rosonina et al. 2009). Interestingly, it was suggested that Sub1 and RPA compete for similar binding sites, as RPA levels increase at active promoters in *sub1Δ* cells (Sikorski et al. 2011). Therefore, *sub1Δ rad9Δ cdc13-1* cells could have a temperature-dependent imbalance in the proteins bound to ssDNA (like telomeric ssDNA and transcription-associated ssDNA) causing defects that are harder to fix due to lack of DDR. Since temperature affects the strength and stability of chemical interactions (as protein-protein or protein-DNA interactions) it might happen that between 20°C and 23°C, pathways promoting cell viability become more stable.

3.3.5. ***SKI2***

SKI2 deletion also showed strong interactions with both *cdc13-1* and *yku70Δ*. Yet, follow-up experiments showed that Ski2 role at telomeres might be indirect and related to genetic/proteomic instability caused by loss of transcriptional fidelity (caused by an impairment in the Ski-related mRNA degradation pathway). Loss of transcriptional fidelity can turn into loss of replication fidelity if the proteins responsible for proof-reading are defective. Ski2 is part of the Ski complex (with Ski3 and Ski8) that, together with Ski7, acts as a co-factor for the cytoplasmic exosome to degrade mRNAs (Brown et al. 2000; Araki et al. 2001). It was observed that *SKI2* deletion in telomere defective cells led to varied phenotypes (regarding fitness and mitochondrial function) in cells with identical genotypes. Nonetheless, with different degrees, *ski2Δ* consistently suppressed *cdc13-1* temperature sensitivity.

The Ski complex helps RNA degradation in the cytoplasm and it is not known to translocate to the nucleus where it could have a direct role degrading RNAs that could directly affect telomere biology such as TERRA and *TLC1*. However, although the Ski complex is localised to the cytoplasm, Ski8 was shown to move to the nucleus where it plays a role in double-stranded break formation during meiotic recombination (Arora et al. 2004). One would expect that lack of Ski2 disrupts the complex function, leading to degradation/misfolding/mislocalisation of the remaining components. Therefore, the high genetic instability observed in Ski2 mutants might be related to this role of Ski8 in meiosis, as Ski8 might lose its function in *ski2Δ* cells. For example, *ski* mutants with impaired recombination during meiosis might originate aneuploid progeny, or progeny with duplicated or lacking chromosome fragments.

The capacity of Ski8 to translocate to the nucleus is also remarkable, since Ski8 is part of the PAF1 complex in humans (Zhu et al. 2005). The yeast PAF1 complex (Cdc73, Paf1, Ctr9, Leo1 and Rtf1) is known to be involved in RNA control mainly by regulation of transcription and will be further studied in Chapters 5 and 6. If the interaction of the Ski complex to the transcription machinery (through Ski8) is conserved in yeast, it might happen that *ski* mutants also have defects in mRNA production/transcription (PAF1 complex defects) which would be greatly exacerbated by a defect in the RNA degradation pathway (Ski complex defects).

It was also observed that Ski2 aids the resection of *cdc13-1* even at low temperatures. This suggests that the decrease in single-stranded telomeric DNA might be the main reason why *ski2Δ cdc13-1* cells are more resistant to telomere uncapping at non-permissive temperatures. The way *ski2Δ* affects ssDNA might be as indirect as affecting the levels of a nuclease or a protein that recruits nucleases to telomeres. Consequently, telomere resection would be more inefficient. Another option is related to the fact that transcription at telomeres leads to Exo1-dependent resection (Balk et al. 2014). For example, if the interaction of Ski8 to the PAF1 complex is conserved in yeast, *ski2Δ* mutants might have defective transcription leading to less ssDNA. Although one would think that the ssDNA observed in *cdc13-1* cells is just related to telomere uncapping, it is true that *ski2Δ* affects the ssDNA levels of *cdc13-1* cells even at the permissive temperature of 23°C.

Mutations in the *SKI2* human orthologue, SKI2VL, leads to Trichohepatoenteric syndrome (syndromic diarrhoea), a life-threatening disease (Fabre et al. 2013). Mutations in SKI2VL are not known to be a primary cause of cancer, however

SKI2VL is found mutated in 0.8% of cancers (Gonzalez-Perez et al. 2013). If the data here presented are conserved in humans, perhaps mutations in SKI2VL (leading to its inactivation) help cancer cells to thrive by increasing genetic instability and loss of quality control over defective mRNAs. Also, a capacity to bypass telomere defects would definitely aid tumour progression since telomere maintenance is one of the key features of cancers.

3.4. Future work

3.4.1. DYN1

It would be interesting to assess the DNA damage response in *dyn1Δ* and *dyn1Δ cdc13-1* cells. For example, by assessing Rad53 and H2A phosphorylation and by looking at the presence of Mre11 in the nucleus, it would be possible to see if there are any defects in translocation of DNA damage repair proteins to the damage sites.

3.4.2. UDF2

Ufd2 is an ubiquitin chain assembly factor and therefore is important to protein signalling and degradation. Levels of DDR response proteins could be quantified in *ufd2Δ cdc13-1* versus *cdc13-1* cells to understand if lack of Ufd2 is causing an unbalance in DDR proteins. Since *ufd2Δ cdc13-1* cells do not have less telomeric ssDNA than *cdc13-1* cells, nucleases are not expected to be affected by *ufd2Δ*, and would not be tested at a first stage.

3.4.3. SUB1

Another notable result that would be interesting to address is the *sub1Δ rad9Δ cdc13-1* cold sensitivity at 20°C. A first step to understand this phenomenon would be the deletion of different DDR proteins in the *sub1Δ cdc13-1* background. ssDNA could also be quantified in *sub1Δ rad9Δ cdc13-1* at 20°C versus at 23°C.

3.4.4. *SKI2*

Deletion of *SKI2* in telomere defective cells causes high phenotypic variability. Nevertheless, a follow-up study of the *ski2Δ cdc13-1* cells that are fit at non-permissive temperatures might help unravelling the pathways behind *cdc13-1* bypass. For example, the fittest *ski2Δ cdc13-1* cells could be backcrossed for a couple of generations to understand how the “fit trait” is transmitted. Fit *ski2Δ cdc13-1* strains could then be sequenced to find the mutations responsible for *cdc13-1* bypass. Additionally, chromatin profiling (methylation/ acetylation) could help to understand if the changes are genetic or epigenetic. Another way of testing how direct is the Ski2 role in decreasing *cdc13-1* fitness would be by inserting back *SKI2* in the *ski2Δ cdc13-1* genome (or in a plasmid), and test if the fitness defects increase.

4. Vps74 as a bridge between the Golgi apparatus and the DDR

4.1. Introduction

In Chapter 3, *VPS74* deletion was found to weakly suppress *cdc13-1* fitness defects and strongly enhance *yku70Δ* fitness defects (Figure 3-1). Vps74 (Vacuolar Protein Sorting 74) is a cytoplasmic protein and was first identified as being needed for protein sorting to the vacuole (Bonangelino et al. 2002). Later, Vps74 was shown to be needed for the localisation of glycosyltransferases to the Golgi apparatus (Schmitz et al. 2008). Glycosyltransferases are responsible for protein glycosylation, which is a post-translational modification where a sugar (glycan) chain is attached to the protein (Shental-Bechor and Levy 2008). Protein glycosylation contributes to the correct folding of some proteins, therefore acting as a quality control mechanism (Shental-Bechor and Levy 2008; Xu and Ng 2015). Glycans are also recognised by ER-associated degradation (ERAD) receptors, being therefore important for protein degradation in both yeast and mammals (Xu and Ng 2015).

Another important role for the yeast Vps74 is to regulate the levels of phosphatidylinositol 4-phosphate (PtdIns4P) by interacting and activating Sac1, a phosphoinositide phosphatase membrane protein (Wood et al. 2012). PtdIns4P is mainly known to promote protein trafficking in Golgi (Strahl and Thorner 2007). Additionally, PtdIns4P is the precursor of the second messengers: 1,2-diacylglycerol (DAG) and inositol 1,4,5-trisphosphate (Ins(1,4,5)P₃) (Strahl and Thorner 2007). Ins(1,4,5)P₃ is soluble and diffuses to the nucleus where it is successively phosphorylated to originate Ins(1,4,5,6)P₄, Ins(1,3,4,5,6)P₅ and InsP₆ (Figure 4-1). The latter was shown to have a role in mRNA export, with a decrease in InsP₆ levels leading to an accumulation of polyadenylated mRNA in the nucleus (Wera et al. 2001).

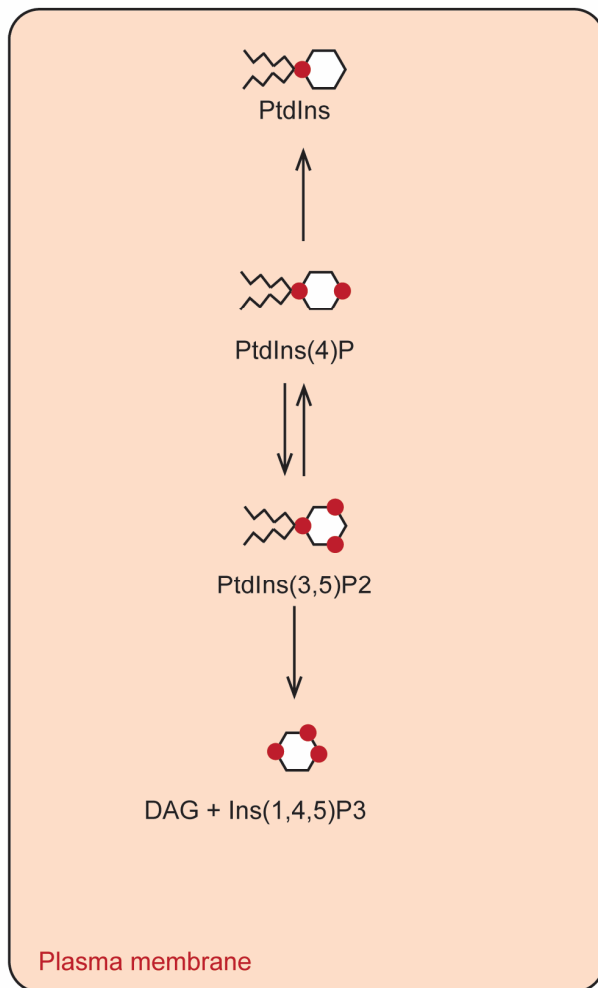
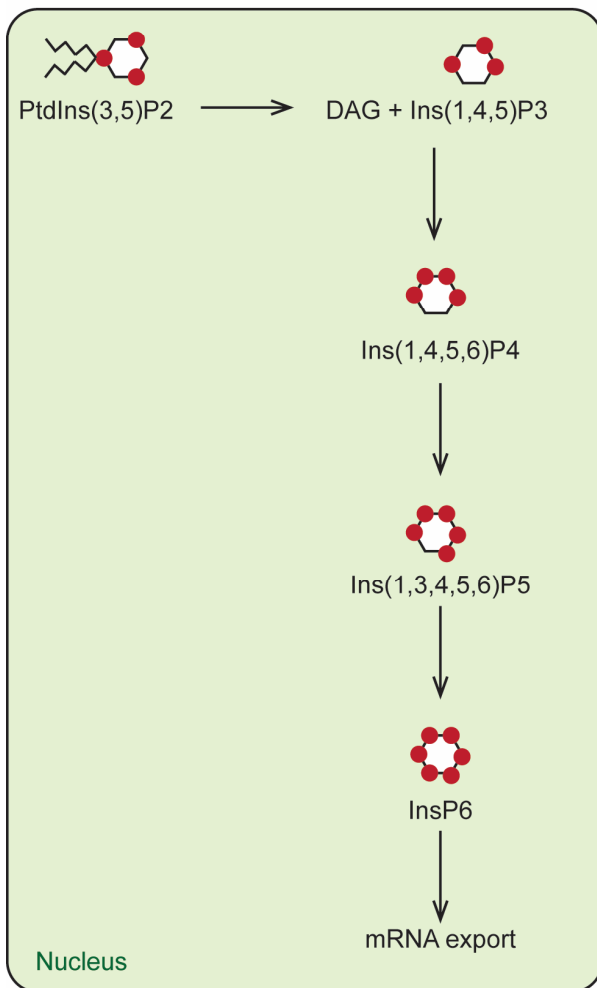
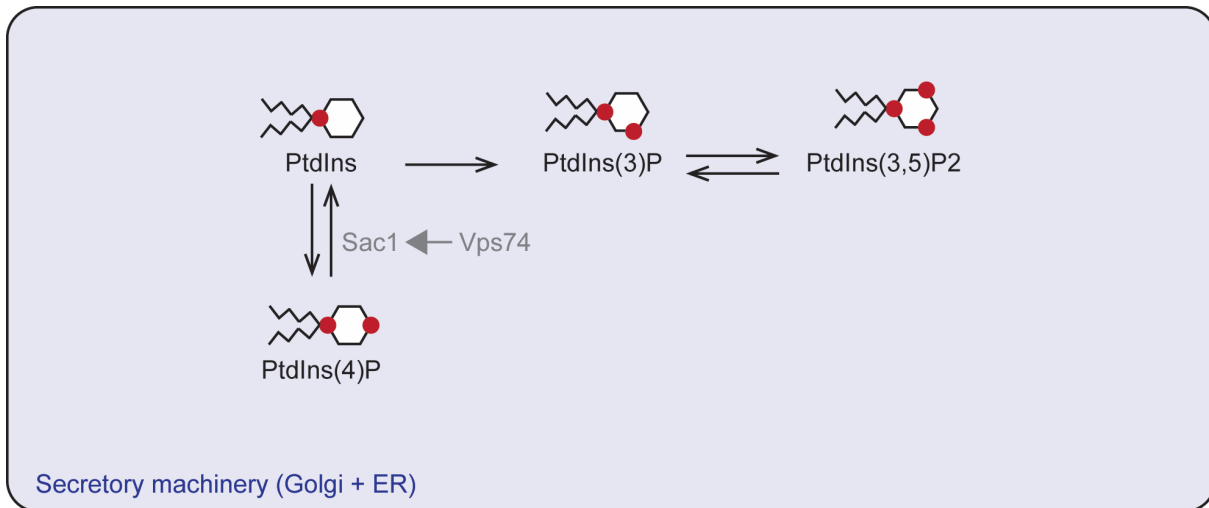


Figure 4-1 Phosphoinositide signalling in yeast. Series of transformations that members of the inositol pathway go through in 3 different cell compartments: Golgi and Endoplasmic Reticulum; Nucleus; and Plasma Membrane. DAG, diacylglycerol. Adapted from (Wera et al. 2001).

4.1.1. Inositol signalling and telomeres

Experiments with the enzymes involved in inositol signalling have suggested that the inositol signalling affects telomere length (Saiardi et al. 2005; York et al. 2005). For instance, Ins(1,3,4,5,6)P5 and InsP6 can be converted into the diphosphoryl inositols PP-IP4 and PP-IP5 through the action of Kcs1 (Saiardi et al. 2000). *kcs1Δ* cells have longer telomeres and low PP-IP4 levels. Also, *ipk1Δ* (*IPK1*, inositol polyphosphate kinase 1) cells have shorter telomeres and high PP-IP4 levels. Therefore, PP-IP4 was suggested to be a negative regulator of telomere length (Saiardi et al. 2005; York et al. 2005). Inositol levels can also affect the levels of complex sphingolipids such as inositol-phosphoceramide (IPC), that are originated by sphingolipid maturation in the ER and Golgi (Dickson and Lester 1999). Sphingolipids are part of eukaryotic membranes and play a role in signal transduction pathways (Bartke and Hannun 2009). A study showed that depletion of a protein involved in sphingolipid homeostasis, Arv1, affects the transcription of many genes involved in telomere maintenance (such as *SIR3* and *EST3*) (Ikeda et al. 2015).

4.1.2. Golgi and the DNA damage response

In 2014, Farber-Katz and colleagues showed that the Golgi responds to DNA damage (Farber-Katz et al. 2014). The experiments in mammalian cells showed that Golgi became fragmented after camptothecin (CPT)-induced DNA damage. Golgi fragmentation would persist even after DNA lesions were repaired. This response to DNA damage was dependent on GOLPH3, *VPS74* mammalian orthologue, which was phosphorylated by DNA-PK (a DNA damage protein kinase), increasing GOLPH3-MYO18A interaction (Farber-Katz et al. 2014). MYO18A is a myosin that links Golgi membranes to the cytoskeleton (Dippold et al. 2009). These data suggested that Golgi can “sense” DNA damage and respond to it, however, it is not yet known what are the implications and consequences of this response.

Interestingly, GOLPH3 is an oncogene, reinforcing the idea that this gene is involved in maintaining genetic stability (Scott et al. 2009).

The yeast Golgi composition is very similar to that of the mammalian Golgi, however its organization strongly varies, with the yeast Golgi being more disorganized than the mammalian Golgi (Figure 4-2). Also, the kinase DNA-PK, which is the link between the nucleus (where the DNA damage occurs) and Golgi (GOLPH3) in

mammalian cells, is not conserved in yeast. Thus, it is not clear if/how yeast Golgi also responds to DNA damage. Although the mammalian kinases ATM and ATR, respectively Tel1 and Mec1 in yeast, were not shown to be required for DNA-damage-induced Golgi dispersal in mammalian cells, they might be in a simple organism like yeast (Farber-Katz et al. 2014).

The purpose of this Chapter was to better understand, in yeast, the possible Golgi (Vps74) role on the DNA damage caused by uncapped telomeres. I was also aiming to get new insights on the role of GOLPH3 (the Vps74 human orthologue) as an oncogene.

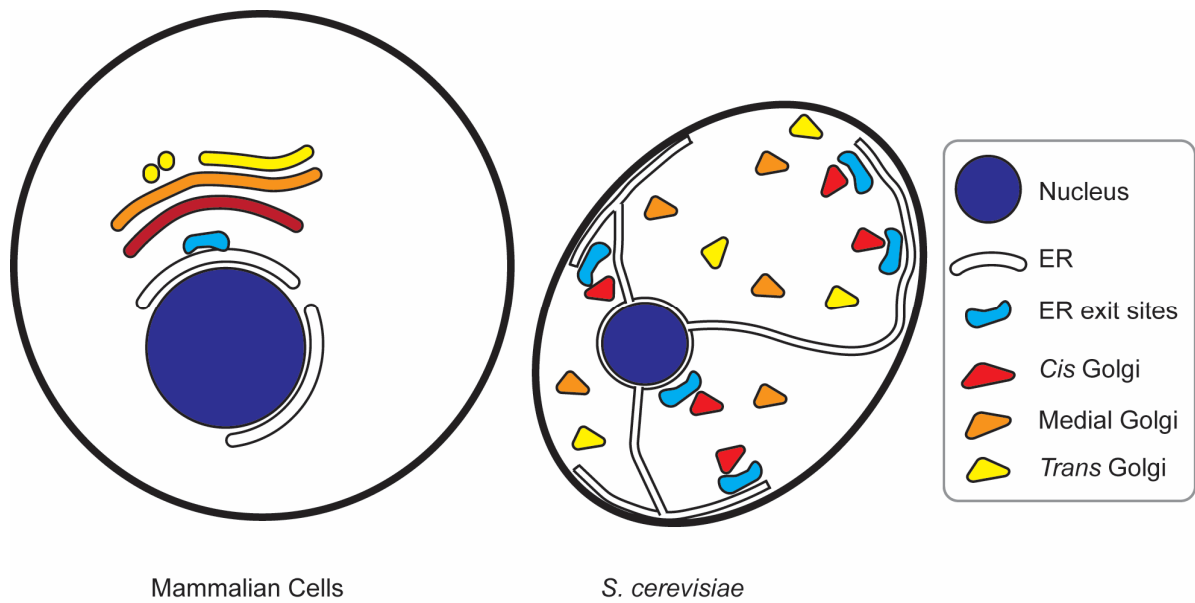


Figure 4-2 Mammalian Golgi versus yeast Golgi. Golgi of mammalian cells (left) shows cisternae-like organization, with *cis* Golgi being closest to the Endoplasmic Reticulum (ER)(that surrounds the nucleus) and the *trans* Golgi being the furthest. ER exit sites are the regions from where vesicles are released. Golgi of *S. cerevisiae* (right) is dispersed throughout the cytoplasm with *cis* Golgi being close to Endoplasmic Reticulum exit sites. As Golgi matures (to medial and *trans* Golgi) it acquires a more disorganized distribution. Adapted from (Verissimo and Pepperkok 2013) and (Glick 2002).

4.2. Results

4.2.1. Golgi structure changes upon DNA damage

It was previously shown that the mammalian Golgi is fragmented in response to DNA damage (Farber-Katz et al. 2014). Therefore, I asked if yeast Golgi also responds to DNA damage. In order to answer that question I used microscopy. Fluorescently tagged Rer1 and Sec7, proteins that respectively localise to *cis* and *trans* Golgi, were used as Golgi markers (Matsuura-Tokita et al. 2006). Centromeric plasmids carrying *RER1* or *SEC7* fused to enhanced green fluorescent protein (EGFP) were transformed into *WT* and *cdc13-1* cells (the latter was used to induce telomeric DNA damage). A preliminary experiment showed that the EGFP signal obtained was highly variable (which I attributed to a variation in plasmid copy number). In order to decrease signal variability between cells, the *EGFP-RER1* and *SEC7-EGFP* constructs (and *ADH1* promoter they were associated with) were cloned into an integrative plasmid (inside the *URA3* gene). Finally, the constructs *EGFP-RER1::URA3* and *SEC7-EGFP::URA3* (and the *ADH1* promoter) were integrated at the *ura3-1* locus in *WT* and *cdc13-1* cells.

DSBs and replication fork stalling (two forms of DNA damage) were induced by addition of 0.1% (w/v) of methyl methanesulfonate (MMS) or 200 mM of hydroxyurea (HU), respectively. Additionally, *cdc13-1* cells were exposed to 36°C to induce telomere uncapping. DNA damage was induced for 180 min before live-cell imaging was performed.

Figure 4-3 shows that both *cis* (Rer1) and *trans* (Sec7) Golgi can be observed as an organized structure, spread throughout the cell (bright green dots). *cdc13-1* cells did not show any noticeable structural changes in Golgi upon induction of telomere uncapping (by exposure at 36°C, Figure 4-3). Note that *cdc13-1* cells after 180 min at 36°C, showed a dumbbell shape, accompanied by an increase in cell size, which is caused by cell cycle arrest in G2/M. MMS and HU-treated cells do not show such a strong dumbbell phenotype, likely because they are arresting in S phase (Friedel et al. 2009).

HU treatment did not noticeably cause significant changes in Golgi structure, although it might have caused some fragmentation in *trans* Golgi (Sec7-EGFP), since the signal seems slightly weaker. If not a technical issue this might suggest reduced

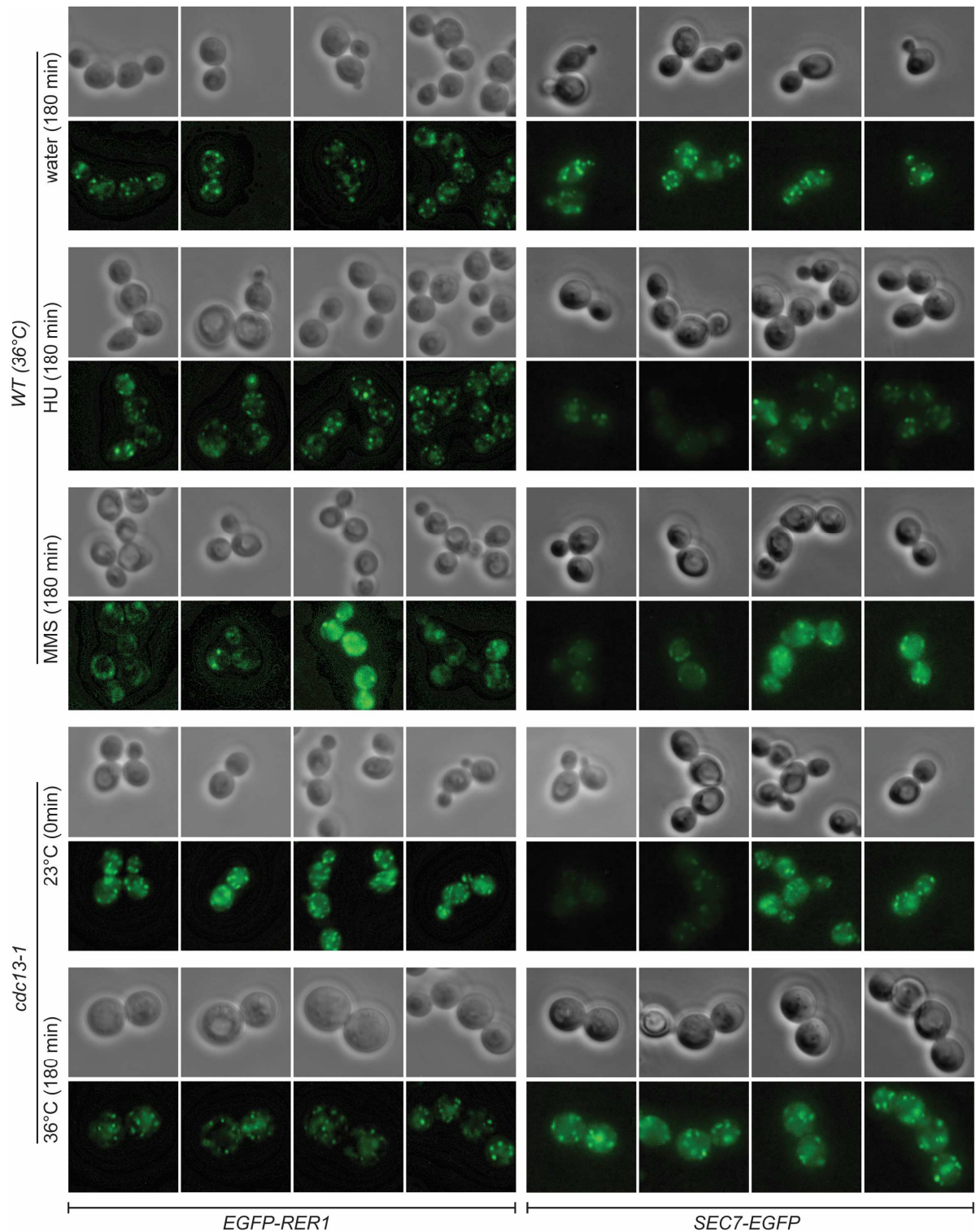


Figure 4-3 Yeast presents Golgi structural changes upon DNA damage. Cultures were grown overnight at 23°C until exponential phase ($OD_{600} \sim 0.4$). Temperature was shifted to 36°C and *WT* cultures were subdivided into 3 cultures, to which HU (200mM), MMS (0.1%, w/v) or water was added. *WT* (with the drugs) and *cdc13-1* cells were photographed (1000X magnification) either before the temperature shift (0min) or after 180 min of treatment. A representative sample is shown here and additional pictures are in Appendix E. Strains used were: *WT EGFP-RER1*, 10001; *cdc13-1 EGFP-RER1*, 10003; *WT SEC7-EGFP*, 10002; and *cdc13-1 SEC7-EGFP*, 10004. Pictures were treated as described in section 2.3.23.

trans Golgi signal, or less Sec7-EGFP being delivered to *trans* Golgi. MMS treatment seemed to have caused both *cis* (Rer1) and *trans* (Sec7) Golgi fragmentation or dissolution since the number of brighter dots that stand out from the background is reduced.

Since *cdc13-1* cells seem to be arresting at a different phase of the cell cycle, compared to MMS and HU-treated cells, it can happen that Golgi responsiveness/fragmentation is affected by the cell cycle. Consequently, other sources of telomeric DNA damage (for example *yku70Δ*) should be tested.

MMS is an alkylating agent that causes base mispairing and replication block while HU blocks replication by exhausting the dNTPs pool. The preliminary results here presented suggest that Golgi is more sensitive to MMS treatment. It is also possible that HU treatment was not efficient and did not cause the same level of DNA damage as the MMS treatment.

Another issue with this experiment is that upon DNA damage induction (by the addition of MMS or HU) temperature was also shifted to 36°C. Consequently, the cells are exposed to an additional source of stress: temperature. It is therefore important to repeat these experiments at 30°C. Additionally, a control for a general effect of cell-cycle arrest (independent of DNA damage) needs to be used to control for specificity of the Golgi response. Also, a positive control to Golgi disruption should be used to better recognise the structural changes that happen when Golgi is damaged.

I conclude that yeast Golgi structure, like mammalian Golgi, gets fragmented upon cytotoxic DNA damage (and replication block). I also conclude that Golgi does not respond to telomeric DNA damage caused by uncapped telomeres. Importantly, these conclusions must be confirmed by performing a better controlled experiment.

4.2.2. Exo1 and Rad24 decrease, whereas Mre11 increases, *vps74Δ* cell fitness

I observed that deletion of *VPS74* causes fitness defects at any temperature, but the decreased fitness is more evident at 23°C and 38°C (Figure 3-1 and Figure 4-4). *VPS74* genetically interacts with both *cdc13-1* and *yku70Δ* (Figure 3-1) suggesting a role for Vps74 in telomere maintenance and/or in the DDR. To test if *vps74Δ* fitness defects were caused by checkpoint activation, various members of the DDR were

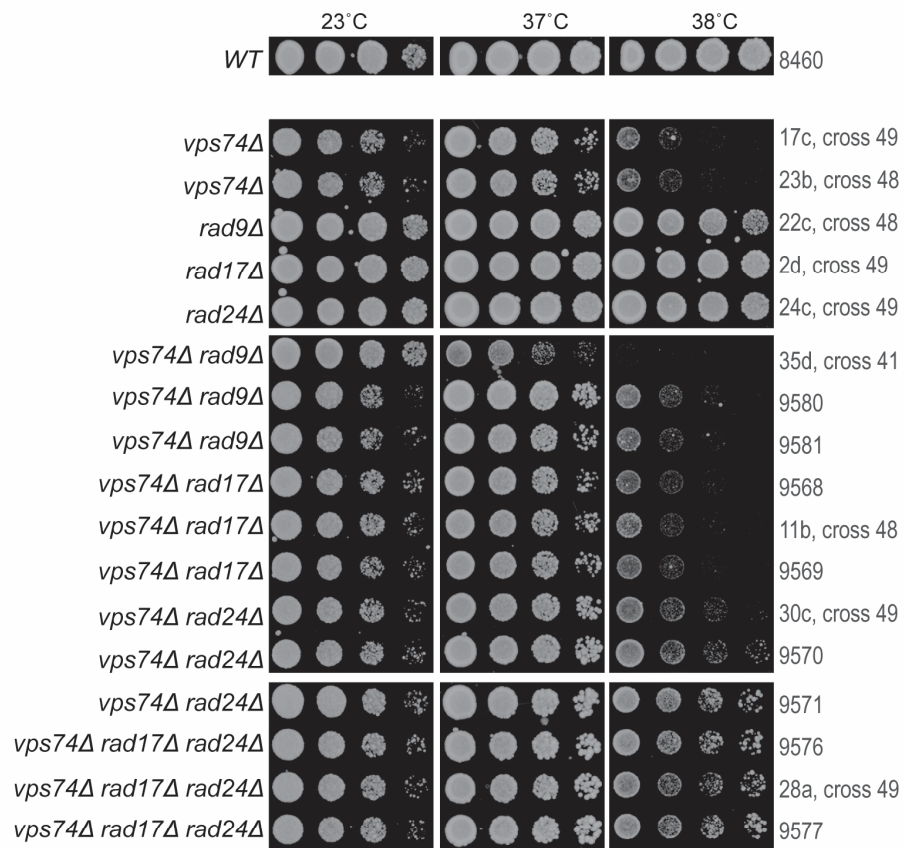
deleted in the *vps74Δ* background. Interactions with *rad9Δ*, *rad17Δ*, *rad24Δ*, *exo1Δ* and *mre11Δ* were tested (Figure 4-4). Table 4-1 (page 120) summarises these genetic interactions and others observed in this Chapter.

I noted that deletion of either *RAD9* or *RAD17* did not affect *vps74Δ* growth at 38°C (Figure 4-4A). Surprisingly, deletion of *RAD24*, that acts in the same pathway as *RAD17*, did suppress *vps74Δ* fitness defects at 38°C (Figure 4-4A). Also, simultaneous deletion of *RAD24* and *RAD17* suppress *vps74Δ* fitness defects (Figure 4-4A). This suggests that activation of DDR checkpoint proteins causes fitness defects at 38°C in *vps74Δ* cells, indicating that deletion of *VPS74* causes some sort of DNA damage. The difference between *rad17Δ* and *rad24Δ* phenotypes suggest that in the *vps74Δ* context, Rad24 might maintain some function outside the common pathway where Rad24 loads Rad17 (and Mec3/Ddc1) to the DNA lesion. It is important though to confirm these results with a different arrangement of the strains in the plate. This is because the rectangular plate where the spot test was performed was arranged in 3 columns (of 4 dilutions each) (Figure 4-4B). In the last column, the highly diluted cells had no competition (for nutrients, for example), while in the first and second columns they had. The last column had one *vps74Δ rad24Δ* and all the *vps74Δ rad17Δ rad24Δ* strains, therefore the fitness suppression observed might be affected by nutrient accessibility. Nevertheless, the difference between *vps74Δ rad17Δ rad24Δ* cells and *vps74Δ* cells seems too big to be solely due to nutrient accessibility differences.

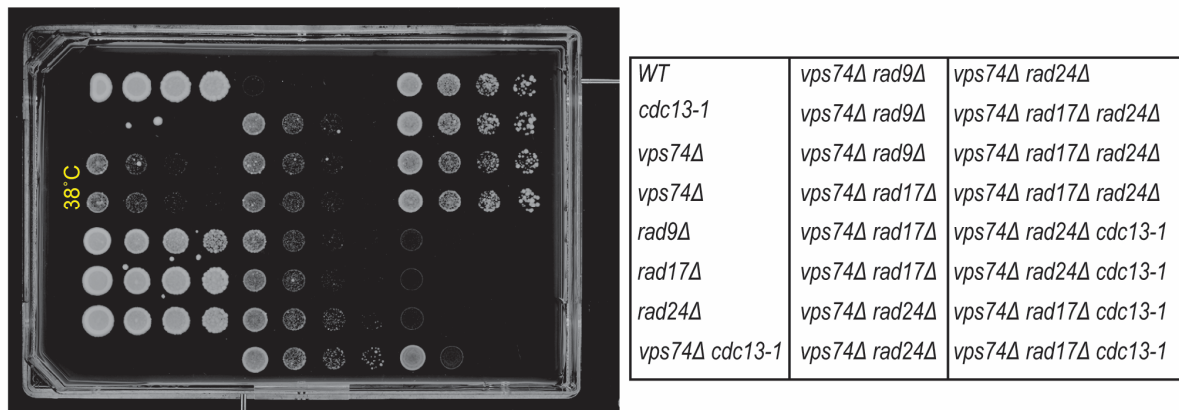
EXO1 deletion weakly suppressed *vps74Δ* fitness defects at 38°C (Figure 4-4C), suggesting that *VPS74* deletion causes DNA damage that involved Exo1-mediated resection. Finally, *MRE11* deletion strongly enhanced *vps74Δ* fitness defects (Figure 4-4D). *mre11Δ* also strongly enhances *yku70Δ* fitness defects and *yku70Δ vps74Δ* are synthetically sick (Figure 3-1) (Maringele and Lydall 2002). This strengthens the idea that Yku70 and Vps74 act in parallel to maintain the genome integrity and that Mre11 has a role maintaining the viability of *yku70Δ* and *vps74Δ* cells.

I conclude that *VPS74* deletion induces fitness defects that are dependent on Exo1, and Rad24. On the other hand Mre11 increases the fitness of *vps74Δ* cells. I suggest that Vps74 either promotes genomic stability and/or contributes to the DDR.

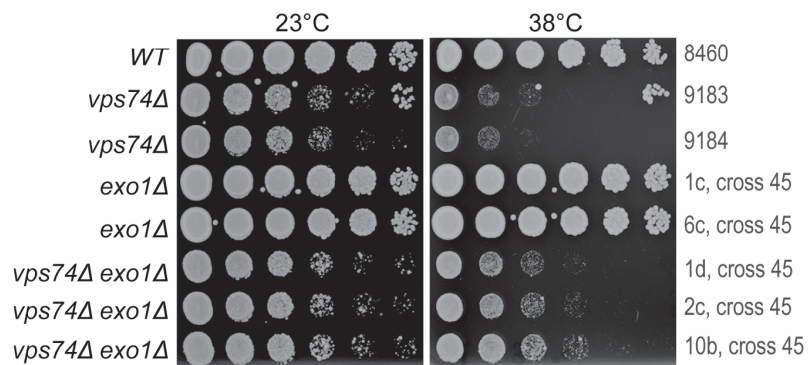
A



B



C



D

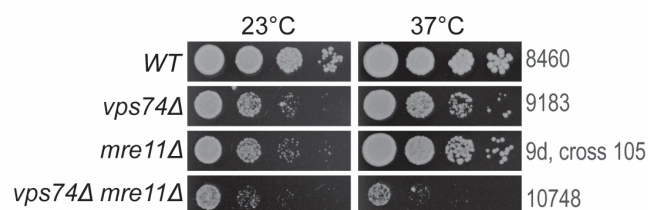


Figure 4-4 *vps74Δ* fitness defects are suppressed by *exo1Δ* and *rad24Δ* but not *rad17Δ* or *rad9Δ*, and are enhanced by *mre11Δ*. **A, C and D)** Saturated cultures of the genotypes indicated were serially diluted across YEPD agar plates and grown for 3 days at the temperatures indicated. All strains at each temperature were grown on a single plate but have been cut and pasted to allow better comparisons. When the strain number is not shown, the number of the spore and the cross is shown. These strains were not frozen, but the phenotype is representative of the genotype. **B)** Original plate from the strains in A) at 38°C.

4.2.3. Exo1, but not Sae2, contribute to fitness defects of *yku70Δ vps74Δ* cells

The most striking result involving Vps74 was perhaps the strong synthetic sickness observed in *yku70Δ vps74Δ* cells, which suggested that Vps74 and Yku70 work together to maintain cell fitness by parallel pathways (Figure 3-1). From Figure 4-4 it was inferred that Vps74 itself is involved in maintaining genomic integrity since deletion of some DDR proteins increased fitness of *vps74Δ* cells. Exo1 is a major player in the cell-cycle arrest that happens in *yku70Δ* cells, due to its role resecting the *yku70Δ* uncapped telomeres (Maringele and Lydall 2002). Therefore, I speculated that the lower fitness of *yku70Δ vps74Δ* cells could be suppressed by *exo1Δ*. If so, this could suggest that Vps74 is somehow involved in maintaining proper telomere capping.

To test the involvement of Exo1 in *yku70Δ vps74Δ* fitness defects, *EXO1* was deleted in *yku70Δ vps74Δ* cells. *SAE2*, which encodes for an endonuclease involved in DNA repair, was also deleted to better understand the role of different nucleases in *yku70Δ vps74Δ* cells (Figure 4-5). Figure 4-5A shows that *exo1Δ* strongly suppresses *yku70Δ vps74Δ* fitness defects at 35°C and 36°C. In Figure 4-5B a different strain of *yku70Δ vps74Δ* seems to be even more defective than the DLY10017 strain in Figure 4-5A, showing some phenotypic variability between *yku70Δ vps74Δ* cells. In all cases, *yku70Δ vps74Δ* cells are always substantially less fit than *yku70Δ* or *vps74Δ* cells and *exo1Δ* always strongly suppresses *yku70Δ vps74Δ* fitness defects.

Interestingly, *SAE2* deletion did not affect the fitness of *yku70Δ vps74Δ* cells (Figure 4-5B). One explanation for such a difference between *sae2Δ* and *exo1Δ*, is that *vps74Δ yku70Δ* fitness defects are triggered by accumulation of long molecules of ssDNA (dependent of Exo1, but not on Sae2). Additionally, *sae2Δ* enhanced *yku70Δ* fitness defects but not *vps74Δ* fitness defects and did not further decrease fitness defects of *yku70Δ vps74Δ* or *yku70Δ vps74Δ exo1Δ* cells. Such results show that Sae2 contributes to the fitness of *yku70Δ* cells (which is the opposite to the role of Exo1 in *yku70Δ* cells).

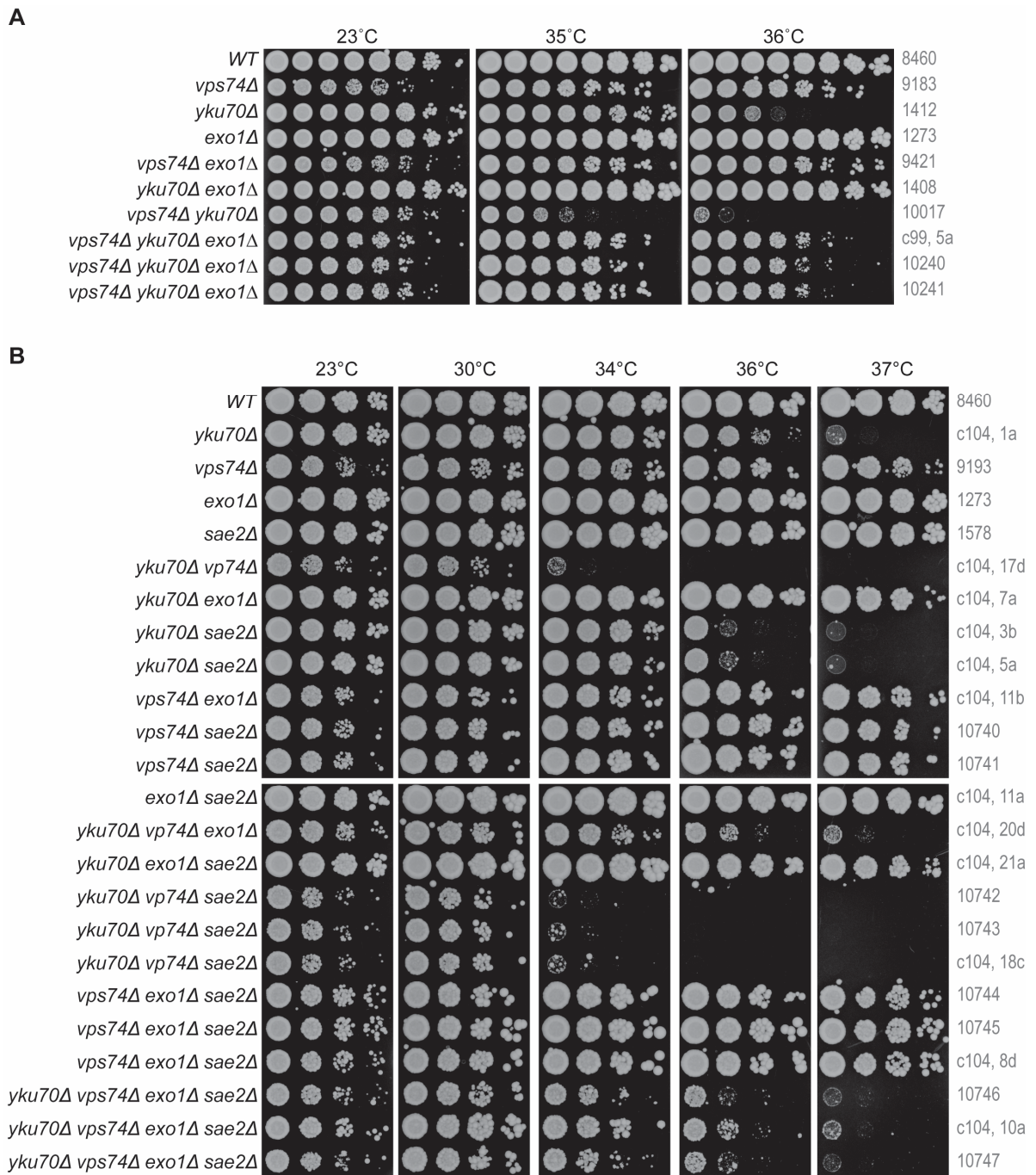


Figure 4-5 *vps74Δ yku70Δ* fitness defects are suppressed by *exo1Δ* but not *sae2Δ*. A and B) Saturated cultures of the genotypes indicated were serially diluted across YEPD agar plates and grown for 3 days at the temperatures indicated. All strains at each temperature were grown on a single rectangular plate but have been cut and pasted to allow better comparisons. When the strain number is not shown, the number of the spore and the cross is shown. These strains were not frozen, but the phenotype is representative of the genotype.

It was also noticeable that *vps74Δ sae2Δ* strains grow slightly better than *vps74Δ* cells at 37°C (Figure 4-5B). It seems that *sae2Δ* and *exo1Δ* suppress *vps74Δ* fitness defects (but not *vps74Δ yku70Δ*). Such result suggests that *vps74Δ* fitness defects are at least in part due to nuclease activity, independently of the extension of the resection. Perhaps *vps74Δ* cells still have protection mechanism against Exo1 extensive resection and the small fitness defects observed at 38°C are caused by low levels of short ssDNA molecules and consequent DDR activation.

These data show that Exo1, but not Sae2, contributes to the fitness defects of cells simultaneously lacking Yku70 and Vps74. This suggests that increased DNA resection might be responsible for *yku70Δ vps74Δ* poor cell growth.

4.2.4. Vps74 slightly increases telomeric ssDNA of *cdc13-1* cells and decreases the ssDNA of *yku70Δ* cells

Since *yku70Δ vps74Δ* fitness defects are suppressed by *EXO1* deletion, I hypothesized that *yku70Δ vps74Δ* fitness defects were caused by an increase in telomeric ssDNA. To test this hypothesis, the ssDNA of *vps74Δ yku70Δ* (with and without *EXO1*) was measured by In-gel assay using a telomeric probe. ssDNA of *vps74Δ cdc13-1* cells was also assessed since those cells grow better than *cdc13-1* cells, which also accumulate high ssDNA levels (Booth et al. 2001). The In-gel assay uses a probe that anneals to the telomere end in native telomeres that were previously cut with an endonuclease (XhoI in this case). Hypothetically, XhoI will only cut dsDNA, therefore the In-gel assay can reveal 2 types of information: 1) the amount of ssDNA present in the sample (by the band intensity); and 2) the extension of the resection (by the length of the bands) (Appendix D).

vps74Δ cells, like *WT* cells, do not show significant levels of telomeric ssDNA (Figure 4-6A, B). As expected, *cdc13-1* cells accumulate long fragments of ssDNA (Intermediate) (Figure 4-6A, B). Additionally, *yku70Δ* cells accumulate small fragments of ssDNA (Low). *exo1Δ* cells, like *WT* and *vps74Δ* cells do not show increased telomeric ssDNA. Interestingly, *VPS74* deletion slightly decreases *cdc13-1* ssDNA (Intermediate), which might explain the weak suppression of *cdc13-1* fitness defects upon *VPS74* deletion (Figure 3-1). *yku70Δ vps74Δ* cells, when compared to

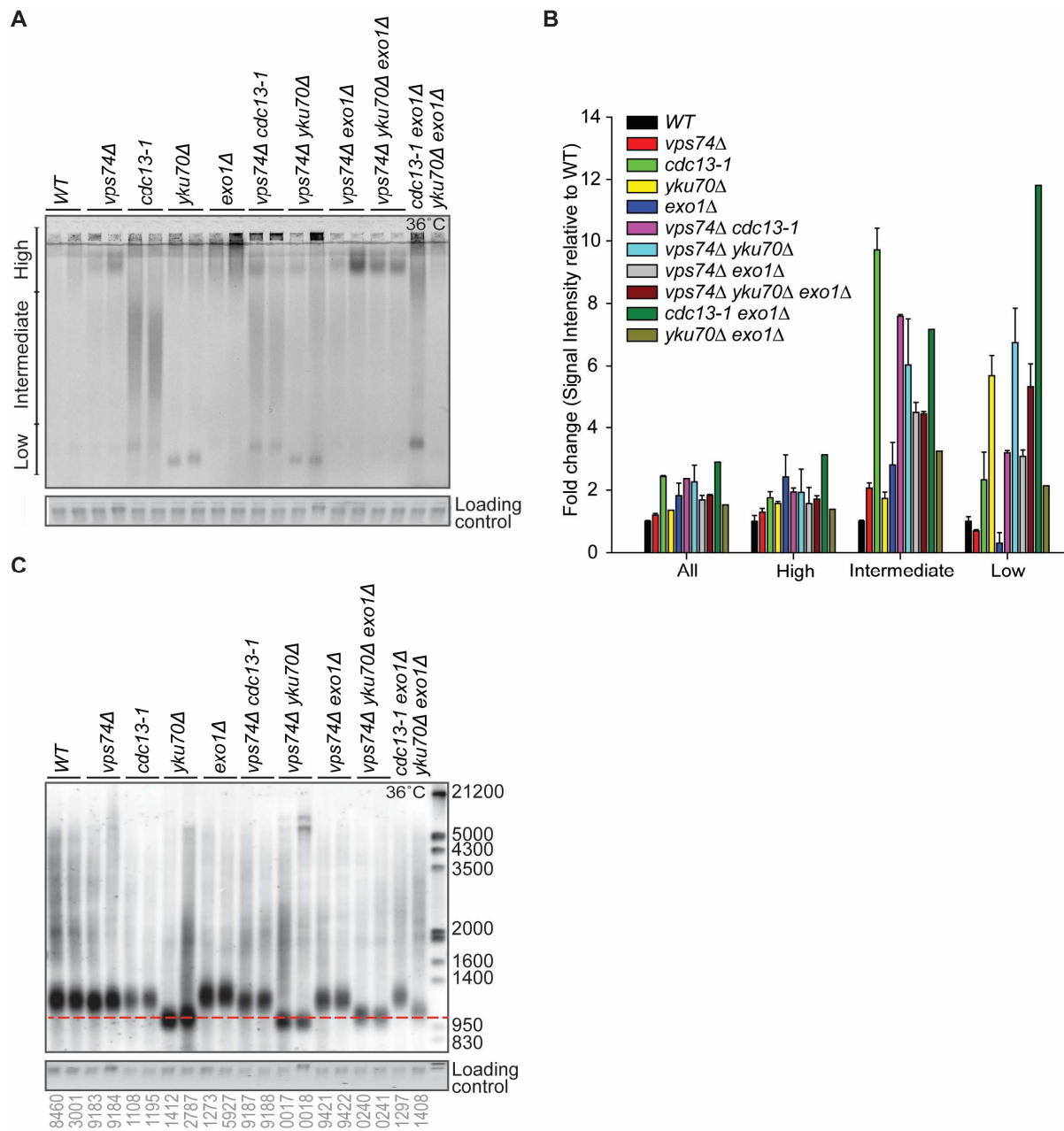


Figure 4-6 *vps74Δ* decreased telomeric ssDNA of *cdc13-1* cells and increased *yku70Δ* ssDNA. **A) Cell cultures of the indicated genotypes were grown overnight to exponential at 23°C and a further 4h at 36°C. DNA was extracted using the phenol method and ssDNA in the TG repeats was measured by In-gel assay. **B)** The gel in **A)** was horizontally divided in 3 parts (High, Intermediate, and Low). For each lane, the signal in each part was quantified and divided by the loading control signal. Quantifications were made using the ImageJ software. **C)** DNA from cultures in **A)** were analysed by Southern Blot using a telomeric probe.**

yku70Δ or *vps74Δ* cells, had slightly increased ssDNA levels (Intermediate), and no difference in the smaller ssDNA fragments (Low) (Figure 4-6B). As expected, *yku70Δ exo1Δ*, *vps74Δ exo1Δ* and *yku70Δ vps74Δ exo1Δ* all have very low levels of telomeric ssDNA since Exo1 is a main effector of telomeric resection. Although *yku70Δ vps74Δ* have more of the long telomeric ssDNA products, it does not seem to correlate with fitness, since the fitness defects of those cells are quite dramatic. This suggests that Vps74 plays a small role in the protection of telomeres against resection and that increased telomeric ssDNA in *vps74Δ yku70Δ* cells is at least part of what makes these cells less fit.

The DNA analysed in Figure 4-6A was further analysed by Southern blot to see if Vps74 contributed to telomere length maintenance of normal and uncapped telomeres (Figure 4-6C). Due to the nature of the DNA preparation (4h at 36°C followed by Phenol extraction), only terminal fragments were observed, nonetheless it is clear that *vps74Δ* cells have telomeres of similar length to the *WT* cells (Figure 4-6C). Interestingly, *yku70Δ vps74Δ* cells have slightly shorter telomeres when compared to *yku70Δ* cells, while *yku70Δ vps74Δ exo1Δ* telomere length is similar to that observed in *yku70Δ* cells. Although *yku70Δ vps74Δ* telomeres are not much shorter than *yku70Δ* telomeres, a small difference might be enough to reach a certain threshold and trigger a stronger DNA damage response against those defective telomeres. Therefore, it is reasonable that extremely short telomeres, together with more ssDNA, are a main cause for *yku70Δ vps74Δ* fitness defects.

I conclude that Vps74 does not affect the telomere length of wild-type telomeres, but plays a minor role increasing the length of *yku70Δ* cells, with short telomeres. Additionally Vps74 plays a minor role in the protection of *yku70Δ* uncapped telomeres against resection having the opposite role in *cdc13-1* cells.

4.2.5. Rad27 contributes to the fitness of *vps74Δ* cells

Rad27, a flap endonuclease, was described to be involved in Okazaki fragment processing (Rossi and Bambara 2006). Exo1 also displays a 5' flap endonuclease activity (weaker than Rad27) and I found that Exo1 decreases the fitness of *vps74Δ* and *vps74Δ yku70Δ* cells (Tishkoff et al. 1997; Lee and Wilson 1999). Since *exo1Δ* strongly suppresses *vps74Δ yku70Δ* fitness defects and weakly suppresses *vps74Δ* fitness defects, I wondered if *rad27Δ* could also suppress *vps74Δ yku70Δ* and

vps74Δ fitness defects. To test this, *RAD27* was deleted in *vps74Δ yku70Δ* and *vps74Δ* cells, and fitness assessed by spot test.

Deletion of *RAD27* in *vps74Δ*, *yku70Δ* and *yku70Δ vps74Δ* cells seems to be associated with a small phenotypic variability in cells with a similar genotype (Figure 4-7). Such variability can be related to genetic or epigenetic variability (related for example to accumulation of mutations or alterations in chromatin modifiers) or can be due to variability in the proteome. Indeed, *rad27Δ* cells were previously shown to have telomeric repeat instability, being subjected to expansions and contractions of the telomeric repeats (Parenteau and Wellinger 1999). The successive passaging and backcross of such strains could help identify the origin of such variability. Nevertheless, overall Rad27 contributes to the fitness of *vps74Δ* and *yku70Δ* cells in a similar extent (Figure 4-7, 36°C). Such result is the opposite of that observed for Exo1 (Exo1 decreases the fitness of *vps74Δ* and *yku70Δ vps74Δ* cells), supporting the idea that the poor fitness of *vps74Δ yku70Δ* cells is related to increased ssDNA. In agreement with such model is the fact that *rad27Δ* cells have higher levels of telomeric ssDNA (Parenteau and Wellinger 1999). It is therefore not surprising that *rad27Δ* enhances *yku70Δ vps74Δ* fitness defects (at ≥36°C), since it might increase the already high levels of telomeric ssDNA.

I conclude that Rad27, unlike Exo1, contributes to the fitness of *vps74Δ* cells. I suggest that Rad27 helps control the high levels of ssDNA in *vps74Δ yku70Δ* cells (and perhaps in *vps74Δ* cells).

4.2.6. Mec1 decreases the fitness of *vps74Δ* and *yku70Δ vps74Δ* cells

To better understand the role of Vps74 (and Yku70) in the DNA damage response, I next tested the role of Mec1 in the fitness of cells lacking Vps74 (Figure 4-8). Mec1 is a phosphoinositide (PI)-3-kinase-related essential protein kinase (Kato and Ogawa 1994; Naito et al. 1998). Mec1 plays a central role in the DDR, activating Chk1 and Rad53. Despite being an essential gene, *MEC1* (and *RAD53*) can be deleted if *SML1* (which acts downstream of Mec1 and Rad53) is also deleted (Zhao et al. 1998).

Figure 4-8 shows that *mec1Δ (sml1Δ)* suppresses both *vps74Δ* and *yku70Δ vps74Δ* fitness defects, at 38°C and at 35°C, respectively. Also, as previously reported *mec1Δ (sml1Δ)* suppresses *yku70Δ* fitness defects. This result suggests that Vps74 has a similar, but parallel, role to Yku70.

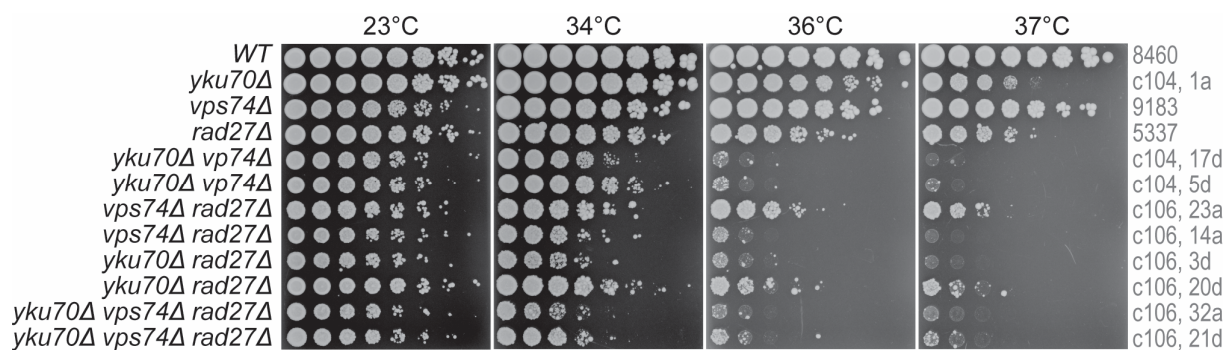


Figure 4-7 *rad27Δ* enhances *vps74Δ* and *yku70Δ* fitness defects. Saturated cultures of the genotypes indicated were serially diluted across YEPD agar plates and grown for 3 days at the temperatures indicated. All strains at each temperature were grown on a single rectangular plate. When the strain number is not shown, the number of the spore and the cross is shown. Cells with *RAD27* deleted, were not frozen due to the high phenotypic variability.

I conclude that Mec1 decreases the fitness of *vps74Δ* cells. I suggest that *vps74Δ* and *vps74Δ yku70Δ* cells have telomere defects that activate the Mec1 checkpoint protein. Due to the fact that Mec1 also responds to genomic DNA damage and replication block, it is also possible that *vps74Δ* and *vps74Δ yku70Δ* cells have damage outside the telomeres.

4.2.7. Sgs1 has no effect on the fitness of *vps74Δ* cells and Rad53 and Chk1 decrease the fitness of *yku70Δ vps74Δ* cells

During DDR, Mec1 phosphorylates Rad53, Rad9 and Chk1, and in turn Rad9 stimulates the activation of Rad53 and Chk1 (Emili 1998; Blankley and Lydall 2004; Ma et al. 2006). Upstream of Mec1, the Sgs1 helicase and Exo1, have the important role of resecting the DNA to initiate the DDR (Balogun et al. 2013). Sgs1, Rad53 and Chk1 role in maintaining the fitness of *vps74Δ* and *yku70Δ vps74Δ* cells was tested in order to better understand the place of Vps74 in the DDR (Figure 4-9). Again, the spot test assay was used to understand the effects that deletion of *SGS1*, *RAD53* and *CHK1* have in the fitness of cells lacking Vps74 (and Yku70) (Figure 4-9).

Figure 4-9A shows that *sgs1Δ* has little effect on *vps74Δ* or *yku70Δ vps74Δ* fitness defects, but strongly suppresses *yku70Δ* temperature sensitivity at 34°C and 36°C. This is in agreement with my previous results that showed that *EXO1* deletion (which works with Sgs1 to resect DNA) more strongly suppresses *yku70Δ* fitness defects than *vps74Δ* fitness defects (Figure 4-5) (Zhu et al. 2008). These results suggest that the nuclease function of Exo1 plays a relevant role decreasing the fitness of *vps74Δ* and *yku70Δ vps74Δ* cells, and that this function is independent of Sgs1.

RAD53 deletion suppressed *vps74Δ yku70Δ*, but not *vps74Δ*, fitness defects (Figure 4-9A). This suggests that activation of Rad53 checkpoint is not a major reason for *vps74Δ* fitness defects at 38°C. Rad53 checkpoint activation seems however to be important for the decreased fitness of *vps74Δ yku70Δ* cells.

As explained in the previous section, Chk1 is doubly activated by Rad9 and Mec1 upon DDR activation. Figure 4-9B shows that *chk1Δ* strongly suppresses *yku70Δ vps74Δ* fitness, but does not affect *vps74Δ* fitness defects at 38°C. It was consequently concluded that Chk1 does not affect the cell fitness of *vps74Δ* cells, but decreases the cell fitness of *yku70Δ vps74Δ* cells.

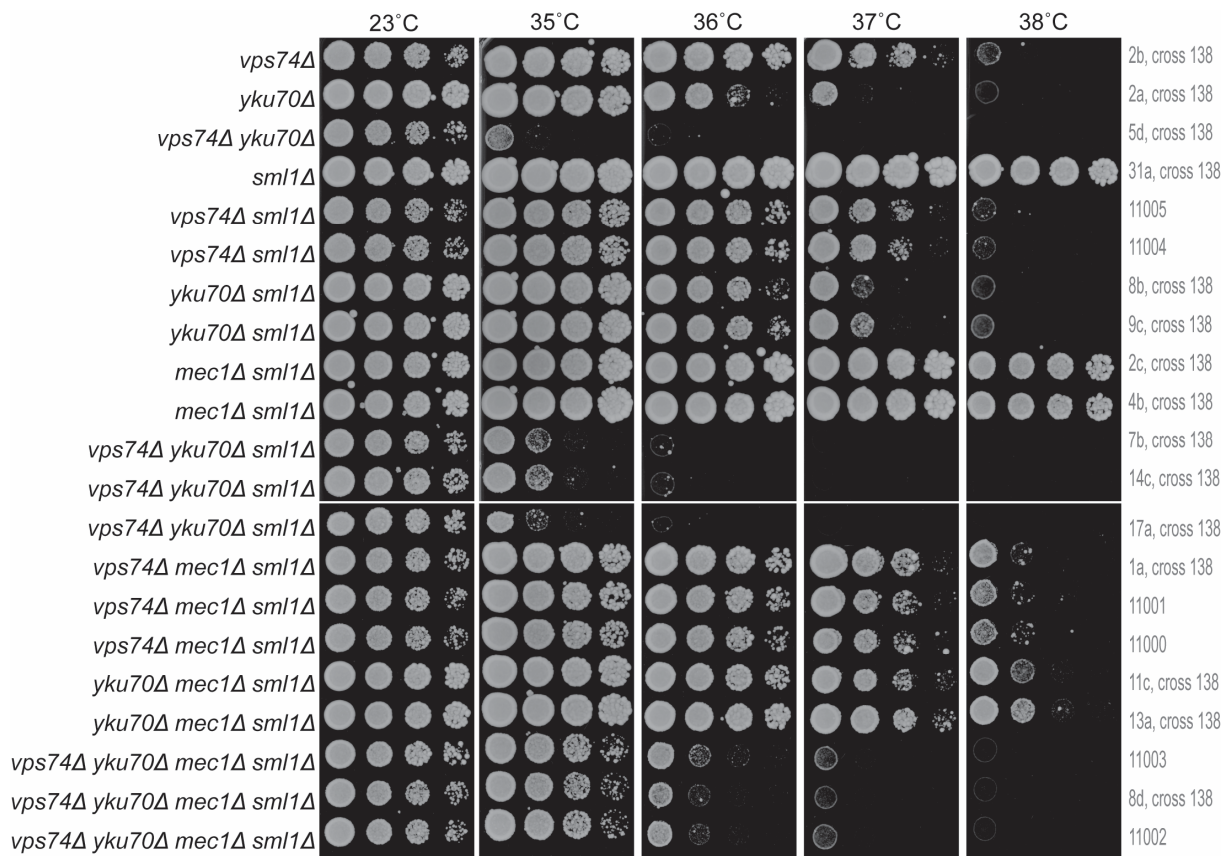


Figure 4-8 *mec1Δ sml1Δ* suppresses *vps74Δ* and *yku70Δ vps74Δ* fitness defects. Saturated cultures of the genotypes indicated were serially diluted across YEPD agar plates and grown for 3 days at the temperatures indicated. All strains at each temperature were grown on a single plate but have been cut and pasted to allow better comparisons. When the strain number is not shown, the number of the spore and the cross is shown. These strains were not frozen, but the phenotype is representative of the genotype.

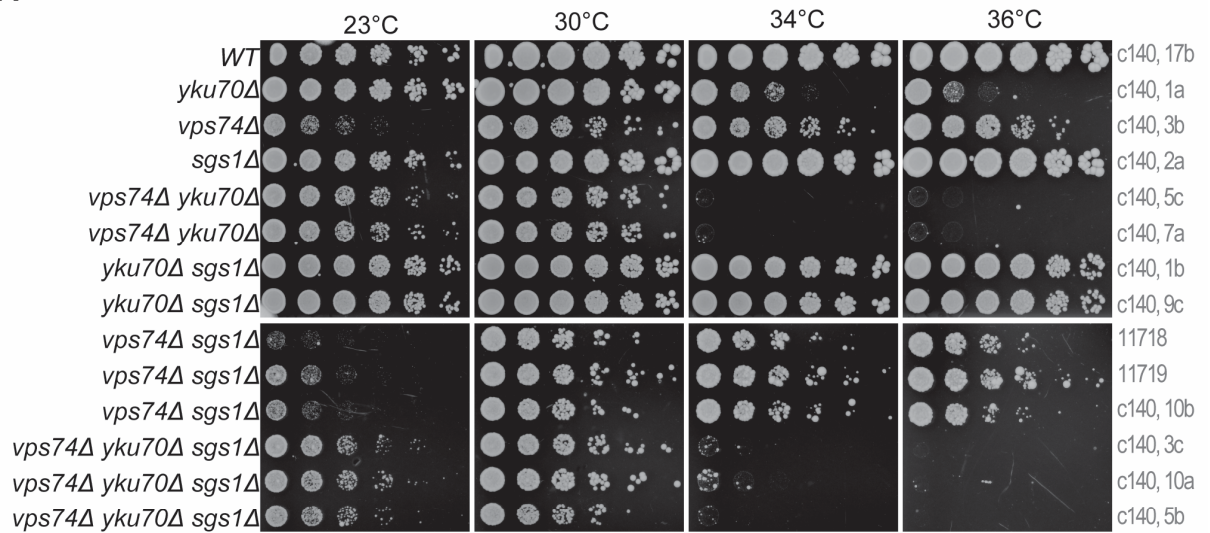
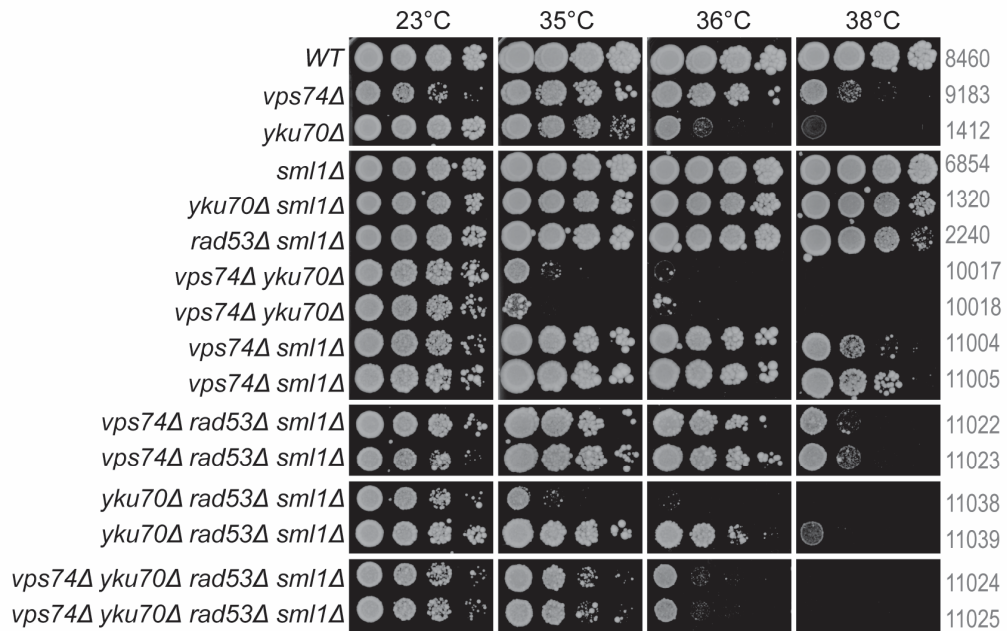
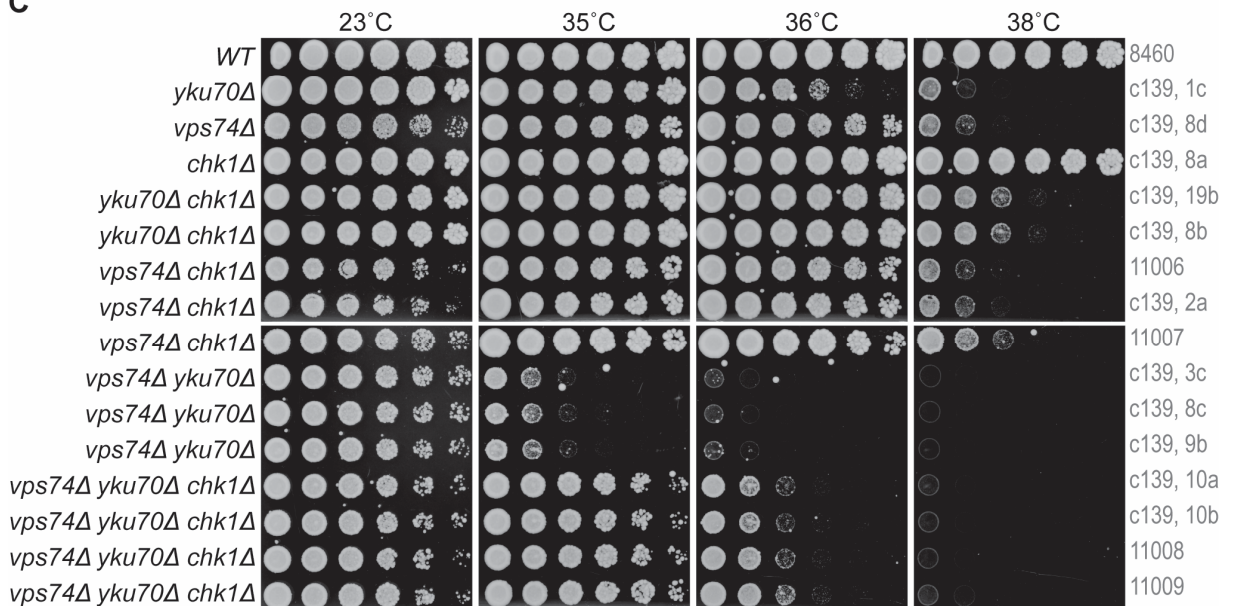
A**B****C**

Figure 4-9 *rad53Δ* and *chk1Δ* suppress *yku70Δ vps74Δ* fitness defects. A-C) Saturated cultures of the genotypes indicated were serially diluted across YEPD agar plates and grown for 3 days at the temperatures indicated. All strains at each temperature were grown on a single plate but have been cut and pasted to allow better comparisons. When the strain number is not shown, the number of the spore and the cross is shown. These strains were not frozen, but the phenotype is representative of the genotype.

I conclude that Rad53 and Chk1 decrease the fitness of *yku70Δ vps74Δ* cells but do not affect *vps74Δ* cell fitness. I suggest that the poor fitness of *vps74Δ yku70Δ* cells is due to the activation of the checkpoint pathway that involves Rad53 and Chk1. I also see evidence that *vps74Δ* cells itself do not strongly activate Rad53 and Chk1.

4.2.8. Vps74 contributes to genome stability

Table 4-1 shows the genetic interactions described in the previous sections of this Chapter. It is clear that fitness of *vps74Δ* cells is dependent on DDR proteins (or vice versa), with *mre11Δ* and *rad27Δ* enhancing *vps74Δ* fitness defects. Suppressors of *vps74Δ* comprise *exo1Δ*, *sae2Δ*, *rad24Δ* and *mec1Δ*. Although the synthetic sickness between *yku70Δ* and *vps74Δ* can additionally be suppressed by *chk1Δ* and *rad53Δ*, those suppressors are also strong suppressors of *yku70Δ* sickness. This could suggest that lack of Vps74 exacerbates the fitness defects of *yku70Δ* cells, and that the fitness defects observed in *yku70Δ vps74Δ* cells are mainly due to the disruption of Yku70-related functions. This could happen if *vps74Δ* cells have DNA damage that is dependent on Yku70 to be efficiently repaired. The role of Vps74 in the DDR could be direct or indirect, for example by promoting the transport and maturation of relevant proteins.

Table 4-1 Genetic interactions between *vps74Δ* or *vps74Δ yku70Δ* and members of the DDR. Summary of the effects observed in the spot tests presented in this Chapter. The effects several deletions (first column) in the fitness of *WT*, *yku70Δ*, *vps74Δ* or *yku70Δ vps74Δ* cells (header) are shown. *WT* growth was considered to be +++++, cells that grow better than the respective header will have more "+" (shaded green) and cells that grow worse than the respective header will have less "+" (shaded red). Blue means that phenotype was inferred from the literature. N.d., not determined.

	<i>WT</i>	<i>yku70Δ</i>	<i>vps74Δ</i>	<i>vps74Δ yku70Δ</i>
<i>rad9Δ</i>	+++++	+++++	+++++	N.d.
<i>exo1Δ</i>	+++++	+++++	+++++	+++++
<i>rad17Δ</i>	+++++	+++++	+++++	N.d.
<i>rad24Δ</i>	+++++	+++++	+++++	N.d.
<i>mre11Δ</i>	+++	+	+	+
<i>sae2Δ</i>	+++++	++++	+++++	+++++
<i>rad27Δ</i>	++++	++	++	++
<i>mec1 sml1Δ</i>	+++++	+++++	+++++	+++++
<i>rad53 sml1Δ</i>	++++	+++++	+++++	+++++
<i>sgs1Δ</i>	+++++	+++++	+++++	+++++
<i>chk1Δ</i>	+++++	+++++	+++++	+++++

4.2.9. Vps74 is potentially phosphorylated by Rad53

The mammalian Vps74 (GOLPH3) is phosphorylated by DNA-PK upon DNA damage leading to Golgi dispersal (Farber-Katz et al. 2014). In yeast, Vps74 has not yet been associated with DNA damage, but Vps74 seems to have many potential sites that could be phosphorylated upon DNA damage (Cherry et al. 2012). Table 4-2 shows 30 potential phosphorylation sites that I found bioinformatically (the 30 more likely, out of 39). It is interesting to find that my analysis retrieved Rad53, a DNA damage checkpoint, as a potential kinase.

Other kinases comprise the WEE kinase group (Swe1), the Haspin kinase group (Alk1 and Alk2) and the CAMKL group (Kin4 and Kin2). The three kinase groups have been directly or indirectly associated with the DDR: Swe1 was shown to have checkpoint function by delaying mitosis through a repressive phosphorylation of Cdc28 (Booher et al. 1993); Alk1 and Alk2 are phosphorylated upon DNA damage (Nespoli et al. 2006); and members of the CAMKL group of kinases were also shown to take part in checkpoint signalling pathways involving cellular division (D'Aquino et al. 2005). CK1 (Yck1 and Yck2), a casein kinase, was also found to potentially

phosphorylate a considerable number of Vps74 sites. Yck1 and Yck2 are bound to the plasma membrane and are most known to respond to glucose changes (Vancura et al. 1993; Vancura et al. 1994; Reddi and Culotta 2013).

The bioinformatics analysis of Vps74 potential phosphorylation sites strengthens the idea that Vps74 might be modified in the response to nuclear cues. Vps74 modifications would activate a downstream signalling pathway in order to respond to those nuclear cues.

Table 4-2 Vps74 potential phosphorylation sites. Group-based Prediction System (GPS) v3.0 software (available online at <http://gps.biocuckoo.org/>) was used to find potential kinase phosphorylation sites using the Vps74 amino acid sequence available in SGD (Xue et al. 2008; Cherry et al. 2012). Position: the position of the site which is predicted to be phosphorylated; Code: the residue which is predicted to be phosphorylated; Kinase: the regulatory kinase which is predicted to phosphorylate the site; Peptide: the predicted phosphopeptide with 7 amino acids upstream and 7 amino acids downstream around the modified residue; Score: the value calculated by GPS algorithm to evaluate the potential of phosphorylation. Results are organized in descending order according to the score values. In red are the sites that were previously reported as being phosphorylated in SGD (not necessarily by the kinases identified by the software).

Position	Code	Kinase	Peptide	Score
260	Y	WEE	LALICGSYGANVLEN	14
2	S	CK1	*****MSTLQRRRV	11.631
196	T	Haspin	VDKGVLRTEMKNFFL	11
27	T	Haspin	IHSSANNTKGDKIAN	10
116	S	PEK	KIRILDDSARKRFDL	9.909
339	S	CK1	AGVFEVFSRMDMLL*	9.7
14	S	CAMKL	RRVNRADSGDTSSIH	9.535
226	S	RAD53	AIKRRVLSVLVSRNM	9.453
136	T	NAK	EVIDSSKTGEVLLDE	9.4
226	S	CAMKL	AIKRRVLSVLVSRNM	9.203
236	S	CAMKL	VSRNMELSYNEYFPE	9.028
237	Y	AGC	SRNMELSYNEYFPET	8.667
270	T	RAD53	NVLENLTTLEYEKR	8.528
19	S	CK1	ADSGDTSSIHSSANN	8.508
2	S	CK1	*****MSTLQRRRV	6.993
56	S	NEK	IAYDPEESKLRDNIN	6.393
259	S	WEE	TLALICGSYGANVLE	6.333
124	S	Bud32	ARKRFDLSERLIEVI	6.25
157	S	Bud32	NDEPLSISNWIDLLS	6.25
307	S	CK1	KETELGVSVNLNKEV	6.007
18	S	CK1	RADSGDTSSIHSSAN	5.986
18	S	PLK	RADSGDTSSIHSSAN	5.708
2	S	RSK	*****MSTLQRRRV	5.183

133	S	ULK	RLIEVIDSSKTGEVL	5.077
282	S	RSK	EKRDKAISRAEEIMA	4.915
19	S	PLK	ADSGDTSSIHSSANN	4.682
56	S	PLK	IAYDPEESKLRDNIN	4.636
22	S	STE11	GDTSSIHSSANNTKG	3.318
14	S	CAMK	RRVNRADSGDTSSIH	2.752
292	S	STE	EEIMAQFSQYPFDE	2.36

4.2.10. Vps74 and Sac1 contribute to cell fitness through independent pathways

It was suggested that Vps74 is involved in the DNA damage response, either causing the damage, or contributing to its repair (Table 4-1). However, Vps74 is a cytoplasmic protein, mainly described as a sensor of PtdIns4P that activates Sac1 by physically interacting with Sac1. Therefore, it is extremely unlikely that Vps74 plays a direct role at the nucleus to aid DDR (however it cannot be excluded that Vps74 could translocate to the nucleus upon a stimulus). There are at least 3 major pathways through which Vps74 might affect the DNA damage response: 1) DDR protein maturation; 2) Inositol signalling; 3) Vps74 might be an active player in a signal transduction pathway that affects DDR.

The fact that Vps74 affects maturation/levels of DDR proteins is not likely since proteins that are known to affect protein maturation in Golgi were not found to behave like *vps74Δ* in high-throughput screens (Addinall et al. 2011). The hypothesis that Vps74 affects the DDR through the inositol signalling would likely depend on Sac1, since Sac1 is the protein that effectively acts over the PtdIns4P pool. Although in the *Saccharomyces* Genome Database *sac1Δ* and *vps74Δ* do not share many characteristics (*sac1Δ* cells seem to have more extensive fitness defects), it is still possible that Vps74 and Sac1 work together just in one pathway, but still affect other pathways independently. Therefore, to test whether Vps74 is affecting the DDR, in the nucleus, by affecting the inositol signalling, Sac1 was deleted in an *yku70Δ vps74Δ exo1Δ* background (Figure 4-10).

Figure 4-10 clearly shows that *vps74Δ* and *sac1Δ* are synthetically sick. The poor fitness of *vps74Δ sac1Δ* cells is already observable during spore germination (Figure 4-10A). Even at 23°C *vps74Δ sac1Δ* cells show very low fitness, which is not affected by deletions of *YKU70* and/or *EXO1* (Figure 4-10B). This result clearly shows that Vps74 and Sac1 are in different pathways to maintain the fitness of yeast cells.

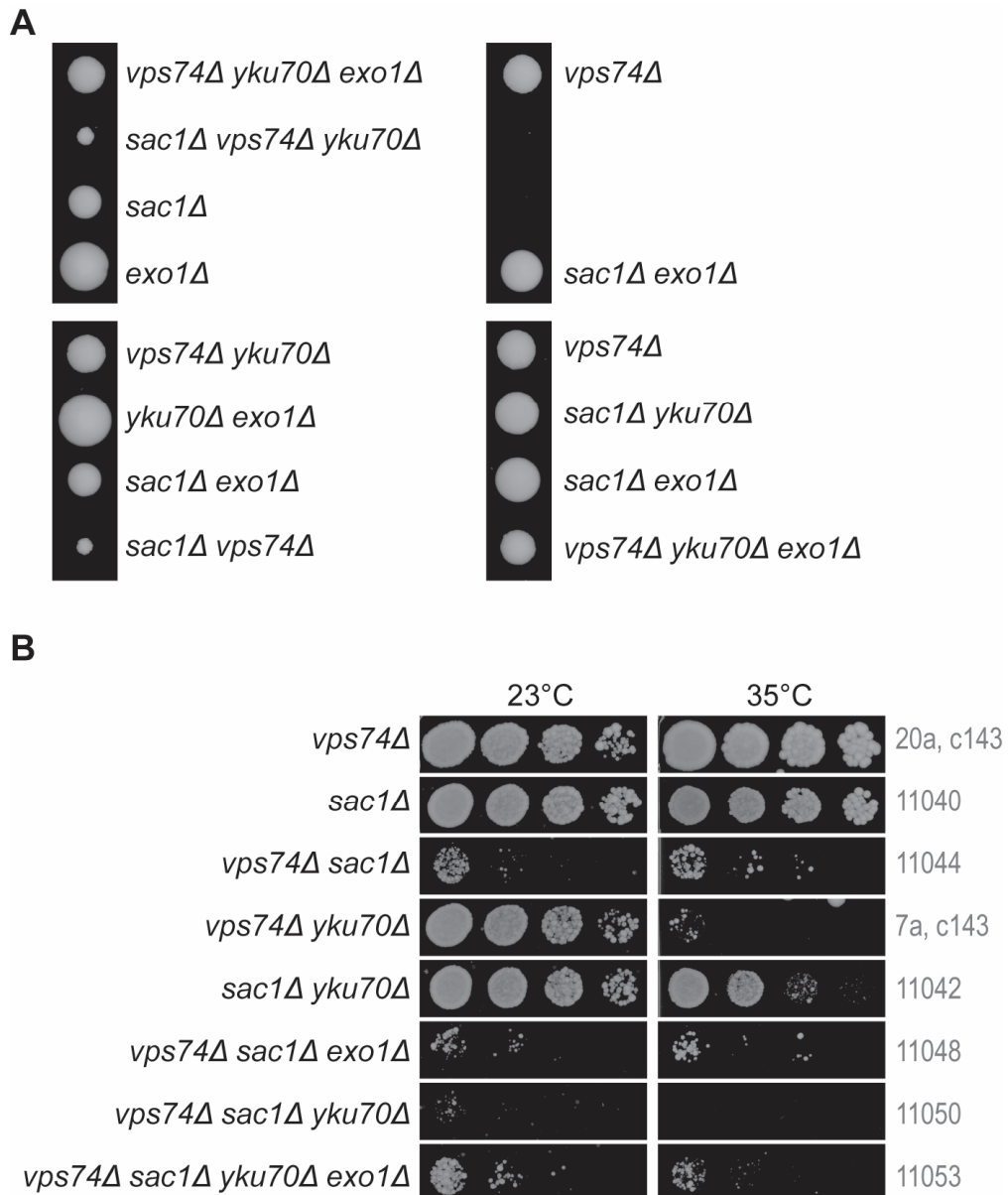


Figure 4-10 *vps74Δ* and *sac1Δ* are synthetically sick. **A)** Diploids were sporulated and spores were separated by tetrad dissection and plates were incubated for 5 days at 23°C before photographing. Representative colonies of each genotype are shown. **B)** Saturated cultures of the genotypes indicated were serially diluted across YEPD agar plates and grown for 3 days at the temperatures indicated. All strains at each temperature were grown on a single plate but have been cut and pasted to allow better comparisons. When the strain number is not shown, the number of the spore and the cross is shown. These strains were not frozen, but the phenotype is representative of the genotype.

Furthermore, *yku70Δ vps74Δ* are less fit than *yku70Δ sac1Δ* at 35°C, suggesting that Vps74 has a role in telomere defective cells that is independent of Sac1. Additionally, *SAC1* deletion enhances *yku70Δ* fitness defects, but not as strongly as *VPS74* deletion. Since Vps74 affects Sac1 activity, and therefore affects inositol levels, but Vps74 plays a stronger role maintaining *yku70Δ* cell fitness than Sac1, it is likely that Sac1 too affects *yku70Δ* fitness independently of the inositol pathway. Sac1 is perhaps important for the maturation of DDR-related proteins.

I conclude that Vps74 and Sac1 act in parallel to maintain cell fitness. Thus, Vps74 role in DDR/telomere biology is likely independent of the inositol pathway. I also showed that Sac1 is needed for the fitness of *yku70Δ* cells. Consequently, both Vps74 and Sac1 contribute to the fitness of *yku70Δ*, and are simultaneously needed for the fitness of *WT* cells.

4.2.11. Deletion of *SAC1* affects tryptophan intake

When I first deleted *SAC1*, I used a hygromycin (*HYG*) marker to replace the *SAC1* ORF. At the same time, and in the same diploids *SAE2* was also deleted with a tryptophan (*TRP1*) marker. After diploid sporulation and tetrad dissection, I noticed that *sac1::HYG* cells were extremely unfit and originated small colonies and *sac1::HYG sae2::TRP1* cells were much fitter (Figure 4-11, red *versus* green). Although this seemed a very exciting result, *sac1::HYG* extensive fitness defects were not suppressed by *exo1::LEU2* (or any other gene I deleted without the *TRP1* marker). Additionally, *SAC1* mutants were shown to have low levels of membrane phosphatidylserine (PS) (Tani and Kuge 2014). Low PS, in turn, affects tryptophan uptake from the surrounding environment, which leads to tryptophan insufficiency when the cell cannot internally produce tryptophan (Nakamura et al. 2000). I therefore hypothesized that *sac1::HYG* cells are sick because they lack tryptophan and that *sae2::TRP1* suppresses *sac1::HYG* fitness defects due to the *TRP1* marker (and the capacity to synthesise tryptophan) and not loss of Sae2 function.

To test if *sac1Δ* cells are defective in tryptophan uptake I compared the growth of *sac1::HYG* (with and without extra tryptophan supplementation in the medium) to *sac1::TRP1* (Figure 4-12). Indeed *sac1::HYG* (c127) grow worse than *sac1::TRP1* (c142) (compare the small colonies to the big colonies within each cross).

Supplementation of *sac1::HYG* cells with 10 mg/mL tryptophan slightly increased colony size, but colonies kept growing significantly slower than wild-type colonies. Importantly, there is no evidence that *vps74Δ* cells have any issue uptaking tryptophan neither in the literature nor in my results. For example *vps74Δ yku70Δ* fitness defects are suppressed by *exo1::LEU2* and *exo1::URA3*, while *sac1::HYG* fitness defects could only be suppressed by the presence of the *TRP1* marker.

I conclude that the fitness of *sac1Δ* cells is affected by the *TRP1* marker suggesting defects in tryptophan uptake. Therefore, to avoid fitness defects related to tryptophan levels, *SAC1* should be deleted with the *TRP1* marker to allow cells to produce tryptophan.

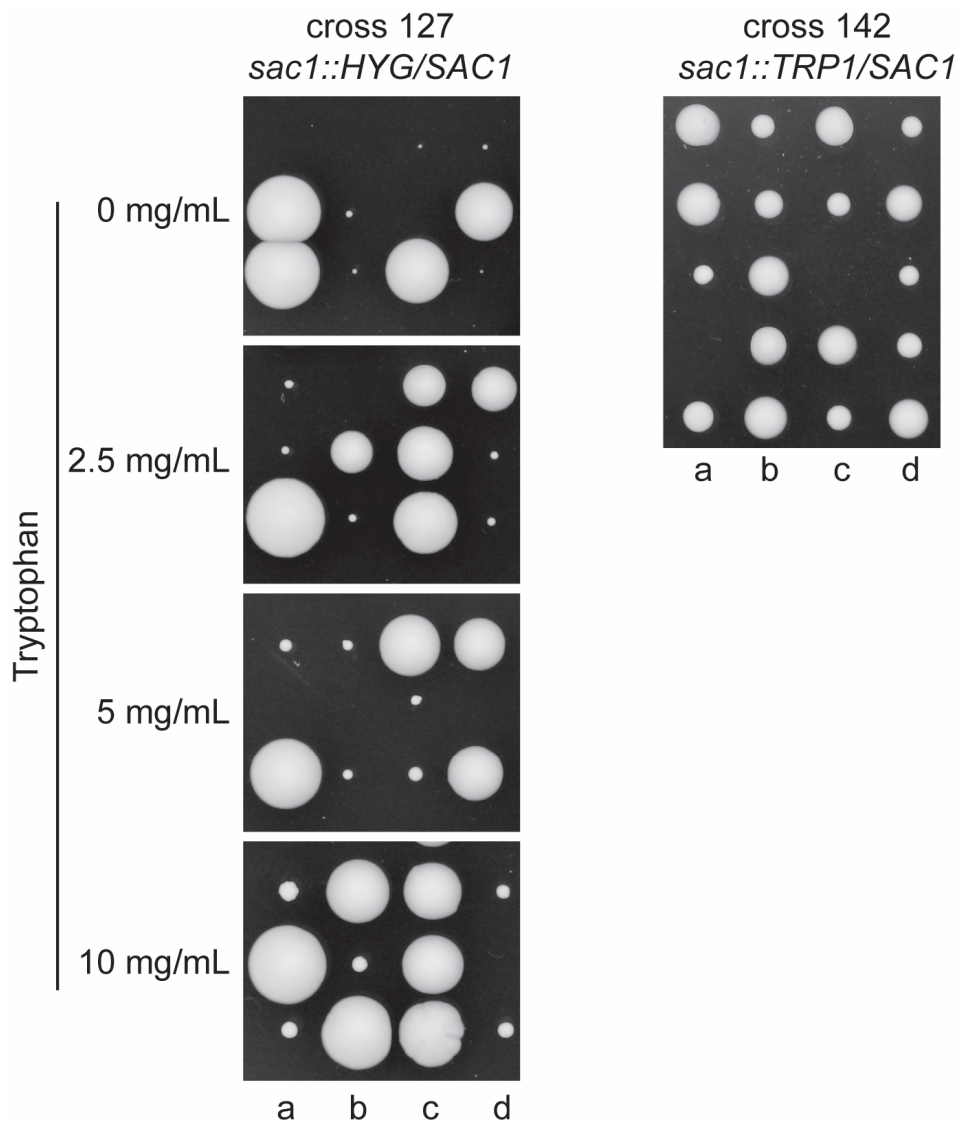


Figure 4-12 *SAC1* deletion affects the cell capacity to uptake tryptophan from the medium. Diploids were generated by deleting *SAC1* with a hygromycin (c127) or a tryptophan (c142) marker. Spores were separated by tetrad dissection and plates were incubated for 10 (c127) or 5 (c142) days at 23°C before photographing. Spores from c127 were also dissected onto plates supplemented with 200 μ L of a 2.5 mg/mL, 5 mg/mL or 10 mg/mL L-tryptophan solution.

4.3. Discussion/Conclusion

The work in this Chapter showed that Vps74 plays an important role maintaining cell fitness and evidence that in Vps74 absence the DDR is activated. A strong genetic interaction between *vps74Δ* and *yku70Δ*, together with a milder interaction between *vps74Δ* and *cdc13-1*, suggested a role for Vps74 at telomeres. *VPS74* role at telomeres, and indeed in DDR, was especially provocative due to the fact that Vps74 is not a nuclear protein and up to date no role for the yeast protein has been suggested at telomeres. Unfortunately, it was not possible to separate a telomeric role of Vps74 from a role elsewhere in the genome. Actually, the data here presented points towards a more general role of Vps74 in maintaining genome integrity throughout the genome. This is in agreement with the notion that GOLPH3 (Vps74 mammalian orthologue) is an oncogene since *GOLPH3* overexpression could for example improve cellular fitness.

How Vps74 would contribute to the maintenance of genomic stability is not clear, but mammalian data showed that increased GOLPH3 levels led to cancer (by activation of the mTOR signalling) (Scott et al. 2009). Interestingly, a yeast mTOR orthologue, TORC1 (Tor1 and Tor2), has been associated with telomere maintenance and DDR. For instance, TORC1 inhibition leads to telomere shortening and decreased Yku70 levels (Ungar et al. 2011). Also, rapamycin, a drug that inhibits TORC1, could strongly suppress *cdc13-1* fitness defects after the cells were exposed to 37°C and put back to 23°C (Klermund et al. 2014). Such effect of rapamycin on *cdc13-1* cell fitness was related to the maintenance of checkpoint proteins in an active (phosphorylated) state to prevent adaptation/cell division while the cells were at non-permissive temperatures (Klermund et al. 2014). Interestingly, *vps74Δ* weakly suppresses *cdc13-1* fitness defects, in agreement with less active TORC1 caused by *VPS74* deletion. In *yku70Δ vps74Δ* cells, prolonged checkpoint activation would perhaps justify the poor fitness and the reason why deletion of checkpoint proteins suppress the fitness defects. Another more general role for a TORC2 (Tor2) pathway is to maintain genome stability upon mild DSB induction (Weisman et al. 2014). This role is in agreement with a model where Vps74 and Tor2 (and Tor1) collaborate to maintain genome stability. The fact that *vps74Δ* cells show mild fitness defects even at 23°C might suggest slower division/prolonged cell cycle. Prolonged cell cycle could happen if cell checkpoints are being activated by DNA damage.

Vps74 is a cytoplasmic protein, thus a direct role of this protein in the nucleus is unlikely. However, like its human orthologue, it might act as a signal transducer for the DNA damage response. If Vps74 was indeed part of a DNA damage signalling pathway, lack of Vps74 activation could lead to prolonged DNA damage (TORC1 activation for instance), perhaps due to delays in the response or lack of activation of the DDR effector proteins. Bioinformatic analysis of Vps74 phosphorylation sites revealed 39 potential sites (Table 4-2). Indeed Vps74 might be a direct target of Rad53, which also has a small presence in the cytoplasm (Table 4-2) (Smolka et al. 2006). It is therefore possible that Vps74 is important for an effective DDR, being part of signalling cascade. Further work will be required to understand the role of Vps74 in the DDR.

Vps74 has also a small effect on telomere length of *yku70Δ* telomere defective cells. Since *vps74Δ* cells do not have short telomeres, Vps74 role at telomeres is dependent on Yku70 absence. A possible explanation is that *vps74Δ* cells accumulate DNA damage sites and the DDR proteins (including Tel1, for example) are mobilized to those DNA damage sites throughout the genome. A redistribution of some DDR proteins from the telomere to the genome in cells with uncapped telomeres (*yku70Δ* cells) might leave the telomere more prone to resection and less prone to amplification. Such redistribution was already shown to happen upon replication stress and DNA damage, with fluorescent microscopy analysis revealing relocation of checkpoint proteins and the Sir complex (Martin et al. 1999; Tkach et al. 2012).

The results here described suggest that Vps74 is involved/affects the DDR (Figure 4-13). I suggest that Vps74 is part of a signalling pathway that responds to naturally occurring DNA lesions (replicative damage or telomere shortening, for example). Lack of Vps74 would therefore delay the repair of the DNA lesions or just prolong the activation of the DNA damage checkpoints (through the TORC1 pathway, for instance). Lack of Vps74 activity could therefore lead to accumulation of unfixed DNA lesions.

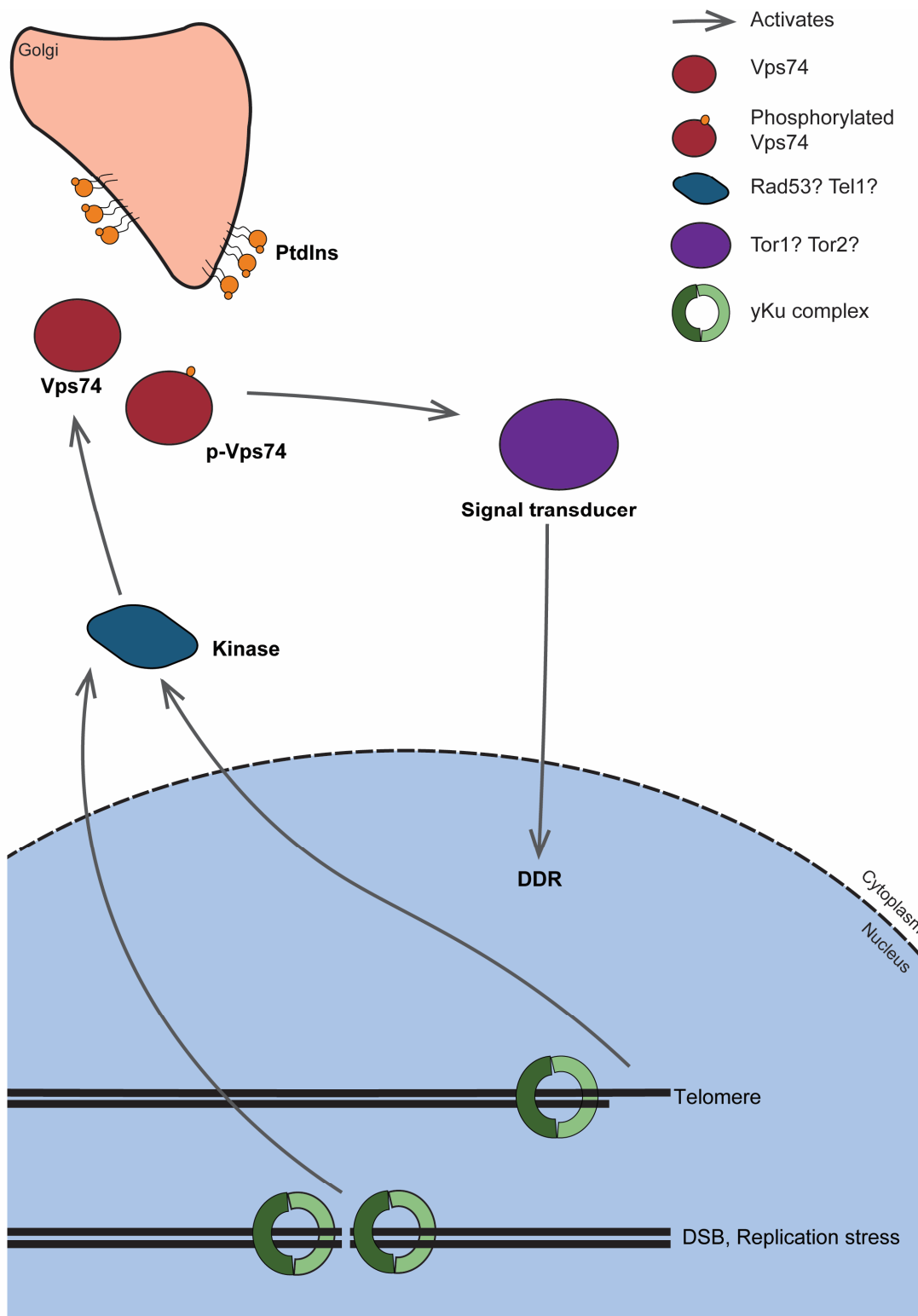


Figure 4-13 Model for a role of Vps74 in the DDR. Natural occurring DNA lesions (due to replicative stress) or uncapped telomere ends are recognised by the Ku complex. DNA checkpoints are activated and Vps74 is phosphorylated (p-Vps74) by a kinase like Rad53, Yck1/Yck2, Alk1/Alk2, etc. p-Vps74 would then initiate a signal transduction signal, perhaps through the Tor1/Tor2 to aid the DDR. Vps74 might act to amplify the DNA response, without being essential for it.

4.4. Future work

The interactions of *VPS74* to various members of the DDR relate *Vps74* to the DDR pathway. It is still unclear if lack of *Vps74* causes DNA damage to induce the DDR or if it disrupts an efficient DDR. A way of testing if lack of *Vps74* is causing DNA damage is to, by western-blot, test the phosphorylation states of Rad53 and histone H2A in *vps74Δ* cells (with and without deletions of the genes here found to genetically interact with *vps74Δ*). Pulse-field gel could also be helpful to detect any major chromosomal abnormalities caused by the proposed genomic instability in *Vps74*-defective cells.

To test whether *Vps74* is involved in the DNA damage response, CPT, MMS, HU, UV resistance of *vps74Δ* cells could be tested and later compared to the resistance of the double and triple mutants containing *vps74Δ* generated in this work. Additionally, to test whether *Vps74* affects genetic stability through the Tor1/Tor2 pathway, *vps74Δ* cells could be exposed to rapamycin. If the Tor1/Tor2 pathway is functional, addition of rapamycin should further decrease cell fitness.

Moreover, since GOLPH3 is phosphorylated in mammalian cells and *Vps74* has many potential phosphorylation sites, *Vps74* phosphorylation could be tested. A possible way of testing *Vps74* phosphorylation is to tag the protein, and search for a gel shift by western blot (using anti-tag antibodies). It would be interesting to see if *Vps74* is phosphorylated in *yku70Δ* cells and upon exposure to DNA damaging agents. Additionally, how this phosphorylation would change with the deletions that suppress *vps74Δ yku70Δ* fitness defects could also be addressed. Mutation of hypothetical phosphorylation sites in *Vps74* followed by spot test assay could also indicate if *Vps74* lack of phosphorylation is responsible for the fitness defects observed in *vps74Δ* cells. *Vps74* phosphorylation upon DNA damage would strongly suggest this protein as part of the DDR.

vps74Δ decreased the fitness of otherwise wild-type cells and *yku70Δ* cells. In humans, cancers often show overexpressed GOLPH3 (*VPS74* orthologue), which confer them resistance to DNA damaging agents (Buschman et al. 2015). It would be interesting to see if *VPS74* overexpression in *WT* and telomere defective cells would also increase its fitness and resistance to DNA damage agents. If so, further studies in yeast could be very helpful for the design of treatment strategies in GOLPH3-positive cancers.

Another useful tool to find a place for Vps74 (together with Yku70) in the DDR is to perform a genome wide-screen (SGA, synthetic genetic array) to get a broader view of the genetic interactions of *vps74Δ* vs *yku70Δ* vs *yku70Δ vps74Δ*. Such experiment would allow the identification of the proteins (or functional group) that contribute to the fitness of *vps74Δ* cells.

Finally, it would be interesting to see how *vps74Δ* cells die or arrest at 38°C. A simple microscopic examination with DAPI staining of *vps74Δ* cells at 30°C versus 38°C could help define in which cell-cycle phase the cells arrest/die. Knowing when the cells arrest/die would help to characterize Vps74 functions in DDR. For example, if cells arrest with a dumbbell shape, that might suggest telomere dysfunction.

5. Adjacent gene effect reveals synthetic genetic interactions between the PAF1 complex and the ESCRT machinery

5.1. Introduction

The PAF1 complex is an important and widely conserved protein complex, with many reported functions that affect transcript levels (Tomson and Arndt 2013). Cdc73 was shown to have a role in telomere defective cells (Figure 3-1). Cdc73 together with Paf1, Ctr9, Rtf1 and Leo1, is part of the yeast PAF1 complex (Mueller and Jaehning 2002). In the human PAF1 complex, hRtf1 is not stably associated with the complex which contains instead hSki8 (Figure 5-1A) (Zhu et al. 2005; Chu et al. 2013).

5.1.1. The PAF1 complex and transcription regulation

The PAF1 complex was first identified as a complex that binds RNA pol II (Wade et al. 1996). It localizes in the nucleus where it is involved in transcriptional regulation (Squazzo et al. 2002; Chen et al. 2009; Kim et al. 2010; Crisucci and Arndt 2011), histone modifications (Krogan et al. 2003a), control of Poly(A) site utilization (Penheiter et al. 2005), etc. The PAF1 complex was also associated with the generation of double-stranded breaks during meiosis and regulation of promotor proximal pausing by RNA pol II (Chen et al. 2015; Gothwal et al. 2015; Yu et al. 2015). In fission yeast, the PAF1 complex was associated with repression of small-RNA-mediated epigenetic gene silencing (Kowalik et al. 2015). In budding yeast, reduced levels of *TLC1* RNA (RNA template required for telomerase function) in *cdc73Δ*, *paf1Δ* or *ctr9Δ* cells suggested that loss of telomerase RNA might contribute to the cell growth defects of cells depleted of the PAF1 complex components (Singer and Gottschling 1994; Betz et al. 2002). Consistent with this, growth and telomere length defects of cells depleted of the PAF1 complex components could be partially recovered by *TLC1* overexpression (Betz et al. 2002).

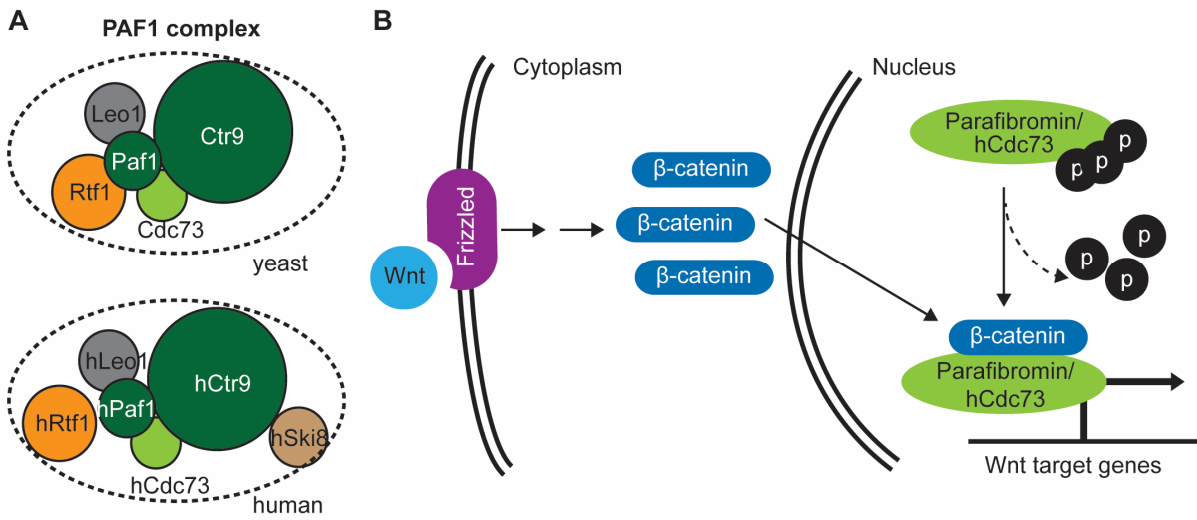


Figure 5-1 The PAF1 complex is conserved between yeast and humans and is involved in the Wnt pathway. A) Cartoons representing the composition of the PAF1 complex in yeast and human cells (Tomson and Arndt 2013). **B)** Cartoon illustrating the role of Cdc73 in Wnt signalling. Cdc73 dephosphorylation allows binding to β -catenin, helping to induce transcription of Wnt target genes. Other members of the complex are thought to stabilize Cdc73- β -catenin interaction (Takahashi et al. 2011a).

5.1.2. The PAF1 complex and cancer

The PAF1 complex has been implicated in cancer biology since mutations in the human *CDC73* can cause cancer (Gonzalez-Perez et al. 2013). For instance, mutations in human *CDC73* (*HRPT2*, that encodes Parafibromin) lead to hyperparathyroidism-jaw tumour syndrome (HPT-JT), parathyroid carcinoma and familial isolated hyperparathyroidism (FIHP) (Jackson et al. 2015; Verdelli et al. 2015). The *Cdc73* orthologue in *Drosophila melanogaster* has been shown to play an important role in the canonical Wnt signalling pathway by directly associating with Armadillo (β -catenin orthologue in *Drosophila*) (Figure 5-1B) (Mosimann et al. 2006). Co-immunoprecipitation studies have also suggested an indirect interaction between *Leo1* and β -catenin, suggesting a role for the whole PAF1 complex in the Wnt signalling pathway, which is known to be mutated in cancers (Mosimann et al. 2006; MacDonald et al. 2009).

5.1.3. Different roles for different PAF1 complex components

Although *Cdc73*, *Paf1*, *Ctr9*, *Rtf1* and *Leo1* form a protein complex, deletion of individual PAF1 complex components differently affect the cellular levels of the remaining complex members: *Ctr9* loss leads to a decrease of *Paf1*, *Rtf1* and *Leo1*; *Paf1* loss leads to a decrease of *Rtf1*, *Ctr9* and *Cdc73*; *Cdc73* loss causes a decrease of *Rtf1*; while neither *Rtf1* nor *Leo1* loss affect the levels of the other members of the complex (Mueller et al. 2004). Structural studies have revealed *Ctr9* as the scaffold protein for the PAF1 complex in humans, while studies in yeast revealed that upon *CDC73* or *RTF1* deletions the other members of the complex remain associated with each other but do not associate to RNA pol II (Nordick et al. 2008; Chu et al. 2013).

Deletion of individual PAF1 complex members in yeast leads to distinct phenotypes (Betz et al. 2002). For example, *ctr9 Δ* and *paf1 Δ* cause similarly severe growth defects, *cdc73 Δ* and *rtf1 Δ* cause mild growth defects and *leo1 Δ* causes no growth defects (Betz et al. 2002). Since both *Rtf1* and *Cdc73* are required for the association of the PAF1 complex with RNA pol II but their deletion does not cause extensive growth defects it was suggested that a major role of the PAF1 complex is independent of RNA pol II related functions (Mueller and Jaehning 2002; Mueller et al. 2004). In humans, *hSki8* is a component of both PAF1 complex and the Ski

complex (which is needed for the exosome dependent 3'-5' mRNA decay) which reveals a connection between the PAF1 complex and RNA surveillance (Zhu et al. 2005).

5.1.4. *CDC73* and its adjacent gene, *VPS36*

In yeast, *CDC73* is adjacent to *VPS36*, and large-scale surveys have shown that *cdc73Δ* and *vps36Δ* strains share many characteristics, for example reduced telomere length (Askree et al. 2004), heat sensitivity (Betz et al. 2002; Sinha et al. 2008) and decreased resistance to hygromycin B and hydroxyurea (Betz et al. 2002; Dudley et al. 2005; Fell et al. 2011). For these reasons, it has been suggested that *CDC73* and *VPS36* might demonstrate a neighbouring gene effect, or in other words, that the deletion of the coding sequence of one gene affects the function of the other (Ben-Shitrit et al. 2012). *VPS36* is widely conserved among eukaryotes and encodes a protein that is part of the ESCRT (Endosomal Sorting Complexes Required for Transport)-II complex (Teo et al. 2004). The ESCRT-II complex is composed of Snf8, Vps25 and Vps36. The deletion of any of the ESCRT-II members causes short telomeres in *S. cerevisiae* (Rog et al. 2005).

The ESCRT machinery is composed of ESCRT-0 (Vps27 and Hse1), ESCRT-I (Stp22, Mvb12, Vps37 and Vps28), ESCRT-II and ESCRT-III (Snf7, Vps20, Vps24 and Did4) (Schuh and Audhya 2014). The main described function for the ESCRT complex is the remodelling of membranes, which is related to its role in the multivesicular body (MVB) pathway and cytokinesis (Schmidt and Teis 2012). One of the functions of the MVB pathway is to sort ubiquitylated membrane proteins for degradation in lysosomes (Schmidt and Teis 2012). During this process each of the ESCRT complexes assemble on endosomes in a sequential manner (Schmidt and Teis 2012). More recently the ESCRT III complex has been shown to be required for nuclear envelope repair after rupture caused by mammalian cell migration (Raab et al. 2016).

The main aim of this Chapter was to understand if a neighbouring gene effect occurred between *CDC73* and *VPS36* and was responsible, or partly responsible, for the phenotypic differences between *cdc73Δ* cells and cells carrying deletions of other components of the PAF1.

5.2. Results

5.2.1. The PAF1 complex affects telomere defective strains

Genome-wide screens showed *cdc73Δ* as an enhancer of *cdc13-1* fitness defects (Addinall et al. 2011). Additionally, *leo1Δ* and *rtf1Δ* had similar phenotype to *cdc73Δ* in the screen data (also as enhancers of *cdc13-1* fitness defects) (Figure 5-2). *LEO1*, *RTF1* and *CDC73* each encode members of the PAF1 complex (together with *CTR9* and *PAF1*), and the similarity of *leo1Δ*, *rtf1Δ* and *cdc73Δ* effects on *cdc13-1* cells strongly suggested a role for the PAF1 complex on telomere defective strains.

5.2.2. Members of the PAF1 complex interact differently with *cdc13-1*

In order to confirm and extend the high-throughput data, all five members of the PAF1 complex (*CDC73*, *PAF1*, *CTR9*, *RTF1* and *LEO1*) were deleted in a different genetic background (W303) (Figure 5-3). The knockouts were created in diploid cells heterozygous for *cdc13-1* and *rad9Δ* (Figure 5-3A) so that after sporulation and tetrad dissection one could clarify the role of PAF1 complex when telomeres and/or when DNA damage checkpoint pathways are defective. *RAD9* encodes a DNA damage checkpoint protein, part of the DNA damage response (DDR), and its deletion suppresses *cdc13-1* fitness defects (Weinert and Hartwell 1993).

Analysing the colonies derived from each germinated spore it was noticed that *cdc73Δ*, *leo1Δ* and *rtf1Δ* spores formed bigger colonies than *paf1Δ* and *ctr9Δ* spores (squares in Figure 5-3B). This is in agreement with previous reports, which showed that *paf1Δ* and *ctr9Δ* cells have much more pronounced growth defects than *cdc73Δ*, *leo1Δ* and *rtf1Δ* cells (Betz et al. 2002). Deletion of *RAD9* had no noticeable effect on the fitness of strains with PAF1 complex deletions (pentagons in Figure 5-3B), suggesting that the growth defects observed in the PAF1 complex deletion strains are likely not due to DNA damage. On the other hand, *cdc13-1* seemed to greatly enhance the *paf1Δ* and *ctr9Δ* growth defects while the effect on *cdc73Δ*, *leo1Δ* or *rtf1Δ* fitness was much milder (circles on Figure 5-3B). Triple mutants (triangles on Figure 5-3B), containing *cdc73Δ*, *leo1Δ* or *rtf1Δ* deleted in a *rad9Δ cdc13-1* background, revealed no consistent differences on colony size when compared to the other mutants shown (single and double mutants: squares, pentagons and circles on

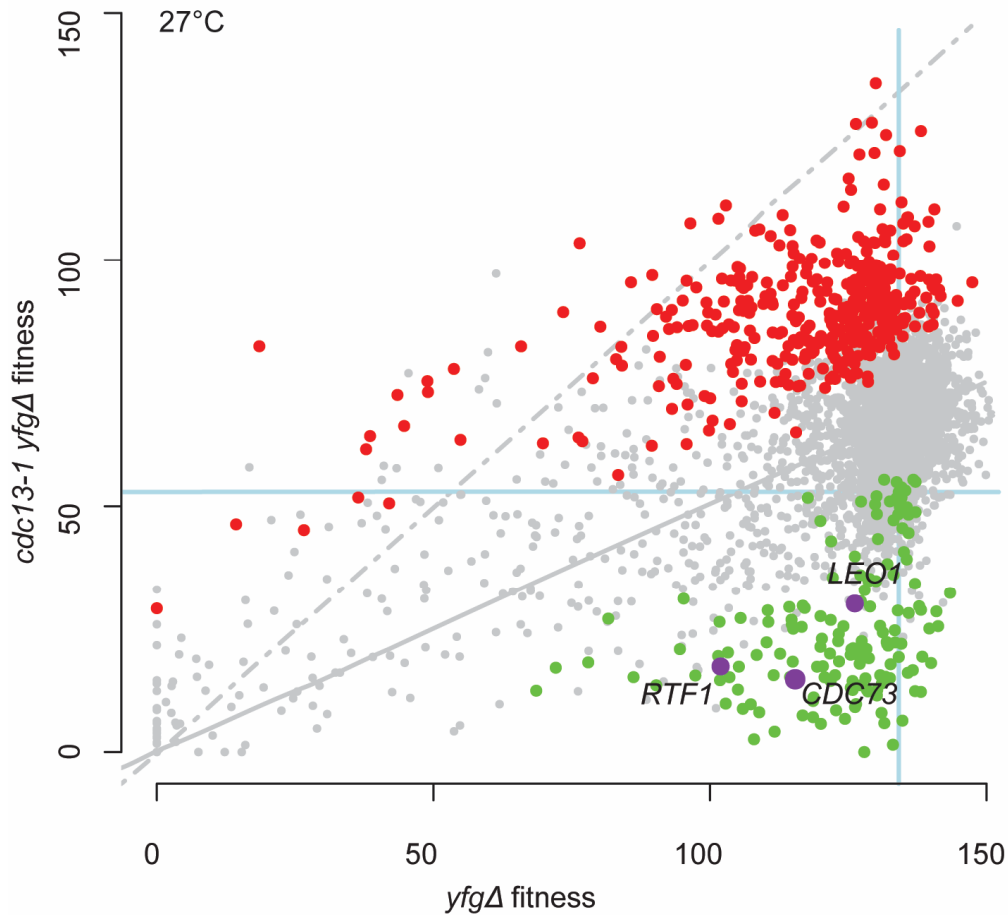


Figure 5-2 The *PAF1* complex affects telomere defective strains. The yeast genome knock out collection (~4200 strains) was crossed with *cdc13-1* or *ura3Δ*. Double mutants were then grown on solid agar plates and the fitness was measured at 27°C (Addinall et al. 2011). Each dot indicates the effect of a gene deletion (*yfgΔ*) on the fitness of *cdc13-1* or *ura3Δ*. Represented by grey dots are all the deletions that did not significantly alter the fitness of *cdc13-1*. Green dots represent gene deletions that are enhancers of the *cdc13-1*, red dots are suppressors and the purple dots represent the fitness of *CDC73*, *RTF1* and *LEO1* deletions.

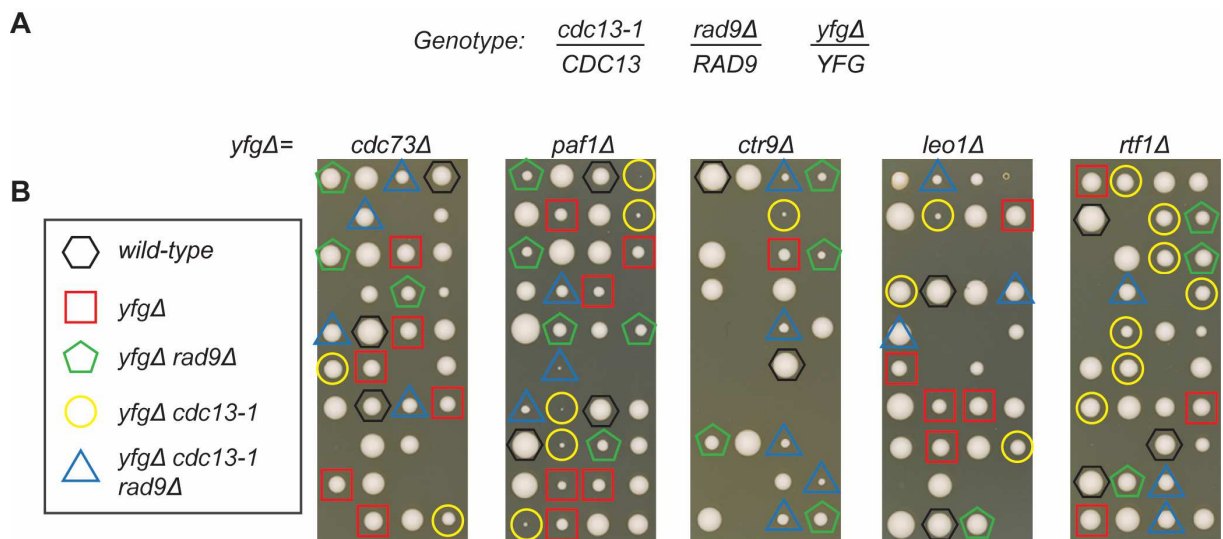


Figure 5-3 PAF1 complex genes interact differently with *cdc13-1*. **A)** One allele of each of the PAF1 complex members (*yfgΔ*: *cdc73Δ*, *paf1Δ*, *ctr9Δ*, *leo1Δ* or *rtf1Δ*) was deleted in diploid cells with the genotype *RAD9/rad9Δ CDC13/cdc13-1* (DDY227). **B)** Resulting diploids were sporulated and tetrads dissected onto YEPD plates. Germinated spores grew for 6 days at 23°C before being photographed.

Figure 5-3B). However, *paf1Δ rad9Δ cdc13-1* and *ctr9Δ rad9Δ cdc13-1* formed bigger colonies than *paf1Δ cdc13-1* and *ctr9Δ cdc13-1* respectively (triangles versus circles on Figure 5-3B). Since *rad9Δ* suppresses *cdc13-1* growth defects, the bigger colonies of *paf1Δ rad9Δ cdc13-1* and *ctr9Δ rad9Δ cdc13-1* when compared to *paf1Δ cdc13-1* and *ctr9Δ cdc13-1* are expected and confirm that *paf1Δ cdc13-1* and *ctr9Δ cdc13-1* poor fitness is indeed related to telomere defects (Weinert and Hartwell 1993).

Overall, these experiments revealed pronounced synthetic growth defects in *paf1Δ cdc13-1* and *ctr9Δ cdc13-1* strains, but not in *cdc73Δ cdc13-1*, *leo1Δ cdc13-1* or *rtf1Δ cdc13-1* strains, suggesting that *paf1Δ* and *ctr9Δ* strains are more sensitive to telomere defects than *cdc73Δ*, *leo1Δ* or *rtf1Δ*. The results in W303 strains clearly show that the deletion of different PAF1 complex components can have different effects on fitness of telomere defective *cdc13-1* cells.

5.2.3. Cdc73, Paf1 and Ctr9 induce *TLC1* RNA

cdc73Δ, *paf1Δ* and *ctr9Δ* were all previously shown to cause a decrease in *TLC1* (telomerase component 1) RNA levels and a corresponding decrease in telomere length in the BY and JJ yeast genetic backgrounds (Mozdy et al. 2008). In order to confirm that the same pattern is observed in the W303 genetic background, I measured *TLC1* RNA levels and telomere length in cells (W303 genetic background) with each of the PAF1 complex components deleted (Figure 5-4).

Deletion of *CDC73*, *PAF1* and *CTR9* caused a decrease in *TLC1* RNA to around 20%, while *LEO1* deletion decreased *TLC1* RNA to 40% and *RTF1* deletion halved *TLC1* RNA (Figure 5-4A). Accordingly, *leo1Δ* and *rtf1Δ* cells have seemingly normal telomeres while *cdc73Δ*, *paf1Δ* and *ctr9Δ* cells have short telomeres as observed in the Southern blot in Figure 5-4B. Between *cdc73Δ*, *paf1Δ* and *ctr9Δ* cells, *cdc73Δ* seem to cause the biggest decrease in telomere length, followed by *paf1Δ*, and finally by *ctr9Δ*.

I conclude that Cdc73, Paf1 and Ctr9 strongly regulate/induce *TLC1* levels while Leo1 and Rtf1 play a minor role. Consequently, cells lacking Cdc73, Paf1 or Ctr9 have short telomeres.

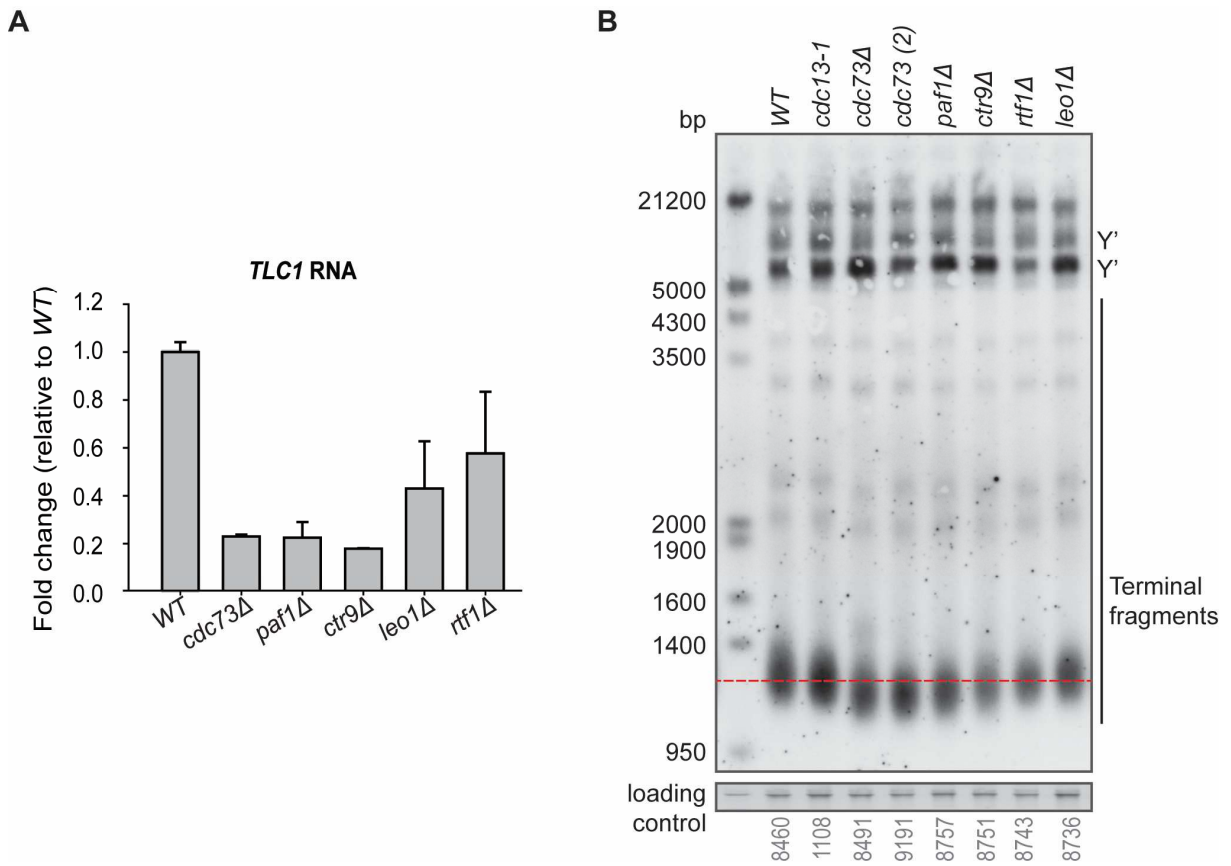


Figure 5-4 PAF1 complex increases *TLC1* RNA levels in W303. A) qRT-PCR analysis of *TLC1* RNA expression levels. RNA from two independent strains of each genotype was measured. The “error” bars indicate the means of the two strains analysed. Each value was normalized to the levels of *BUD6* mRNA (Addinall et al. 2011). *WT*: DLY8490, 3001; *cdc73Δ*: DLY8490, 8491; *paf1Δ*: DLY8757, 8758; *ctr9Δ*: DLY8751, 8752; *leo1Δ*: DLY8736, 8737; *rtf1Δ*: DLY8743, 8744. **B)** Telomeric Southern blot was performed using a probe against the Y'+TG sequence (Maringele and Lydall 2004) in order to analyse the telomere structure.

5.2.4. *TEN1* mRNA is increased in *paf1Δ* and *ctr9Δ* strains

paf1Δ, *ctr9Δ* and *cdc73Δ* mutations all reduce *TLC1* RNA levels to similar amounts, and have similar effects on telomere length, but *paf1Δ* and *ctr9Δ* strains most strongly enhance growth defects of telomere defective *cdc13-1* strains (Figure 5-3 and Figure 5-4). Therefore it was wondered if *paf1Δ*, *ctr9Δ* and *cdc73Δ* affected other relevant, telomere related, transcripts. mRNA levels of the three CST complex members, *CDC13*, *STN1* and *TEN1* were therefore measured (Figure 5-5A). Members of the PAF1 complex had little effect on *CDC13* mRNA. However, interestingly, *paf1Δ* and *ctr9Δ*, but not *cdc73Δ*, increased *TEN1* mRNA levels, with perhaps also a small increase in *STN1* mRNA. This effect of *PAF1* and *CTR9* on *TEN1* mRNA might contribute to the poor fitness caused by *paf1Δ* and *ctr9Δ* mutations in both *CDC13* and *cdc13-1* backgrounds (Figure 5-3B). Consistent with this idea increased Ten1 was shown to inhibit telomerase activity in yeast and plants (Qian et al. 2009a; Leehy et al. 2013).

To test if the high levels of *TEN1* in *paf1Δ* and *ctr9Δ* cells exacerbate the defects caused by lower levels of telomerase (due to reduced levels of *TLC1* RNA), leading to particularly poor growth of these strains, *TEN1* and *STN1* were expressed in *cdc73Δ* strains (Figure 5-5B). If higher *TEN1* levels, together with low *TLC1* RNA cause fitness defects in *paf1Δ* and *ctr9Δ* strains, and since *TLC1* levels are also low in *cdc73Δ* strains, one could expect that expressing *TEN1* in *cdc73Δ* strains, would decrease its fitness. However, no significant decrease in *cdc73Δ* strains expressing *TEN1* was found when compared to cells expressing the vector plasmid. The lack of effect after *TEN1* expression might be due to incapacity of the centromeric plasmid used to properly increase Ten1 levels. A very low decrease in fitness of cells expressing *STN1* from a 2 micron plasmid (when compared to the vector) can be seen at 23°C and 36°C. Since *STN1* is also reported to repress telomerase recruitment it seems that *cdc73Δ* strains slightly benefit from not having high levels of the CST components that repress telomerase recruitment (when compared to *paf1Δ* and *ctr9Δ*) (Grandin et al. 2000). The effects observed after expression of *STN1* are very modest, suggesting that the main factor(s) that cause *PAF1* or *CTR9* deletions to be much more harmful than *CDC73* deletion in cells with uncapped telomeres is still to be identified.

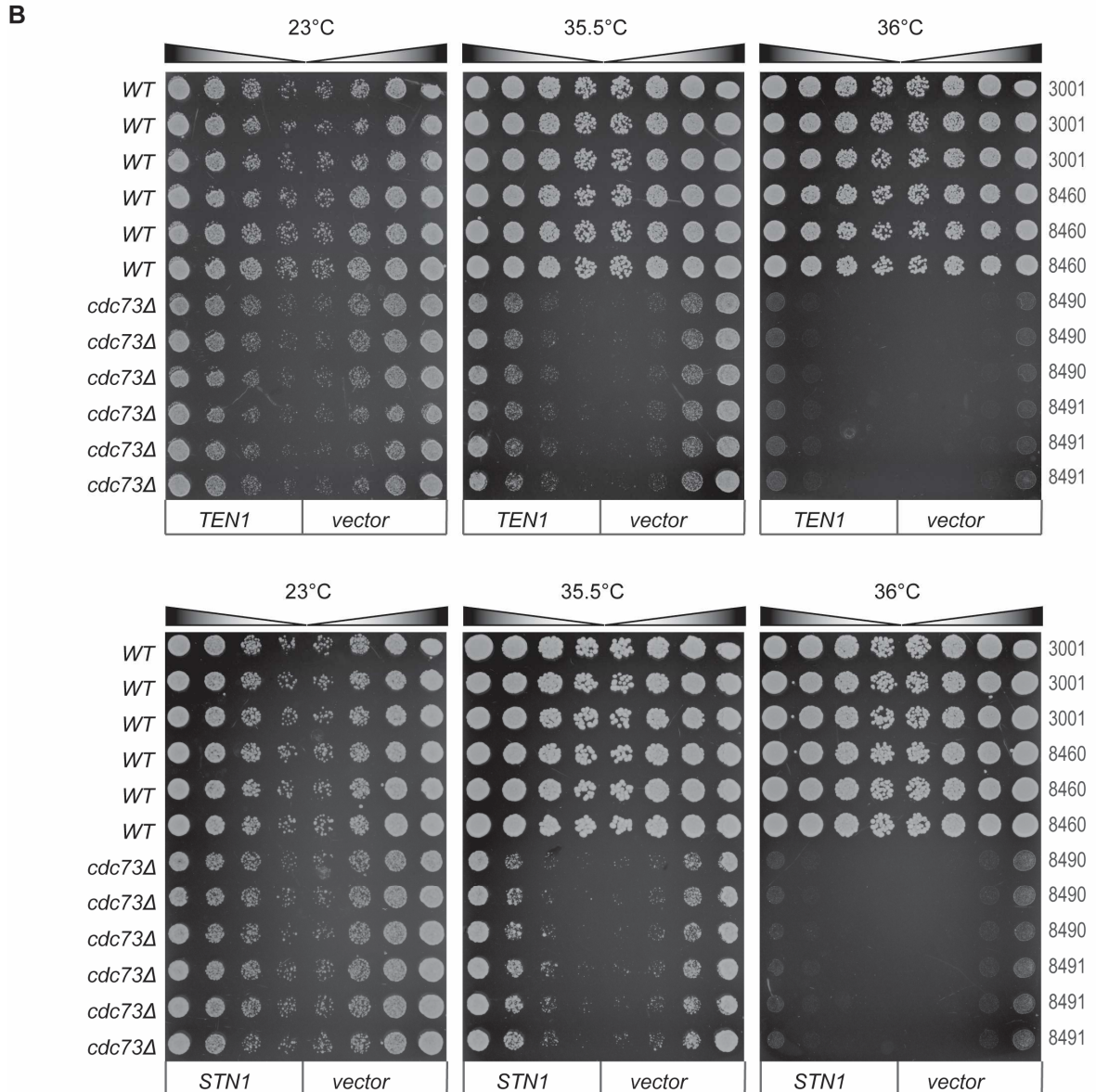
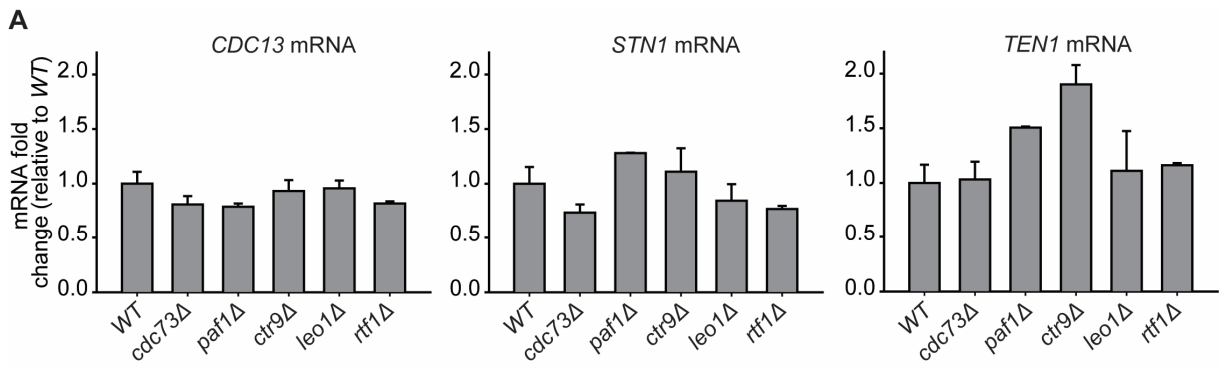


Figure 5-5 PAF1 and CTR9 regulate TEN1 mRNA. A) qRT-PCR analysis of *CDC13*, *STN1* and *TEN1* mRNA expression levels in strains with one of the PAF1 complex members deleted. The mean is indicated and the “error” bars indicate the two independent measurements. Each value was normalized to the levels of *BUD6* mRNA (Addinall et al. 2011). *WT*, 8460 and 3001; *cdc73Δ*, 8490 and 8491; *paf1Δ*, 8757 and 8758; *ctr9Δ*, 8751 and 8752; *leo1Δ*, 8736 and 8737; *rtf1Δ*, 8743 and 8744. **B)** Two independent *WT* strains and two *cdc73Δ* strains were transformed with a plasmid carrying *TEN1* (pDL1495), *STN1* (pDL1755) or the corresponding empty vector (pDL1726 or pDL1756). From each transformation three pools of >10 colonies were tested by spot test: cells were cultivated overnight at 23°C and then serial dilutions of the saturated overnight culture were spotted onto solid –URA (*TEN1*) or –LEU (*STN1*) plates and incubated at different temperatures for 2 days.

5.2.5. Synthetic sickness and neighbouring gene effect between *CDC73* and adjacent gene *VPS36*

I have confirmed that *cdc73Δ*, *paf1Δ* and *ctr9Δ* similarly regulate *TLC1* RNA. It was also previously shown that *cdc13-1 tlc1Δ* survivors, with rearranged telomeres, exhibited better growth than *cdc13-1* cells with normal telomeres (Tsai et al. 2002). Therefore, the substantial higher fitness of *cdc73Δ cdc13-1* versus *paf1Δ cdc13-1* and *ctr9Δ cdc13-1* cells, led us to think that maybe Cdc73 and Paf1/Ctr9 have an additional and distinct role affecting the telomere integrity. One explanation for the different phenotypes of *cdc73Δ* versus *paf1Δ* and *ctr9Δ* would be if *cdc73Δ* affected the function of a neighbouring gene, and if the neighbouring gene also affected fitness in *cdc13-1* strains.

CDC73 is adjacent to *VPS36* (separated by 204 bp) and *vps36Δ* and *cdc73Δ* have been suggested to cause a neighbouring gene effect (deletion of one ORF affects the function of the adjacent gene). To test if interactions between *VPS36* and *CDC73* could help explain the unusual properties of *cdc73Δ* strains, five related gene disruption constructs were created (Figure 5-6A). The effects of the constructs were analysed in *CDC13*, *cdc13-1* and *rad9Δ* backgrounds to determine their role on cell fitness. Their effects on telomere length and *TLC1* RNA levels were also measured. The data is shown in Figure 5-6.

The strongest phenotype observed demonstrates a synthetic genetic interaction between *CDC73* and *VPS36* and comes from analysis of construct 5, which deletes the C termini of both proteins, and most likely completely inactivates both proteins (Figure 5-6B, D). Construct 5 causes a strong temperature sensitive phenotype in *CDC+* strains, much stronger than the temperature sensitivity observed in *cdc73Δ* strains (construct 5 versus 1 and 2) (Figure 5-6B). This results shows that Cdc73 and Vps36 work in separate pathways to affect cell fitness at high temperatures and that a synthetic genetic interaction occurs when both genes are disrupted.

The spatial organisation of *CDC73* and *VPS36* suggested that standard, complete ORF replacement of *CDC73* might affect the 3' UTR of *VPS36* and vice versa. The fact that construct 5 caused a more severe growth phenotype than construct 1 suggests that construct 1 only partially reduces Vps36 function. Consistent with this hypothesis there is a small difference in fitness between constructs 1 and 2 in all combinations of *cdc13-1* and *rad9Δ* backgrounds (Figure 5-6B-E). Importantly,

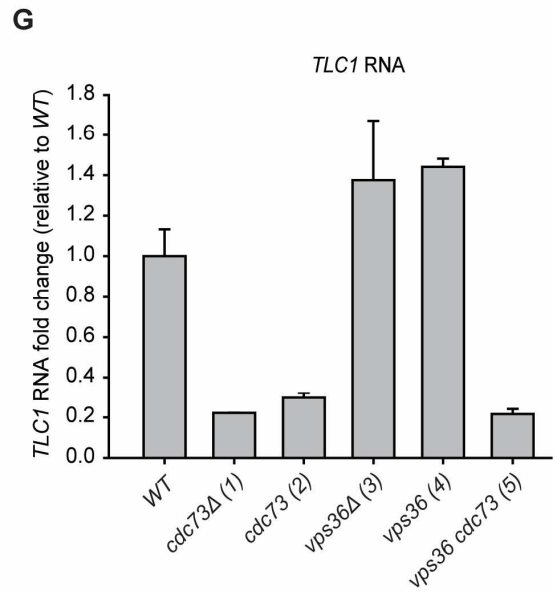
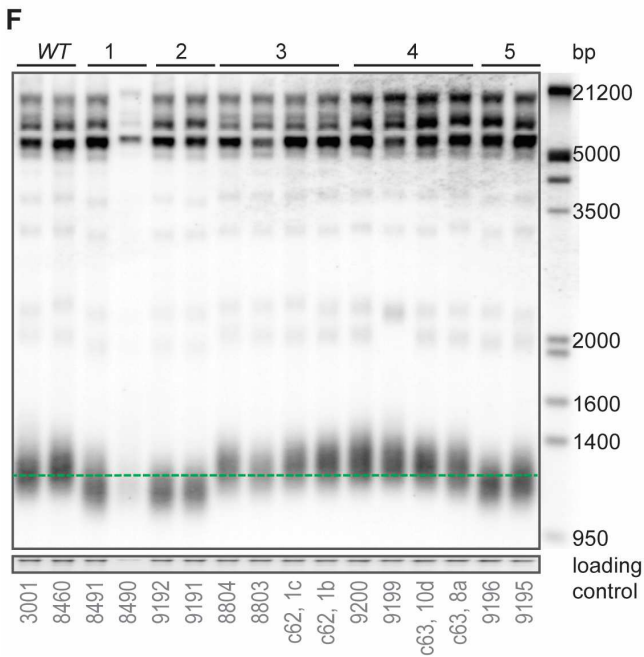
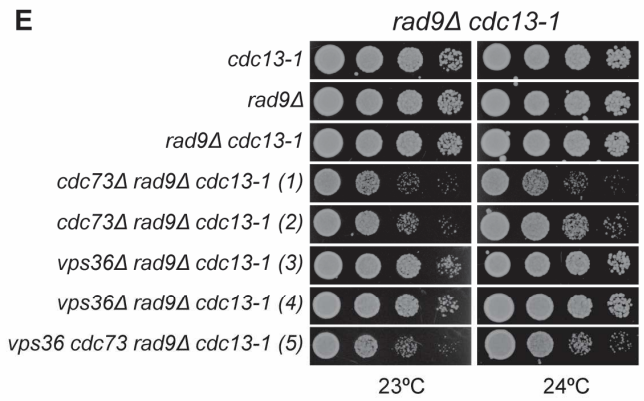
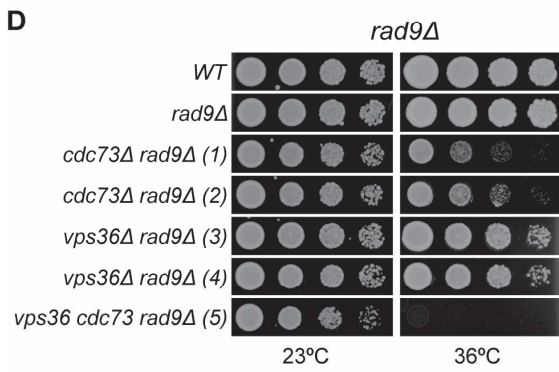
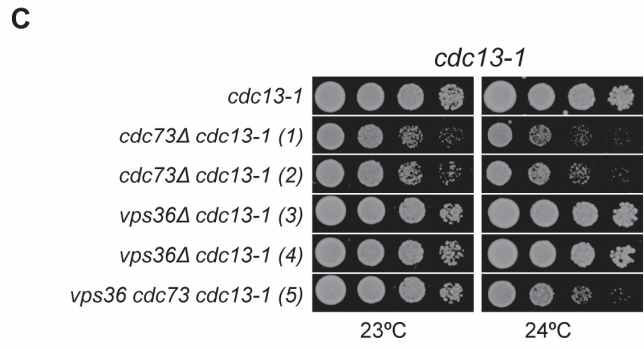
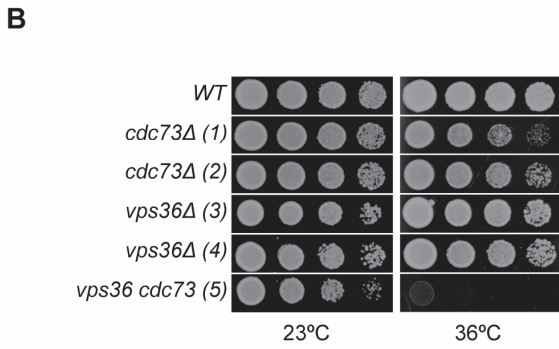
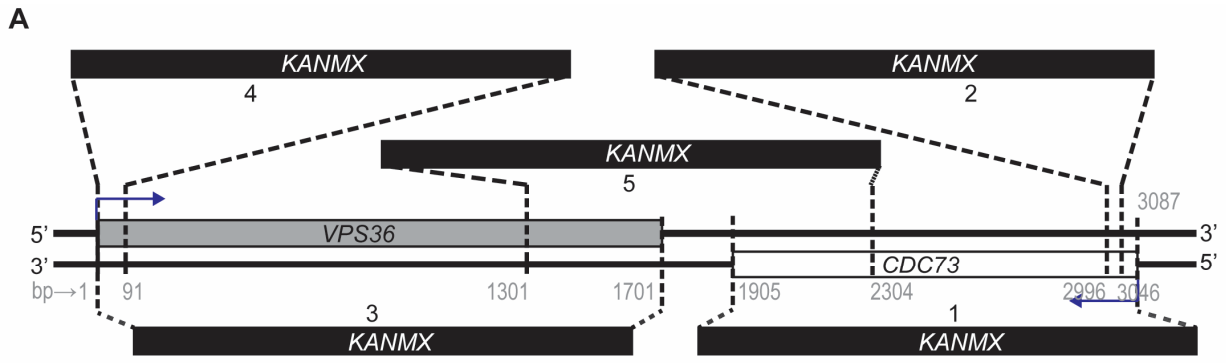


Figure 5-6 *CDC73* and its adjacent gene *VPS36* interact. **A)** Map representing the relative position of *CDC73* and its adjacent gene *VPS36*, together with 5 different constructs used for the deletion of *CDC73*, *VPS36* or both. **B, C, D and E)** Each of the constructs described in A were introduced in the following yeast genetic backgrounds: *CDC13⁺ RAD9⁺* (B), *cdc13-1 RAD9⁺* (C), *CDC13⁺ rad9Δ* (D) or *cdc13-1 rad9Δ* (E). The resulting strains were cultivated overnight at 23°C. Serial dilutions of the saturated overnight cultures were then spotted onto solid YEPD plates and incubated at 23°C and 36°C (B and D) or 23°C and 24°C (C and E) for 2 days. At each temperature, all strains were grown on the same YEPD plate. Fitness of *cdc13-1* strains was measured as soon as possible after spore germination. Four different strains for each genotype were analysed and a representative strain is shown. No strain numbers were generated for these specific strains. Strain numbers for independent strains with identical genotypes can be found in Appendix A. **F)** Telomeric Southern blot was performed using a probe against the Y'+TG sequence (Maringele and Lydall 2004) in order to analyse the telomere structure of the strains described in A. **G)** qRT-PCR analysis of *TLC1* mRNA expression levels in the strains described in A. mRNA from two independent strains was measured. The mean is indicated and the "error" bars indicate the two independent measurements. Each value was normalized to the levels of *BUD6* mRNA (Addinall et al. 2011). The strains used are in the strain table (Appendix A) and were also analysed in F.

construct 2 (with *VPS36* unaffected, therefore the true *cdc73Δ* phenotype) is a weaker enhancer of decreased *cdc13-1* fitness defects than construct 1 (used throughout this thesis). The better fitness caused by construct 2 suggests that the fitness differences between *cdc73Δ* and *pafl1Δ* or *ctr9Δ* cells are not caused by an adjacent gene effect, since *pafl1Δ* and *ctr9Δ* are considerably less fit than *cdc73Δ* (Figure 5-3).

The three constructs that inactivate Cdc73 each caused short telomeres and decreases in *TLC1* RNA (constructs 1, 2, 5 Figure 5-6F and G). Interestingly lack of Vps36 (constructs 3 and 4) caused slightly increased *TLC1* levels and slightly longer telomeres (Figure 5-6F and G). Furthermore it seems that construct 5, disrupting *CDC73* and *VPS36* caused slightly longer telomeres than *cdc73Δ* alone (constructs 1 and 2). This result is not in agreement with the previously reported short telomere phenotype of *vps36Δ* cells and will be further addressed in section 5.2.7 (Rog et al. 2005).

I conclude that the standard *cdc73Δ* mutation (construct 1) is partially interfering with *VPS36* activity, most likely by affecting the *VPS36* UTR. I see no detectable fitness difference between the standard *vps36Δ* and a *VPS36* N terminal disruption in *cdc13-1* mutants (compare constructs 3 and 4, Figure 5-6C). Overall there are both a synthetic genetic interaction between *VPS36* and *CDC73* and a neighbouring gene effect on *VPS36* function caused by the standard *cdc73Δ* construct.

5.2.6. Expression of *VPS36* on a plasmid decreases *cdc73Δ cdc13-1* fitness

To better understand the role of *CDC73*, *VPS36* and *YLR419W* (the other gene adjacent to *CDC73*) in *cdc73Δ cdc13-1* strains, each gene was cloned in a centromeric plasmid to permit complementation testing. Heterozygous *cdc73Δ cdc13-1* diploids were transformed with each plasmid and spores carrying a plasmid expressing *CDC73*, *VPS36* or *YLR419W* were germinated and fitness assessed.

cdc73Δ cdc13-1 cells carrying an empty plasmid (vector) grow better than *cdc13-1* cells at non-permissive temperatures (27°C and 28°C) (Figure 5-7). This is in agreement with the suppressing role of *CDC73* observed in Figure 3-1 but is opposite to what is observed in Figure 5-6C (*cdc73Δ cdc13-1* cells are less fit than *cdc13-1* cells at 24°C) and in high-throughput screens (Addinall et al. 2011). The reasons for this discrepancy will be addressed in Chapter 6.

It was observed, as expected, that expression of *CDC73* rescued the *cdc13-1* fitness in *cdc73Δ cdc13-1* strains (Figure 5-7). This shows that *CDC73* deletion is largely responsible for the *cdc73Δ cdc13-1* better growth at semi-permissive temperatures. The expression of *VPS36* from a plasmid enhanced *cdc73Δ cdc13-1* thermo-sensitivity. This effect of the expression of *VPS36* on *cdc73Δ cdc13-1* fitness might be due to an increase of Vps36 in the cells which is reported to cause growth defects (Sopko et al. 2006). Therefore it is likely that the *cdc73Δ cdc13-1* strains in Figure 5-7 are expressing more *VPS36* than is physiologically typical, showing that the cells are very sensitive to changes in Vps36 homeostasis. Since *VPS36* is part of a protein sorting pathway it is possible that too much Vps36 will lead to the dysregulation of protein levels (Bowers and Stevens 2005). Finally, the expression of *YLR419W* on a plasmid both enhanced and suppressed the *cdc73Δ cdc13-1* fitness defect (Figure 5-7). This heterogeneity is typical of a population that might be rearranging their telomeres and such phenotype will be explained in Chapter 6.

Altogether, these results show that Vps36 overexpression enhances the fitness defects of *cdc73Δ cdc13-1*. It was also suggested (from sections 5.2.4 and 5.2.6) that *cdc73Δ cdc13-1* cells are very sensitive to changes in Vps36 levels perhaps due to the fact that *CDC73* deletion causes a protein unbalance that would be addressed by protein degradation pathways.

5.2.7. ESCRT-II complex does not affect telomere length in W303

In contrast to the data here presented, a *VPS36* deletion was previously reported to cause short telomeres (Figure 5-6) (Askree et al. 2004). Therefore the telomere length in *snf8Δ* or *vps25Δ* strains, defective in other members of the ESCRT-II complex, was also measured. No strong effects on telomere length were observed upon deletion of any of the ESCRT-II complex components (Figure 5-8). My experiments are performed in the W303 genetic background, and cells were cultured at 23°C, whereas the published experiments were in the BY4742 background, and cells were most likely cultured at 30°C. It seems that the effect of the ESCRT-II complex on telomere length is dependent on the genetic background and/or temperature. I conclude that ESCRT-II components do not (always) regulate telomere length in yeast.

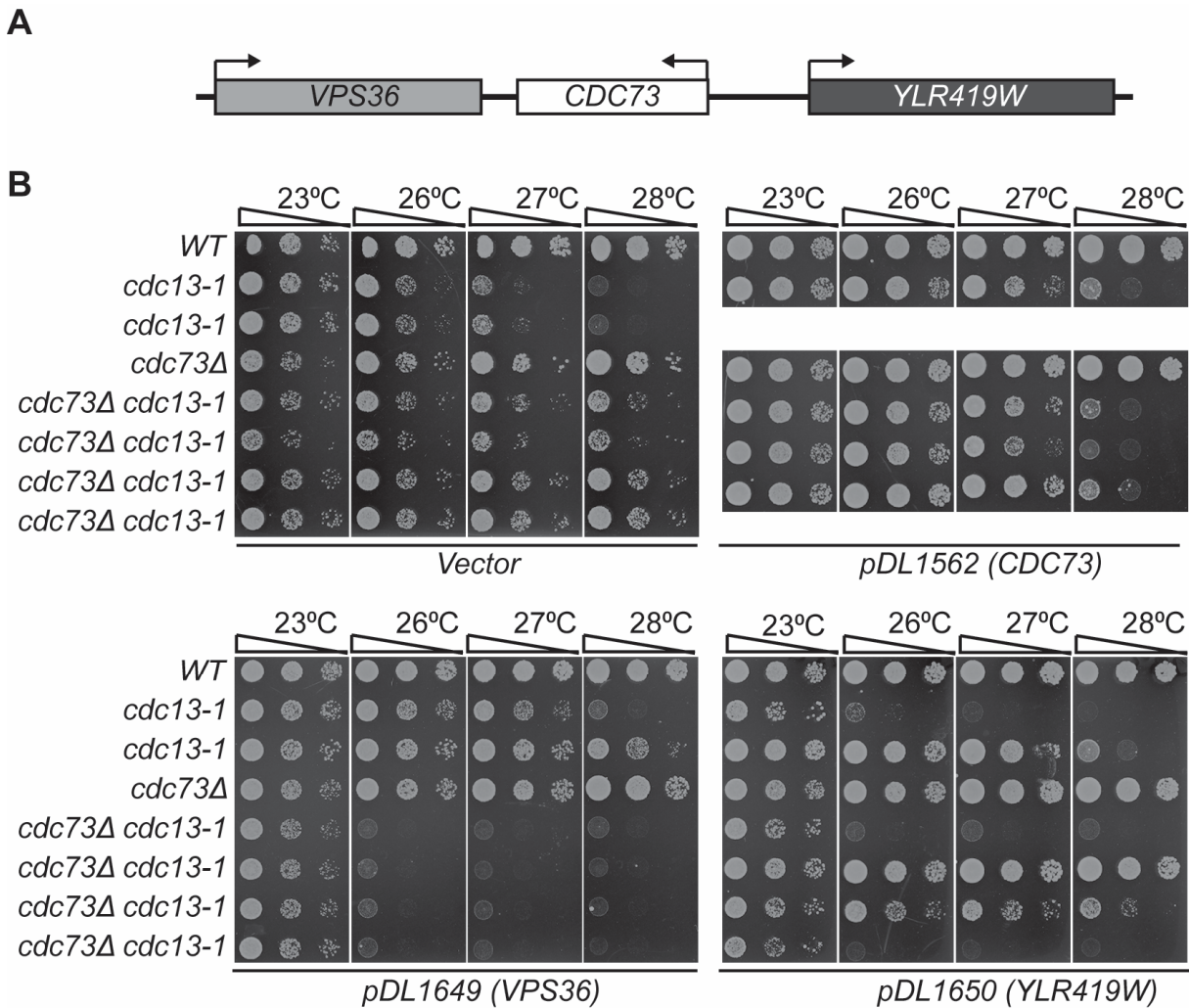


Figure 5-7 Expression of *CDC73* adjacent genes in plasmids suggests that *VPS36* might be affected in *cdc73Δ* strains. A) Cartoon representing the relative organization of *CDC73* and its adjacent genes: *VPS36* and *YLR419W*. **B)** The diploid *CDC73/cdc73Δ RAD9/rad9Δ CDC13/cdc13-1* was transformed with plasmids carrying the *CDC73* gene (pDL1562) and each one of its adjacent genes *VPS36* (pDL1649) or *YLR419W* (pDL1650). The vector was transformed into haploid cells. Diploids were sporulated and the strains carrying each of the plasmids were selected. These strains were then tested by spot test: cells were cultivated overnight at 23°C and then serial dilutions of the saturated overnight culture were spotted onto solid -Ura plates and incubated at different temperatures for 5 days. No strain numbers were generated for these specific strains.

5.2.8. The PAF1 complex regulates *VPS36* transcription

Since *Cdc73* is part of the PAF1 complex that is involved in transcriptional regulation I wondered whether the interactions between *CDC73* and *VPS36* were due, in part, to transcriptional regulation of *VPS36* mRNA by the PAF1 complex. To test this, *VPS36* mRNA levels were measured in strains with disruptions of *CDC73* (constructs 1 and 2, Figure 5-6A) and in strains with the other PAF1 complex components deleted (Figure 5-9A). Interestingly, *VPS36* mRNA is decreased when each of the PAF1 complex components is deleted, with little difference between deletion and N-terminal disruption of *CDC73* (constructs 1 and 2). Similar to what has been seen in other phenotypes, such as growth on germination plates (Figure 5-3B), *leo1Δ* and *rff1Δ* disruptions showed milder effects on *VPS36* RNA levels. Expression of the other adjacent gene to *CDC73*, *YLR419W*, was also tested in *cdc73Δ* cells and found to be unaltered (Figure 5-9B). I conclude that *VPS36* is a new transcriptional target of the PAF1 complex.

5.2.9. *vps36Δ* is synthetically lethal with *paflΔ* or *ctr9Δ* but not with *cdc73Δ*, *rff1Δ* or *leo1Δ*

Given that *VPS36* and *CDC73* function independently to maintain cell fitness, particularly at high temperature, I wanted to know what role, if any, *VPS36* played in the fitness of other PAF1 complex deletion strains. To address this question, I crossed *vps36Δ* (Figure 5-6A, disruptions 3 and 4) to strains carrying *paflΔ*, *ctr9Δ*, *rff1Δ* or *leo1Δ* mutations (Figure 5-10A). Note that fitness of *cdc73Δ vps36Δ* double mutants was previously tested in Figure 5-6B and found to be decreased when compared to single mutants. Interestingly, viable *vps36Δ paflΔ* or *vps36Δ ctr9Δ* double mutants could not be identified but all other double mutants could. Although this synthetic lethality between *vps36Δ* and *paflΔ* or *ctr9Δ* has not been previously reported, both *PAF1* and *CTR9* deletions were reported to show synthetic growth defects with deletions affecting ubiquitination pathways (*UBP6*) or multivesicular body/protein sorting pathways (*VPS21*, *VPS71* and *VPS72*). Since *Vps36* (as part of ESCRT-II) is involved in sorting ubiquitinated proteins for degradation through the multivesicular body pathway, the findings here reported are in line with the previously described genetic interactions of *PAF1/CTR9* and members of the multivesicular

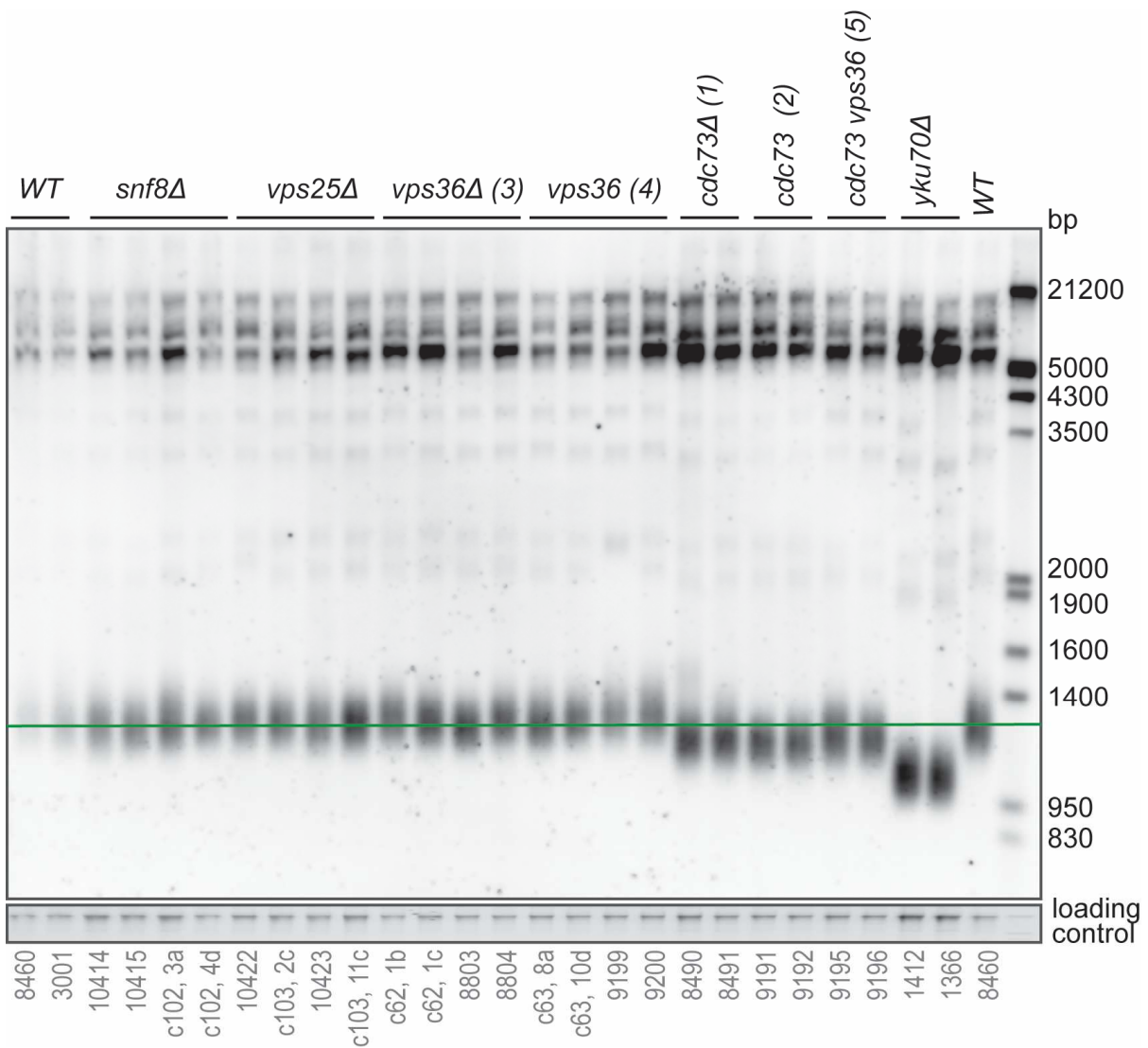


Figure 5-8 ESCRT-II complex components do not regulate W303 telomere length. Telomeric Southern blot was performed as in Figure 5-6F. For each *VPS* mutant, the first two strains (left to right) are described in Appendix A, while the last two were taken from germination plates and never frozen. SYBR safe staining was used as loading control.

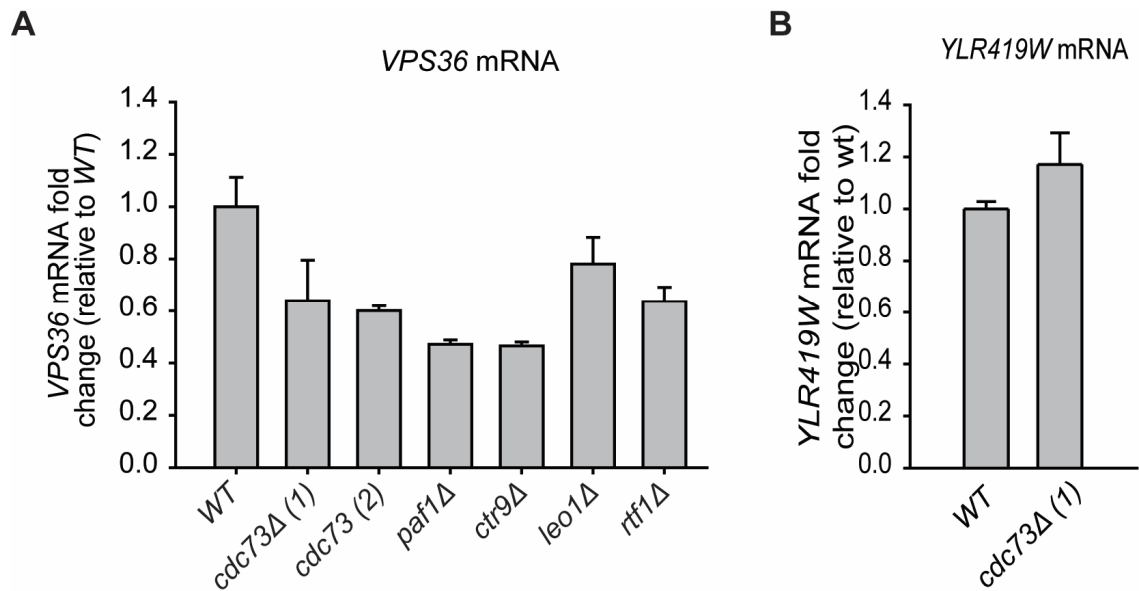
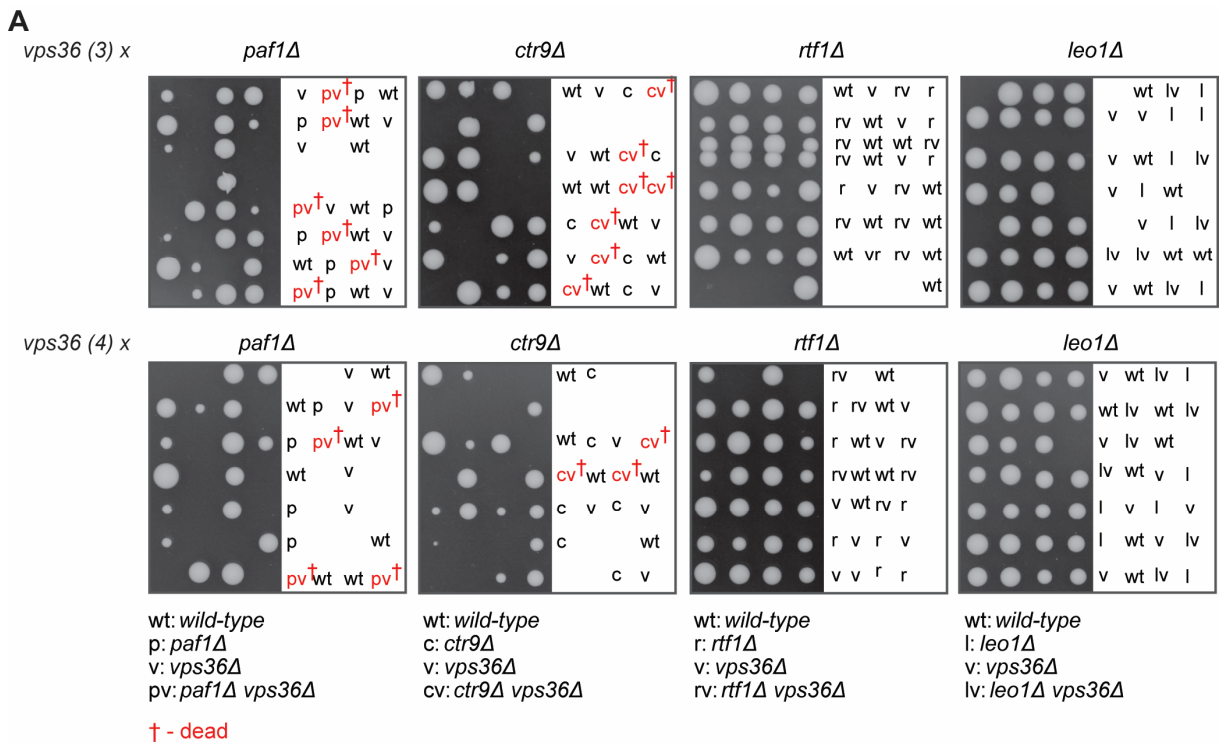


Figure 5-9 PAF1 complex controls *VPS36* expression. A and B) qRT-PCR analysis of *VPS36* and *YLR419W* mRNA expression levels in strains with one of the PAF1 complex members deleted. mRNA from two independent strains was measured. The mean is indicated and the “error” bars indicate the two independent measurements. Each value was normalized to the levels of *BUD6* mRNA (Addinall et al. 2011). WT, 8460 and 3001; *cdc73Δ* (1), 8490 and 8491; *cdc73* (2), 9191 and 9192; *paf1Δ*, 8757 and 8758; *ctr9Δ*, 8751 and 8752; *leo1Δ*, 8736 and 8737; *rtf1Δ*, 8743 and 8744.

body degradation pathway (Krogan et al. 2003b; Teo et al. 2004; Larabee et al. 2005; Collins et al. 2007). These results show that Vps36 and the PAF1 complex, specifically *PAF1* and *CTR9*, work together to support cell viability.

PAF1 and *CTR9* deletions were shown to decrease *TLC1* RNA levels, leading to short telomeres (Mozdy et al. 2008). Telomere shortening in *ctr9Δ* cells could be bypassed by overexpression of *TLC1*. Additionally, deletion of ESCRT components in other yeast backgrounds was shown to cause a short telomere phenotype (Askree et al. 2004). Although I did not see any decrease in telomere length in ESCRT II deletion mutants, I hypothesised that in a *paf1Δ/ctr9Δ* background, deletion of ESCRT mutants caused extensive telomere shortening, causing cell cycle arrest. To test this hypothesis I asked if *TLC1* RNA could rescue *vps36Δ paf1Δ* synthetic lethality. Importantly, I saw no effect of a *TLC1* expressing plasmid (versus vector) on the viability of *vps36Δ paf1Δ* (from 79 viable spores carrying *TLC1*, none was *vps36Δ paf1Δ*) (Figure 5-10B).

I conclude that Vps36 and Paf1/Ctr9 work in independent pathways to maintain cell viability, with simultaneous lack of function of Vps36 and Paf1 or Ctr9 leading to cell death. Furthermore, the synthetic lethality between *vps36Δ* and *paf1Δ* is unlikely to be related to the decreased levels of *TLC1* in *paf1Δ* cells. These results suggest that Paf1 and Ctr9 are more essential for cell viability than the remaining components of the PAF1 complex.



B

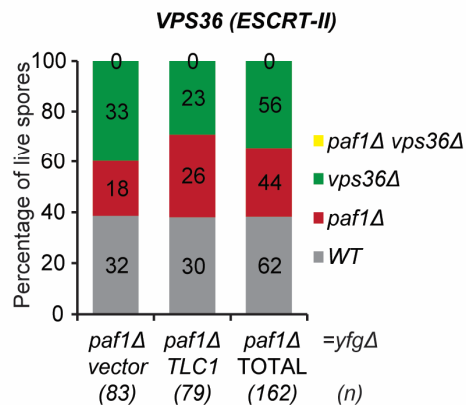


Figure 5-10 *vps36Δ* is synthetically lethal with *paf1Δ* or *ctr9Δ* but not with *rtf1Δ* or *leo1Δ*. **A** *vps36Δ* (Figure 5-6A, constructs 3 and 4) were crossed to *paf1Δ* (DLY8757), *ctr9Δ* (DLY8751), *rtf1Δ* (DLY8743) or *leo1Δ* (DLY8736) strains and diploid cells were obtained. Diploids were sporulated and tetrads dissected onto YEPD plates, where germinated spores grew for 6 days at 23°C before being photographed. **B** A *vps36Δ paf1Δ* heterozygous diploid was transformed with a centromeric plasmid carrying *TLC1* (pDL751) or a vector plasmid (pDL1713). Random spore analysis was used to get haploid strains: the diploids carrying the plasmids were sporulated and spotted onto –URA plates. After 7 days at 23°C colonies were genotyped. The percentage of each genotype in the total was plotted. *n* represents the total number of colonies (cells) genotyped.

5.2.10. *paf1Δ* and *ctr9Δ* are synthetically lethal with deletions of ESCRT-I, ESCRT-II and ESCRT-III components

To test if the synthetic lethality between *paf1Δ/ctr9Δ* and *vps36Δ* is conserved among other components of the ESCRT machinery (ESCRT-0 to ESCRT-III), I performed random spore analysis of diploids carrying simultaneous deletions of PAF1 complex components and ESCRT components. I tested interactions between the PAF1 complex and *VPS27* (ESCRT-0), *STP22* (ESCRT-I), *SNF8* (ESCRT-II), *VPS25* (ESCRT-II) and *SNF7* (ESCRT-III). Interestingly, and in agreement with the interactions observed between *PAF1/CTR9* and *VPS36*, *PAF1* and *CTR9* could not be deleted in cells carrying deletions of any of the ESCRT-I, ESCRT-II or ESCRT-III components (Figure 5-11). Importantly, 8 (in 88) *paf1Δ vps27Δ* and 1 (in 35) *ctr9Δ vps27Δ* cells were found alive, suggesting that *Vps27* (ESCRT-0) is not as important as downstream ESCRT components for the viability of *paf1Δ* or *ctr9Δ* cells.

I conclude that PAF1 complex (through Paf1 and Ctr9) work together with the ESCRT machinery to maintain cell viability.

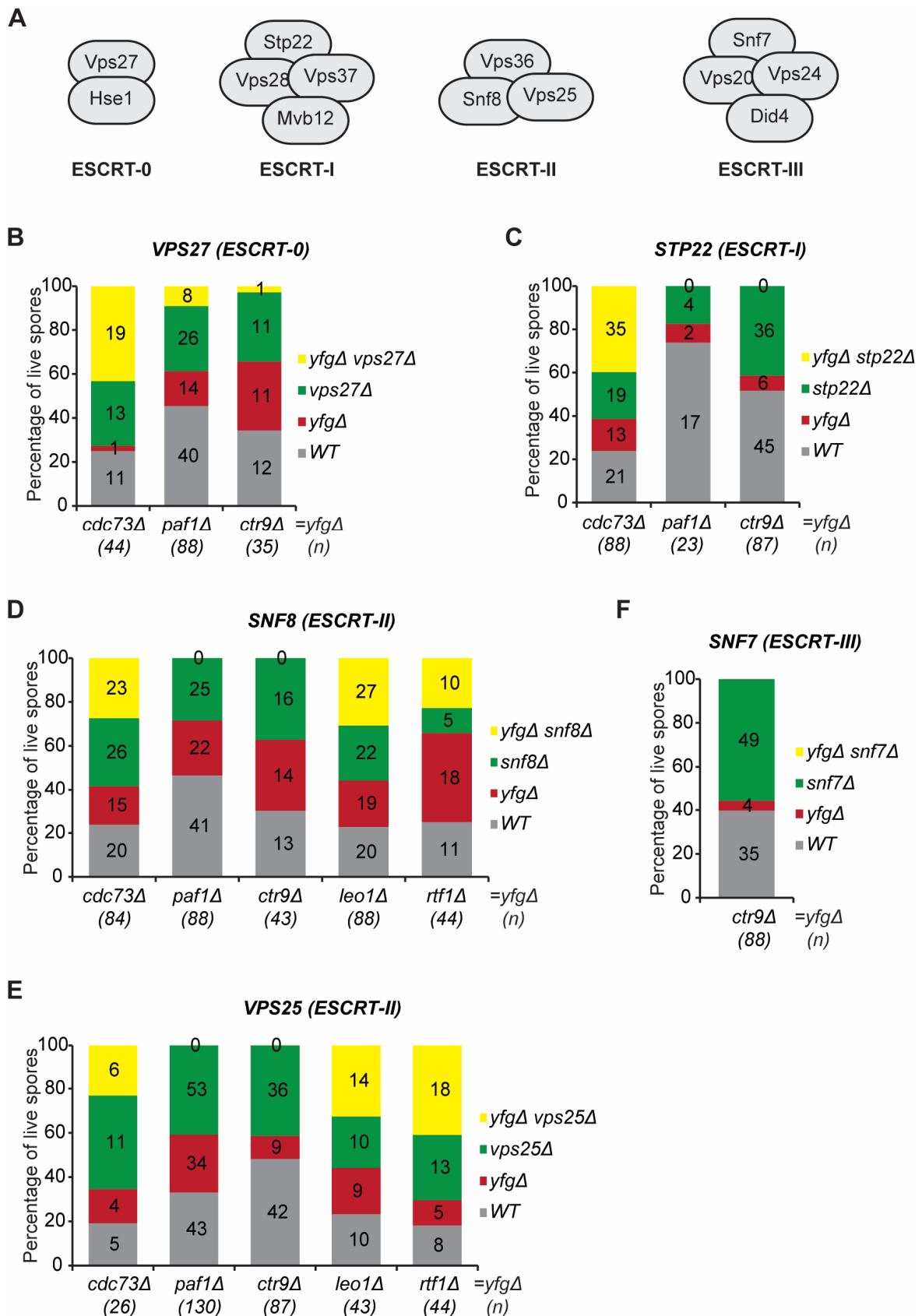


Figure 5-11 *paf1Δ* and *ctr9Δ* are synthetically lethal with deletions of many ESCRT components. **A)** Schematic representation of the components of the yeast ESCRT-0, ESCRT-I, ESCRT-II and ESCRT-III complexes. **B-E)** Strains carrying deletions of different components of the PAF1 complex were crossed with *vps27Δ* (B), *stp22Δ* (C), *snf8Δ* (D), *vps25Δ* (E) or *snf7Δ* (F) strains. Data was analysed as described in Figure 5-10B.

5.3. Discussion

The PAF1 complex binds RNA polymerase, is highly conserved among eukaryotes and plays roles in human disease such as cancer. The PAF1 complex affects the amount of numerous RNAs by affecting transcriptional and post-transcriptional processes (Penheiter et al. 2005; Tomson and Arndt 2013). Here, it was investigated how the PAF1 complex affects fitness of yeast cells with defective telomeres to help explore the potential relevance of these interactions to cancer.

The experiments in this Chapter show that the PAF1 complex has numerous effects on telomere biology and the data is summarized by Figure 5-12. A new set of interactions between the PAF1 complex and components of the ESCRT machinery have also been described. For instance, I found that Paf1 and Ctr9 are essential for viability in cells with defects in ESCRT-I, ESCRT-II or ESCRT-III complexes. All the data here described, and much of the literature, support the view that Ctr9 and Paf1 are the most critical members of the PAF1 complex. Conversely, Leo1 and Rtf1 are the least critical (auxiliary) members of the PAF1 complex, and Cdc73 is somewhere in-between.

Consistent with previous reports, the results here described find that the PAF1 complex is needed to achieve normal, high levels of *TLC1* (telomerase component) RNA (Mozdy et al. 2008). Leo1 and Rtf1 have lesser effects than Cdc73, Ctr9 and Paf1 on *TLC1* levels (Pathway a, Figure 5-12). Also, I show for the first time that all the PAF1 complex components induce *VPS36* transcript levels, with a stronger role for Paf1 and Ctr9 (Pathway b, Figure 5-12). On the other hand Ctr9 and Paf1 reduce levels of *TEN1* mRNA (affecting a member of the telomere capping complex, CST) (Pathway c, Figure 5-12) while other components of the PAF1 complex had comparatively small effects. Thus, in summary, PAF1 complex components show complex effects on levels of three transcripts that affect telomere biology: *TLC1*, *VPS36* (perhaps also through *TLC1* RNA regulation) and *TEN1*.

CDC73 is adjacent to *VPS36* and the pair have been suggested to exhibit a neighbouring gene effect. In this Chapter I confirmed that the *CDC73* disruption partially reduces *VPS36* function (and by this criterion is causing a neighbouring gene effect) (Pathway d, Figure 5-12). This is in agreement with a model where the *cdc73Δ* mutation affects *VPS36* 3' UTR.

In addition to the neighbouring gene effect, there are other more important (*trans*) interactions between the PAF1 complex and *VPS36*. First, *Cdc73* and the other members of the PAF1 complex are required for normal, high *VPS36* mRNA levels. In addition *vps36Δ* exacerbates the temperature sensitive phenotype of *cdc73Δ* mutants. Furthermore, there is a synthetic lethal interaction in cells with defective ESCRT-I, ESCRT-II and ESCRT-III machineries and *ctr9Δ* or *paf1Δ* mutations. This suggests that the ESCRT machinery functions redundantly with Ctr9/Paf1 to maintain yeast cell viability (Pathway e, Figure 5-12).

How the PAF1 complex and the ESCRT components function together to maintain yeast cell fitness is not clear. The higher sensitivity of ESCRT deletion mutants to 6-azauracil suggested that the ESCRT pathway plays a role in transcription elongation (Song et al. 2014). Importantly, ESCRT proteins physically associate with 3' regions of actively transcribed genes (Song et al. 2014). Thus, since the PAF1 complex facilitates transcription, *paf1Δ vps36Δ* and *ctr9Δ vps36Δ* might have exacerbated transcriptional defects that are not compatible with life.

Another hypothesis is that double mutants (carrying deletions of both PAF1 and ESCRT complex components) could have increased levels of transcription-replication fork collisions. Paf1 (together with Ino80) was shown to be important for RNA pol II degradation to avoid transcription-replication fork collision (Poli et al. 2016). Additionally, many have shown that Rpb1 is ubiquitylated upon DNA damage, marking RNA pol II for degradation (Huibregtse et al. 1997; Beaudenon et al. 1999; Somesh et al. 2005; Chen et al. 2007). Since the ESCRT machinery is involved in the sorting of ubiquitylated proteins for degradation, it is possible that the ESCRT complex is involved in the degradation of RNA pol II. If true, the combined effects of loss of PAF1 (less signalling for RNA pol II degradation) and loss of ESCRT (less capacity to degrade RNA pol II) could cause irreversible stalling in replication forks, leading to cell cycle arrest.

Irrespective of the precise mechanism it is plausible that the synthetic lethal interactions between *paf1Δ* or *ctr9Δ* and ESCRT component deletions are based, at least in part, on their functions at telomeres (Pathways e,f, Figure 5-12). *Vps36* and the ESCRT II complex are connected with telomere biology. In this Chapter I saw slightly higher levels of *TLC1* RNA in *vps36Δ* strains and this correlates with telomere length increases, whereas others reported that *vps36Δ* caused a short telomere phenotype (Rog et al. 2005). This discrepancy might be due to a difference in the

genetic background, temperature, or other environmental conditions that might be different in my experiments when compared to the previously reported experiments. Indeed, telomere length can be affected by environmental conditions such as temperature and ethanol concentration (Romano et al. 2013). The ESCRT-II complex role on telomere function might be due to a role in telomerase turnover, or in the turnover of other proteins involved in telomerase turnover/transcription repression.

An important new insight comes from the observation that Paf1 and Ctr9, the critical members of the PAF1 complex, inhibit *TEN1* mRNA accumulation. It is known that in plant and yeast cells that high levels of Ten1 can inhibit telomerase recruitment (Qian et al. 2009a; Leehy et al. 2013). Thus a *ctr9Δ* mutation causing a reduction in *TLC1* RNA combined with an increase in *TEN1* mRNA will be more harmful to telomere function, and cell fitness, than a *cdc73Δ* mutation which just affects *TLC1* RNA levels. I could only observe a very modest effect on *STN1* expression (also a telomerase repressor) in *cdc73Δ* strains, showing that although contributing to cell sickness, high Ten1 levels are perhaps just a small fraction of what makes *paf1Δ cdc13-1* and *ctr9Δ cdc13-1* cells sick. Since the PAF1 complex is needed for proper levels of hundreds of transcripts, it might just be that one of those altered transcripts is required at normal levels in telomere defective strains.

Finally, the interactions here described between the PAF1 complex and *VPS36* might be relevant to health in higher eukaryotes. In *Drosophila*, the *VPS36* orthologue was reported to affect the Hedgehog (Hh) pathway (Yang et al. 2013). The Hedgehog pathway, conserved between vertebrate and invertebrates (Nussleinvolhard and Wieschaus 1980; Huangfu and Anderson 2006), is involved in embryonic and post-embryonic development and has a strong role on neural stem cell maintenance (Ahn and Joyner 2005; Balordi and Fishell 2007; Ingham et al. 2011; Briscoe and Therond 2013). Interestingly, Ctr9 has been shown to regulate dopamine transporter trafficking (essential for proper neural function) in mammalian cells (De Gois et al. 2015), and could therefore potentially play a role like the Hedgehog pathway in neural stem cells.

Furthermore, both Hedgehog (Vps36) and Wnt (PAF1 complex) signalling pathways are constitutively active in many cancers (Taipale and Beachy 2001) and common regulators like XSufu have been identified in *Xenopus* (Min et al. 2011).

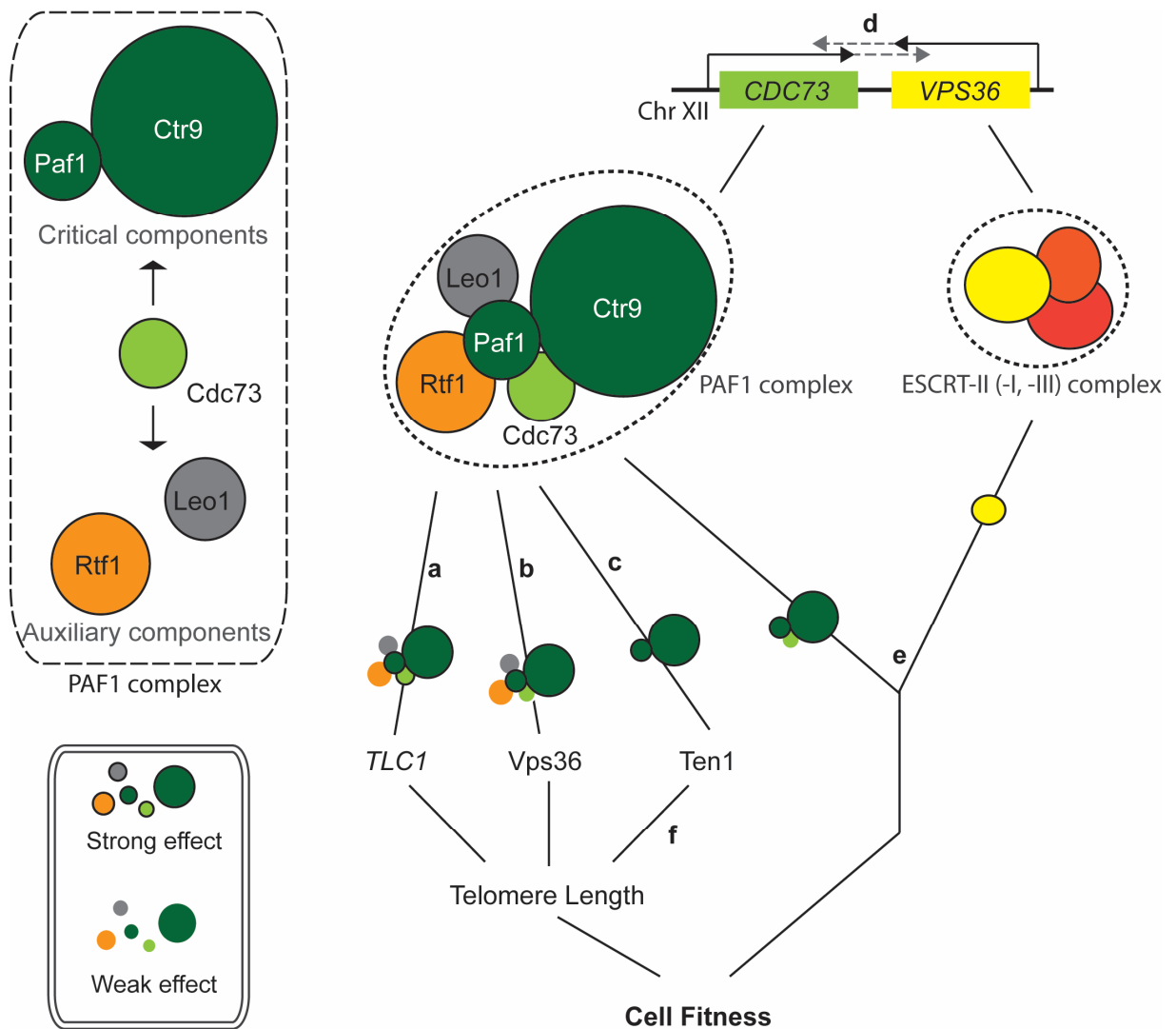


Figure 5-12 Cartoon for the regulation of cell viability by the PAF1 complex. The Paf1 complex is composed of Cdc73, Paf1, Ctr9, Leo1 and Rtf1. The Paf1 complex promotes the expression in *trans* of both *TLC1* (**a**) and *VPS36* (**b**), while Paf1 and Ctr9 repress the expression of *TEN1* (**c**). Additionally, *CDC73* and *VPS36* interact in *cis* (**d**). Telomere maintenance is essential for cell viability and Ten1 has a repressive effect over telomere lengthening while *TLC1* promotes telomere lengthening. Therefore, the PAF1 complex, mainly through Paf1 and Ctr9, maintains cell viability by promoting telomere integrity. Ctr9 and Paf1, together with Vps36, contribute to cell viability (**e**) through a mechanism that I cannot yet define, although it might be related to a role of Vps36 at telomeres (**f**).

Thus, a better understanding of the cross-talk between the Hedgehog and Wnt pathways could be helpful. The links between the PAF1 complex, Vps36 and telomere biology in yeast may help to understand the role of the human PAF1 complex in cancer.

5.4. Future work

It would be interesting to see if *TLC1* overexpression rescues the fitness defects of *paf1Δ cdc13-1* and *ctr9Δ cdc13-1* (in comparison to *cdc73Δ cdc13-1*). This would show if the low *TLC1* levels (caused by deletion of *CDC73*, *PAF1* and *CTR9*) have a critical role in the low fitness of *paf1Δ cdc13-1* and *ctr9Δ cdc13-1* cells. A hypothesis is that such expression would recover *cdc73Δ cdc13-1* fitness defects (at very low passage) more than *paf1Δ cdc13-1* and *ctr9Δ cdc13-1* fitness defects.

6. PAF1 complex components regulate TERRA and telomere function

6.1. Introduction

In the previous Chapter it was shown that *CDC73* deletion slightly affects the function of its adjacent gene *VPS36*. However it was also concluded that this neighbouring gene effect is not responsible for the phenotypic differences caused by deletion of *CDC73* versus deletion of *PAF1* or *CTR9*. Therefore, the reason why different components of the PAF1 complex affect cells with uncapped telomeres so differently is still to be addressed.

6.1.1. The PAF1 complex and RNA metabolism

The PAF1 complex has been mainly associated with transcription, either by facilitating elongation or by stalling RNA pol II at promoter-proximal sites after transcription initiation (Tomson and Arndt 2013; Chen et al. 2015). The opposing functions of the same complex suggest that the PAF1 complex depends on interaction partners to perform some of its functions. Other roles of the PAF1 complex happen after transcription termination. For instance, the yeast PAF1 complex was shown to promote normal poly(A) length, with *paf1Δ* cells having RNAs with shorter poly(A) tails (Mueller et al. 2004). The same control over poly(A) length was observed in human cells depleted of PAF1 (Nagaike et al. 2011). It was suggested that a reduced recruitment of termination factors in cells lacking PAF1 complex components caused less efficient polyadenylation (Nordick et al. 2008). A physical interaction between the PAF1 complex and the most important deadenylase complex (CCR4-NOT) was also described in yeast (Chang et al. 1999). Also, extended 3'-UTRs have been shown for the nonpolyadenylated small nucleolar RNAs (snoRNAs) in *paf1Δ* cells (Sheldon et al. 2005). An abnormal polyadenylation signal is often associated with increased instability and increased RNA decay (Garneau et al. 2007). Thus, the PAF1 complex regulates mRNA levels also by promoting normal poly(A), since abnormal poly(A) tails are a signal for mRNA degradation.

Interestingly, in humans, hSki8, a member of the SKI complex (involved in cytoplasmic RNA decay) is found to associate with the PAF1 complex (Zhu et al. 2005). This suggests a direct link between the PAF1 complex (transcription) and RNA degradation pathways.

6.1.2. Different functions for different PAF1c components

The PAF1 complex components form a multi-protein complex, however there is increasing evidence in mammalian cells that different components perform different functions. In mouse muscle cells, Rtf1 does not bind other PAF1 complex components but another protein, Ski8, does (Yang et al. 2016). In HeLa cells, Rtf1 regulates the expression of a distinct subset of genes to other PAF1 complex components (Cao et al. 2015). Furthermore, the idea that different PAF1 components perform different functions is suggested by the fact that Cdc73 is more often found mutated in cancer than other PAF1 complex components (An et al. 2016). In yeast there is also evidence that different PAF1 components perform different functions. In *S. pombe*, the PAF1 complex (through Paf1 and Leo1) influences chromatin state by enhancing histone turnover (Sadeghi et al. 2015). Additionally, loss of Cdc73, Paf1 or Ctr9 reduces Pol II CTD Ser2-P while loss of Rtf1 or Leo1 have little effect (Nordick et al. 2008). Yeast *paf1Δ* and *ctr9Δ* cells are very unfit while *cdc73Δ*, *leo1Δ* and *rtf1Δ* cells are quite fit (Betz et al. 2002; Mozdy et al. 2008). Despite the evidence that different components of the PAF1 complex perform different functions few studies have systematically addressed their different functions. The aim of this Chapter is to better understand how different PAF1 complex components affect telomere biology in budding yeast.

6.2. Results

6.2.1. PAF1 complex components affect fitness in different ways

To clarify the roles of PAF1 components, the fitness of all five members of the complex was tested by spot test. As has been reported before, *paf1Δ* and *ctr9Δ* caused fitness defects in otherwise wild-type cells, while *cdc73Δ*, *leo1Δ* and *rtf1Δ* had minimal effects (Figure 6-1) (Betz et al. 2002). Interestingly, and in contrast to published high-throughput data (Figure 5-2), in W303, *cdc73Δ cdc13-1* cells were clearly fitter than *cdc13-1* cells (Figure 6-1) (Addinall et al. 2011). This better fitness of *cdc73Δ cdc13-1* is also the opposite of what was observed in Figure 5-6C (where fitness was assessed very early after spore germination). *paf1Δ* and *ctr9Δ* demonstrated a strong synthetic sick phenotype with *cdc13-1* at 23°C (Figure 6-1). I conclude that distinct members of the PAF1 complex play specialized roles in both telomere proficient and telomere defective cells.

6.2.2. Loss of CDC73 in telomere defective strains leads to telomere rearrangements

Telomerase-defective yeast cells use recombination dependent mechanisms to rearrange telomeres and bypass the need for telomerase (Lundblad and Blackburn 1993). It was previously shown that *cdc13-1 tlc1Δ* strains, lacking telomerase, and with rearranged telomeres, grew better than comparable *cdc13-1* cells (Tsai et al. 2002). Furthermore cells with rearranged telomeres can tolerate complete loss of *CDC13* (Larrivee and Wellinger 2006). Therefore I hypothesised that the *cdc73Δ cdc13-1* strains shown in Figure 6-1 might be very fit when compared to the high-throughput data (Figure 3-1A), because the telomeres had rearranged. Consistent with this hypothesis, *cdc73Δ* strains have short telomeres due to low telomerase RNA levels (Figure 5-4) (Mozdy et al. 2008). Additionally, in low-throughput experiments, many more cell divisions between spore germination on tetrad dissection plates and fitness measurements occur than in typical genome-wide experiments and this might provide time for telomere rearrangements to occur. Consistent with my hypothesis, *cdc73Δ cdc13-1* and *cdc73Δ yku70Δ* strains each showed extensively rearranged telomeres, similar to other telomere defective strains, *mre11Δ yku70Δ* and *tlc1Δ* cells (Figure 6-2B, lanes 9-12). As previously reported,

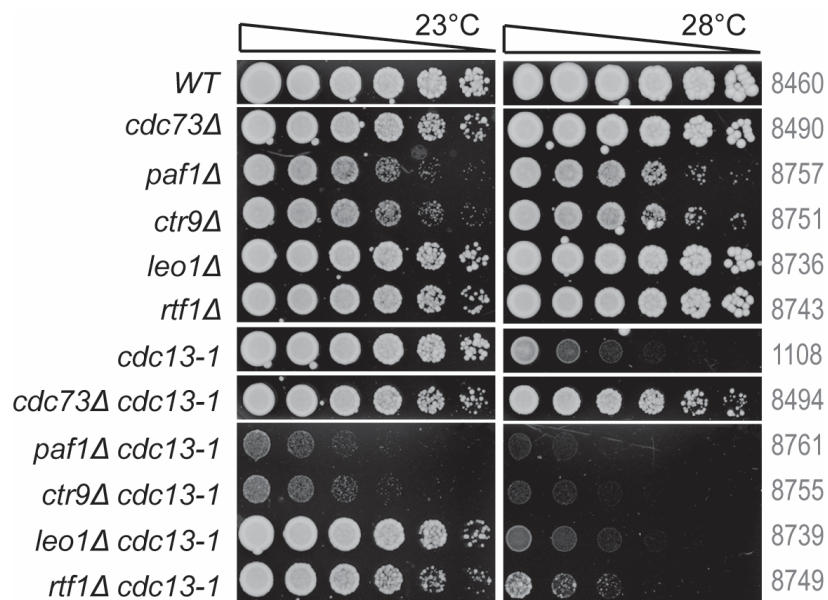


Figure 6-1 Paf1 and Ctr9, but not Cdc73, are needed for fitness of telomere defective cells. Serial dilutions (5-fold) of saturated overnight cultures, grown at 23°C, were spotted onto YEPD plates and incubated for 2 days at the indicated temperatures. All strains at each temperature were grown on a single plate but have been cut and pasted to allow better comparisons.

cdc73Δ strain telomeres were short but not as short as *yku70Δ* strains (Figure 6-2B, lanes 7-8) (Mozdy et al. 2008).

To possibly relate fitness changes to telomere rearrangements, *cdc73Δ yku70Δ* and *cdc73Δ yku80Δ* cells were passaged three times and their telomere structure was assessed by Southern blot (Figure 6-2C-E). Figure 6-2D shows that both *cdc73Δ yku70Δ* and *cdc73Δ yku80Δ* cells form colonies of variable sizes by passage 1 (with mainly small colonies), recovering by passage 3. Accordingly, *cdc73Δ yku70Δ* telomeres seem to lose terminal fragments and become rearranged with increasing passage (Figure 6-2E). Also, it is noticeable at passage 1 that telomeres of *cdc73Δ yku70Δ* and *cdc73Δ yku80Δ* cells are shorter than telomeres of *yku70Δ* cells, reinforcing the idea that initial *cdc73Δ yku70Δ* reduced cell fitness is related to telomere defects. Again, *cdc73Δ* cells show slightly shorter telomeres than *WT* cells (Figure 6-2E). I conclude that lack of *CDC73* in telomere defective cells (*yku70Δ* and *cdc13-1*) leads to telomere rearrangements. Therefore, telomere rearrangements in *cdc73Δ cdc13-1* cells could explain the comparatively high fitness of these cells when compared to *paflΔ cdc13-1* and *ctr9Δ cdc13-1* cells.

6.2.3. *cdc73Δ cdc13-1* cells recover from fitness defects faster than *paflΔ cdc13-1* or *ctr9Δ cdc13-1*

cdc73Δ, *paflΔ* and *ctr9Δ* cells have lower *TLC1* levels and consequently have shorter telomeres (Figure 5-4) (Mozdy et al. 2008). Telomere rearrangements in *cdc73Δ cdc13-1* cells were confirmed in Figure 6-2 and are very likely to be the reason why those cells are so fit. Since *paflΔ* and *ctr9Δ* cause similar telomere shortening to *cdc73Δ* it is possible that *paflΔ cdc13-1* and *ctr9Δ cdc13-1* can also recover from the extensive fitness defects. To test this hypothesis, *cdc73Δ cdc13-1* and *paflΔ cdc13-1* cells were passaged several times (Figure 6-3A). Additionally, the fitness at different passages was assessed by spot test (Figure 6-3B).

Figure 6-3 shows that *cdc73Δ cdc13-1* cells do not present fitness defects at any passage (in agreement with the results in Figure 5-3). Also *cdc73Δ cdc13-1* cells are able to grow at high temperatures from very early passages, suggesting that they rearrange their telomeres very early (Figure 6-3B). On the other hand, at 23°C, *paflΔ cdc13-1* cells are very unfit at passages 1 and 2, and slightly recover by passage 3.

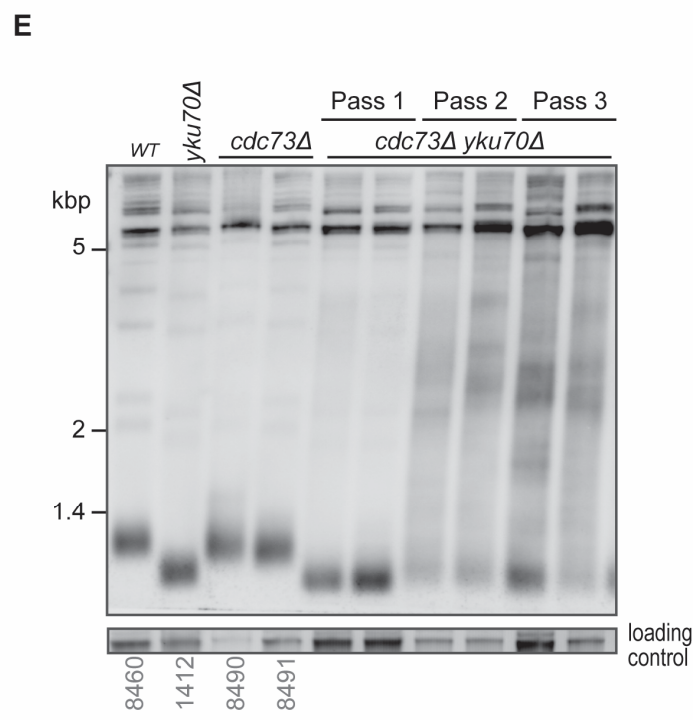
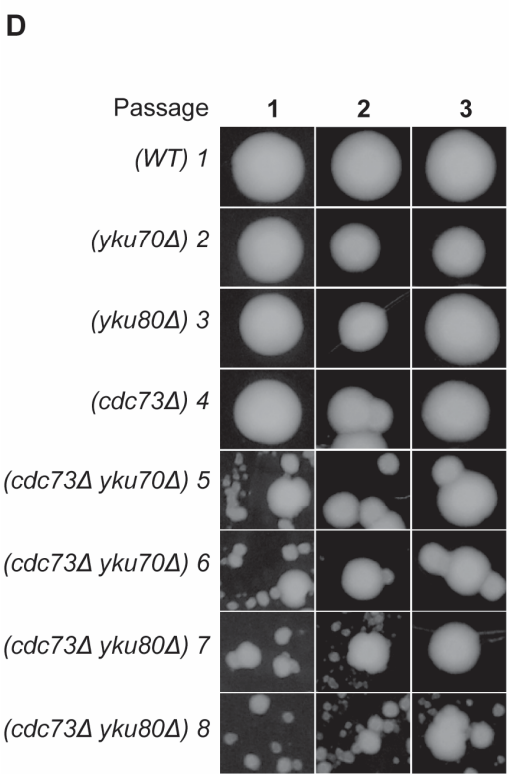
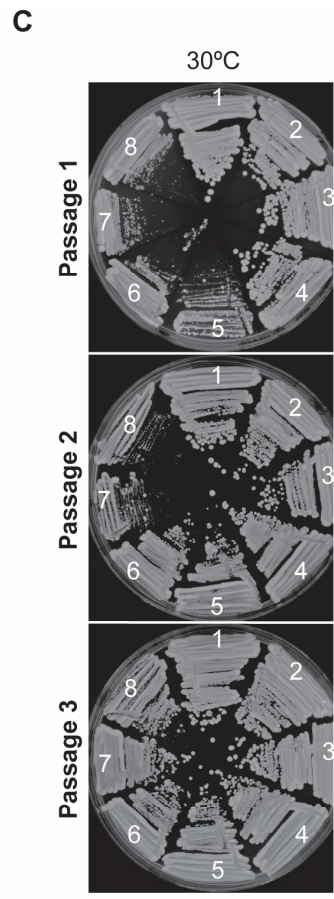
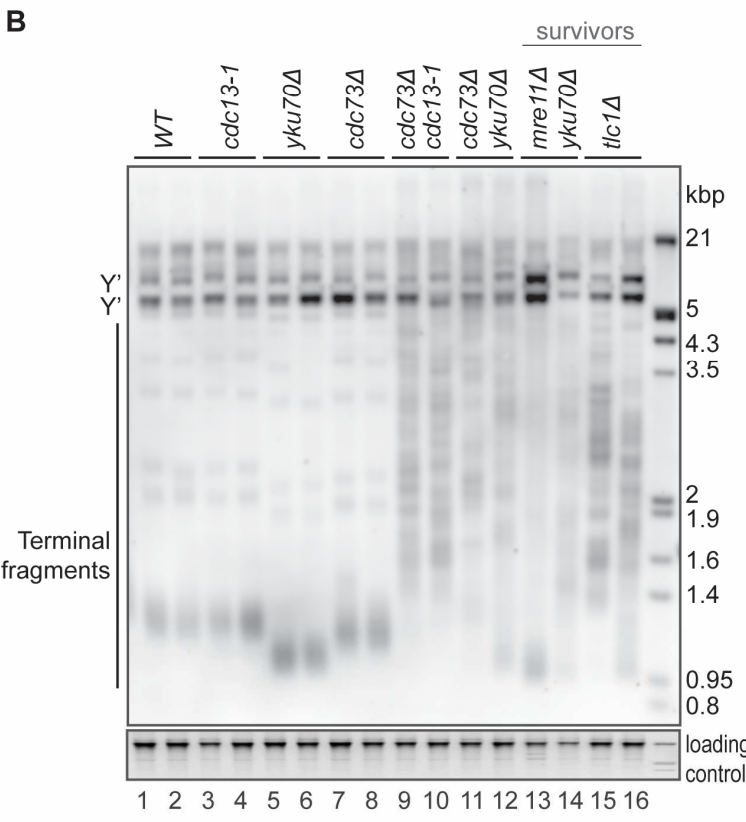
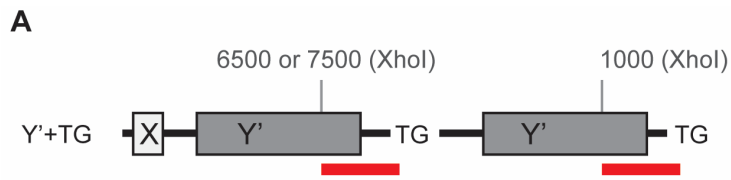


Figure 6-2 *cdc73Δ* induces telomere rearrangements in telomere defective cells. **A)** The locations of a telomere Southern blot probe as well as XhoI sites (adapted from Maringele and Lydall 2004). The probe recognizes both Y' and TG sequences. Distance from the centromeric start of the TG repeats is indicated. **B)** Two independent strains for each genotype were analysed by Southern blot using the probe in A) *mre11Δ yku70Δ* and *tlc1Δ* strains are type I and type II survivors, respectively (Maringele and Lydall 2004). SYBR safe staining used as loading control. The strains used were: *WT*, 8460 and 3001; *cdc13-1*, 1108 and 1195; *yku70Δ*, 1412 and 1366; *cdc73Δ*, 8490 and 8491; *cdc73Δ cdc13-1*, 8494 and 8495; and *cdc73Δ yku70Δ*, 8594 and 8595. **C)** Passage tests were performed by taking cells directly from germination plates and spreading them onto a fresh YEPD plate (passage 1). The plates were incubated at 30°C for 2 days, and then a pool of colonies passaged to a new fresh YEPD plate (passage 2). **D)** Representative colony or group of colonies for each strain passaged in C). For each passage the colonies shown were on the same plate. **E)** Telomere Southern blot as described in B). Strains used were: *WT*, 8460; *cdc73Δ*, 8490 and 8491. *cdc73Δ yku70Δ* cells were from fresh germination plates and not given strain numbers.

Interestingly, although *paf1Δ cdc13-1* cells seem to recover fitness with increasing passages at 23°C (Figure 6-3A), those cells never grow at non-permissive temperatures (as for example *cdc73Δ cdc13-1* cells) (Figure 6-3B). This suggests that *paf1Δ cdc13-1* cannot tolerate the telomere defects caused by *cdc13-1*. Thus, Paf1 might be needed for the fitness of cells with rearranged telomeres. Therefore, it is important to confirm that the *paf1Δ cdc13-1* cells with improved fitness indeed have telomere rearrangements. I conclude that Cdc73 plays a role decreasing the fitness of *cdc13-1* telomere defective cells. On the other hand, Paf1 increases the fitness of *cdc13-1* cells. Also, I suggest that Cdc73 and Paf1 (like Ctr9) affect telomere biology by a pathway independent of *TLC1* RNA regulation.

6.2.4. Paf1 and Ctr9, but not Cdc73, reduce TERRA levels

In principal, the short telomere phenotype of *cdc73Δ* cells, in combination with a *cdc13-1* induced telomere defect, explains the rapid telomere rearrangements and high fitness of *cdc73Δ cdc13-1* cells. However, *cdc73Δ*, *paf1Δ* and *ctr9Δ* mutations each similarly decrease *TLC1* RNA levels and telomere length, while *leo1Δ* and *rtf1Δ* have smaller effects on *TLC1* levels and telomere length (Figure 5-4) (Mozdy et al. 2008). Yet, Figure 6-1 and Figure 6-3 show that *cdc73Δ cdc13-1* cells were very fit, and in contrast *paf1Δ cdc13-1* and *ctr9Δ cdc13-1* cells were very unfit, suggesting that these fitness phenotypes were unrelated to *TLC1* levels or telomere length.

Telomere rearrangements occur in telomere defective cells via homologous recombination in both mammals and yeast (Bryan et al. 1997; Teng and Zakian 1999). TERRA (telomeric repeat containing RNA) has been suggested to facilitate this recombination, due to the presence of recombination stimulatory RNA-DNA hybrids between TERRA and telomeric DNA (Balk et al. 2013; Arora et al. 2014). Therefore, it was hypothesized that the effects Cdc73, Paf1 and Ctr9 have on TERRA levels might explain the fitness differences between *cdc73Δ cdc13-1* versus *paf1Δ cdc13-1* and *ctr9Δ cdc13-1* strains. To test this hypothesis, TERRA levels were measured in *cdc73Δ*, *paf1Δ*, *ctr9Δ*, *leo1Δ* and *rtf1Δ* strains, as well in *sir4Δ* strains, previously reported to affect TERRA levels (Iglesias et al. 2011). In addition *yku70Δ* and *mre11Δ* strains with short telomere phenotypes were examined since *cdc73Δ*, *paf1Δ* and *ctr9Δ* strains have short telomeres and shortening telomeres were suggested to induce TERRA (Cusanelli et al. 2013; Moravec et al. 2016).

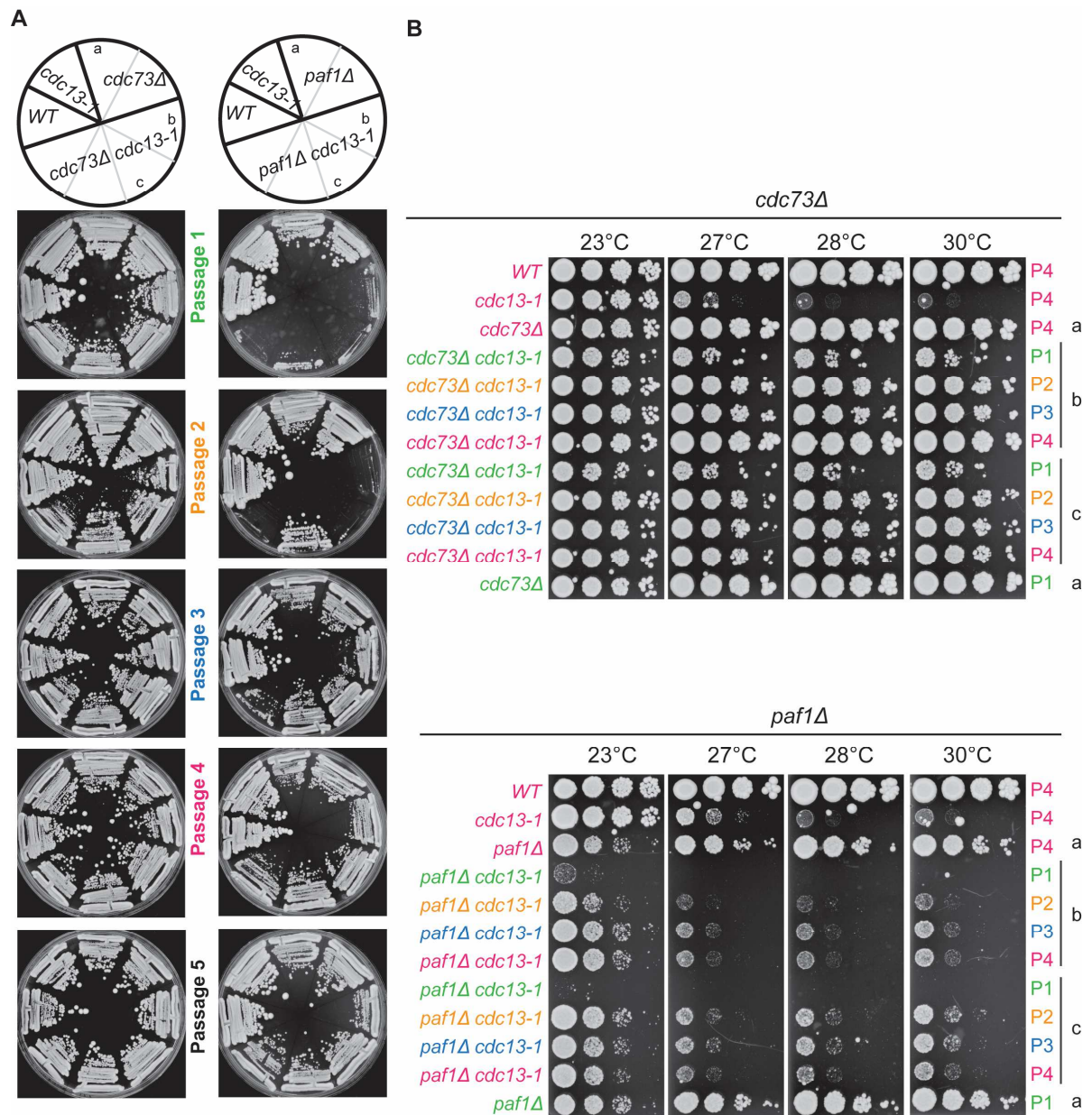


Figure 6-3 *cdc73Δ cdc13-1* do not show fitness defects while *paf1Δ cdc13-1* recover from severe fitness defects by passage 3. A) Passage tests were performed as described in Figure 6-2C with the difference that plates were incubated at 23°C for 4 days. a, b and c correspond to the strains examined by spot test in B). B) A pool of colonies from the strains in A) was inoculated in liquid media, grown overnight at 23°C and the fitness was assessed by spot test at different temperatures. *cdc73Δ* and *paf1Δ* strains at each temperature were grown on a single rectangular plate. No strains originated from this experiment were given strain numbers.

TERRA from several telomeres, including 1L, 10R, 13R and 15L, was measured and the results are shown in Figure 6-4. It was found that Paf1 and Ctr9 strongly repress TERRA levels, while other PAF1 components had much smaller effects (Figure 6-4B-G). As previously reported *sir4Δ* caused increased TERRA levels to values very similar to those of *paf1Δ* and *ctr9Δ* (Iglesias et al. 2011). Additionally, *mre11Δ* and *yku70Δ* (which have short telomeres) slightly increased TERRA levels (Figure 6-4D-G).

Short telomeres are expected to induce TERRA transcription to promote telomerase recruitment and consequent telomere elongation (Cusanelli et al. 2013; Moravec et al. 2016). *cdc73Δ* cells have short telomeres but TERRA levels similar to *WT* cells (Figure 5-4, Figure 6-2 and Figure 6-4) (Mozdy et al. 2008). Since Cdc73 is involved in the direct interaction of the PAF1 complex to RNA pol II, I hypothesised that Cdc73 is required for TERRA transcription (Mueller and Jaehning 2002; Mueller et al. 2004). To test this hypothesis, TERRA levels of *cdc73Δ paf1Δ* and *cdc73Δ ctr9Δ* cells were measured. Deletion of *CDC73* in *paf1Δ* or *ctr9Δ* cells did not decrease TERRA levels (Figure 6-4 D-G), showing that Cdc73 is not needed for high TERRA levels in these contexts.

Figure 6-4H and I shows that Paf1 and Ctr9 do not affect TERRA levels in telomeres that contain Y' repeats. Sir4, involved in histone deacetylation, as reported before, does not affect TERRA levels in Y'-telomeres (TERRA in Y'-telomeres was suggested to be regulated by Rap1, through Rif1 and Rif2) (Figure 6-4H, I) (Iglesias et al. 2011). The lack of increased TERRA from Y' telomeres together with the similar increased TERRA from X telomeres in *paf1Δ*, *ctr9Δ* and *sir4Δ* cells, suggests that Paf1 and Ctr9 might regulate TERRA through a similar pathway to Sir4.

I conclude that Paf1 and Ctr9, but not Cdc73, Rtf1 and Leo1, repress TERRA levels. Also, the idea that short telomeres cause increased TERRA levels is not verified in *cdc73Δ* cells, which have short telomeres, but normal levels of TERRA.

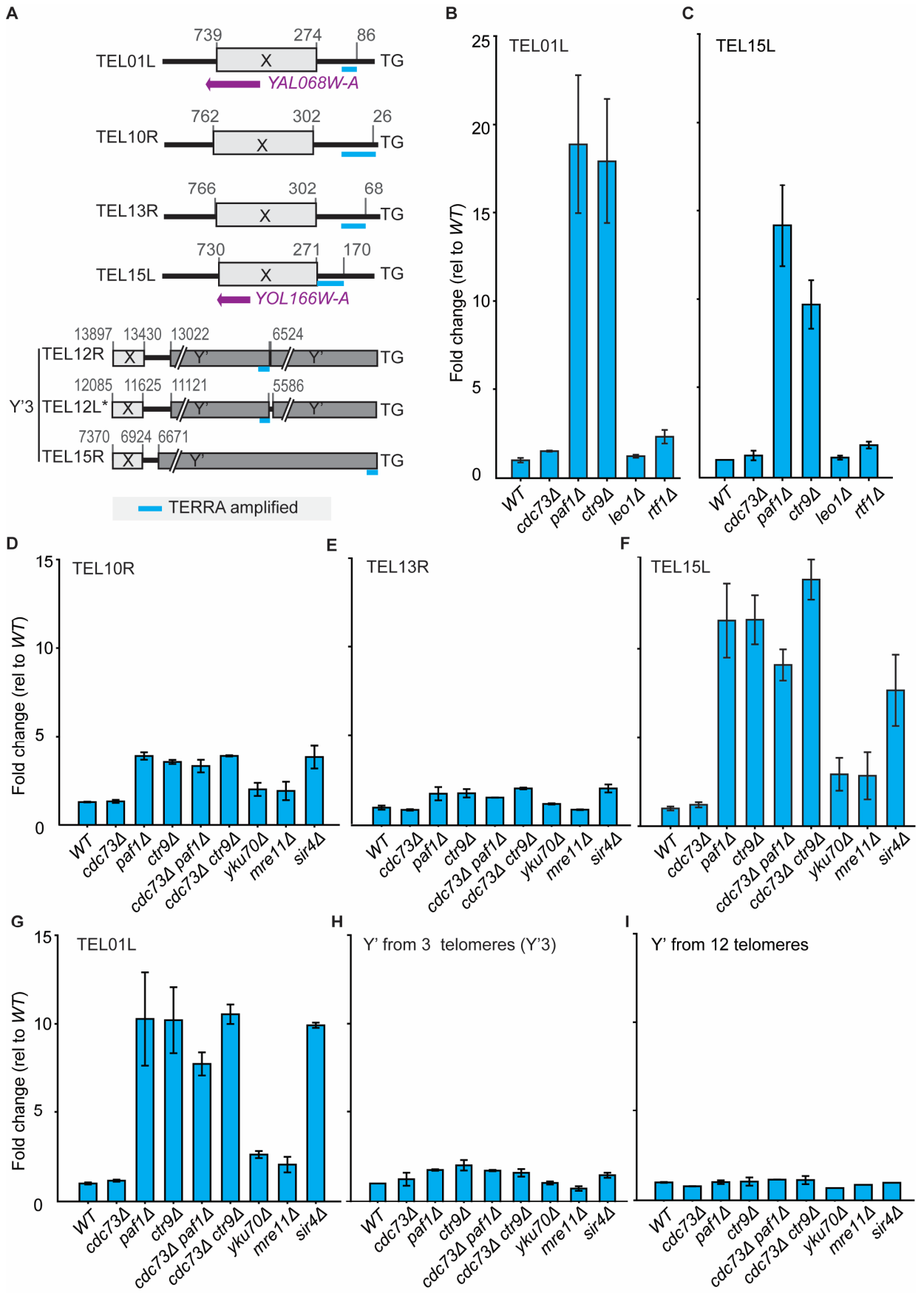


Figure 6-4 Paf1 and Ctr9, but not Cdc73, repress TERRA expression. A) The TERRA loci (blue) on different telomeres (for example telomere 1L, TEL01L) amplified during qRT-PCR TERRA measurements. Genes used to assess silencing (Figure 6-10) are represented in purple. Distance from the centromeric start of the TG repeats is indicated. **B-I)** RNA from two independent strains of each genotype was measured by qRT-PCR. The “error” bars indicate the means of the two strains analysed. Each value was normalized to *ACT1* mRNA. Values in B) and C) are from an independent experiment from D) to I). Strains used were: *WT*, 8460 and 3001; *cdc73Δ*, 8490 and 8491; *paf1Δ*, 8757 and 8758; *ctr9Δ*, 8751 and 8752; *leo1Δ*, 8736 and 8737; *rtf1Δ*, 8743 and 8744; *sir4Δ*, 5692 and 5693; *cdc73Δ paf1Δ*, 10959 and 10960; *cdc73Δ ctr9Δ*, 10961 and 10962; *yku70Δ*, 1412 and 1366; and *mre11Δ*, 2041 and 4457.

6.2.5. Telomere length is not a main regulator of TERRA expression in PAF1 complex mutants

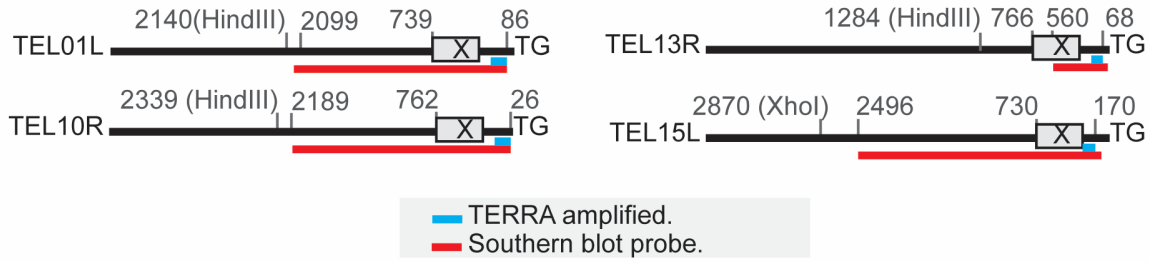
The length of yeast telomeres has a heterogeneous nature, varying inside a cell population, but also between the telomeres inside the same cell (Shampay and Blackburn 1988). Such heterogeneity requires mechanisms of sensing and responding to the telomere shortening of a single telomere. TERRA was suggested to play such role, being more expressed upon telomere shortening in order to nucleate telomerase and promote telomere lengthening in *cis* (Cusanelli et al. 2013; Moravec et al. 2016).

Since *cdc73Δ* cells were shown to have, on average, short telomeres, but no increase in TERRA levels, I hypothesized that perhaps the particular telomeres analysed for TERRA were not short in *cdc73Δ* cells. To test this hypothesis and to test the correlation between TERRA and telomere length, the cells that were analysed for TERRA in Figure 6-4 were also analysed for telomere length of the telomeres from where TERRA was expressed (Figure 6-5). Telomere length was measured by Southern blot using probes against the Y'+TG repeats (for overall telomere length assessment) and the 1L, 15L, 10R and 13R telomeres.

Figure 6-5 shows that, the overall telomere length measured using the Y'+TG probe is representative of the telomere lengths of the 1L, 15L, 10R and 13R telomeres. *cdc73Δ* (lanes 3 and 4), *paf1Δ* (lanes 5 and 6) and *ctr9Δ* (lane 7) cells have equally short telomeres (but differently affect TERRA, Figure 6-4). *yku70Δ* (lanes 8-10), *yku80Δ* (lanes 19 and 20) and *mre11Δ* (lanes 11 and 12) have shorter telomeres but less TERRA RNA than *paf1Δ* and *ctr9Δ* cells. Telomeres of *cdc73Δ paf1Δ* (lanes 15 and 16) and *cdc73Δ ctr9Δ* (lanes 17 and 18) cells are as short as the single mutants (and have TERRA levels similar to those of *paf1Δ* and *ctr9Δ* cells, Figure 6-4). *rif1Δ* (lane 25) telomere length was measured as a control for long telomeres (Teixeira et al. 2004). Interestingly, and opposite to previously published data, *sir4Δ* cells (lanes 13 and 14) have slightly long telomeres (Hass and Zappulla 2015). The reason for the difference between my data and previously published data is unclear, but my data shows that *sir4Δ* cells with long telomeres can have high TERRA levels.

I conclude that there is little correlation between telomere length and TERRA levels between *cdc73Δ*, *paf1Δ*, *ctr9Δ*, *mre11Δ*, *yku70Δ* or *sir4Δ* cells (Figure 6-4 and Figure 6-5).

A



B

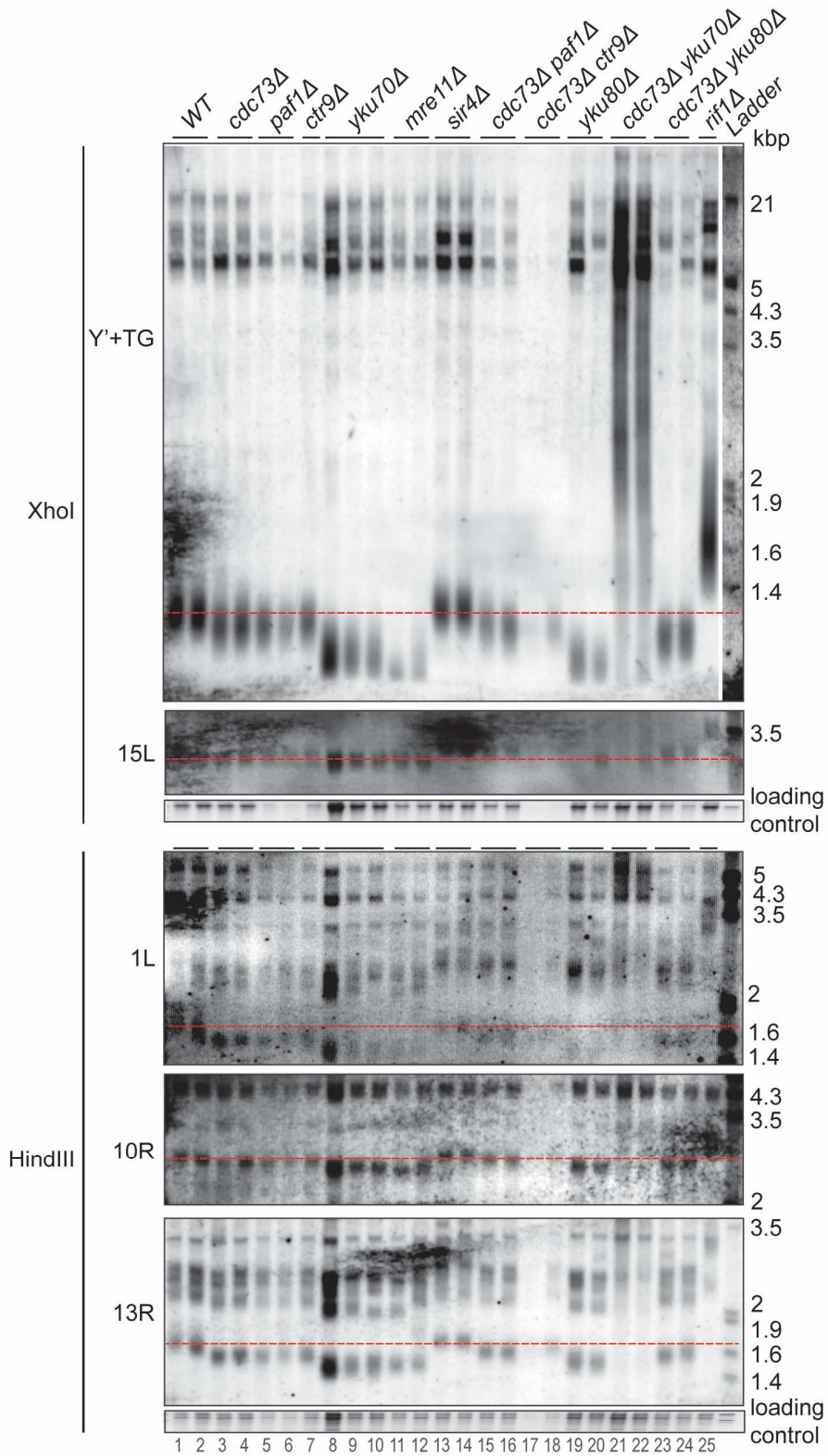


Figure 6-5 Telomere length in strains with PAF1 components deleted. A) Cartoon representing the annealing sites of the probes used in B) (red) and the TERRA loci (blue) analysed in Figure 6-4. **B)** Telomeric Southern blot performed after XhoI (top 3 panels) or HindIII (bottom 3 panels) digestion. The DNA digested with XhoI was first probed for telomere 15L and then for Y'+TG sequences. The DNA digested with HindIII was first probed for telomere 1L and then for telomeres 10R and 13R. The DNA analysed is from the same cultures that originated the data in Figure 6-4 (one exponentially growing culture was divided into two pellets used to extract either RNA or DNA). *yku80Δ* strains are 4310 and 4311; *cdc73Δ yku70Δ*, 8594 and 8595; *cdc73Δ yku80Δ*, 8702 and 8703; *rif1Δ*, 4451. The remaining strain numbers are the same as in Figure 6-4.

6.2.6. *RNH1* overexpression does not affect *paf1Δ cdc13-1* fitness

Elevated TERRA levels might lead to increased levels of RNA-DNA hybrids (between TERRA and the telomere end). RNA-DNA hybrids, or R-loops, are created when an RNA molecule anneals to DNA (Thomas et al. 1976). In yeast, RNA-DNA hybrids are eliminated by RNase H1 and RNase H2, whose catalytic subunits are encoded by *RNH1* and *RNH201*, respectively (Arudchandran et al. 2000; Jeong et al. 2004). R-loops, are a physical barrier for replication causing activation of the DDR and genomic instability (Gan et al. 2011). For example, while the RNA anneals to one of the dsDNA molecules, the exposure of the remaining ssDNA molecule can activate the DDR (Skourti-Stathaki and Proudfoot 2014). Additionally, accumulation of telomeric RNA-DNA hybrids was shown to lead to telomere loss and cellular senescence (Balk et al. 2013).

In section 6.2.4 I showed that Paf1 and Ctr9 repress TERRA levels, while Cdc73 does not. Furthermore, deletion of *PAF1* and *CTR9* in a telomere defective background (*cdc13-1*) causes extensive fitness defects while deletion of *CDC73* does not (Figure 6-1). Therefore, I hypothesised that *paf1Δ cdc13-1* and *ctr9Δ cdc13-1* cells grow poorly due to an increased number of R-loops which exacerbate *cdc13-1* telomere defects. To test this hypothesis, *RNH1* (which resolves RNA-DNA hybrids) was overexpressed in a plasmid in *paf1Δ cdc13-1* cells (Figure 6-6).

Figure 6-6 shows that overexpression of *RNH1* does not cause visible changes in the fitness of *paf1Δ* and *cdc13-1* cells when compared to the cells containing the empty vector. Data for *paf1Δ cdc13-1* cells are unclear since those cells are extremely sick at any temperature. Lack of effect of *RNH1* expression in *paf1Δ* cell fitness could suggest that RNA-DNA hybrids are not the reason for the poor growth of *paf1Δ cdc13-1* and *ctr9Δ cdc13-1* cells. However, this experiment lacks a positive control (a strain whose fitness undoubtedly benefits from *RNH1* overexpression). Thus, in the experiment in Figure 6-6 one does not know if overexpression of *RNH1* is indeed decreasing the levels of RNA-DNA hybrids in *paf1Δ cdc13-1* cells.

I conclude that overexpression of *RNH1* in *paf1Δ cdc13-1* cells does not cause fitness changes. However, whether this is informative about the role of RNA-DNA hybrids in cell fitness is unclear.

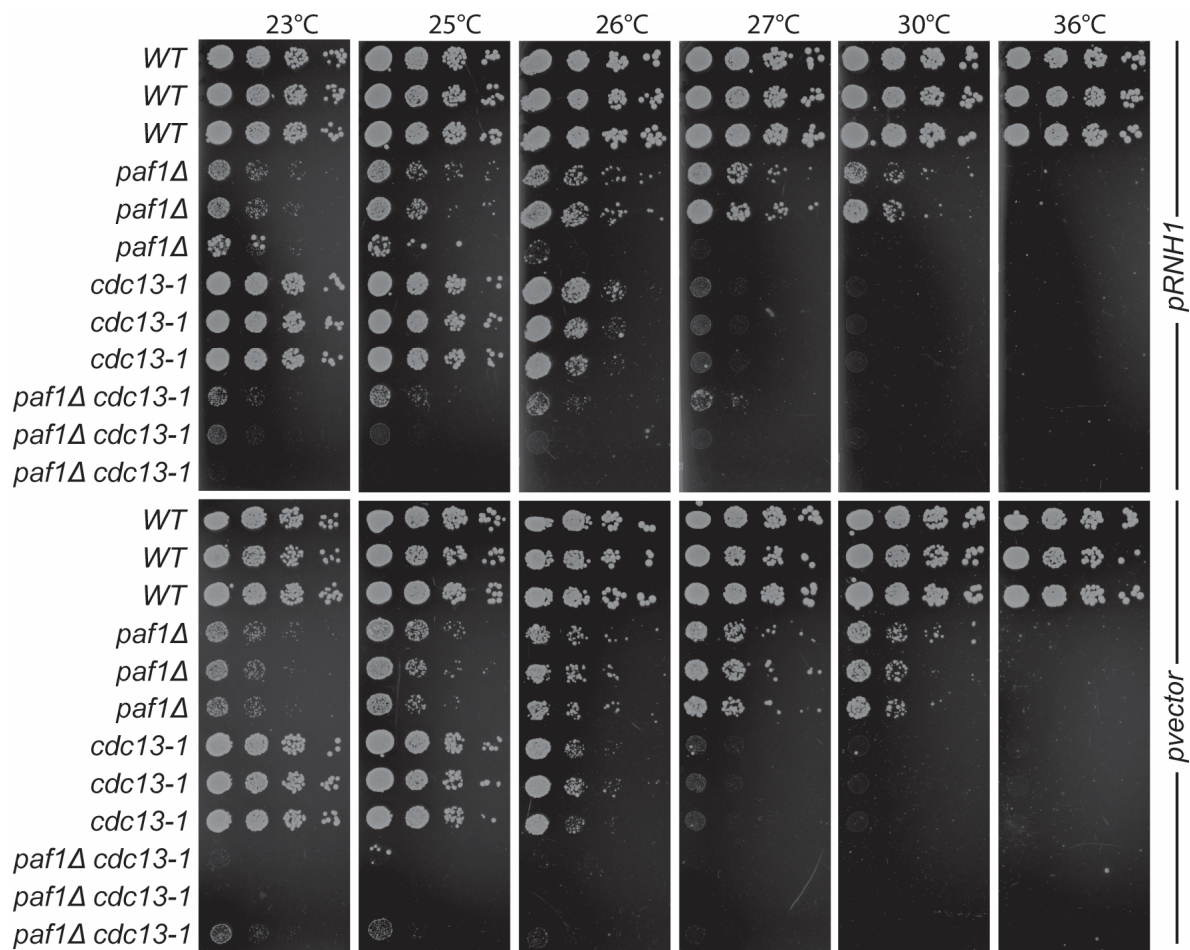


Figure 6-6 *RNH1* overexpression does not affect *paf1Δ cdc13-1* fitness. The strains indicated were independent strains picked from plasmid-bearing spores (from diploid DDY598 transformed with pDL1702 or pDL1703). Serial dilutions of the cell cultures were spotted on –Ura plates and grown for 5 days before photographing. The strains shown do not have strain numbers since they were not frozen. All strains at each temperature were grown on a single plate.

6.2.7. Paf1 and Ctr9 repress TERRA independently of the Sir complex

The effects of Paf1 and Ctr9 on TERRA were as strong as Sir4, one of the strongest known repressors of TERRA (Figure 6-4) (Iglesias et al. 2011). This led to the speculation that Paf1/Ctr9 and the Sir complex regulate TERRA through the same pathway. To test this, TERRA levels in *sir4Δ paf1Δ* and *sir4Δ ctr9Δ* double mutants was assessed (Figure 6-7). Interestingly, *sir4Δ paf1Δ* and *sir4Δ ctr9Δ* cells had TERRA levels 4 to 8 times higher than the corresponding single mutants. This shows that Paf1/Ctr9 represses TERRA through a pathway that is independent of the Sir complex. Figure 6-7E shows that the increased levels of TERRA in *paf1Δ* and *ctr9Δ* cells (compared for instance with *cdc73Δ* cells) are not due to differences in the amount of DNA from where the TERRA is being expressed (caused for example by deletions or duplications of a chromosome portion).

Reports in *S. cerevisiae* show that increased TERRA expression causes telomere shortening while reports in *S. pombe* suggest that higher TERRA expression increases telomere length (Pfeiffer and Lingner 2012; Moravec et al. 2016). Since *paf1Δ sir4Δ* and *ctr9Δ sir4Δ* cells had extremely high TERRA levels (higher than each single mutant), I next tested how TERRA levels correlate with telomere length in those cells. Figure 6-8 shows that disruption of *SIR4* further reduced the length of the already short telomeres of *paf1Δ*, *ctr9Δ* or *cdc73Δ* cells. This suggests that in *paf1Δ sir4Δ* and *ctr9Δ sir4Δ* cells there is indeed a correlation between high TERRA levels and short telomeres. Interestingly, deletion of *DOT1* (involved in telomere silencing, like *SIR4*) caused slightly longer telomeres than the *WT*, just like *sir4Δ* (Figure 6-8) (Takahashi et al. 2011b). Such result supports a model where disruption of telomere silencing promotes telomere lengthening (more like what is observed in *S. pombe*).

I conclude that Paf1 and Ctr9 repress TERRA independently of the Sir complex. I also found a correlation between extremely high levels of TERRA and very short telomere length in *paf1Δ sir4Δ* and *ctr9Δ sir4Δ* cells. However it is not clear which feature appears first: if short telomeres cause high TERRA, or if high TERRA causes telomere shortening (data in literature is also not concordant in this matter).

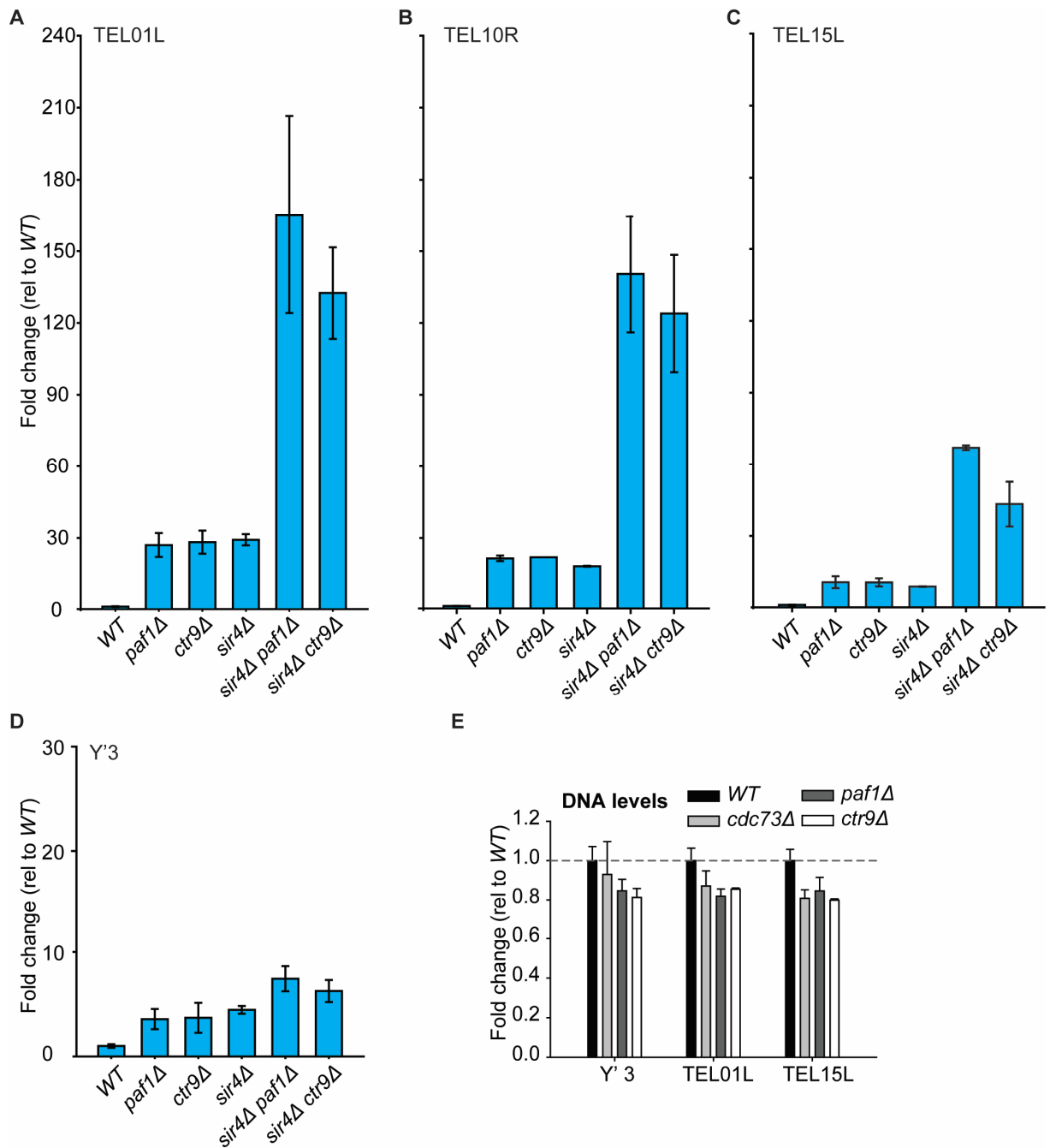


Figure 6-7 Paf1 and Ctr9 repress TERRA expression independently of the Sir complex. **A - D)** RNA from two independent strains of each genotype was measured by qRT-PCR. The “error” bars indicate the means of the two strains analysed. Each value was normalized to *ACT1* mRNA. **E)** qPCR analysis of Y'3, TEL01L and TEL15L loci. DNA from two independent strains of each genotype was measured. The “error” bars indicate the two positions of the means of the two strains analysed. Each value was normalized to the levels of *ACT1* DNA. *WT*, *paf1Δ*, *ctr9Δ* and *sir4Δ* strain numbers are the same as in Figure 6-4. *sir4Δ paf1Δ* strains are 11154 and 11155 and *sir4Δ ctr9Δ* strains are 11156 and 11157.

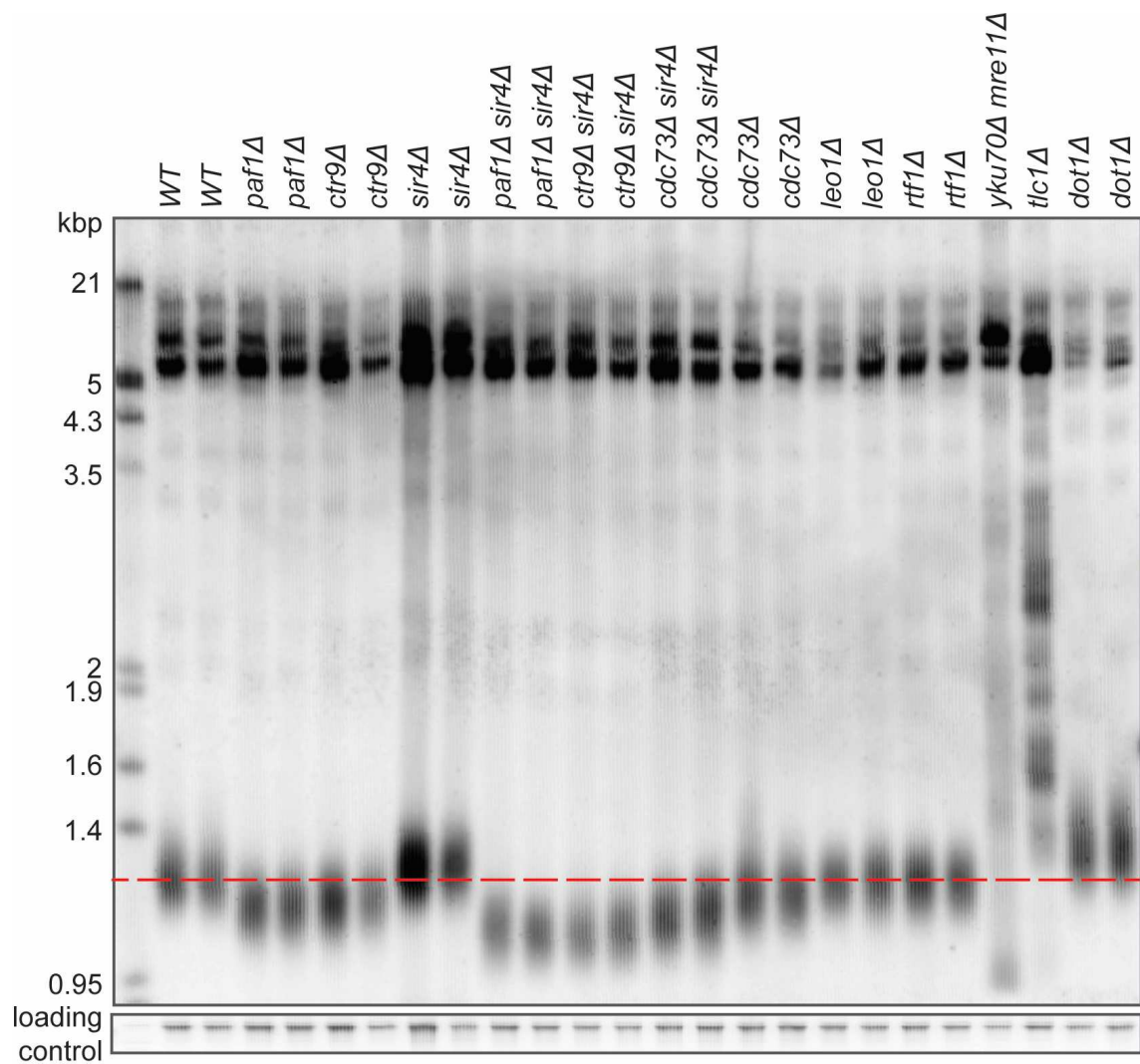


Figure 6-8 *sir4Δ* shortens *paf1Δ* and *ctr9Δ* telomeres. Telomeric Southern blot performed as described in Figure 6-2. Strain numbers as described in Figure 6-4 and Figure 6-7. *yku70Δ mre11Δ* strain is 1845; *tlc1Δ* is 2146; and *dot1Δ* are 7850 and 7851.

6.2.8. Paf1, Ctr9 and Cdc73 have distinct roles in telomere silencing

The PAF1 complex binds RNA pol II and controls RNA levels via a number of routes including regulation of histone modifications, transcription, poly(A) processing and promoter-proximal pausing of RNA pol II (Penheiter et al. 2005; Crisucci and Arndt 2011; Chen et al. 2015). Systematic analysis of *paf1Δ* and *ctr9Δ* strains shows that the PAF1 complex reduces about three times as many transcripts as it increases (Penheiter et al. 2005). Interestingly, in the context of regulating TERRA levels, Paf1 and Rtf1 have been reported to help silence telomeres (Krogan et al. 2003a). Therefore, it was hypothesised that the PAF1 complex could be regulating TERRA levels by silencing telomeres through a parallel pathway to the Sir complex. To test telomere silencing, *URA3* expression near the 7L telomere was measured (Figure 6-9) (Gottschling et al. 1990; Fourel et al. 1999).

Figure 6-9B shows that *paf1Δ*, *ctr9Δ* and *rtf1Δ* cells were unable to silence expression from the telomere 7L while *cdc73Δ* and *leo1Δ* cells were proficient at silencing. These results confirm and extend previous experiments that showed that Paf1, Ctr9 and Rtf1 promote telomere silencing (the role of other members of the PAF1 complex was not tested) (Krogan et al. 2003a; Marton and Desiderio 2008). Once again it was observed that different PAF1 complex components have different functions. Furthermore there was a clear lack of correlation between telomere silencing and TERRA expression, in particular *rtf1Δ* cells were perhaps the most defective at silencing 7L (most similar to *sir4Δ* mutants), but had very small effects on TERRA levels (Figure 6-4). It was however plausible that the lack of correlation between silencing and TERRA levels was an artefact of the artificial telomere used to measure silencing.

Interestingly, *sir4Δ* suppressed the fitness defects of *paf1Δ* and *ctr9Δ* cells at 34°C (Figure 6-9, SC media), even though *paf1Δ sir4Δ* and *ctr9Δ sir4Δ* cells have shorter telomeres than *paf1Δ* or *ctr9Δ* cells (Figure 6-8). Perhaps it is relevant to note that *rtf1Δ*, which is important for telomere silencing (Figure 6-9), also represses *paf1Δ* fitness defects (Mueller and Jaehning 2002; Krogan et al. 2003a). Therefore one hypothesis is that loss of telomere silencing increases *paf1Δ* and *ctr9Δ* cell fitness (maybe due to chromatin remodelling caused by an unbalanced acetylation/methylation ratio).

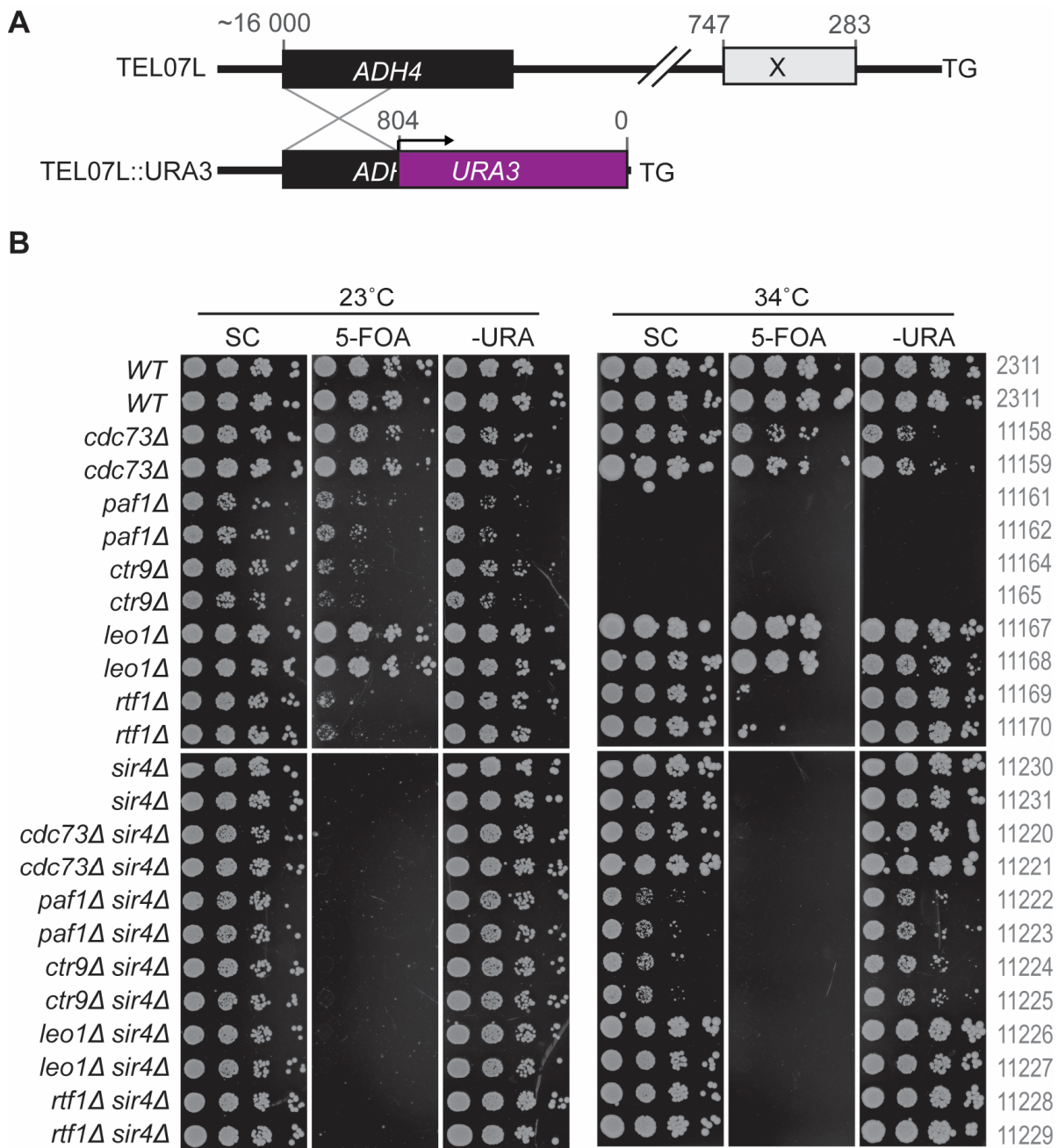


Figure 6-9 Paf1, Ctr9 and Rtf1, but not Cdc73 and Leo1, affect telomere silencing. **A**) Insertion of a *URA3* gene at the *ADH4* locus to measure telomere silencing (Gottschling et al. 1990; Fourel et al. 1999). **B**) Silencing was measured by growth on plates lacking uracil (-URA), containing 5-Fluoroorotic acid (5-FOA) or synthetic complete media (SC). All strains have the *TEL07L::URA3* construct. All strains at each temperature were grown on a single plate.

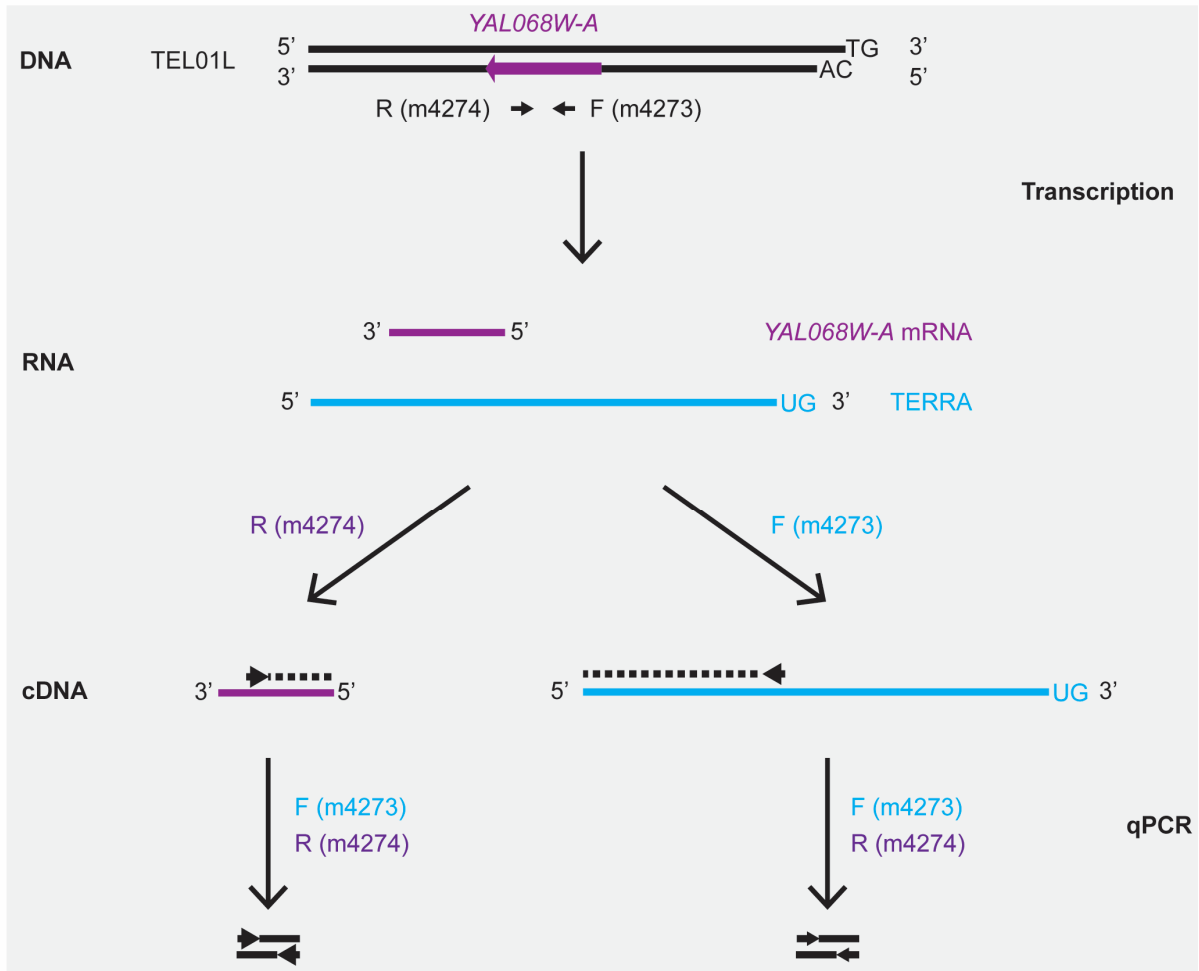
I conclude that Paf1, Ctr9 and Rtf1 promote telomere silencing, while Cdc73 and Leo1 do not. Such conclusion is in agreement with previously reported data, although my data is the first systematic analysis of the role of each PAF1 complex component in telomere silencing.

6.2.9. Paf1 and Ctr9 repress TERRA transcription more than other telomeric transcripts

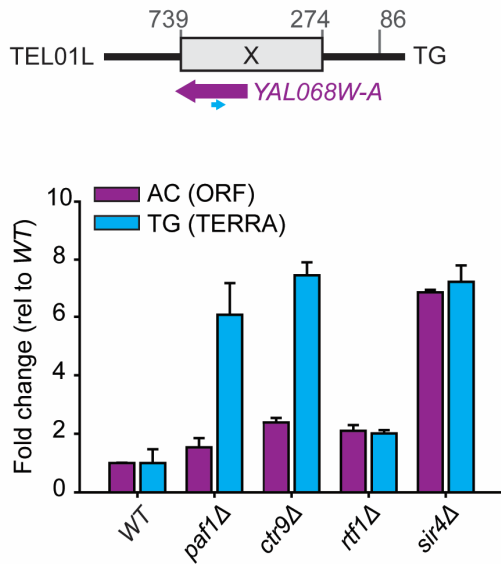
To further investigate the relationship between TERRA and silencing I examined natural telomere silencing by measuring transcripts from telomeres 1L (*YAL068W-A*) and 15L (*YOL166W-A*) (Figure 6-10). To distinguish gene silencing from TERRA, transcripts on opposite strands were measured (Figure 6-10A). Interestingly, at natural telomeres, the roles of Paf1 and Ctr9 were different to Rtf1 and to Sir4. As expected *sir4Δ* cells show high levels of both telomeric ORF transcripts and TERRA, consistent with a general telomere-silencing defect. *paf1Δ* and *ctr9Δ* cells showed moderately increased ORF transcript levels near telomeres, but much larger increase of RNA from the opposite strand (TERRA) (*sir4Δ*, *paf1Δ* and *ctr9Δ* have similarly high TERRA). This confirms the idea that Paf1 and Ctr9 strongly repress TERRA but have a weaker effect on general telomeric gene silencing, which is consistent with the spot test assays in Figure 6-9. Interestingly, Rtf1 had a similar effect to Paf1 and Ctr9 in repressing *YAL068W-A* transcription at the 1L telomere, and barely any effect on *YOL166W-A* transcription, suggesting a role for Rtf1 in telomere silencing, but not in TERRA transcription.

I conclude that Paf1, Ctr9 and Rtf1 contribute broadly and similarly to telomere gene silencing, while Cdc73 and Leo1 do not. However, Paf1 and Ctr9 strongly repress TERRA, by a Sir4-independent pathway, while Cdc73, Leo1 and Rtf1 play smaller roles repressing TERRA.

A



B



C

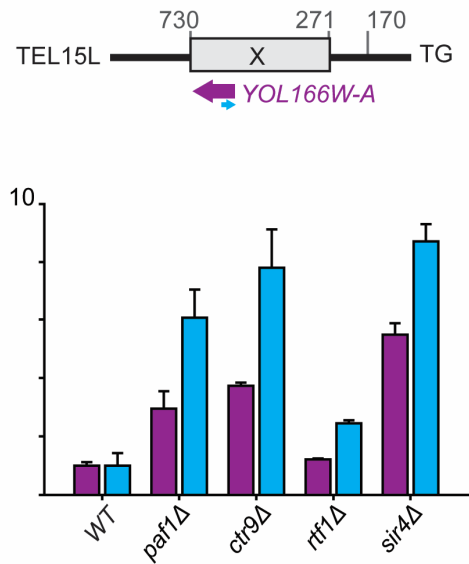


Figure 6-10 Paf1 and Ctr9 repression of telomeric transcript does not perfectly correlate with TERRA repression.**A)** To compare transcription from ORFs in the AC-rich (antisense) strand (*YAL068W-A*) versus the TG-rich (sense) strand (TERRA), two independent cDNA synthesis reactions were performed. For *YAL068W-A* mRNA measurements, the reverse primer (m4274) was used. For TERRA measurements, the forward primer (m4273) was used. qPCR was then performed to each cDNA using both forward and reverse primers. **B and C)** qRT-PCR to measure telomeric RNA at *YAL068W-A* (B) and *YOL166W-A* loci (C), as described in A). Purple bars represent the transcription from the AC-rich DNA strand and blue bars represent transcription from the TG-rich DNA strand (TERRA). RNA from two independent strains of each genotype was measured and “error” bars indicate the means of the two strains analysed. Each value was normalized to *ACT1* mRNA. Strain numbers as described in Figure 6-4.

6.2.10. The PAF1 complex does not regulate mating locus silencing

To test if the PAF1 complex components also affect mating type locus silencing I quantified the expression of the *a1* factor in *MAT α* strains (Figure 6-11). If the mating type locus is properly silenced, *MAT α* cells should not express the *a1* factor from the mating type locus, since *a1* is only expressed in *MAT α* cells (Herskowitz 1989). Figure 6-11 shows that indeed deletion of each of the PAF1 complex components in *MAT α* strains did not affect repression of the *a1* factor in those cells.

I conclude that, opposite to what happens at telomeres, none of the PAF1 complex components promote, or is essential, for mating locus silencing. I suggest that the PAF1 complex play a specialized role at telomeres, perhaps by interaction with telomeric proteins.

6.2.11. Paf1 promotes RNA, especially TERRA, degradation

RNA levels can be regulated by at least two different ways: transcription and degradation. The Sir complex, a histone deacetylase complex, represses transcription and regulates TERRA by this pathway (Iglesias et al. 2011). Paf1 and Ctr9 were shown to repress TERRA by an independent pathway to the Sir complex (Figure 6-7) and were also shown to repress TERRA more strongly than telomere ORFs (Figure 6-10). Consequently, I hypothesised that Paf1 and Ctr9 were repressing TERRA by promoting TERRA degradation. To test this hypothesis, RNA decay was measured in *paf1 Δ* versus *WT* cells using the Anchor-Away technique (Haruki et al. 2008). In the version of the Anchor-Away technique used here, a subunit of RNA pol II (Rpb1) is removed from the nucleus upon addition of rapamycin, stopping transcription (Haruki et al. 2008). This allows the determination of the RNA half-life for different transcripts (Table 6-1, Figure 6-12).

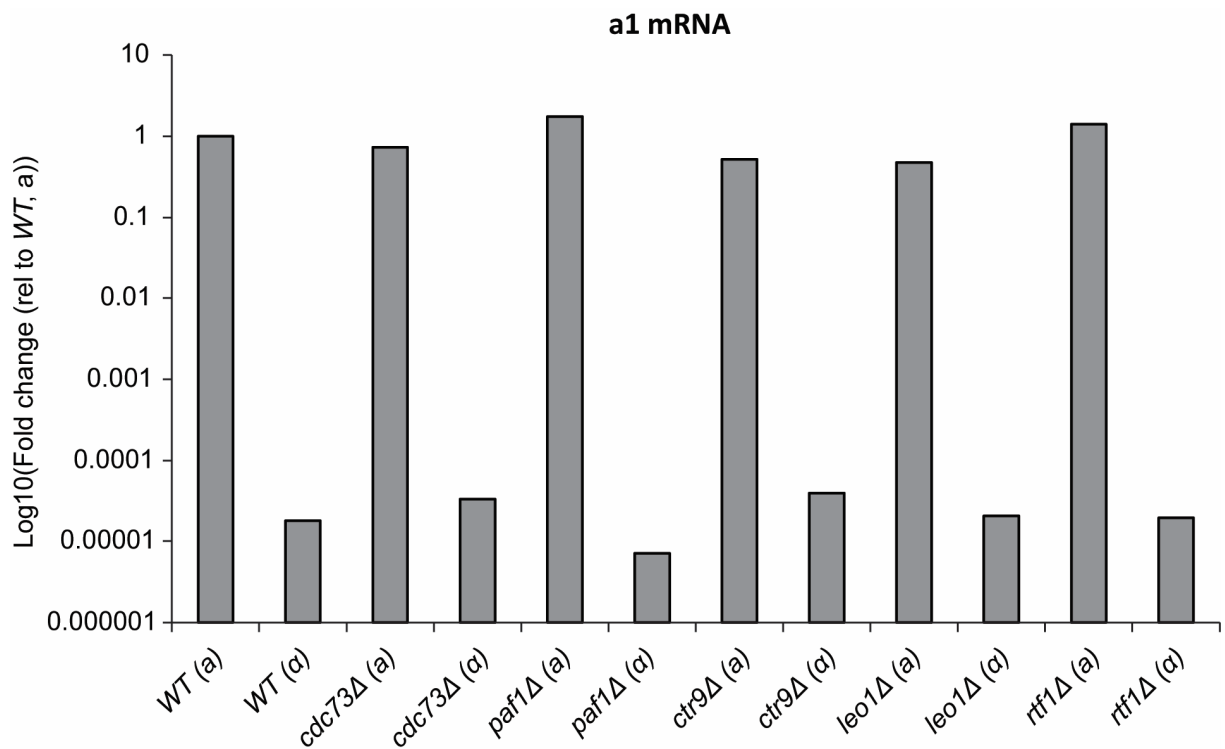


Figure 6-11 Deletion of PAF1 components in *MAT α* cells does not affect a1 mRNA levels. qRT-PCR analysis of a1 RNA expressed from the *MAT* locus. One strain for each mating type was used. Data is presented in the Log10 scale. Strains are as described in Figure 6-4. For each genotype the smaller strain number corresponds to the *MAT α* strain.

Figure 6-12 shows that in *WT* (Anchor-Away background) or *paf1Δ* cells addition of DMSO did not cause major changes in RNA levels. In *WT* cells addition of rapamycin caused the RNA to decrease over time suggesting that indeed transcription stopped after rapamycin addition (Figure 6-12). Additionally, in *WT* cells, TERRA half-life was similar to *ACT1* and *BUD6* mRNA (housekeeping) (Table 6-1). Interestingly, in *paf1Δ* cells, an overall increase in RNA half-life was observed, with the half-life of housekeeping genes increasing 2 to 6 fold (Table 6-1). However, a much more severe effect on TERRA half-life could be observed in *paf1Δ* cells, with basically no degradation of TERRA from telomeres 1L, 10R and 15L, corresponding to a 600 fold increase in half-life of TERRA RNA (Figure 6-12 and Table 6-1).

I concluded that Paf1 (and presumably Ctr9) repress TERRA levels likely by promoting RNA degradation. I also show that Paf1 promotes degradation of RNAs throughout the genome but plays a stronger role at telomeres. The stronger effect at telomeres is in agreement with the role of the PAF1 complex in silencing telomeres but not the mating type locus (Figure 6-9 and Figure 6-11). I suggest that the PAF1 complex plays a specialized role at telomeres.

Table 6-1 RNA half-life. RNA half-life was calculated as described in Materials and Methods using the graphs in Figure 6-12. A half-life of 20000 min was given when no RNA decrease was observed over 60 min (a positive slope was observed). Fold changes of the *paf1Δ* half-life relative to the *WT* averages can be found in brackets. N. d., not determined.

	Half-life (min)			
	<i>WT</i> 1 (11213)	<i>WT</i> 2 (11213)	<i>paf1Δ</i> (11218)	<i>paf1Δ</i> (11232)
<i>ACT1</i>	25	26	85 (3.3X)	45 (1.8X)
<i>BUD6</i>	15	17	91 (5.6X)	104 (6.5X)
1L TERRA	21	21	19694 (938X)	68 (3.2X)
10R TERRA	36	N. d.	20000 (555X)	20000 (555X)
15L TERRA	21	32	20000 (755X)	20000 (755X)

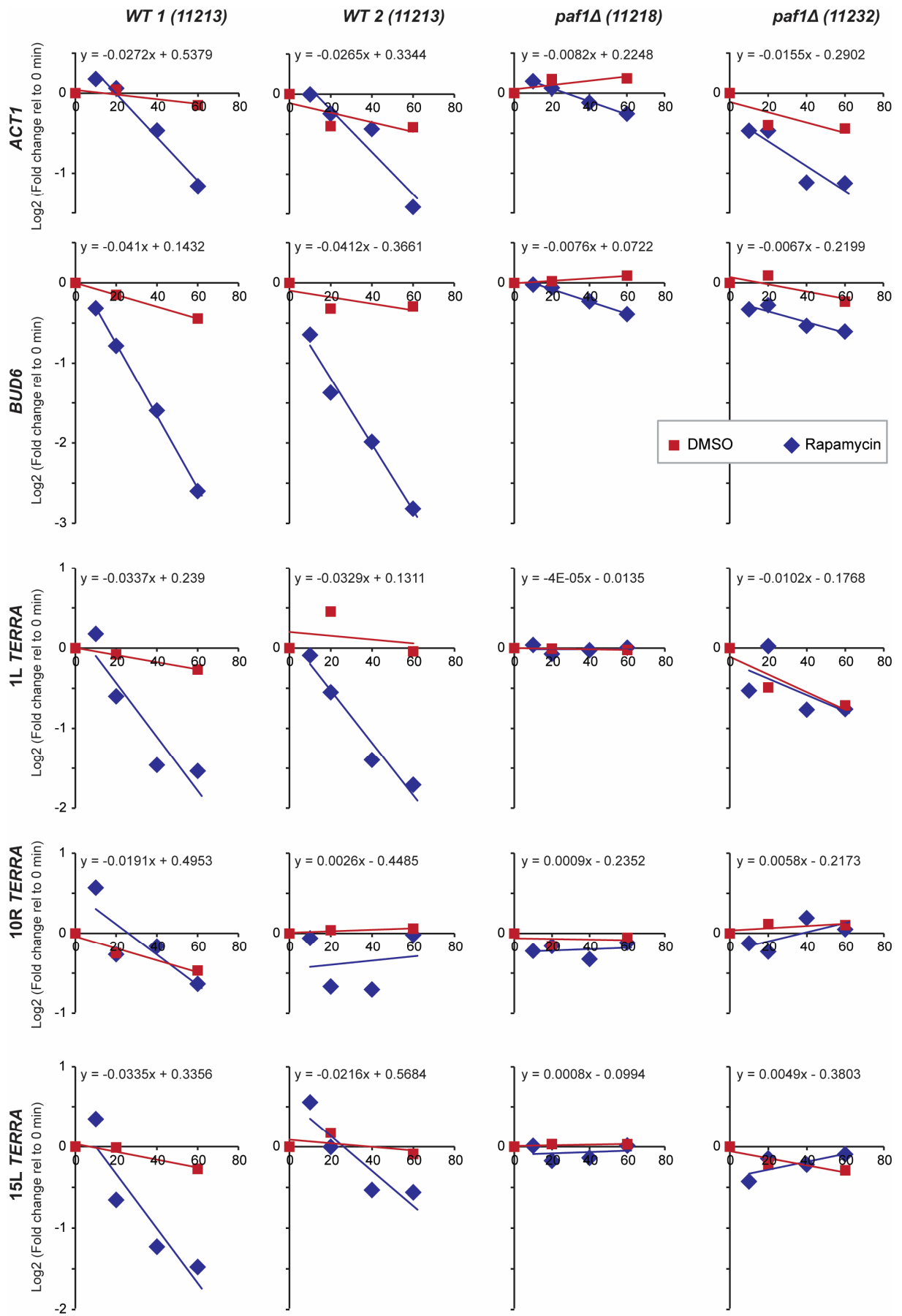


Figure 6-12 Paf1 promotes RNA degradation. qRT-PCR of *ACT1*, *BUD6* and *TERRA* from 3 different telomeres (1L, 10R and 15L) in *WT* and *paf1Δ* strains (in the Anchor-Away background). Total RNA was isolated from cells harvested at 0, 10, 20, 40 and 60 min after rapamycin (blue) was added to the media or 0, 20, 40 and 60 min after addition of DMSO (red). RNA levels were measured for each time-point and normalized for the amount of 7S RNA. The fold change from the 0 min time point was obtained and the data was plotted as a function of time starting from the 10 min time-point. The line that best represent each set of data is represented (defined by Microsoft Excel) and the equation ($y=mx+b$) of the line for the rapamycin experiment is shown. Two independent experiments were performed: experiment 1: *WT1* (11213) and *paf1Δ* (11218); experiment 2: *WT2* (11213) and *paf1Δ* (11232).

6.2.12. Nmd2 and Ski2 do not strongly affect TERRA levels

RNA quality control is an essential mechanism to maintain cell function as it prevents the generation of defective proteins (van Hoof and Wagner 2011). mRNA quality is assessed at various stages, from transcription initiation/elongation, to splicing and polyadenylation (Garneau et al. 2007). Consequently, the cell has a variety of mRNA surveillance-pathways acting both in the nucleus as well as in the cytoplasm (Garneau et al. 2007). Since Paf1 (and likely Ctr9) is repressing TERRA levels at least in part by promoting its degradation I decided to measure TERRA levels in cells defective in two independent mRNA decay pathways: the nonsense-mediated mRNA decay and the cytoplasmic exosome.

Figure 6-13 shows that *NMD2* (part of the nonsense-mediated mRNA decay) deletion slightly increases TERRA RNA from 1L and 15L but to a much lesser extent than *PAF1* deletion. *SKI2* (adaptor of the cytoplasmic exosome) deletion did not affect TERRA levels at telomeres 1L or 15L. I conclude that Paf1 represses TERRA by promoting its degradation by a pathway that is likely independent of the nonsense-mediated mRNA decay and the cytoplasmic exosome-dependent pathways.

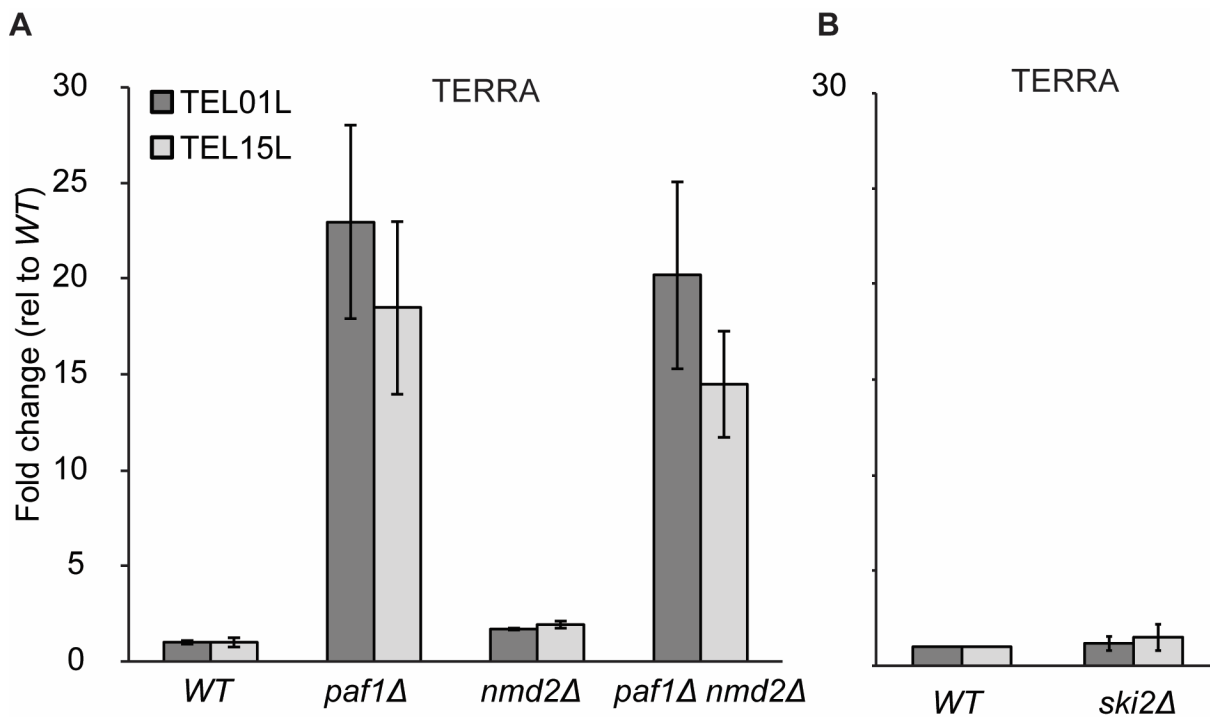


Figure 6-13 Nmd2 weakly represses TERRA and Ski2 does not affect TERRA. qRT-PCR analysis of TERRA RNA in *nmd2*Δ (A) and *ski2*Δ (B) strains. Strain numbers are: *WT*, 8460 and 3001; *paf1*Δ, 8757 and 8758; *nmd2*Δ, 4528 and 4765; *paf1*Δ *nmd2*Δ, 10117 and 10118; and *ski2*Δ, 8844 and 8845.

6.3. Discussion

In order to understand the role of the different components of the PAF1 complex in telomere biology, each component was assessed for a role in: a) fitness of telomere defective cells; b) telomere length; and c) TERRA regulation. I could clearly show that components of the PAF1 complex play distinct roles in regulating telomere biology, as summarised in Figure 6-14A. Paf1 and Ctr9 contribute most to fitness of wild-type cells and telomere defective *cdc13-1* cells. Interestingly, Cdc73, which like Paf1 and Ctr9 affects telomerase levels, has the opposite effect and reduces fitness of *cdc13-1* cells. Leo1 and Rtf1 have minimal effects on fitness. Paf1 and Ctr9 strongly reduce TERRA levels, while Cdc73, Leo1 and Rtf1, the other PAF1 components, play a minor role in this context. Paf1, Ctr9 and Rtf1 affect telomere gene silencing while Cdc73 and Leo1 do not. Overall the data in this Chapter suggests that Paf1 and Ctr9 are the core components of the Paf1 complex, affecting TERRA and with other components affecting specific aspects of telomere biology such as telomere silencing and *TLC1* RNA levels.

I propose a model where the PAF1 complex affects telomere function by at least three pathways (p1, p2, p3) (Figure 6-14). p1 affects TERRA levels, p2 affects histone modifications and transcription, but does not greatly affect TERRA, and p3 affects *TLC1* RNA abundance and therefore telomerase activity. My experiments show that the Paf1/Ctr9 dependent p1 affects TERRA levels through an alternative pathway to the Sir complex. RNA decay experiments suggested that p1 promotes TERRA degradation. Paf1, Ctr9 and Rtf1-dependent p2 affects silencing and is distinguished from p1 by the fact Rtf1 effects on TERRA are much milder than Paf1/Ctr9 (Figure 6-14A). Rtf1 is required for H3K4 and H3K79 methylation, via recruitment of COMPASS and Dot1 (Krogan et al. 2003a) and p2 might work via this route. Paf1, Ctr9 and Cdc73 affect *TLC1* RNA levels, telomerase activity and telomere length in p3.

A

	<i>wt</i>	<i>paf1Δ</i>	<i>ctr9Δ</i>	<i>cdc73Δ</i>	<i>leo1Δ</i>	<i>rtf1Δ</i>
Fitness	++++	++	++	+++	+++	+++
<i>cdc13-1</i> fitness	++++	+	+	+++ ++	++	++
<i>TLC1</i> /Telomere length	++++	+	+	+	++	++
<i>TERRA</i>	++++	++++ ++++	++++ ++++	++++	++++	+++ ++
Silencing	++++	++	++	++++	++++	++
Pathways affected (see B)		1,2,3	1,2,3	3		2

B

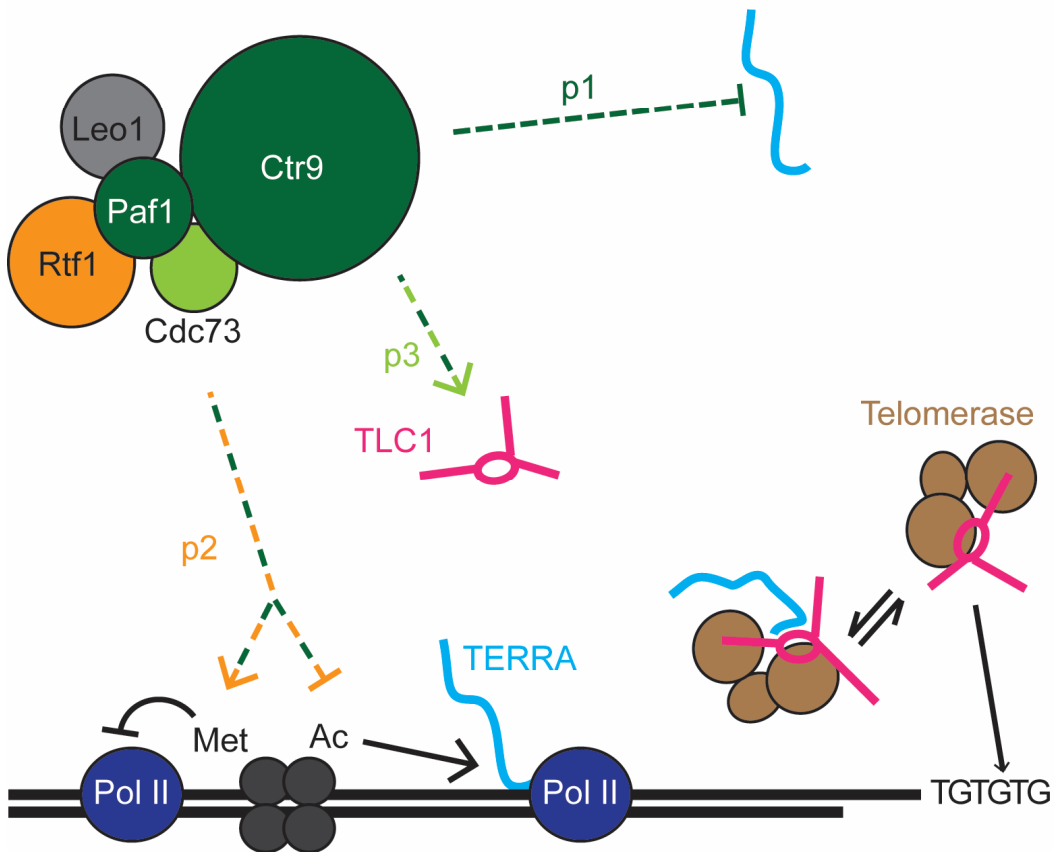


Figure 6-14 The role the PAF1 complex components in telomere function. A) Effects caused by deletions of PAF1 complex components. “++++” are the values of “Fitness”, “*TLC1*/Telomere length”, “*TERRA*” or “Silencing” (first column) observed in *WT* cells. Mutations that cause a decrease in the parameters in the first column will have less “+” (shaded red), while more “+” (shaded green) represent an increase in the parameters in the first column. **B)** Model for how the PAF1 complex affects telomere biology. Paf1 and Ctr9 are needed for the integrity of the PAF1 complex and all its functions. A major role for Paf1 and Ctr9 is to affect *TERRA* levels (p1). A *TERRA-TLC1* interaction impairs telomerase function causing fitness defects. Rtf1, Paf1 and Ctr9 stimulate histone methylation to reduce RNA Pol II transcription (p2). Cdc73, Paf1 and Ctr9, affect *TLC1* levels (p3). Leo1 (gray) is the least important Paf1 component and has the mildest phenotypes.

How Paf1 promotes TERRA degradation (more than *BUD6* and *ACT1* mRNA for example) is not totally clear. One hypothesis is that lack of Paf1 function would decrease TERRA polyadenylation (in yeast all TERRA RNA is adenylated) (Luke et al. 2008). It has been suggested both in budding and fission yeast that polyadenylated TERRA does not tend to anneal to the telomere ends, while non-adenylated, G-rich TERRA does (Porro et al. 2010; Moravec et al. 2016). It is possible that in *paf1Δ* cells TERRA is bound to the telomere more tightly (RNA:DNA hybrids), stabilizing and protecting it from degradation, and therefore increasing its half-life. A challenge to such a model is the fact that altered poly(A) tail length, by mutations in polyadenylation proteins, was shown to destabilize TERRA (Luke et al. 2008; Porro et al. 2010). The RNA half-life increase in *paf1Δ* cells observed for *ACT1* and *BUD6*, must be related to an overall role of Paf1 controlling poly(A) tail length, but due to the special nature of TERRA and telomeres (a noncoding RNA), TERRA might be more strongly stabilized than other coding RNAs in *paf1Δ* cells. Additionally, the fact that in *paf1Δ* cells I cannot see an increase in *ACT1* and *BUD6* mRNA levels (while half-life increase 3-6 fold) suggests that cells can compensate for that increased half-life (maybe decreasing transcription rate). Another hypothesis is that Paf1 directly regulates the levels or presence at telomeres of a member of the RNA decay pathway, promoting TERRA degradation. A difference in effect at telomeres (TERRA) versus the remaining chromosome (*BUD6* and *ACT1*) might be again due to the special composition in proteins/interactions at telomeres. I suggest that the PAF1 complex has an essential role maintaining telomere homeostasis particularly due the unique telomere microenvironment.

Early experiments suggested that telomere length is not a major regulator of TERRA levels (Iglesias et al. 2011) while more recent experiments suggested that it might be (Arnoult et al. 2012; Cusanelli et al. 2013; Moravec et al. 2016). My data supports the view that telomere length is not a primary regulator of TERRA because there is little correlation between telomere length and TERRA levels in PAF1 complex mutants, *mre11Δ* or *yku70Δ* strains. However, interestingly it was observed that *paf1Δ sir4Δ* mutants, with very high levels of TERRA, had very short telomeres, suggesting that under certain conditions telomere length does relate to TERRA levels. Whether telomere shortening is a cause or consequence of increased TERRA levels, is not clear.

There are many reasons for yeast strains to grow poorly but the fitness defects caused by loss of *PAF1*, *CTR9* or *CDC73* can be partially rescued by overexpression of *TLC1*, showing that fitness defects are due at least in part to low levels of *TLC1* (Betz et al. 2002). It is notable that *paf1Δ* and *ctr9Δ* cells are less fit than *cdc73Δ* strains, both with and without *cdc13-1*. In the previous Chapter, Paf1 and Ctr9 were shown to be important to maintain low levels of *TEN1* and *STN1* mRNA. I suggest that the poor fitness caused by *paf1Δ* and *ctr9Δ* in telomere defective cells is because of the high levels of TERRA, Ten1 and Stn1. High levels of TERRA, Ten1 and Stn1 in *paf1Δ* and *ctr9Δ* mutants could directly interfere with telomere capping function and/or further reduce the amount of active telomerase in such cells. TERRA inhibits telomerase activity *in vitro* (Redon et al. 2010) and telomerase contributes directly to making a functional telomere cap (Vega et al. 2007). Additionally, Ten1 represses telomerase recruitment to the telomere (Qian et al. 2009a; Leehy et al. 2013). It is also known that increased levels of TERRA can interact with Ku, even though this interaction does not affect the binding capacity of Ku to *TLC1* or the telomere, it promotes telomere shortening (Pfeiffer and Lingner 2012) and consistent with this I have shown the very high levels of TERRA, in *paf1Δ sir4Δ* and *ctr9Δ sir4Δ* cells correlate with very short telomeres. Finally, telomeres have complex relationships with DNA damage proteins, because DNA damage proteins, like Ku, ATM and ATR, are important for telomere physiology, yet in the context of telomeres do not induce their usual DNA damage responses such as NHEJ or cell cycle arrest. The PAF1 complex too interacts with DDR proteins, to avoid replication-transcription fork collision (Poli et al. 2016). Perhaps in *paf1Δ* and *ctr9Δ* cells, the high levels of TERRA (causing R-loops, increasing transcription) and low levels of *TLC1* (maybe slowing down telomere replication), together with less efficient mechanism to avoid replication-transcription fork collision, leads to replication block and activation of the DDR. Still, such a model might not explain how *paf1Δ sir4Δ* cells, with very short telomeres and very high TERRA levels are fitter than *paf1Δ* cells (that have longer telomeres and lower TERRA).

The observation that loss of Cdc73 suppresses the fitness defects of telomere defective *cdc13-1* strains is striking. Similar effects in human cells may help explain why large numbers of mutations in Cdc73, but not other PAF1 components, are found in human cancers (An et al. 2016). For instance, *cdc73Δ* cells are able to maintain cell division even when the telomeres are defective (which is a major signal for cell cycle arrest), just like cancer cells. It is perhaps the capacity of *cdc73Δ* cells

to maintain normal levels of TERRA, Ten1 and Stn1, that allows those cells to avoid extensive DDR activation upon Cdc13 inactivation. My results also clarified some of the specific roles of each PAF1 complex component, and reinforced the reason why this complex evolved to be as it is. For instance, the PAF1 complex plays such an important role promoting cell fitness through Paf1 and Ctr9, that it seems that Cdc73 functions as a “brake”, to decrease fitness and avoid proliferation of defective cells. Since the PAF1 complex has such a broad role controlling the expression of so many transcripts, it just makes sense that the complex has its own “supervisor”, Cdc73, a protein with seemingly opposing functions to the main complex proteins.

6.4. Future work

Future work will be required to understand the mechanism(s) by which Paf1 and Ctr9 promote TERRA degradation. Northern blot and/or sequencing could help understand if TERRA polyadenylation is altered in *paf1Δ/ctr9Δ* cells. Cross of *rat1-1* mutants, which are known to degrade TERRA (Luke et al. 2008), to *paf1Δ* and *ctr9Δ* cells would maybe say if Paf1 and Ctr9 are promoting TERRA degradation by the Rat1 pathway. It would also be interesting to show the amount of TERRA that is annealed to telomeres versus the TERRA that is free and able to diffuse in the nucleus. This could be done by comparing TERRA RNA in samples treated with Rnh1 and/or Rnh201 versus untreated samples, or by measuring TERRA in a soluble fraction versus an insoluble (chromatin) fraction. Finally, RNA immunoprecipitation assays could help to define if the increased levels of TERRA molecules are interacting with telomerase.

7. Overall Perspectives

My data shows that yeast genome-wide screens are a good starting point to find relevant interactions between a variety of cellular processes, telomere function and cancer. I briefly demonstrated a role at telomeres for proteins involved in mRNA decay, ubiquitination and cellular transport. I further described a set of complex interactions between a Golgi component (*Vps74*) and the telomeres as well as members of the DDR. Perhaps, my most interesting findings showed a set of intricate interactions between a transcription auxiliary complex (PAF1 complex) and various components of telomere biology. My data on both *VPS74* and *CDC73* (member of the PAF1 complex) helped to elucidate the role of their human orthologues in cancer. Shortly, *Vps74* (oncogene) seems to be involved in DDR and promotes cell fitness, and *Cdc73* (tumour suppressor gene) seems to decrease cell fitness and regulate telomere function.

Of important note are the differences in the fitness defects caused by the same gene deletions in distinct yeast genetic backgrounds (S288C and W303). In most cases I saw that deletions in the W303 background caused less severe fitness defects than deletions in the S288C background, but the trend was maintained. *CDC73* deletion in the *cdc13-1* background was the only deletion that caused opposite effects in the two genetic backgrounds (W303 and S288C). I attributed the higher fitness of *cdc73Δ cdc13-1* W303 cells to telomere rearrangements that happened due to the different way of obtaining these strains (compared to the S288C strains used in the high-throughput screens). Nevertheless, this comparison between two yeast genetic backgrounds shows that one must be cautious when generalizing the results observed in one genetic background to all *S. cerevisiae* genetic backgrounds (or higher eukaryotes). The use of different genetic backgrounds and techniques to validate results seems to be a minimum requirement to reach conclusions that can be generalised with a higher degree of certainty.

7.1. *VPS74*

The genetic interactions described in Chapter 4, between *Vps74*, *Yku70* and various members of the DDR response did not give much away about the molecular mechanism behind such interactions. Nevertheless it is tempting to speculate on how *Vps74*, a cytoplasmic protein involved in Golgi homeostasis, interacts with the DDR

and/or telomeres. I suggest that Vps74 affects the DNA damage response and that it is important to maintain genomic stability.

Although the most obvious cases of DNA damage come from external factors, like UV and drugs such as MMS or HU, yeast also have internal sources of DNA damage. Yeast cells grown in the lab have access to high nutrient levels which allows those cells to replicate fast with a doubling time of around 90 min at 30°C (Herskowitz 1988). During this period, replication and transcription happen simultaneously and the cells rely on DDR proteins to promote RNA pol degradation and avoid fork collision which could lead to replication defects (Poli et al. 2016). Also, replication of some DNA regions is inherently more difficult and prone to breakage (Azvolinsky et al. 2009). Telomeres are sources of replication stress as are secondary DNA structures, chromatin compaction, misincorporation of ribonucleotides, etc. (Mazouzi et al. 2014). Thus, I suggest that Vps74, by a mechanism that is still not clear, helps the cell to cope with naturally occurring DNA lesions. Lack of Vps74 would perhaps lead to DNA damage accumulation and chromosome instability. One possibility is that Vps74, like GOLPH3, stimulates the TORC1 pathway affecting the DDR (Scott et al. 2009). Vps74 inactivation decreases TORC1 activity, which in turn, as previously reported, affects checkpoint activation (prolongs Rad53 phosphorylation) (Klermund et al. 2014). Interference with Rad53 activation could as a result increase genomic instability and decrease cell fitness (by checkpoint activation and cell cycle arrest).

Similar to other oncogenes, GOLPH3 (*VPS74* in yeast) overexpression is observed in many cancers and is associated with increased resistance to DNA damaging agents (Buschman et al. 2015). Such observation is in agreement with my findings that lack of Vps74 (hypothetically the opposite to *VPS74* overexpression) causes slower growth, promotes genetic instability and decreases the fitness of *yku70Δ* cells with uncapped telomeres. Perhaps overexpression of GOLPH3 leads to telomere protection and increased resistance to genetic instability. Also if GOLPH3/Vps74 concentration is high, and since it is a DNA-PK target, it could be titrating important checkpoint kinases in detriment of the activation of more important DDR pathways. It cannot also be excluded that overexpression of GOLPH3 leads to loss of the protein function (by for example GOLPH3 protein aggregation).

7.2. PAF1 complex

Chapters 5 and 6 demonstrated how the PAF1 complex and how its components perform different, and sometimes seemingly opposing, functions at telomeres (Figure 7-1). I showed that Paf1 and Ctr9 are the core components of the PAF1 complex in all the parameters studied: repressors of TERRA (p1), *TEN1* and *STN1* (p2) (m)RNA, inducers of *VPS36* (p3) and *TLC1* (p5) transcription and telomere silencing (p6) and important for cell fitness (Figure 7-1). I also found evidence that Paf1 (and likely Ctr9) repress TERRA by promoting its degradation. Cdc73 induced *TLC1* (p5) transcription and had an important role reducing the fitness of telomere defective cells. I also show a neighbouring gene effect between *CDC73* and *VPS36* (p4). The reason why Paf1 and Ctr9 are more important to many of the cellular functions I studied is not totally clear. It might be because Paf1 and Ctr9 are the proteins that hold the complex together, and without them all the PAF1 complex functions are compromised. Such idea is supported by the decreased levels of all other components in *paf1Δ* or *ctr9Δ* cells, but is challenged by the fact that *rtf1Δ* suppresses *paf1Δ* fitness defects (Mueller and Jaehning 2002; Mueller et al. 2004). Paf1 and Ctr9 might also be essential for a set of specific protein-protein interactions that are important for telomere maintenance.

Vps36, a member of the ESCRT-II complex, is involved in protein sorting for degradation, as part of a multi-step pathway that involves five ESCRT complexes (ESCRT-0, -I, -II, -III and the Vps4 complex) (Schmidt and Teis 2012). I described for the first time a synthetic lethality between *vps36Δ* (ESCRT-II) and *paf1Δ* or *ctr9Δ* in budding yeast. Importantly, this interaction was conserved among other members of the ESCRT machinery (ESCRT-I, -II, -III). The reason for such interaction (ESCRT complex components with *PAF1/CTR9*) is not clear, but it might be related to a common role in the DDR and protein degradation. For instance, Paf1 was shown to be important for RNA pol II degradation to avoid replication-transcription fork collision (Poli et al. 2016). So maybe the PAF1 complex and the ESCRT complex work in parallel to aid RNA pol II degradation and avoid fork stalling and DDR. Additionally, mammalian data showed that during cell migration DNA damage increases while the nuclear envelope opens, and those transient openings are repaired by the ESCRT-III (Raab et al. 2016). Although in yeast the nuclear envelope remains closed during mitosis, it is not unlikely that ESCRT-III still plays some kind of role maintaining nuclear envelope integrity, perhaps related to telomere clustering at the nuclear

periphery for example (Smoyer and Jaspersen 2014). Since ESCRT-II and ESCRT-III are part of the same pathway, Vps36 can be contributing to avoid DNA damage response activation and Paf1 and Ctr9 to keep the telomeres intact.

The PAF1 complex has many functions and it is still striking how cells lacking Cdc73, having short telomeres, can so easily maintain their fitness when their telomeres are damaged. This strongly suggests that Cdc73 contributes to the mechanism that induce cell cycle arrest or death of defective cells, in agreement with a described tumour suppressor gene role in humans. Interestingly, *cdc73Δ* cells, with short telomeres, can maintain their TERRA levels at a normal level, suggesting that, if conserved in humans, cancers triggered by *CDC73* depletion will have normal R-loop distribution. *cdc73Δ* cells might benefit from low TERRA levels, since TERRA is also suggested to activate the DDR (by promoting Mre11 recruitment to uncapped telomeres in humans), and maybe *cdc73Δ* cells can proliferate by avoiding extensive activation of DDR mechanisms (Porro et al. 2014). In this line, it would be interesting to see how *cdc73Δ cdc13-1* cells would react to a forced increase in TERRA RNA. Interestingly, R-loops seem to be increased in telomerase-negative cancers (Arora et al. 2014). It would therefore be interesting to understand the characteristics of the cancers caused by *HPRT2 (CDC73)* mutations, to see if some of the characteristics are as I see in yeast (telomerase-, ALT+, normal TERRA).

Overall, I show that the yeast orthologues of two important cancer-related proteins (Vps74 and Cdc73) play important roles maintaining telomere biology in yeast. I suggest that Vps74 plays a role in general DDR and Cdc73 has an important role at telomeres, decreasing the fitness of telomere defective cells. Importantly, I unravelled an important telomere role for Cdc73 complex partners, Paf1 and Ctr9. Paf1 and Ctr9 repress TERRA, Ten1 and Stn1 and strongly increase the fitness of telomere defective cells.

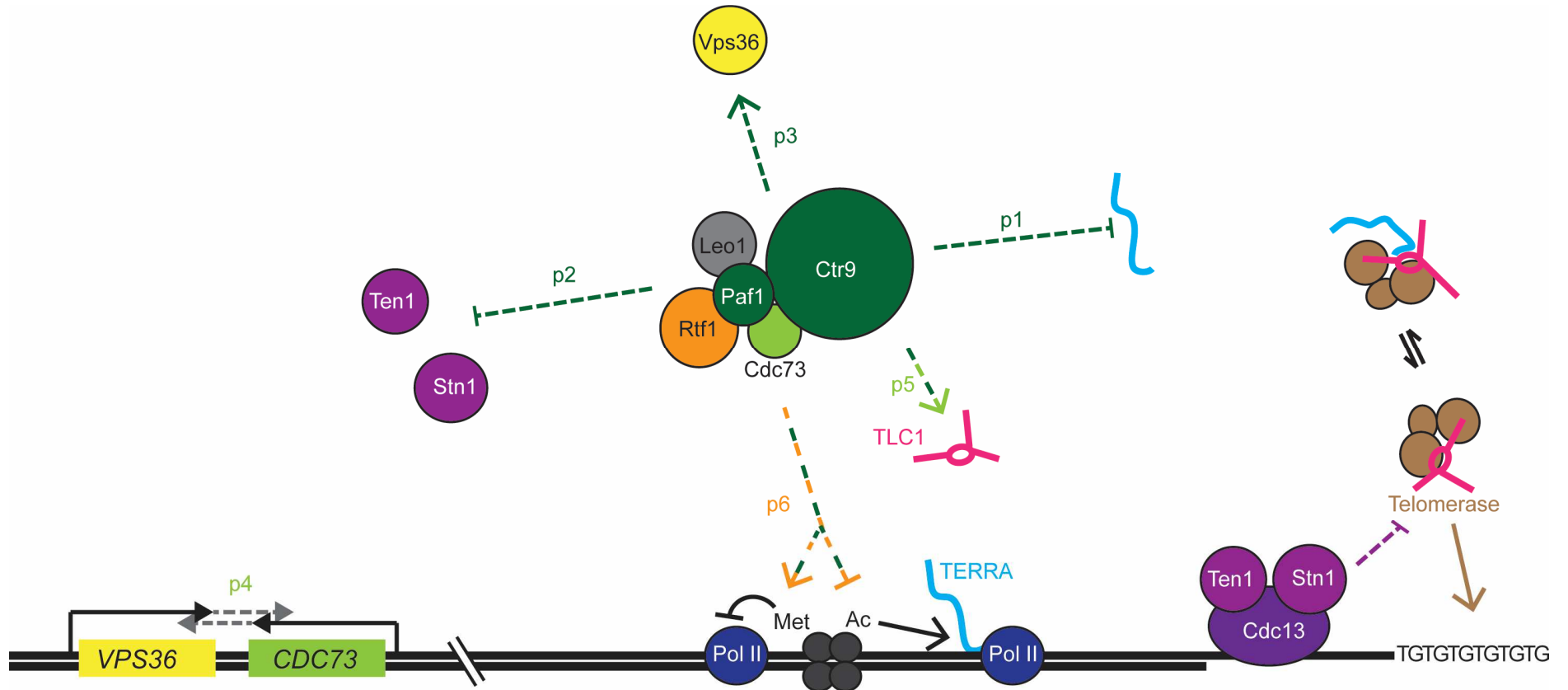


Figure 7-1 Model for the many roles of the different PAF1 complex components at telomeres. Paf1 and Ctr9 repress TERRA (p1), *TEN1* and *STN1* (p2). TERRA, Ten1 and Stn1 negatively affect telomerase function. Paf1 and Ctr9 also induce *VPS36* (p3). *VPS36* in turn is part of a neighbouring gene effect with *CDC73* (p4). Paf1, Ctr9 and Cdc73 induce *TLC1* (p5). Paf1, Ctr9 and Rtf1 promote telomere silencing (p6).

Appendix A

List of the strains used in this thesis. All strains are in the W303 background.

DLY	Genotype	Origin
159	<i>MATa, rad24::TRP1</i>	Lydall collection
1108	<i>MATa cdc13-1-int</i>	Lydall collection
1195	<i>MATalpha cdc13-1-int</i>	Lydall collection
1255	<i>MATa cdc13-1int rad9::HIS3</i>	Lydall collection
1257	<i>MATa cdc13-1int rad24::TRP1</i>	Lydall collection
1258	<i>MATalpha cdc13-1int rad24::TRP1</i>	Lydall collection
1273	<i>MATalpha exo1::LEU2 RAD5</i>	Lydall collection
1296	<i>MATa cdc13-1-int exo1::LEU2</i>	Lydall collection
1297	<i>MATalpha cdc13-1-int exo1::LEU2</i>	Lydall collection
1366	<i>MAT alpha yku70::HIS3 RAD5</i>	Lydall collection
1408	<i>MAT a yku70::HIS3 exo1::LEU2 RAD5</i>	Lydall collection
1412	<i>MATa yku70::HIS3 RAD5</i>	Lydall collection
1585	<i>MAT alpha rad9::KANMX</i>	Lydall collection
1696	<i>MATalpha exo1::LEU2 cdc13-1-int rad24::TRP1</i>	Lydall collection
1697	<i>MATalpha exo1::LEU2 cdc13-1-int rad24::TRP1</i>	Lydall collection
1700	<i>MATa exo1::LEU2 rad24::TRP1</i>	Lydall collection
1701	<i>MATalpha exo1::LEU2 rad24::TRP1</i>	Lydall collection
1845	<i>MAT a yku70::HIS3 mre11::hisG::URA3 RAD5</i>	Lydall collection
2041	<i>MATalpha mre11::hisG::URA3 RAD5</i>	Lydall collection
2147	<i>MAT alpha tlc1::HIS3 RAD5</i>	Lydall collection
2234	<i>MATa rad9::LEU2 RAD5 CDC+</i>	Lydall collection
2821	<i>MATalpha yku70::LEU2 ebs1::KANMX6 ADE+</i>	Lydall collection
3001	<i>MATalpha ade2-1 trp1-1 can1-100 leu2-3,112 his3-11,15 ura3 GAL+ psi+ ssd1-d2 RAD5</i>	Lydall collection
4026	<i>hmi1::KANMX6</i>	Lydall collection
4310	<i>MATalpha yku80::HIS3</i>	Lydall collection
4311	<i>MATa yku80::HIS3</i>	Lydall collection
4451	<i>MATalpha rif1::URA3</i>	Lydall collection
4457	<i>MATalpha mre11::URA3</i>	Lydall collection
5692	<i>MAT a sir4::HIS3</i>	Lydall collection

5693	<i>MAT a sir4::HIS3</i>	Lydall collection
7850	<i>DELho DELhml::ADE1 MATalpha DELhmr::ADE1 ade1 leu2-3,112 lys5 trp1::hisG ura3-52 ade3::GAL10::HO dot1::KANMX6</i>	Lydall collection
7851	<i>DELho DELhml::ADE1 MATalpha DELhmr::ADE1 ade1 leu2-3,112 lys5 trp1::hisG ura3-52 ade3::GAL10::HO dot1::KANMX6</i>	Lydall collection
8460	<i>MATa ade2-1 trp1-1 can1-100 leu2-3,112 his3-11,15 ura3 GAL+ psi+ ssd1-d2 RAD5</i>	Lydall collection
8490	<i>MATa cdc73::KANMX6</i>	This work
8491	<i>MATalpha cdc73::KANMX6</i>	This work
8492	<i>MATa cdc73::KANMX6 rad9::HIS3</i>	This work
8493	<i>MATalpha cdc73::KANMX6 rad9::HIS3</i>	This work
8494	<i>MATa cdc13-1 int cdc73::KANMX6</i>	This work
8495	<i>MATalpha cdc13-1 int cdc73::KANMX6</i>	This work
8496	<i>MATa cdc13-1 int cdc73::KANMX6 rad9::HIS3</i>	This work
8497	<i>MATalpha cdc13-1 int cdc73::KANMX6 rad9::HIS3</i>	This work
8594	<i>MATa yku70::HIS3 cdc73::KANMX6</i>	This work
8595	<i>MATalpha yku70::HIS3 cdc73::KANMX6</i>	This work
8596	<i>MATa rad24::TRP1 cdc73::KANMX6</i>	This work
8597	<i>MATlpha rad24::TRP1 cdc73::KANMX6</i>	This work
8598	<i>MATa cdc13-1int rad24::TRP1 cdc73::KANMX6</i>	This work
8599	<i>MATalpha cdc13-1int rad24::TRP1 cdc73::KANMX6</i>	This work
8607	<i>MATa cdc73::KANMX6 cdc13-1 p::URA3::CDC73</i>	This work
8608	<i>MATa acdc73::KANMX6 rad9::HIS3 cdc13-1 p::URA3::CDC73</i>	This work
8609	<i>MATa cdc73::KANMX6 cdc13-1 p::URA3</i>	This work
8610	<i>MATa cdc73::KANMX6 rad9::HIS3 cdc13-1 p::URA3</i>	This work
8702	<i>MATa yku80::HIS3 cdc73::KANMX6</i>	This work
8703	<i>MATalpha yku80::HIS3 cdc73::KANMX6</i>	This work
8732	<i>MATa cdc73::KANMX6 exo1::LEU2</i>	This work
8733	<i>MATalpha cdc73::KANMX6 exo1::LEU2</i>	This work
8734	<i>MATa cdc73::KANMX6 exo1::LEU2 cdc13-1</i>	This work
8735	<i>MATalpha cdc73::KANMX6 exo1::LEU2 cdc13-1</i>	This work
8736	<i>MATa leo1::KANMX6</i>	This work
8737	<i>MATalpha leo1::KANMX6</i>	This work
8738	<i>MATalpha leo1::KANMX6 ra9::HIS3</i>	This work
8739	<i>MATa leo1::KANMX6 cdc13-1</i>	This work
8740	<i>MATalpha leo1::KANMX6 cdc13-1</i>	This work
8741	<i>MATa leo1::KANMX6 rad9::HIS3 cdc13-1</i>	This work
8742	<i>MATalpha leo1::KANMX6 rad9::HIS3 cdc13-1</i>	This work
8743	<i>MATa rtf1::KANMX6</i>	This work
8744	<i>MATalpha rtf1::KANMX6</i>	This work
8745	<i>MATa rtf1::KANMX6 rad9::HIS3</i>	This work
8746	<i>MATalpha rtf1::KANMX6 rad9::HIS3</i>	This work
8747	<i>MATa rtf1::KANMX6 rad9::HIS3 cdc13-1</i>	This work
8748	<i>MATalpha rtf1::KANMX6 rad9::HIS3 cdc13-1</i>	This work
8749	<i>MATa rtf1::KANMX6 cdc13-1</i>	This work
8750	<i>MATalpha rtf1::KANMX6 cdc13-1</i>	This work
8751	<i>MATa ctr9::KANMX6</i>	This work
8752	<i>MATalpha ctr9::KANMX6</i>	This work
8752	<i>MATalpha ctr9::KANMX6</i>	This work
8753	<i>MATa ctr9::KANMX6 rad9::HIS3</i>	This work

8753	<i>MATa ctr9::KANMX6 rad9::HIS3</i>	This work
8753	<i>MATa ctr9::KANMX6 rad9::HIS3</i>	This work
8753	<i>MATa ctr9::KANMX6 rad9::HIS3</i>	This work
8754	<i>MATalpha ctr9::KANMX6 rad9::HIS3</i>	This work
8755	<i>MATalpha ctr9::KANMX6 cdc13-1</i>	This work
8756	<i>MATa ctr9::KANMX6 rad9::HIS3 cdc13-1</i>	This work
8757	<i>MATa paf1::KANMX6</i>	This work
8758	<i>MATalpha paf1::KANMX6</i>	This work
8759	<i>MATa paf1::KANMX6 rad9::HIS3</i>	This work
8760	<i>MATalpha paf1::KANMX6 rad9::HIS3</i>	This work
8761	<i>MATalpha paf1::KANMX6 cdc13-1</i>	This work
8762	<i>MATa paf1::KANMX6 rad9::HIS3 cdc13-1</i>	This work
8763	<i>MATalpha paf1::KANMX6 rad9::HIS3 cdc13-1</i>	This work
8768	<i>MATa cdc73::KANMX6 est1::natMX</i>	This work
8769	<i>MATalpha cdc73::KANMX6 est1::natMX</i>	This work
8803	<i>MATa vps36::KANMX6</i>	This work
8804	<i>MATalpha vps36::KANMX6</i>	This work
8805	<i>MATa vps36::KANMX6 rad9::HIS3</i>	This work
8806	<i>MATalpha vps36::KANMX6 rad9::HIS3</i>	This work
8807	<i>MATa vps36::KANMX6 cdc13-1 int</i>	This work
8808	<i>MATalpha vps36::KANMX6 cdc13-1 int</i>	This work
8809	<i>MATa vps36::KANMX6 rad9::HIS3 cdc13-1 int</i>	This work
8810	<i>MATalpha vps36::KANMX6 rad9::HIS3 cdc13-1 int</i>	This work
8811	<i>MATa ylr419w::KANMX6</i>	This work
8812	<i>MATalpha ylr419w::KANMX6</i>	This work
8812	<i>MATalpha ylr419w::KANMX6</i>	This work
8813	<i>MATa ylr419w::KANMX6 rad9::HIS3</i>	This work
8814	<i>MATalpha ylr419w::KANMX6 rad9::HIS3</i>	This work
8815	<i>MATa ylr419w::KANMX6 cdc13-1 int</i>	This work
8816	<i>MATalpha ylr419w::KANMX6 cdc13-1 int</i>	This work
8817	<i>MATa ylr419w::KANMX6 cdc13-1 int rad9::HIS3</i>	This work
8818	<i>MATalpha ylr419w::KANMX6 cdc13-1 int rad9::HIS3</i>	This work
8828	<i>bas1::KANMX6</i>	This work
8829	<i>bas1::KANMX6</i>	This work
8830	<i>bas1::KANMX6 rad9::HIS3</i>	This work
8831	<i>bas1::KANMX6 rad9::HIS3</i>	This work
8832	<i>bas1::KANMX6 cdc13-1 int</i>	This work
8833	<i>bas1::KANMX6 cdc13-1 int</i>	This work
8834	<i>bas1::KANMX6 rad9::HIS3 cdc13-1 int</i>	This work
8835	<i>bas1::KANMX6 rad9::HIS3 cdc13-1 int</i>	This work
8836	<i>ufd2::KANMX6</i>	This work
8837	<i>ufd2::KANMX6</i>	This work
8838	<i>ufd2::KANMX6 rad9::HIS3</i>	This work
8839	<i>ufd2::KANMX6 rad9::HIS3</i>	This work
8840	<i>ufd2::KANMX6 cdc13-1 int</i>	This work
8841	<i>ufd2::KANMX6 cdc13-1 int</i>	This work
8842	<i>ufd2::KANMX6 rad9::HIS3 cdc13-1 int</i>	This work
8843	<i>ufd2::KANMX6 rad9::HIS3 cdc13-1 int</i>	This work
8844	<i>MATalpha ski2::KANMX6</i>	This work

8845	<i>MATa ski2::KANMX6</i>	This work
8846	<i>ski2::KANMX6 rad9::HIS3</i>	This work
8847	<i>ski2::KANMX6 rad9::HIS3</i>	This work
8848	<i>ski2::KANMX6 cdc13-1 int</i>	This work
8849	<i>ski2::KANMX6 cdc13-1 int</i>	This work
8850	<i>ski2::KANMX6 rad9::HIS3 cdc13-1 int</i>	This work
8851	<i>ski2::KANMX6 rad9::HIS3 cdc13-1 int</i>	This work
8852	<i>sla2::KANMX6</i>	This work
8853	<i>sla2::KANMX6</i>	This work
8854	<i>sla2::KANMX6 cdc13-1 int</i>	This work
8855	<i>sla2::KANMX6 cdc13-1 int</i>	This work
8856	<i>sla2::KANMX6 rad9::HIS3 cdc13-1 int</i>	This work
8857	<i>sla2::KANMX6 rad9::HIS3 cdc13-1 int</i>	This work
8858	<i>dyn1::KANMX6</i>	This work
8859	<i>dyn1::KANMX6</i>	This work
8860	<i>dyn1::KANMX6 rad9::HIS3</i>	This work
8861	<i>dyn1::KANMX6 rad9::HIS3</i>	This work
8862	<i>dyn1::KANMX6 cdc13-1 int</i>	This work
8863	<i>dyn1::KANMX6 cdc13-1 int</i>	This work
8864	<i>dyn1::KANMX6 cdc13-1 int rad9::HIS3</i>	This work
8865	<i>dyn1::KANMX6 cdc13-1 int rad9::HIS3</i>	This work
8866	<i>inp52::KANMX6</i>	This work
8867	<i>inp52::KANMX6</i>	This work
8868	<i>inp52::KANMX6 rad9::HIS3</i>	This work
8869	<i>inp52::KANMX6 rad9::HIS3</i>	This work
8870	<i>inp52::KANMX6 cdc13-1 int</i>	This work
8871	<i>inp52::KANMX6 cdc13-1 int</i>	This work
8872	<i>inp52::KANMX6 rad9::HIS3 cdc13-1 int</i>	This work
8873	<i>inp52::KANMX6 rad9::HIS3 cdc13-1 int</i>	This work
8874	<i>fyv10::KANMX6</i>	This work
8875	<i>fyv10::KANMX6</i>	This work
8876	<i>fyv10::KANMX6 rad9::HIS3</i>	This work
8877	<i>fyv10::KANMX6 rad9::HIS3</i>	This work
8878	<i>fyv10::KANMX6 cdc13-1 int</i>	This work
8879	<i>fyv10::KANMX6 cdc13-1 int</i>	This work
8880	<i>fyv10::KANMX6 rad9::HIS3 cdc13-1 int</i>	This work
8881	<i>fyv10::KANMX6 rad9::HIS3 cdc13-1 int</i>	This work
9008	<i>MATa yku70::HIS3 bas1::KANMX6</i>	This work
9009	<i>MATalpha yku70::HIS3 bas1::KANMX6</i>	This work
9010	<i>MATa yku80::HIS3 bas1::KANMX6</i>	This work
9011	<i>MATalpha yku80::HIS3 bas1::KANMX6</i>	This work
9012	<i>MATa yku70::HIS3 ufd2::KANMX6</i>	This work
9013	<i>MATalpha yku70::HIS3 ufd2::KANMX6</i>	This work
9014	<i>MATa yku80::HIS3 ufd2::KANMX6</i>	This work
9015	<i>MATalpha yku80::HIS3 ufd2::KANMX6</i>	This work
9016	<i>MATa yku70::HIS3 ski2::KANMX6</i>	This work
9017	<i>MATalpha yku70::HIS3 ski2::KANMX6</i>	This work
9018	<i>MATa yku80::HIS3 ski2::KANMX6</i>	This work
9019	<i>MATalpha yku80::HIS3 ski2::KANMX6</i>	This work

9020	<i>MATa yku70::HIS3 dyn1::KANMX6</i>	This work
9021	<i>MATalpha yku70::HIS3 dyn1::KANMX6</i>	This work
9022	<i>MATa yku80::HIS3 dyn1::KANMX6</i>	This work
9023	<i>MATalpha yku80::HIS3 dyn1::KANMX6</i>	This work
9024	<i>MATa yku70::HIS3 inp52::KANMX6</i>	This work
9025	<i>MATalpha yku70::HIS3 inp52::KANMX6</i>	This work
9026	<i>MATa yku80::HIS3 inp52::KANMX6</i>	This work
9027	<i>MATalpha yku80::HIS3 inp52::KANMX6</i>	This work
9028	<i>MATa yku70::HIS3 fyv10::KANMX6</i>	This work
9029	<i>MATalpha yku70::HIS3 fyv10::KANMX6</i>	This work
9030	<i>MATa yku80::HIS3 fyv10::KANMX6</i>	This work
9031	<i>MATalpha yku80::HIS3 fyv10::KANMX6</i>	This work
9183	<i>MATa vps74::KANMX6</i>	This work
9184	<i>MATalpha vps74::KANMX6</i>	This work
9185	<i>MATa vps74::KANMX6 rad9::HIS3</i>	This work
9186	<i>MATalpha vps74::KANMX6 rad9::HIS3</i>	This work
9187	<i>MATa vps74::KANMX6 cdc13-1</i>	This work
9188	<i>MATalpha vps74::KANMX6 cdc13-1</i>	This work
9189	<i>MATa vps74::KANMX6 cdc13-1 rad9::HIS3</i>	This work
9190	<i>MATalpha vps74::KANMX6 cdc13-1 rad9::HIS3</i>	This work
9191	<i>MATa cdc73(41-90)::KANMX6</i>	This work
9192	<i>MATalpha cdc73(41-90)::KANMX6</i>	This work
9193	<i>MATa cdc73(41-90)::KANMX6 cdc13-1</i>	This work
9194	<i>MATalpha cdc73(41-90)::KANMX6 cdc13-1</i>	This work
9195	<i>MATa vps36(1302-1701)-cdc73(782-1182)::KANMX6</i>	This work
9196	<i>MATalpha vps36(1302-1701)-cdc73(782-1182)::KANMX6</i>	This work
9197	<i>MATa cdc73(41-90)::KANMX6 cdc13-1</i>	This work
9198	<i>MATalpha cdc73(41-90)::KANMX6 cdc13-1</i>	This work
9199	<i>MATa vps36(1-90)::KANMX6</i>	This work
9200	<i>MATalpha vps36(1-90)::KANMX6</i>	This work
9201	<i>MATa vps36(1-90)::KANMX6 cdc13-1</i>	This work
9202	<i>MATalpha vps36(1-90)::KANMX6 cdc13-1</i>	This work
9421	<i>vps74::KANMX6 exo1::LEU2</i>	This work
9422	<i>vps74::KANMX6 exo1::LEU2</i>	This work
9423	<i>MATa doa1::HPH</i>	This work
9424	<i>MATalpha doa1::HPH</i>	This work
9425	<i>MATa doa1::HPH cdc13-1</i>	This work
9426	<i>MATa doa1::HPH cdc13-1</i>	This work
9427	<i>MATa doa1::HPH rad9::HIS3</i>	This work
9428	<i>MATalpha doa1::HPH rad9::HIS3</i>	This work
9429	<i>MATa doa1::HPH ufd2::KANMX6</i>	This work
9430	<i>MATalpha doa1::HPH ufd2::KANMX6</i>	This work
9431	<i>MATa doa1::HPH ufd2::KANMX6 rad9::HIS3</i>	This work
9432	<i>MATalpha doa1::HPH ufd2::KANMX6 rad9::HIS3</i>	This work
9433	<i>MATa doa1::HPH ufd2::KANMX6 cdc13-1</i>	This work
9434	<i>MATalpha doa1::HPH ufd2::KANMX6 cdc13-1</i>	This work
9435	<i>MATa doa1::HPH ufd2::KANMX6 rad9::HIS3 cdc13-1</i>	This work
9436	<i>MATalpha doa1::HPH ufd2::KANMX6 rad9::HIS3 cdc13-1</i>	This work
9437	<i>MATa doa1::HPH rad9::HIS3 cdc13-1</i>	This work

9438	<i>MATalpha doa1::HPH rad9::HIS3 cdc13-1</i>	This work
9536	<i>MATa ski7::natMX</i>	This work
9537	<i>MATalpha ski7::natMX</i>	This work
9538	<i>MATa ski7::natMX cdc13-1int</i>	This work
9539	<i>MATalpha ski7::natMX cdc13-1int</i>	This work
9540	<i>MATa ski7::natMX rad9::HIS3</i>	This work
9541	<i>MATalpha ski7::natMX rad9::HIS3</i>	This work
9542	<i>MATa ski7::natMX ski2::KANMX6</i>	This work
9543	<i>MATalpha ski7::natMX ski2::KANMX6</i>	This work
9544	<i>MATa ski7::natMX ski2::KANMX6 cdc13-1int</i>	This work
9545	<i>MATalpha ski7::natMX ski2::KANMX6 cdc13-1int</i>	This work
9546	<i>MATa ski7::natMX ski2::KANMX6 rad9::HIS3</i>	This work
9547	<i>MATalpha ski7::natMX ski2::KANMX6 rad9::HIS3</i>	This work
9548	<i>MATa ski7::natMX rad9::HIS3 cdc13-1int</i>	This work
9549	<i>MATalpha ski7::natMX rad9::HIS3 cdc13-1int</i>	This work
9550	<i>MATa ski7::natMX ski2::KANMX6 rad9::HIS3 cdc13-1int</i>	This work
9551	<i>MATalpha ski7::natMX ski2::KANMX6 rad9::HIS3 cdc13-1int</i>	This work
9552	<i>MATa ski8::TRP1</i>	This work
9553	<i>MATalpha ski8::TRP1</i>	This work
9554	<i>MATa ski8::TRP1 cdc13-1int</i>	This work
9555	<i>MATalpha ski8::TRP1 cdc13-1int</i>	This work
9556	<i>MATa ski8::TRP1 rad9::HIS3</i>	This work
9557	<i>MATalpha ski8::TRP1 rad9::HIS3</i>	This work
9558	<i>MATa ski8::TRP1 ski2::KANMX6</i>	This work
9559	<i>MATalpha ski8::TRP1 ski2::KANMX6</i>	This work
9560	<i>MATa ski8::TRP1 ski2::KANMX6 cdc13-1int</i>	This work
9561	<i>MATalpha ski8::TRP1 ski2::KANMX6 cdc13-1int</i>	This work
9562	<i>MATa ski8::TRP1 ski2::KANMX6 rad9::HIS3</i>	This work
9563	<i>MATalpha ski8::TRP1 ski2::KANMX6 rad9::HIS3</i>	This work
9564	<i>MATa ski8::TRP1 ski2::KANMX6 cdc13-1int</i>	This work
9565	<i>MATalpha ski8::TRP1 ski2::KANMX6 cdc13-1int</i>	This work
9566	<i>MATa ski8::TRP1 ski2::KANMX6 rad9::HIS3 cdc13-1int</i>	This work
9567	<i>MATalpha ski8::TRP1 ski2::KANMX6 rad9::HIS3 cdc13-1int</i>	This work
9568	<i>MATa vps74::KANMX6 rad17::LEU2</i>	This work
9569	<i>MATalpha vps74::KANMX6 rad17::LEU2</i>	This work
9570	<i>MATa vps74::KANMX6 rad24::TRP1</i>	This work
9571	<i>MATalpha vps74::KANMX6 rad24::TRP1</i>	This work
9572	<i>MATa vps74::KANMX6 rad17::LEU2 cdc13-1</i>	This work
9573	<i>MATalpha vps74::KANMX6 rad17::LEU2 cdc13-1</i>	This work
9574	<i>MATa vps74::KANMX6 rad24::TRP1 cdc13-1</i>	This work
9575	<i>MATalpha vps74::KANMX6 rad24::TRP1 cdc13-1</i>	This work
9576	<i>MATa vps74::KANMX6 rad24::TRP1 rad17::LEU2</i>	This work
9577	<i>MATalpha vps74::KANMX6 rad24::TRP1 rad17::LEU2</i>	This work
9578	<i>MATa vps74::KANMX6 rad24::TRP1 rad17::LEU2 cdc13-1int</i>	This work
9579	<i>MATalpha vps74::KANMX6 rad24::TRP1 rad17::LEU2 cdc13-1int</i>	This work
9580	<i>MATa vps74::KANMX6 rad9::HIS3</i>	This work
9581	<i>MATalpha vps74::KANMX6 rad9::HIS3</i>	This work
9832	<i>MATalpha vps36::HPH</i>	This work
9833	<i>MATa vps36(1-90)::HPH</i>	This work

9834	<i>MATalpha vps36(1-90)::HPH</i>	This work
9894	<i>ade1-14, his3-200, leu2-3-112, trp1-289 PSI+</i>	Mick Tuite
9895	<i>ade1-14, his3-200, leu2-3-112, trp1-289 PSI-</i>	Mick Tuite
9987	<i>MATa cdc13-1 int ski2::KANMX6</i>	This work
9988	<i>MATalpha cdc13-1 int ski2::KANMX6</i>	This work
9989	<i>MATa ski2::KANMX6 exo1::LEU2</i>	This work
9990	<i>MATalpha ski2::KANMX6 exo1::LEU2</i>	This work
9991	<i>MATa ski2::KANMX6 exo1::LEU2 cdc13-1 int</i>	This work
9992	<i>MATalpha ski2::KANMX6 exo1::LEU2 cdc13-1 int</i>	This work
9993	<i>MATa ski2::KANMX6 exo1::LEU2 rad24::TRP1</i>	This work
9994	<i>MATalpha ski2::KANMX6 exo1::LEU2 rad24::TRP1</i>	This work
9995	<i>MATa ski2::KANMX6 exo1::LEU2 rad24::TRP1 cdc13-1 int</i>	This work
9996	<i>MATalpha ski2::KANMX6 exo1::LEU2 rad24::TRP1 cdc13-1 int</i>	This work
9997	<i>MATalpha paf1::KANMX6 cdc13-1</i>	This work
9998	<i>MATalpha ctr9::KANMX6 cdc13-1</i>	This work
9999	<i>MATalpha rtf1::KANMX6 cdc13-1</i>	This work
10000	<i>MATalpha leo1::KANMX6 cdc13-1</i>	This work
10001	<i>MATa ura3::EGFP-RER1::URA3 GAL+ psi+ ssd1-d2 RAD5</i>	This work
10002	<i>MATa ura3::SEC7-EGFP::URA3 GAL+ psi+ ssd1-d2 RAD5</i>	This work
10003	<i>MATa ura3::EGFP-RER1::URA3 GAL+ psi+ ssd1-d2 RAD5 cdc13-1-int</i>	This work
10004	<i>MATa ura3::SEC7-EGFP::URA3 GAL+ psi+ ssd1-d2 RAD5 cdc13-1-int</i>	This work
10017	<i>MATa vps74::KANMX6 yku70::LEU2</i>	This work
10018	<i>MATalpha vps74::KANMX6 yku70::LEU2</i>	This work
10019	<i>MATalpha vps74::KANMX6 yku80::HIS3</i>	This work
10020	<i>MATalpha vps74::KANMX6 yku80::HIS3</i>	This work
10021	<i>MATa vps74::KANMX6 yku80::HIS3 yku70::LEU2</i>	This work
10022	<i>MATalpha vps74::KANMX6 yku80::HIS3 yku70::LEU2</i>	This work
10055	<i>MATalpha leo1::KANMX6 nmd2::HIS3</i>	This work
10056	<i>MATalpha leo1::KANMX6 nmd2::HIS3</i>	This work
10057	<i>MATalpha leo1::KANMX6 nmd2::HIS3 cdc13-1</i>	This work
10058	<i>MATalpha leo1::KANMX6 nmd2::HIS3 cdc13-1</i>	This work
10059	<i>MATalpha cdc73::KANMX6 nmd2::HIS3</i>	This work
10060	<i>MATalpha cdc73::KANMX6 nmd2::HIS3</i>	This work
10061	<i>MATalpha cdc73::KANMX6 nmd2::HIS3 cdc13-1</i>	This work
10062	<i>MATalpha cdc73::KANMX6 nmd2::HIS3 cdc13-1</i>	This work
10063	<i>MATalpha rtf1::KANMX6 nmd2::HIS3</i>	This work
10064	<i>MATalpha rtf1::KANMX6 nmd2::HIS3</i>	This work
10065	<i>MATalpha rtf1::KANMX6 nmd2::HIS3 cdc13-1</i>	This work
10066	<i>MATalpha rtf1::KANMX6 nmd2::HIS3 cdc13-1</i>	This work
10113	<i>ctr9::KANMX6 nmd2::HIS3</i>	This work
10114	<i>ctr9::KANMX6 nmd2::HIS3</i>	This work
10115	<i>ctr9::KANMX6 nmd2::HIS3 cdc13-1</i>	This work
10116	<i>ctr9::KANMX6 nmd2::HIS3 cdc13-1</i>	This work
10117	<i>paf1::KANMX6 nmd2::HIS3</i>	This work
10118	<i>paf1::KANMX6 nmd2::HIS3</i>	This work
10119	<i>paf1::KANMX6 nmd2::HIS3 cdc13-1</i>	This work
10120	<i>paf1::KANMX6 nmd2::HIS3 cdc13-1</i>	This work
10155	<i>MATa ura3::URA3::EGFP-RER1 GAL+ psi+ ssd1-d2 RAD5 cdc13-1</i>	This work
10157	<i>MATa ura3::URA3::EGFP-RER1 GAL+ psi+ ssd1-d2 RAD5 cdc13-1</i>	This work

10158	<i>MATalpha ura3::URA3::EGFP-RER1 GAL+ psi+ ssd1-d2 RAD5</i>	This work
10159	<i>MATalpha ura3::URA3::EGFP-RER1 GAL+ psi+ ssd1-d2 RAD5</i>	This work
10160	<i>MATalpha ura3::URA3::EGFP-RER1 GAL+ psi+ ssd1-d2 RAD5</i>	This work
10161	<i>MATalpha mon1::KANMX6</i>	This work
10162	<i>MATalpha mon1::KANMX6</i>	This work
10163	<i>MATa mon1::KANMX6 cdc13-1</i>	This work
10164	<i>MATalpha mon1::KANMX6 cdc13-1</i>	This work
10165	<i>MATa mon1::KANMX6 rad9::HIS3</i>	This work
10166	<i>MATalpha mon1::KANMX6 rad9::HIS3</i>	This work
10167	<i>MATa mon1::KANMX6 rad9::HIS3 cdc13-1</i>	This work
10168	<i>MATalpha mon1::KANMX6 rad9::HIS3 cdc13-1</i>	This work
10169	<i>MATa sub1::KANMX6</i>	This work
10170	<i>MATalpha sub1::KANMX6</i>	This work
10171	<i>MATa sub1::KANMX6 cdc13-1</i>	This work
10172	<i>MATalpha sub1::KANMX6 cdc13-1</i>	This work
10173	<i>MATa sub1::KANMX6 rad9::HIS3</i>	This work
10174	<i>MATalpha sub1::KANMX6 rad9::HIS3</i>	This work
10175	<i>MATa sub1::KANMX6 rad9::HIS3 cdc13-1</i>	This work
10176	<i>MATalpha sub1::KANMX6 rad9::HIS3 cdc13-1</i>	This work
10177	<i>MATa sbp1::HPH</i>	This work
10178	<i>MATalpha sbp1::HPH</i>	This work
10179	<i>MATa sbp1::HPH cdc13-1</i>	This work
10180	<i>MATalpha sbp1::HPH cdc13-1</i>	This work
10181	<i>MATa sbp1::HPH rad9::HIS3</i>	This work
10182	<i>MATalpha sbp1::HPH rad9::HIS3</i>	This work
10183	<i>MATa sbp1::HPH rad9::HIS3 cdc13-1</i>	This work
10184	<i>MATa sbp1::HPH rad9::HIS3 cdc13-1</i>	This work
10240	<i>vps74::KANMX6 yku70::HIS3 exo1::LEU2</i>	This work
10241	<i>vps74::KANMX6 yku70::HIS3 exo1::LEU2</i>	This work
10414	<i>MATa snf8::HYG</i>	This work
10415	<i>MATalpha snf8::HYG</i>	This work
10416	<i>MATa snf8::HYG cdc13-1</i>	This work
10417	<i>MATalpha snf8::HYG cdc13-1</i>	This work
10418	<i>MATa snf8::HYG rad9::HIS3</i>	This work
10419	<i>MATalpha snf8::HYG rad9::HIS3</i>	This work
10420	<i>MATa snf8::HYG rad9::HIS3 cdc13-1</i>	This work
10421	<i>MATalpha snf8::HYG rad9::HIS3 cdc13-1</i>	This work
10422	<i>MATa vps25::NAT</i>	This work
10423	<i>MATalpha vps25::NAT</i>	This work
10424	<i>MATa vps25::NAT cdc13-1</i>	This work
10425	<i>MATalpha vps25::NAT cdc13-1</i>	This work
10426	<i>MATa vps25::NAT rad9::HIS3</i>	This work
10427	<i>MATalpha vps25::NAT rad9::HIS3</i>	This work
10428	<i>MATa vps25::NAT rad9::HIS3 cdc13-1</i>	This work
10429	<i>MATalpha vps25::NAT rad9::HIS3 cdc13-1</i>	This work
10458	<i>MATalpha his4-1, kar1-1 L-A, M1, L-BC</i>	This work
10540	<i>MATa ski2::KANMX6 nmd2::HIS3</i>	This work
10541	<i>ski2::KANMX6 nmd2::HIS3</i>	This work
10542	<i>ski2::KANMX6 rad24::TRP1</i>	This work

10543	<i>ski2::KANMX6 rad24::TRP1</i>	This work
10740	<i>MATa vps74::KANMX6 sae2::TRP1</i>	This work
10741	<i>MATalpha vps74::KANMX6 sae2::TRP1</i>	This work
10742	<i>MATa vps74::KANMX6 yku70::HIS3 sae2::TRP1</i>	This work
10743	<i>MATalpha vps74::KANMX6 yku70::HIS3 sae2::TRP1</i>	This work
10744	<i>MATa vps74::KANMX6 exo1::LEU2 sae2::TRP1</i>	This work
10745	<i>MATalpha vps74::KANMX6 exo1::LEU2 sae2::TRP1</i>	This work
10746	<i>MATa vps74::KANMX6 yku70::HIS3 exo1::LEU2 sae2::TRP1</i>	This work
10747	<i>MATalpha vps74::KANMX6 yku70::HIS3 exo1::LEU2 sae2::TRP1</i>	This work
10748	<i>MATa vps74::KANMX6 mre11::URA3</i>	This work
10749	<i>MATalpha vps74::KANMX6 mre11::URA3</i>	This work
10750	<i>MATa vps74::KANMX6 yku70::HIS3 mre11::URA3</i>	This work
10751	<i>MATalpha vps74::KANMX6 yku70::HIS3 mre11::URA3</i>	This work
10752	<i>MATa vps74::KANMX6 exo1::LEU23 mre11::URA3</i>	This work
10753	<i>MATalpha vps74::KANMX6 exo1::LEU23 mre11::URA3</i>	This work
10754	<i>MATa vps74::KANMX6 yku70::HIS3 exo1::LEU23 mre11::URA3</i>	This work
10755	<i>MATalpha vps74::KANMX6 yku70::HIS3 exo1::LEU23 mre11::URA3</i>	This work
10763	<i>ski2::KANMX6 nmd2::HIS3 cdc13-1 int</i>	This work
10764	<i>ski2::KANMX6 nmd2::HIS3 cdc13-1 int</i>	This work
10765	<i>ski2::KANMX6 nmd2::HIS3 exo1::LEU2</i>	This work
10766	<i>ski2::KANMX6 nmd2::HIS3 exo1::LEU2</i>	This work
10767	<i>MATalpha ski2::KANMX6 nmd2::HIS3 rad24::TRP1</i>	This work
10768	<i>MATalpha ski2::KANMX6 nmd2::HIS3 rad24::TRP1</i>	This work
10769	<i>MATa ski2::KANMX6 nmd2::HIS3 exo1::LEU2 cdc13-1</i>	This work
10770	<i>ski2::KANMX6 nmd2::HIS3 exo1::LEU2 cdc13-1</i>	This work
10771	<i>ski2::KANMX6 ski2::KANMX6 nmd2::HIS3 exo1::LEU2 rad24::TRP1 cdc13-1</i>	This work
10772	<i>MATalpha ski2::KANMX6 ski2::KANMX6 nmd2::HIS3 exo1::LEU2 rad24::TRP1 cdc13-1</i>	This work
10773	<i>MATa ski2::KANMX6 sac1::HYG sae2::TRP1</i>	This work
10774	<i>MATalpha ski2::KANMX6 sac1::HYG sae2::TRP1</i>	This work
10786	<i>MATalpha ski2::KANMX6 sac1::HYG sae2::TRP1</i>	This work
10787	<i>MATalpha ski2::KANMX6 sac1::HYG sae2::TRP1</i>	This work
10788	<i>MATa ski2::KANMX6 sac1::HYG sae2::TRP1 vps74::KANMX6</i>	This work
10959	<i>cdc73::HPH paf1::KANMX6</i>	This work
10960	<i>cdc73::HPH paf1::KANMX6</i>	This work
10961	<i>cdc73::HPH ctr9::KANMX6</i>	This work
10962	<i>cdc73::HPH ctr9::KANMX6</i>	This work
10995	<i>MATa sac1::TRP1</i>	This work
10996	<i>MATalpha sac1::TRP1</i>	This work
10997	<i>MATalpha vps74::KANMX6 mec1::TRP1</i>	This work
10998	<i>MATa vps74::KANMX6 yku70::LEU2 mec1::TRP1</i>	This work
10999	<i>MATa vps74::KANMX6 yku70::LEU2 mec1::TRP1</i>	This work
11000	<i>MATa vps74::KANMX6 mec1::TRP1 sml1::HIS3</i>	This work
11001	<i>MATalpha vps74::KANMX6 mec1::TRP1 sml1::HIS3</i>	This work
11002	<i>MATa vps74::KANMX6 yku70::LEU2 mec1::TRP1 sml1::HIS3</i>	This work
11003	<i>MATalpha vps74::KANMX6 yku70::LEU2 mec1::TRP1 sml1::HIS3</i>	This work
11004	<i>MATa vps74::KANMX6 sml1::HIS3</i>	This work
11005	<i>MATalpha vps74::KANMX6 sml1::HIS3</i>	This work
11006	<i>MATa vps74::KANMX6 chk1::HIS3</i>	This work
11007	<i>MATalpha vps74::KANMX6 chk1::HIS3</i>	This work

11008	<i>MATa vps74::KANMX6 yku70::LEU2 chk1::HIS3</i>	This work
11009	<i>MATalpha vps74::KANMX6 yku70::LEU2 chk1::HIS3</i>	This work
11010	<i>MATa vps74::KANMX6 sgs1::NatMX</i>	This work
11011	<i>MATa vps74::KANMX6 yku70::LEU2 sgs1::NatMX</i>	This work
11012	<i>MATalpha vps74::KANMX6 yku70::LEU2 sgs1::NatMX</i>	This work
11013	<i>MATa vps74::KANMX6 yku70::LEU2 mec1::TRP1</i>	This work
11014	<i>MATa mec1::TRP1</i>	This work
11015	<i>MATalpha mec1::TRP1 yku70::LEU2</i>	This work
11016	<i>MATa vps74::KANMX6 mec1::TRP1 yku70::LEU2</i>	This work
11017	<i>MATa rad53::HIS3 yku70::LEU2</i>	This work
11018	<i>MATa rad53::HIS3</i>	This work
11019	<i>MATa rad53::HIS3</i>	This work
11020	<i>MATalpha rad53::HIS3 yku70::LEU2</i>	This work
11021	<i>MATalpha rad53::HIS3 yku70::LEU2 vps74::KANMX6</i>	This work
11022	<i>MATalpha vps74::KANMX6 rad53::HIS3 sml1::URA3</i>	This work
11023	<i>MATalpha vps74::KANMX6 rad53::HIS3 sml1::URA3</i>	This work
11024	<i>MATa vps74::KANMX6 yku70::LEU2 rad53::HIS3 sml1::URA3</i>	This work
11025	<i>MATa vps74::KANMX6 yku70::LEU2 rad53::HIS3 sml1::URA3</i>	This work
11038	<i>yku70::LEU2 rad53::HIS3 sml1::URA3</i>	This work
11039	<i>yku70::LEU2 rad53::HIS3 sml1::URA3</i>	This work
11040	<i>sac1::TRP</i>	This work
11041	<i>sac1::TRP</i>	This work
11042	<i>sac1::TRP yku70::HIS3</i>	This work
11043	<i>sac1::TRP yku70::HIS3</i>	This work
11044	<i>sac1::TRP vps74::KANMX6</i>	This work
11045	<i>sac1::TRP vps74::KANMX6</i>	This work
11046	<i>sac1::TRP exo1::LEU2</i>	This work
11047	<i>sac1::TRP exo1::LEU2</i>	This work
11048	<i>sac1::TRP vps74::KANMX6 exo1::LEU2</i>	This work
11049	<i>sac1::TRP vps74::KANMX6 exo1::LEU2</i>	This work
11050	<i>sac1::TRP vps74::KANMX6 yku70::HIS3</i>	This work
11051	<i>sac1::TRP vps74::KANMX6 yku70::HIS3</i>	This work
11052	<i>sac1::TRP vps74::KANMX6 yku70::HIS3 exo1::LEU2</i>	This work
11053	<i>sac1::TRP vps74::KANMX6 yku70::HIS3 exo1::LEU2</i>	This work
11151	<i>MATalpha vps74::KANMX6 sgs1::NatMX</i>	This work
11152	<i>MATa sir4::HIS3 cdc73::KANMX6</i>	This work
11153	<i>MATalpha sir4::HIS3 cdc73::KANMX6</i>	This work
11154	<i>MATa sir4::HIS3 paf1::KANMX6</i>	This work
11155	<i>MATalpha sir4::HIS3 paf1::KANMX6</i>	This work
11156	<i>sir4::HIS3 ctr9::KANMX6</i>	This work
11157	<i>sir4::HIS3 ctr9::KANMX6</i>	This work
11158	<i>MATa -535 telVII-L URA3 cdc73::KANMX6</i>	This work
11159	<i>MATa -535 telVII-L URA3 cdc73::KANMX6</i>	This work
11160	<i>MATa -535 telVII-L URA3 cdc73::KANMX6</i>	This work
11161	<i>MATa -535 telVII-L URA3 paf1::KANMX6</i>	This work
11162	<i>MATa -535 telVII-L URA3 paf1::KANMX6</i>	This work
11163	<i>MATa -535 telVII-L URA3 paf1::KANMX6</i>	This work
11164	<i>MATa -535 telVII-L URA3 ctr9::KANMX6</i>	This work
11165	<i>MATa -535 telVII-L URA3 ctr9::KANMX6</i>	This work

11166	<i>MATa -535 telVII-L URA3 ctr9::KANMX6</i>	This work
11167	<i>MATa -535 telVII-L URA3 leo1::KANMX6</i>	This work
11168	<i>MATa -535 telVII-L URA3 leo1::KANMX6</i>	This work
11169	<i>MATa -535 telVII-L URA3 rtf1::KANMX6</i>	This work
11170	<i>MATa -535 telVII-L URA3 rtf1::KANMX6</i>	This work
11171	<i>MATa -535 telVII-L URA3 rtf1::KANMX6</i>	This work
11213	<i>MATalpha tor1-1 fpr1::NAT RPL13A-2*FKBP12::TRP1 Rpb1-FRB-KANMX6</i>	
11218	<i>MATalpha tor1-1 fpr1::NAT RPL13A-2*FKBP12::TRP1 Rpb1-FRB-KANMX6 paf1::HPH</i>	
11232	<i>MATalpha tor1-1 fpr1::NAT RPL13A-2*FKBP12::TRP1 Rpb1-FRB-KANMX6 paf1::HPH</i>	
11220	<i>MATa -535 telVII-L URA3 cdc73::KANMX6 sir4::HPH</i>	This work
11221	<i>MATa -535 telVII-L URA3 cdc73::KANMX6 sir4::HPH</i>	This work
11222	<i>MATa -535 telVII-L URA3 paf1::KANMX6 sir4::HPH</i>	This work
11223	<i>MATa -535 telVII-L URA3 paf1::KANMX6 sir4::HPH</i>	This work
11224	<i>MATa -535 telVII-L URA3 ctr9::KANMX6 sir4::HPH</i>	This work
11225	<i>MATa -535 telVII-L URA3 ctr9::KANMX6 sir4::HPH</i>	This work
11226	<i>MATa -535 telVII-L URA3 leo1::KANMX6 sir4::HPH</i>	This work
11227	<i>MATa -535 telVII-L URA3 leo1::KANMX6 sir4::HPH</i>	This work
11228	<i>MATa -535 telVII-L URA3 rtf1::KANMX6 sir4::HPH</i>	This work
11229	<i>MATa -535 telVII-L URA3 rtf1::KANMX6 sir4::HPH</i>	This work
11230	<i>MATa -535 telVII-L URA3 sir4::HPH</i>	This work
11231	<i>MATa -535 telVII-L URA3 sir4::HPH</i>	This work

Appendix B

List of the primers used in this thesis. When a reference is not shown, the oligo was designed by me.

Gene	Primer (m)	Sequence	Use (reference)
Y'12'	395	ACAGCACTTCTACATAGCCCTAAATAGCCCTAAAT	TERRA RNA measurements.
Y'12'	396	GCTTTTGGTTGAACATCCGGGTAAGAG	TERRA RNA measurements.
CDC13	550	TTGGCACGATGATGATTCCGG	RFLP analysis of <i>cdc13-1</i> versus <i>CDC13</i> . (Zubko and Lydall 2006)
CDC13	551	TTCGATCAGGCTTTTCCAGT	RFLP analysis of <i>cdc13-1</i> versus <i>CDC13</i> . (Zubko and Lydall 2006)
KANMX6	1485	CGGATGTGATGTGAGAACTGTATCC	Confirm deletion. (Lydall collection)
STN1	1734	TCGAGCAACTGCAAGAAGAA	RT-qPCR. (Addinall et al. 2011)
STN1	1735	CGAAATGACAAGGAATGCAC	RT-qPCR. (Addinall et al. 2011)
TEN1	1794	ATACACCAAAGTCCGCCAAT	RT-qPCR. (Addinall et al. 2011)
TEN1	1795	CACCAAGTGGTGATTTGACA	RT-qPCR. (Addinall et al. 2011)
TEL15L	2335	TATCCTACTCCACTGCCACTTACCCTG	TERRA RNA measurements. Southern Blot probe.
TEL15L	2336	TGTTAGCGTTTCAATATGGTGGGTAGA	TERRA RNA measurements.
CDC73	2864	AGAATAATAATTTGAGCAAGAAACTGGTGAAAAAATTATGCGG ATCCCCGGGTTAATTAA	Disruption with <i>KANMX6</i> .
CDC73	2866	TTCAATGGCCGAAATACCATTCTTCCGTTTATCGTATTCAGAA TTCGAGCTCGTTTAAAC	Disruption with <i>KANMX6</i> .
CDC73	2868	CAACTCATCGAACACCGAGAC	Insertion check.
CDC73	2870	GCGGCACTTGAGTCCTTATTC	Insertion check.
CDC73	2872	TTTCCACTTTGCCGGTGATTC	Insertion check.
CDC73	2873	ATCAAACCTGGACGCTAGGTATC	Insertion check.
CDC73	2885	ACCGCGGTGGCGGCCGCATAGGCCACTAGTGGATCTGATAT CATCGATGTGGGCTTTGAGCTTTCTGTC	Insertion in plasmid.
CDC73	2886	CAATTTATAAAGACTGGAGGCAATCACAAACCTCCTGCTCGAC GGATCTGTTCTTGGATGAGATTGCGAG	Insertion in plasmid.
LEO1	2887	AAAGTAATCCAATTAGATATACTGGACTATAATTAAGATGCGG ATCCCCGGGTTAATTAA	Disruption with <i>KANMX6</i>
LEO1	2888	TGTACATACTAATATATAAACAAGTAACGTCTCCTCTGAAT TCGAGCTCGTTTAAAC	Disruption with <i>KANMX6</i> .
LEO1	2889	TCAATGAGGGTAACACTGCAAC	Insertion check.
LEO1	2890	GATTTGCTCCTTCTGTGGTTGA	Insertion check.
LEO1	2891	CGACGATGAGGAAGAGGAGG	Insertion check.
LEO1	2892	GGAATGAGAAAGGGTCAACTGAG	Insertion check.
RTF1	2893	AATTGTATTGCACTAATTTGTTGAGAGCACTATAGAAATGCGG ATCCCCGGGTTAATTAA	Disruption with <i>KANMX6</i> .
RTF1	2894	AAATATATTTTTACAAACACTGAAATTGTCCTGCCTACTAGAAT TCGAGCTCGTTTAAAC	Disruption with <i>KANMX6</i> .
RTF1	2895	TGTTGCTGCCTTGAATCATG	Insertion check.
RTF1	2896	GTGCTCTCTGCTCCTCATC	Insertion check.
RTF1	2897	ACTAGGCGAGTTGACCTCTAAG	Insertion check.
RTF1	2898	CCTTGGCACGAAACCATTCA	Insertion check.
PAF1	2899	CAATAGAACAGTGCTCATAATAGTATAAAGGGTCACAATGCG GATCCCCGGGTTAATTAA	Disruption with <i>KANMX6</i> .

PAF1	2900	CAGGTTTAAATCAATCTCCCTTCACTTCTCAATATTCTAGAAT TCGAGCTCGTTTAAAC	Disruption with <i>KANMX6</i> .
PAF1	2901	CACGCAATGAGAACCCTAACCC	Insertion check.
PAF1	2902	CATCAAATCAACCGGCATACCT	Insertion check.
PAF1	2903	GGAGCAACCAGAAGACGTTAAG	Insertion check.
PAF1	2904	GTGTCAGTGTAACTGCTGGTG	Insertion check.
CTR9	2905	GTCTGGTCCATTTGTGTTGAGAGCAAGAAAAAACAATGCGG GATCCCCGGGTTAATTA	Disruption with <i>KANMX6</i> .
CTR9	2906	TTTCTTTAAAGTCTTGATTCTAACCTCGCCTCTTCTTAGAAT TCGAGCTCGTTTAAAC	Disruption with <i>KANMX6</i> .
CTR9	2907	ACCTAGTTCTCACTTCAGGTAC	Insertion check.
CTR9	2908	CAAGTGCAATGGTCAACCAA	Insertion check.
CTR9	2909	CGAGGATGACGATGATGTGG	Insertion check.
CTR9	2910	GATCTCAATGCAGACTCGACC	Insertion check.
VPS36	2975	AAGTGTGTTTTGAAAGTCACTTTTTTTTTTCAAAGATGCGGA TCCCCGGGTTAATTA	Disruption with <i>KANMX6</i> .
VPS36	2976	GTATTACGAGCAGGTAATCAAACCATGCATTATTACTTAGAA TTCGAGCTCGTTTAAAC	Disruption with <i>KANMX6</i> .
VPS36	2977	CATGTCTGGTGCAGTGTATGTAAG	Insertion check.
VPS36	2978	GCTAGATCGTCCAATTCCAACC	Insertion check.
VPS36	2979	TGTGTCGATGAAGGCGATTTAC	Insertion check.
VPS36	2980	CTACTATTTCCACTTTGCCGGTG	Insertion check.
VPS36	2981	ACCGCGGTGGCGGCCGCATAGGCCACTAGTGGATCTGATAT CATCGATGCTTATAGCGTCTTCGATGATG	Insertion in plasmid.
VPS36	2982	CAATTTATAAAGACTGGAGGCAATCACAAACCTCTGCTCGAC GGATGTTCCGATCCAGTTGTGGTG	Insertion in plasmid.
YLR419W	2983	ACTTTACATCGCAATTGCTTTTCTTAATTTTTGATAAATGCGGA TCCCCGGGTTAATTA	Disruption with <i>KANMX6</i> .
YLR419W	2984	ATAATTATTATACAGGGACTACAGTAGGAACTGATTACTAGAA TTCGAGCTCGTTTAAAC	Disruption with <i>KANMX6</i> .
YLR419W	2985	GTCTCGGTGTTTCGATGAGTTG	Insertion check.
YLR419W	2986	GGTTGGATCGTTCATTCTTGCA	Insertion check.
YLR419W	2987	CTATTCATTCACCGGGCATCG	Insertion check.
YLR419W	2988	GTTGTATTATCGACGGAGGGTTG	Insertion check.
YLR419W	2989	ACCGCGGTGGCGGCCGCATAGGCCACTAGTGGATCTGATAT CATCGATTTGTTCCACCACAACCTGGATC	Insertion in plasmid.
YLR419W	2990	CAATTTATAAAGACTGGAGGCAATCACAAACCTCTGCTCGAC GGATGAGGCAGCATGACATGAGTG	Insertion in plasmid.
BAS1	2991	AACAAAATTAGTTTTGTTTAAACTTTTTGTTGTAGCGTTTTCGGA TCCCCGGGTTAATTA	Disruption with <i>KANMX6</i> .
BAS1	2992	AACAATTGAAAGATTTGTGTTTTTTTTTCGGCCTTGCCTTCGAAT TCGAGCTCGTTTAAAC	Disruption with <i>KANMX6</i> .
BAS1	2993	GGTCCGAACAATGCGATGAG	Insertion check.
BAS1	2994	CTCCTTTGCGGATTCGTTTACT	Insertion check.
UFD2	2995	AAAAGTTAACTTTGAAAGTAGAACCTCATTCCATAGATCCGG ATCCCCGGGTTAATTA	Disruption with <i>KANMX6</i> .
UFD2	2996	ATTAGGGTCAATTTTGCAATTTATTCTATCACTTATTATGAAAT TCGAGCTCGTTTAAAC	Disruption with <i>KANMX6</i> .
UFD2	2997	AGTATTCGTGAGAGGCGATAGTC	Insertion check.
UFD2	2998	GGAAGGATCGGTGGTGATTTG	Insertion check.
SKI2	3000	AACCTAACTCACAAAATTTACTGTACTAATACTAATTTATCGGA TCCCCGGGTTAATTA	Disruption with <i>KANMX6</i> .
SKI2	3001	CTTTTATAAACATGACTCACATTGAGAATAAATGAGCTCTGAAT TCGAGCTCGTTTAAAC	Disruption with <i>KANMX6</i> .
SKI2	3002	CTTGCTCAGAACGCCATC	Insertion check.
SKI2	3003	CTTTGGTTCATCGGTGCTCTC	Insertion check.
SLA2	3004	CCATAGCAGTAGTAGTGATAGTACTAGCAGCTAGAACAGGCG GATCCCCGGGTTAATTA	Disruption with <i>KANMX6</i> .
SLA2	3005	ATTAACGTTTATCTTTATATATAAAAAGTACAATTCATGAGAAT TCGAGCTCGTTTAAAC	Disruption with <i>KANMX6</i> .

SLA2	3006	CCGACCCGTTATTGGTGATAATAC	Insertion check.
SLA2	3007	CGTGCTTTCTCTTAGGTGCG	Insertion check.
DYN1	3008	GAGCTTAAATTGGAAAGTACGTCAAACGTTTTTTAGGCACGG ATCCCCGGGTTAATTA	Disruption with <i>KANMX6</i> .
DYN1	3009	AGAAAACCGCGGACAAGCAAGACACGCGTACCTGAAAAGGG AATTCGAGCTCGTTTTAAAC	Disruption with <i>KANMX6</i> .
DYN1	3010	CGATCCCTGCGAAACTATGTTAC	Insertion check.
DYN1	3011	GTCGAACTCTCTCCCATCCAATA	Insertion check.
INP52	3012	ACGCAAAGGCAGCAGAATCAAAAACAAATACTCAGTAGCTCG GATCCCCGGGTTAATTA	Disruption with <i>KANMX6</i> .
INP52	3013	TGATACATATTCTATAAATGCGTAATTTTAGTAACACAATGAAT TCGAGCTCGTTTTAAAC	Disruption with <i>KANMX6</i> .
INP52	3014	TTGTTTGGCGGTTAGTGACG	Insertion check.
INP52	3015	CAGCTTTCGGAACCAATTCCA	Insertion check.
FYV10	3016	CAGAGAAAATGATTATAAATTATAGGAAAGTAGGTAAGCCCGG ATCCCCGGGTTAATTA	Disruption with <i>KANMX6</i> .
FYV10	3017	AAATCTTTATATAAAAAATGCATATAGCTTGAAACTATTGAAT TCGAGCTCGTTTTAAAC	Disruption with <i>KANMX6</i> .
FYV10	3018	TCCCTGGCACTCTCTTTTC	Insertion check.
FYV10	3019	CTAGTGCCAACTCGTCGTCT	Insertion check.
CMK2	3020	ATATTGTTCAAGATCAGCAGAACTTCAATTCGTTGATCAAGAA TTCGAGCTCGTTTTAAAC	Disruption with <i>KANMX6</i> .
CMK2	3021	CATGAAATTCAGAATTTATGACCTCTGACTCCTTGGGCATGCA CTGAGCAGCGTAATCTG	Disruption with <i>KANMX6</i> .
CMK2	3022	AGCGCGAAGAGAATAATTGAGG	Insertion check.
CMK2	3023	CGTAAGATTCAGGTTGACCGC	Insertion check.
INP52	3024	CTCGCTTCATATAGTCTCAACATATTTTTGTTTCGCAATGAAT TCGAGCTCGTTTTAAAC	Disruption with <i>KANMX6</i> .
INP52	3025	CTATCTTTCTAGTTTGTCTGTTTCGATAGGAGATTTTCATGCAC TGAGCAGCGTAATCTG	Disruption with <i>KANMX6</i> .
SLA2	3026	CATATATAAATATATATAAAGAATAGTGAACAATAGAAAGAAT TCGAGCTCGTTTTAAAC	Insertion check.
SLA2	3027	TTTTAAGCGCTTTCTGCAGATCTGAATCTATTCTGGACATGCA CTGAGCAGCGTAATCTG	Insertion check.
CDC73 N-terminal	3120	ATGGCGAACTCATTAGACAGACTGAGAGAACTTAAAGACG GATCCCCGGGTTAATTA	Disruption with <i>KANMX6</i> .
CDC73 N-terminal	3121	CATCACTGGATAGAGTTTCTACCATGGTTGCTTCGTAATGAA TTCGAGCTCGTTTTAAAC	Disruption with <i>KANMX6</i> .
VPS36	3122	ATGGAGTACTGGCATTATGTGGAACTACGTCATCGGGCCCG GATCCCCGGGTTAATTA	Disruption with <i>KANMX6</i> .
VPS36	3123	CTCTGTGCTGTAGAATCTTAGATTTGCCATGGTAAAGACGAA TTCGAGCTCGTTTTAAAC	Disruption with <i>KANMX6</i> .
VPS36 and CDC73	3124	CCGAGTTTAAAGATTTGAACAGTGATACCACTATATGATCGG ATCCCCGGGTTAATTA	Disruption with <i>KANMX6</i> .
VPS36 and CDC73	3125	CAATTTAACTGTTGCAAAATATAAAAACAGTTCCTGCTGGAGAA TTCGAGCTCGTTTTAAAC	Disruption with <i>KANMX6</i> .
VPS36	3151	AAGTGTGTTTTGAAAGTCATTCTTTTTTTTTCAAAGATGCGGA TCCCCGGGTTAATTA	Disruption with <i>KANMX6</i> .
VPS36	3152	ATTCTGCCCTCTGTGCTGTAGAATCTTAGATTTGCCATGAA TTCGAGCTCGTTTTAAAC	Disruption with <i>KANMX6</i> .
VPS74	3153	TTCAAACAAAACTATCTAAAAAATACAAAGCAAAAATCCGG ATCCCCGGGTTAATTA	Disruption with <i>KANMX6</i> .
VPS74	3154	TTTTCTTATGTTTCAAAGAGAGGATTTTTGTTGTTATTTGAAT TCGAGCTCGTTTTAAAC	Disruption with <i>KANMX6</i> .
VPS74	3155	TTGCTTTCTGGGTACGTTGAC	Insertion check.
VPS74	3156	GTATCTCCAGAATCCGCCCTAT	Insertion check.
Telomere	3157	CCCACCACACACCCACACCC	Probe for In-Gel.
SKI3	3213	ACTAAGAACACAGAAAAGAAACCGAAGAGCAGAGGAAATCG TACGCTGCAGGTCGACGG	Disruption with Hygromycin.
SKI3	3214	GTTACATTAAGGTTTGATTGACTATCTCGAATCCAAATTTTCGA TGAATTCGAGCTCGTT	Disruption with Hygromycin.
SKI3	3215	TCAGACCATCCTCATCCTCATC	Insertion Check.
SKI3	3216	GGAACATAATTTGGCAGCGGA	Insertion check.
SKI7	3217	TACGAGGAGGTGGTCTTCGAAACTTACAGTACCACCTGACCG TACGCTGCAGGTCGACGG	Disruption with Nourseothricin.
SKI7	3218	AATAAGTATGAATGCCTAGTATAATTTCTTAGTTGTAGGATCG ATGAATTCGAGCTCGAT	Disruption with Nourseothricin.
SKI7	3219	ATCATAATCTGCCATCGCTGTG	Insertion check.

SKI7	3220	GAGACTGGTCCGCACTTAAA	Insertion check.
SKI8	3221	AGACAAGAAACGAAAAAGAGGTTAATCAAGTATTGAAAAGG AAGATATTCTTTATTGAA	Disruption with Triptofan.
SKI8	3222	TTGTAAGGTTACATGCAATATATCAAGATTTACTAGAGAACA AAATATTAACGTTTACA	Disruption with Triptofan.
SKI8	3223	TGGTGCTTCCTACATCTCTCTC	Insertion check.
SKI8	3224	GTGGTAGCAACAAGGCAT	Insertion check.
DOA1	3225	TCATGTGTGATAGTAAGGTGTAGAGCAGCAGATTTGGAGTCG TACGCTGCAGGTCGACGG	Disruption with Hygromycin.
DOA1	3226	ATCTAGACATTATGTGTTTTATATGATTGCTGTAAAAGTATCGA TGAATTCGAGCTCGTT	Disruption with Hygromycin.
DOA1	3227	TTGCTGACCTTGGCATTTC	Insertion check.
DOA1	3228	CATCCATACAGAGGCATTGTG	Insertion check.
SKI3	3257	ATATGTCCGATATTAACAGCTATTGAAGGAAGCCAAACACGT ACGCTGCAGGTCGACGG	Disruption with Hygromycin.
SKI3	3258	TCCAAATTTTTAGAAACATTCGTTTAGCGCCTTCACTGCATCG ATGAATTCGAGCTCGT	Disruption with Hygromycin.
TLC1	3261	AATGTGCCCGTACATCGAA	RT-qPCR.
TLC1	3262	CGCAAACCTAACCGATGCTT	RT-qPCR.
CDC73	3263	CTATCAGTGAATTCGCCACA	RT-qPCR.
CDC73	3264	ATTCCATTGCTGCACGTGT	RT-qPCR.
YLR419W	3267	TGAAGCCGAGAGCAGATTCTA	RT-qPCR.
YLR419W	3268	GCAGCTTTCAGGCGTTTATG	RT-qPCR.
VPS36	3271	GAACTCGCTTGGGTTGGAAT	RT-qPCR.
VPS36	3272	GGGGTCCTGAAAAACAGGA	RT-qPCR.
BUD6	3275	GACCGGGCACATTTAATCAG	RT-qPCR internal control.
BUD6	3276	TCAGCCTTGTCATAGCTTCG	RT-qPCR internal control.
TEL01L	3556	CGGTGGGTGAGTGGTAGTAAGTAGA	TERRA RNA measurements. (Balk et al. 2013)
TEL01L	3557	ACCCTGTCCCAATCAACCATAC	TERRA RNA measurements. Southern Blot probe. (Balk et al. 2013)
SBP1	3610	CCCCAAAAGAAAGAAGAAAACCTCAAACGAAGAAAAATCG TACGCTGCAGGTCGACGG	Disruption with Hygromycin.
SBP1	3611	AAAAACTCAAGTTAGAAATAGGGATGTGGGTAAGAAGTAATC GATGAATTCGAGCTCGTT	Disruption with Hygromycin.
SBP1	3612	TCACAGGTTGTGGCATAAAGG	Insertion check.
SBP1	3613	CCACTGAAAGTGACAAATGCC	Insertion check.
OPI1	3614	TGTATCAGGACAGTGTTTTTAACGAAGATACTAGTCATTGGGA AGATATTCTTTATTGAA	Disruption with Tryptophan.
OPI1	3615	TTACTGGTGGTAATGCATGAAAGACCTCAATCTGTCTCGGACA AAATATTAACGTTTACA	Disruption with Tryptophan.
OPI1	3616	AAGAATATGACCGCCTGCAAG	Insertion check.
OPI1	3617	CATTCTTCAGCCTTGCCCAA	Insertion check.
SCS2	3618	TGTAGCAGAAGGGTATTCTACAATCTCCGCGAACCTAAGTCG TACGCTGCAGGTCGACGG	Disruption with Nourseothricin.
SCS2	3619	AATATATATTTAGAATACAGCTATATCCTCAATCTCCCTATCGA TGAATTCGAGCTCGAT	Disruption with Nourseothricin.
SCS2	3620	AAACGTGCGTGGTGATCTTAC	Insertion check.
SCS2	3621	GCTGTTGGACGTTTGCTTCT	Insertion check.
MON1	3713	CTATCAAAGTACACAAACGTAGAATCAGTACATCGAACTCG GATCCCCGGGTTAATTA	Disruption with <i>KANMX6</i> .
MON1	3714	ATTAAAGGAAAAAATAATAAAATAACCTCCCTGTCACAAGGAA TTCGAGCTCGTTTAAAC	Disruption with <i>KANMX6</i> .
MON1	3715	AAGCAGTTCAAGCTCACATCC	Insertion check.
MON1	3716	GCTCTTTGCCAAATCTGCTGA	Insertion check.
SUB1	3717	TACACATCAATTTTTCGACATATATACAAACACAAGCGCTCGG ATCCCCGGGTTAATTA	Disruption with <i>KANMX6</i> .
SUB1	3718	TGGAAGACGTTGACATAAGCAAGCTCAACTCCAGGACTAGA ATTCGAGCTCGTTTAAAC	Disruption with <i>KANMX6</i> .
SUB1	3719	ATAGCACTGCACACACACAC	Insertion check.
SUB1	3720	CTTTGGGCTGTTCTTGCTCTT	Insertion check.
SNF8	3844	AAAATGCTTGGCGTAACAGCCAACTTCGAAACTCACTAACCGT ACGCTGCAGGTCGACGG	Disruption with Hygromycin.

SNF8	3845	ACTTAACGCTCATCCACCATTCTGTTCAAGTCAACTATCTCG ATGAATTCGAGCTCGTT	Disruption with Hygromycin.
SNF8	3846	AAGTCCACGTTTCAGGCTTG	Insertion check.
SNF8	3847	GCTGCCAGTCCAAACTGTTT	Insertion check.
VPS25	3848	CTCAGAATTATTCTTGTTCGCGCTAATATAGCAAGTGTATTTCGT ACGCTGCAGGTCGACGG	Disruption with Nourseothricin.
VPS25	3849	AATAGTTTTATTTATCCTCTCGCTCGTGTTTTAAACAACCTCGA TGAATTCGAGCTCGAT	Disruption with Nourseothricin.
VPS25	3850	TTGAGTGAAGTGGGACAGAAC	Insertion check.
VPS25	3851	CTTCTTTGGTCATTTGCGACC	Insertion check.
SAC1	3869	ACGATAATATTTATATACACGTATATTTTCTCGCTAGATCGTA CGCTGCAGGTCGACGG	Disruption with Hygromycin.
SAC1	3870	GGATTTACAATAATCATCATTTTATCACATATAGAACTCATCGA TGAATTCGAGCTCGTT	Disruption with Hygromycin.
SAC1	3871	ATCGTGCCCTTTAAGTGTTGC	Insertion check.
SAC1	3872	GACCCGAACACCTTGATCTT	Insertion check.
SAC1	4076	ACGATAATATTTATATACACGTATATTTTCTCGCTAGATGGAA GATATTCTTTATTGAA	Disruption with Tryptophan.
SAC1	4077	GGATTTACAATAATCATCATTTTATCACATATAGAACTCAACAA AATATTAACGTTTACA	Disruption with Tryptophan.
TEL10R	4089	CGGTTATGGTGGACGGTGGATG	TERRA RNA measurements. (Iglesias et al. 2011)
TEL10R	4090	CCTAACCTATTCTAATCCAACCCTGATAA	Southern Blot probe. TERRA RNA measurements. (Iglesias et al. 2011)
TEL13R	4093	ACGGTTATGGTGCACGATGGG	TERRA RNA measurements. (Iglesias et al. 2011)
TEL13R	4094	TTACCCTCCATTACGCTACCTCC	TERRA RNA measurements. (Iglesias et al. 2011)
Y' 6	4095	GGCTTGGAGGAGACGTACATG	TERRA RNA measurements. (Iglesias et al. 2011)
Y' 6	4096	CTCGCTGTCACTCCTTACCCG	TERRA RNA measurements. (Iglesias et al. 2011)
Y' 4	4097	GGCTTGGAGGAGACGTAAATG	TERRA RNA measurements. (Iglesias et al. 2011)
Y' 4	4098	CCAACTCTCTCATCTACCTTACTCG	TERRA RNA measurements. (Iglesias et al. 2011)
Y' 3	4099	GGCTTGGAGGAGACGTACATG	TERRA RNA measurements. (Iglesias et al. 2011)
Y' 3	4100	CCACACACTCTCTCACATCTACCTC	TERRA RNA measurements. (Iglesias et al. 2011)
ACT1	4101	GTAACATCGTTATGTCCGGTGGTAC	TERRA RNA measurements. (Iglesias et al. 2011)
ACT1	4103	CCAAGATAGAACCACCAATCCAGAC	TERRA RNA measurements. (Iglesias et al. 2011)
CA	4104	CACCACACCCACACACCACCCACA	cDNA production. (Iglesias et al. 2011)
TEL10R	4105	TGACTTAACCTTGGCAGCTTC	Southern Blot probe. (Iglesias et al. 2011)
TEL10R	4108	CGTTTCCGATCTGGATGCTAT	Southern Blot probe. (Iglesias et al. 2011)
TEL1L	4109	ATTAACCTCAATCGCCGCTGG	Southern Blot probe. (Iglesias et al. 2011)
TEL13R	4113	TGGGCTTTATGGGTAAATGG	Southern Blot probe. (Iglesias et al. 2011)
TEL13R	4116	TACCCTGATTTAGCATGTCTCTTA	Southern Blot probe. (Iglesias et al. 2011)
TEL15L	4118	AGTGGAACGCTGATAAACTGC	Southern Blot probe. (Iglesias et al. 2011)
SIR4	4226	GCTTCAACCCACAATACCAAAAAAGCGAAGAAAACAGCCACG TACGCTGCAGGTCGACGG	Disruption with hygromycin.
SIR4	4227	GGTACACTTCGTTACTGGTCTTTTGTAGAATGATAAAAAGTCCG ATGAATTCGAGCTCGTT	Disruption with hygromycin.
SIR4	4228	TTACCATGCTCAAACCGAACC	Insertion check.
SIR4	4229	CAATGGGCAGCCTTCAAAGAT	Insertion check.
a1	4240	GGCGGAAAACATAAACAGAACTCTG	RT-qPCR (Panday et al. 2015).
a1	4241	CCGTGCTTGGGGTGATATTGATG	RT-qPCR (Panday et al. 2015).

YOL166W-A (TEL15L)	4269	GCTTGCCTCAGCGGTCTAT	TERRA and Silencing measurements.
YOL166W-A (TEL15L)	4270	TGGGCCGCCAAATGAGATA	TERRA and Silencing measurements.
YAL068W-A (TEL01L)^{***}	4273	TACCCATAACGCCCATCATT	TERRA and Silencing measurements.
YAL068W-A (TEL01L)^{***}	4274	TGGTGCAAAAGTGGTATAACG	TERRA and Silencing measurements.
7S RNA	4275	GGCAGGAGGCGTGAGGAATC	RT-qPCR.
7S RNA	4276	CCTAACAGCGGTGAAGGTGGAG	RT-qPCR.

*Conserved in 12 different telomeres

**Conserved in 3 different telomeres

***Also recognises TEL03L

Appendix C

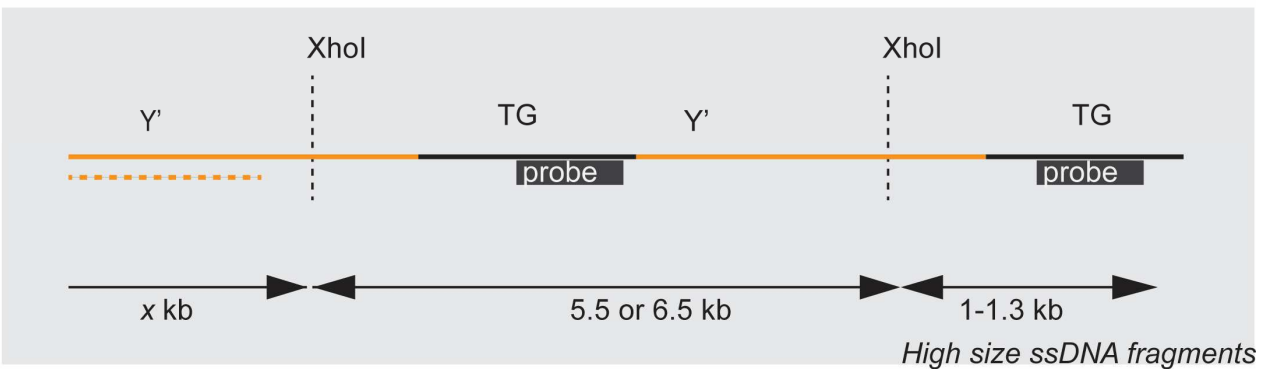
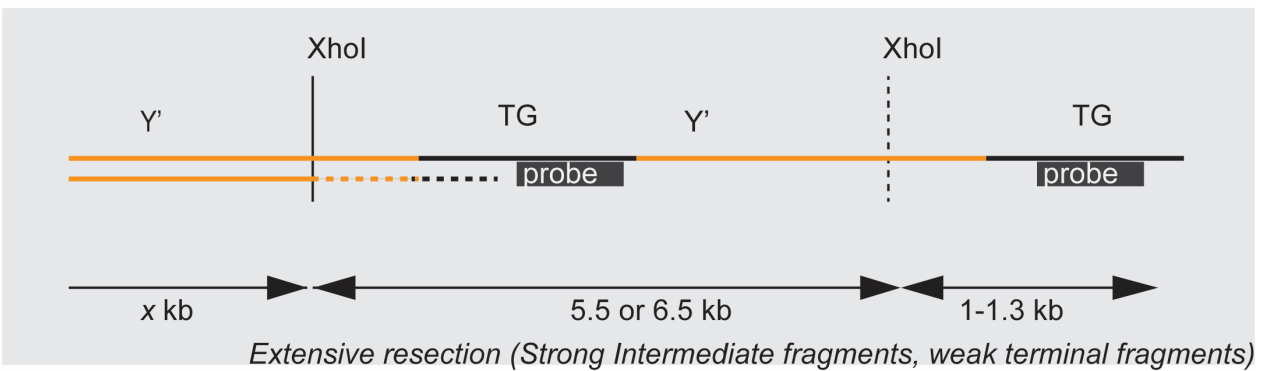
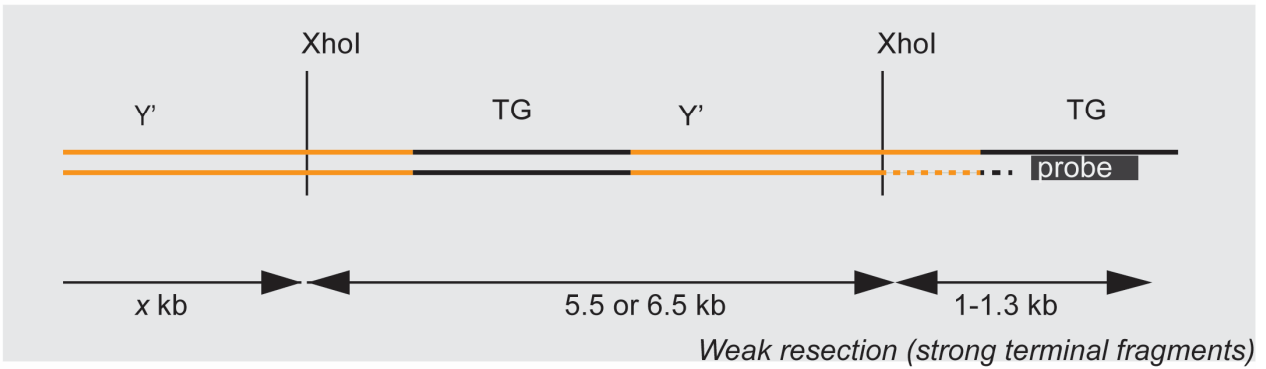
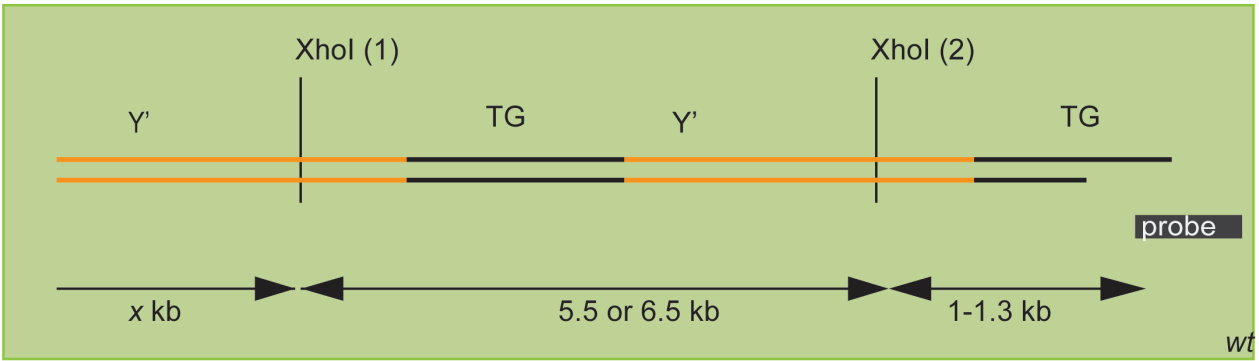
List of the plasmids used in this thesis.

Plasmid number (pDL)	Description	Reference
1042	pFA6a-KANMX6	(Longtine et al. 1998)
1453	pAG36::CAN1. CAN1 cloned as an Xho1, 4.4kb fragment, from 535, into Sal1 site of 1223. For PCR amplification of dominant drug resistance cassette. Nourseothricin resistance gene cloned into pAG22 (pRS316)	(Goldstein and McCusker 1999)
1467	pDL1453 was digested with Asc1 and Sph1. Blunt-ends were generated using DNA polymerase I, Large Klenow fragment (5' fill-in and 3' overhang removal). PDL1467 was then obtained by self-circularization of the linearized vector.	Lydall collection
1495	Plasmid harbouring <i>TEN1</i> . Made by cloning <i>TEN1</i> into pDL1726 (digested with AscI and SphI)	Lydall collection
1562	pDL1467:: <i>CDC73</i> . pDL1467 was digested with AscI and then co-transformed in yeast with a PCR fragment obtained by the amplification of genomic DNA with m2885 and m2886 (<i>CDC73</i> +/- 800bp).	This work
1583	pFA6-hphNT1	(Janke et al. 2004)
1584	pFA6a-natNT2	(Janke et al. 2004)
1614	Expresses GFP-Rer1 fusion protein under the control of the TDH3 promoter	(Matsuura-Tokita et al. 2006)
1615	Expresses mRFP-Gos1 fusion protein under the control of the TDH3 promoter.	(Matsuura-Tokita et al. 2006)
1616	Expresses Sec7-mRFP fusion protein under the control of the ADH1 promoter.	(Matsuura-Tokita et al. 2006)
1618	Expresses Sec7-GFP fusion protein under the control of the ADH1 promoter	(Matsuura-Tokita et al. 2006)
1649	pDL1467:: <i>VPS36</i> . pDL1467 was digested with AscI and then co-transformed in yeast with a PCR fragment obtained by the amplification of genomic DNA with m2981 and m2982 (<i>VPS36</i> +/- 800bp).	This work
1650	pDL1467:: <i>YLR419W</i> . pDL1467 was digested with AscI and then co-transformed in yeast with a PCR fragment obtained by the amplification of genomic DNA with m2989 and m2990 (<i>YLR419W</i> +/- 800bp).	This work
1667	pRS406_eGFP _{RER1} . Vector (pDL745) and Insert (pDL1614) were digested with BamHI and XhoI. Insert contained the <i>TDH3</i> promoter, eGFP-RER1 and <i>CMK1</i> terminator.	This work
1671	pRS406_SEC7eGFP. Vector (pDL745) and Insert (pDL1618) were digested with BamHI and XhoI. Insert contained the <i>TDH3</i> promoter, <i>SEC7</i> -eGFP and <i>CMK1</i> terminator.	This work
1726	pDL1453 was digested with Mlu1 and vector was purified after gel extraction. pDL1726 was obtained by self-circularization of the linearized vector.	Lydall collection
1755	pVL1066. Plasmid containing <i>STN1</i> and its native promoter.	(Gasparyan et al. 2009)
1756	YEplac181. Control vector to use with pDL1755	(Gasparyan et al. 2009)

Appendix D

Cartoon to aid In-Gel interpretation.

Probe: CCCACCACACACCCCACACCC



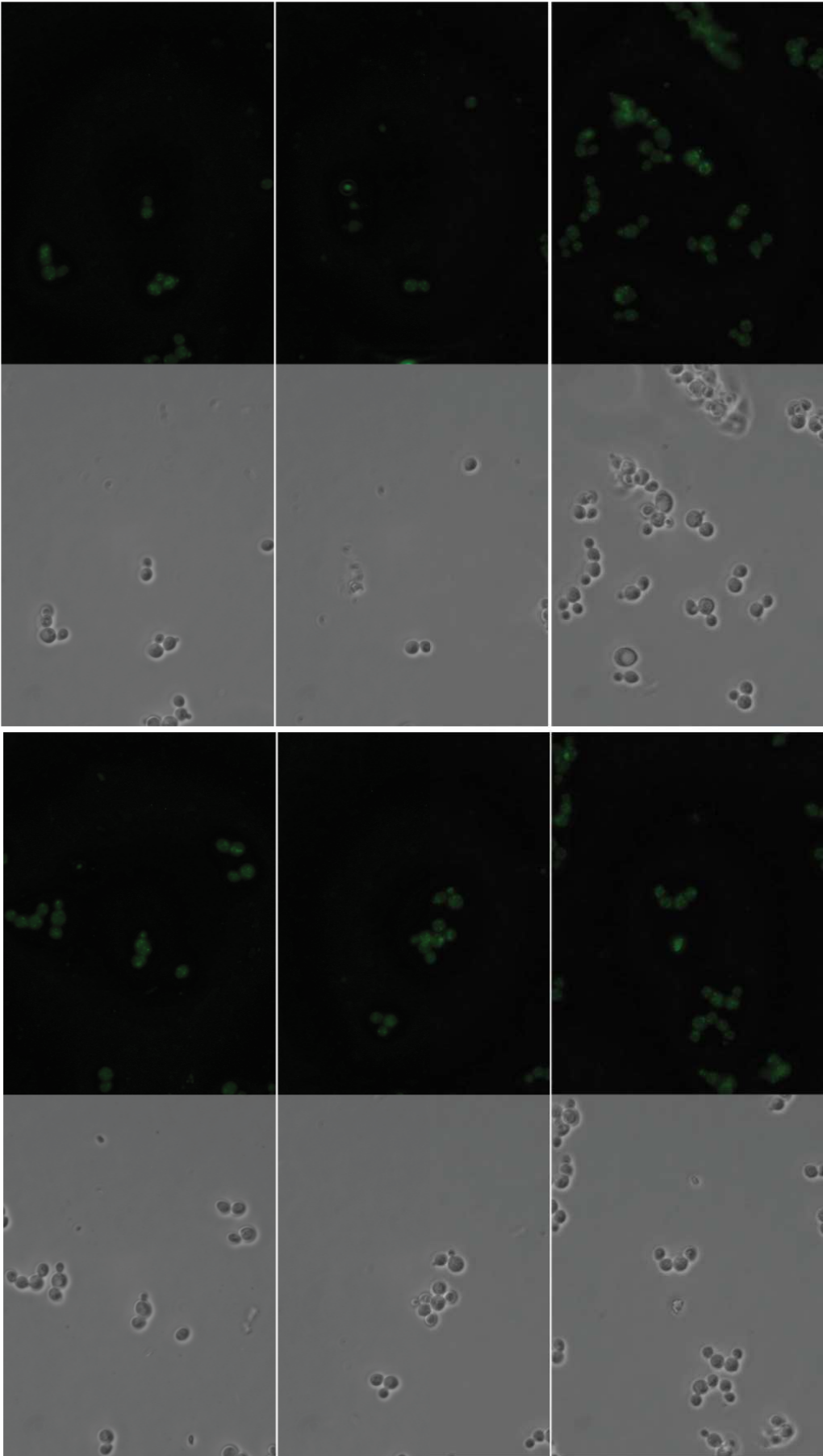
Big ssDNA fragments. DNA was not cut by XhoI (can not cut ssDNA). Might be due to the extraction method.

Intermediate ssDNA fragments. Extensive resection, but should allow XhoI to cut on site 1.

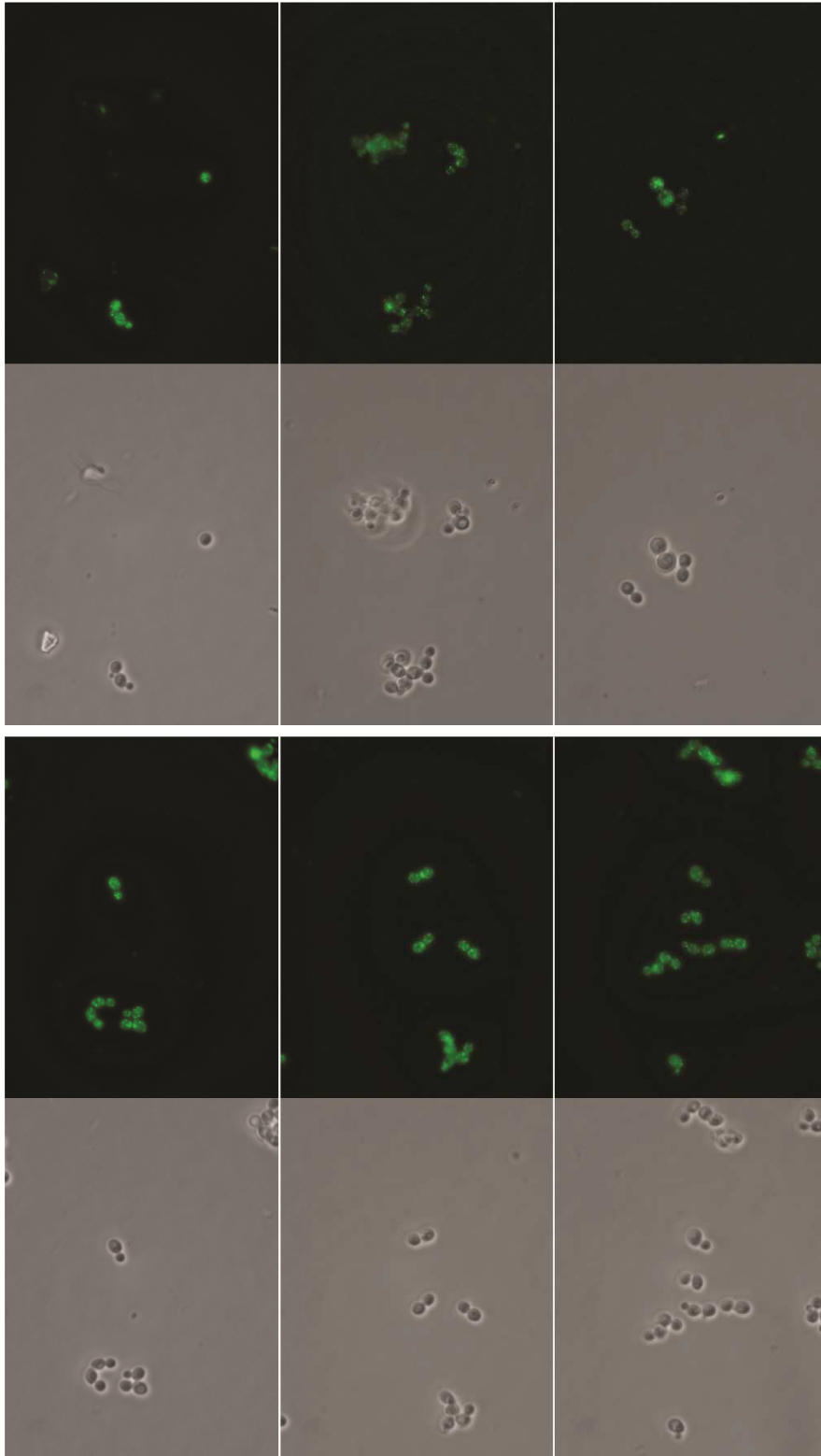
Terminal fragments. XhoI cuts on sites 1 and 2.

Appendix E

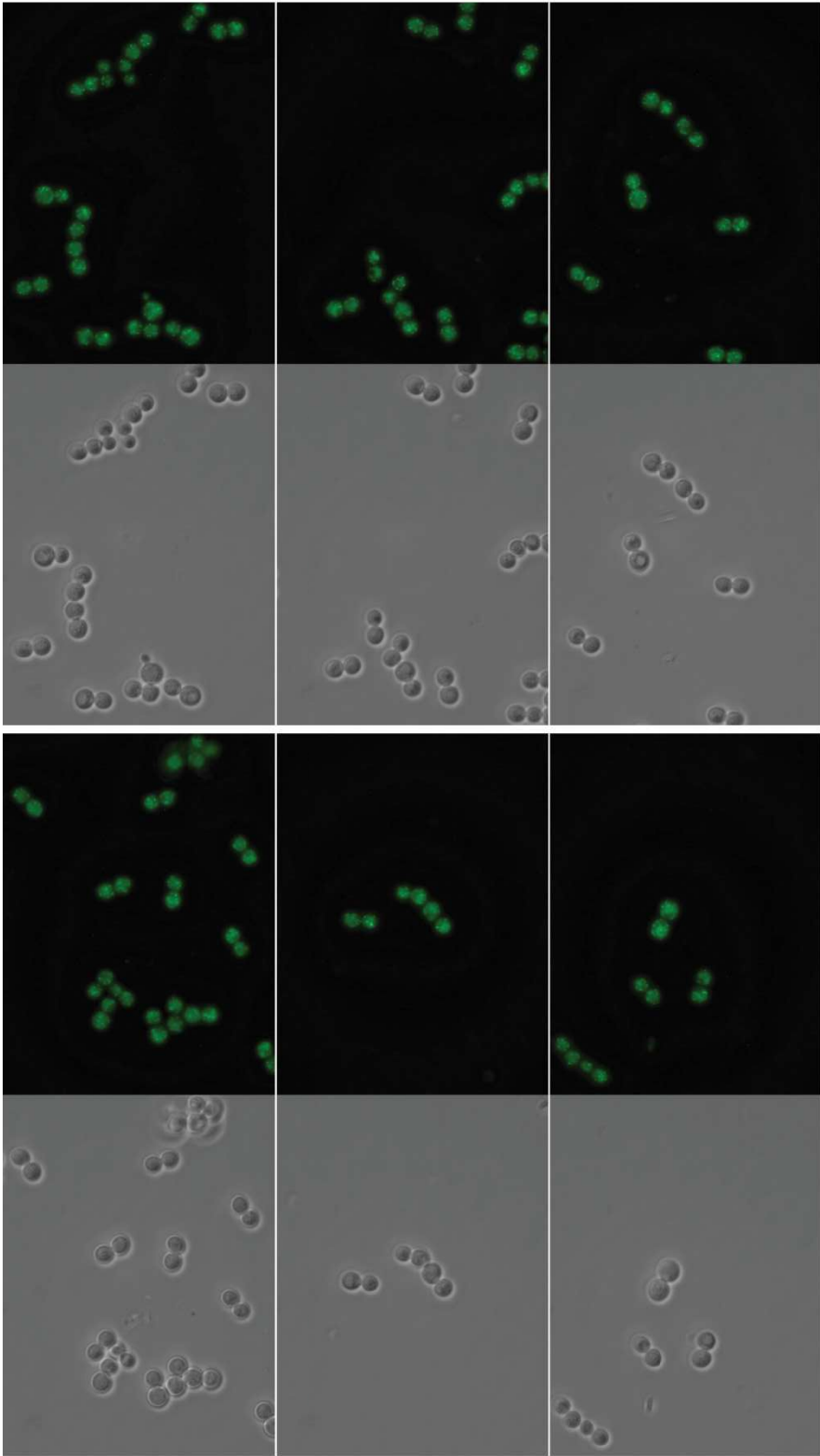
Live yeast cell imaging of EGFP-Rer1 and Sec7-EGFP (Sections 2.3.23 and 4.2.1). Strain, treatment (water, HU or MMS), time (0 or 180 min) and temperature are indicated under each group of images



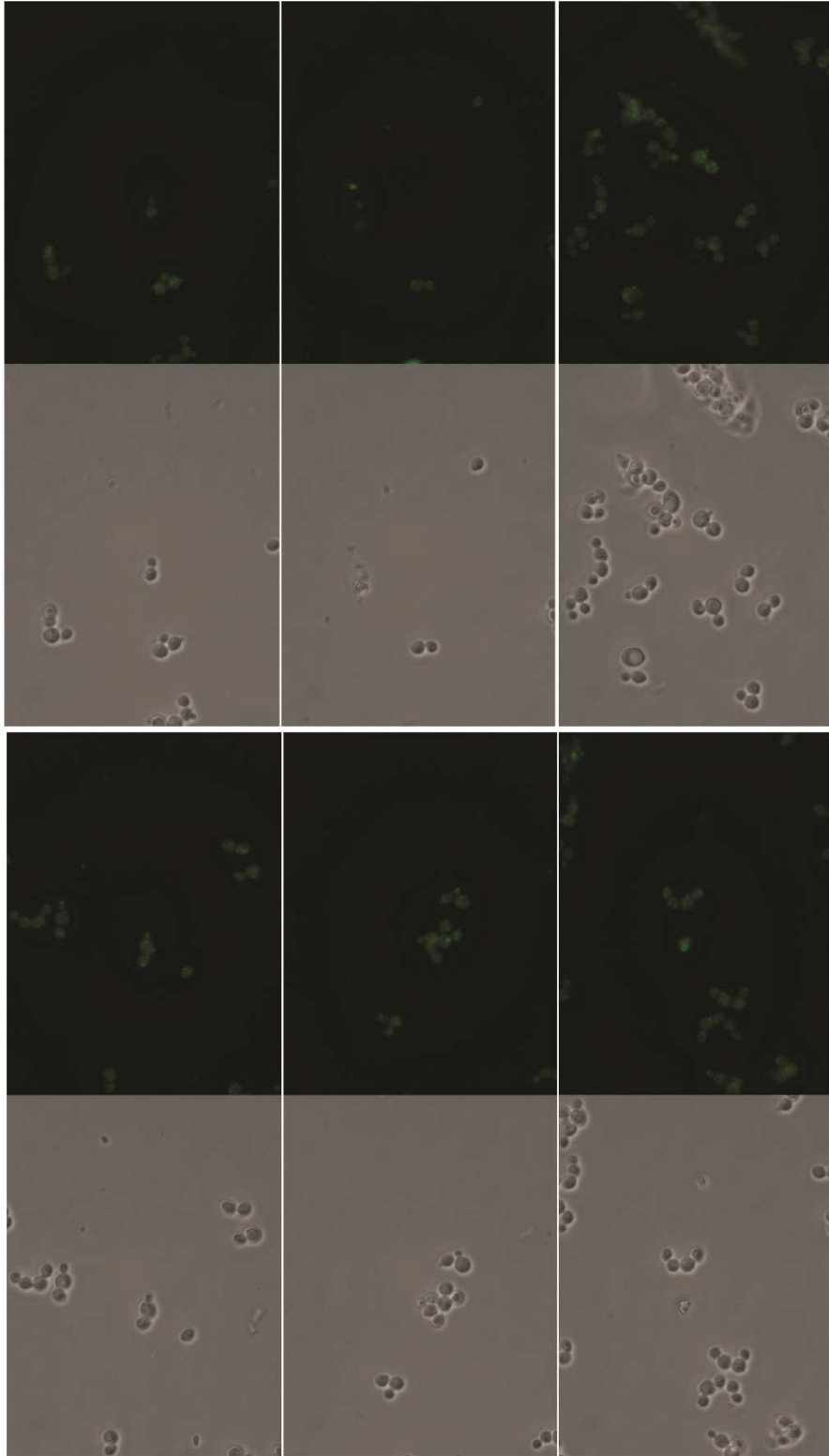
EGFP-Rer1, WT, water, 180 min, 36°C



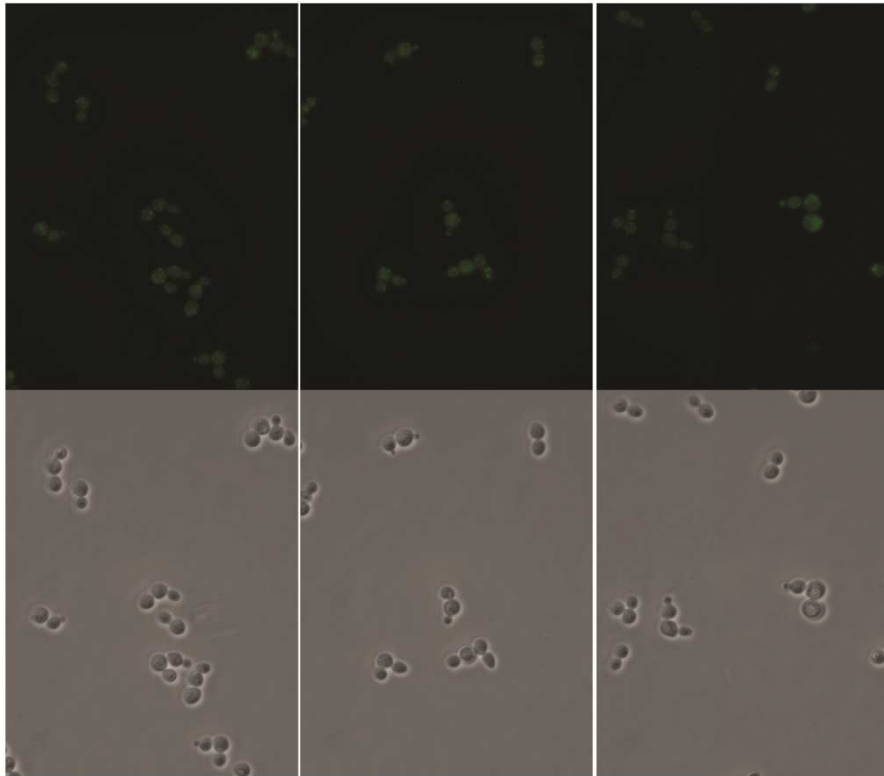
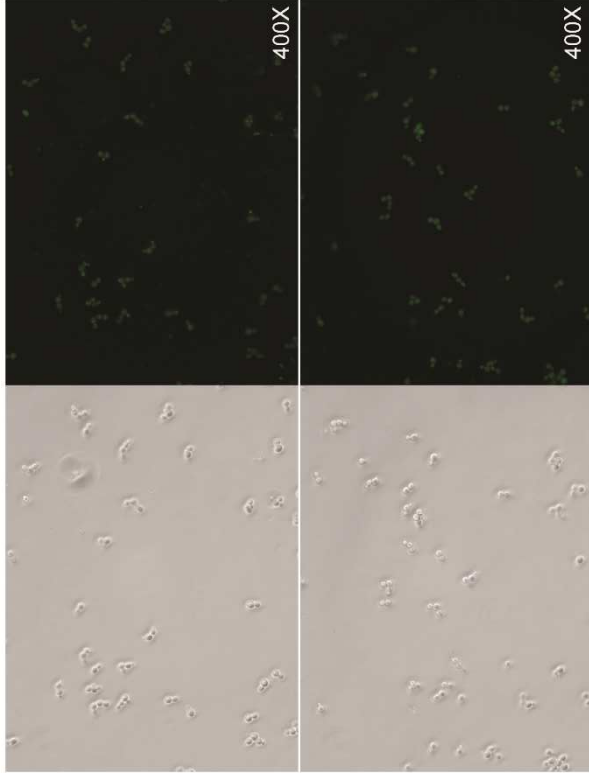
EGFP-Rer1, *cdc13-1*, 0 min, 23°C



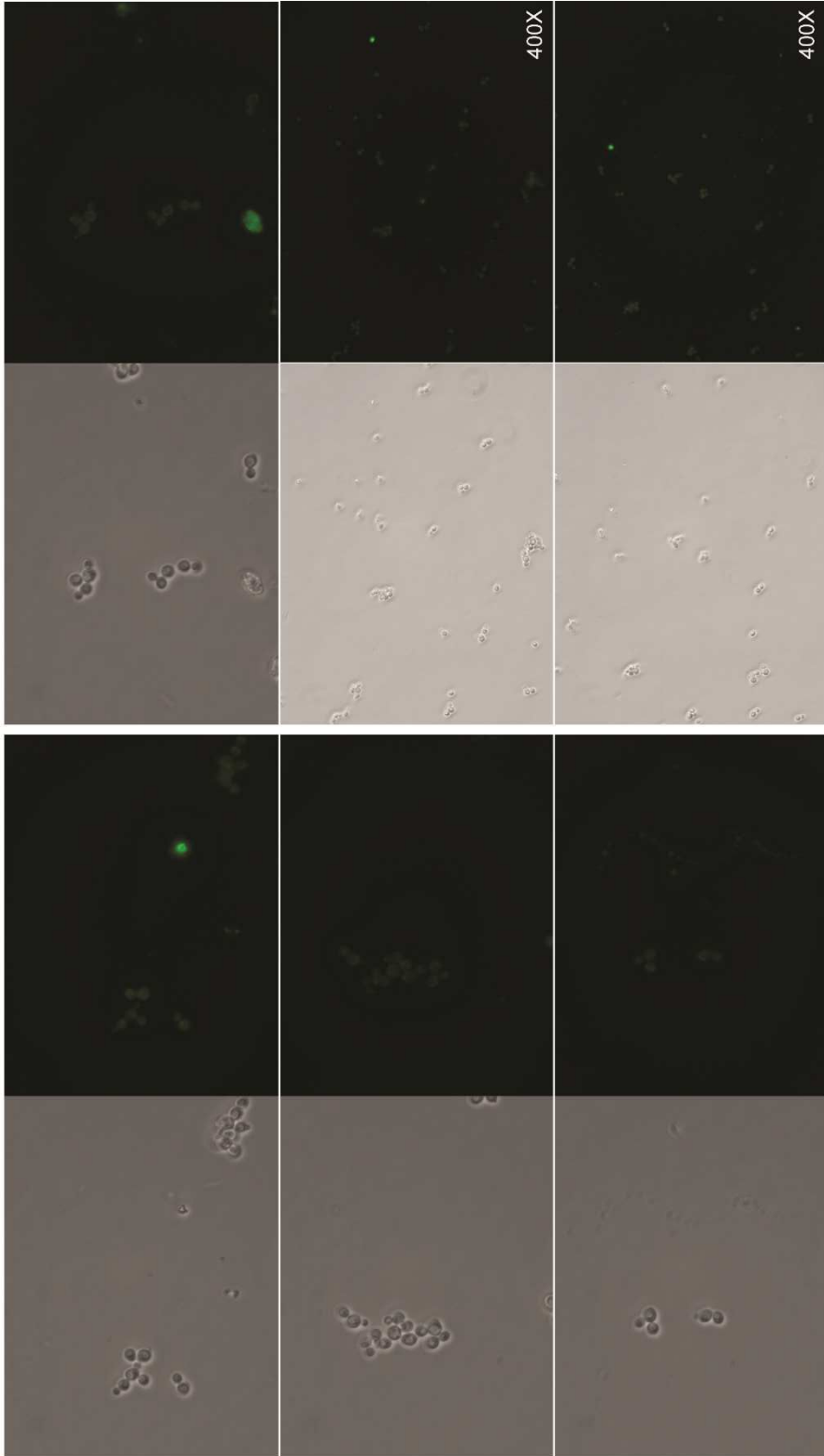
EGFP-Rer1, *cdc13-1*, 180 min, 36°C

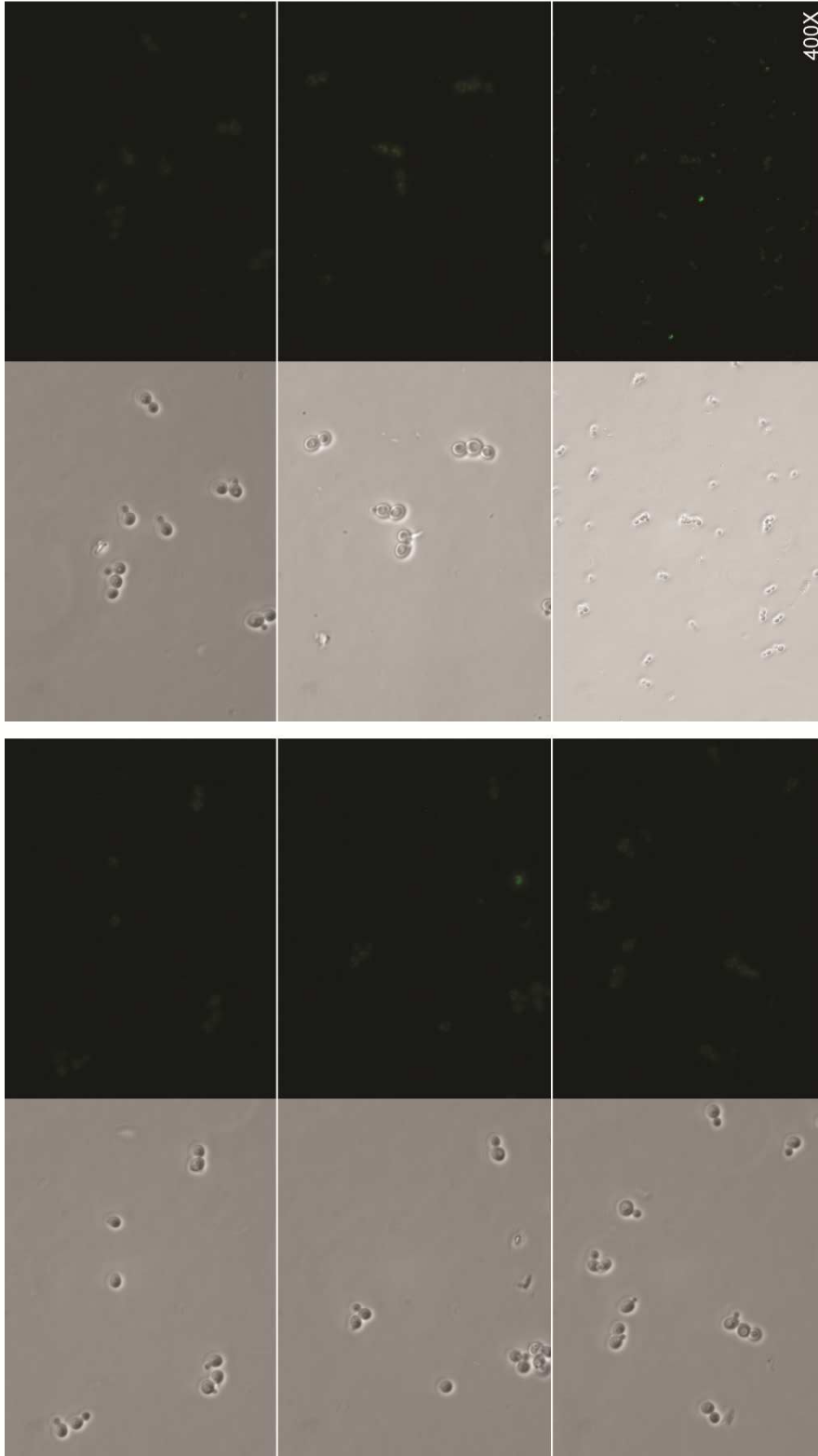


EGFP-Rer1, WT, water, 180 min, 36°C

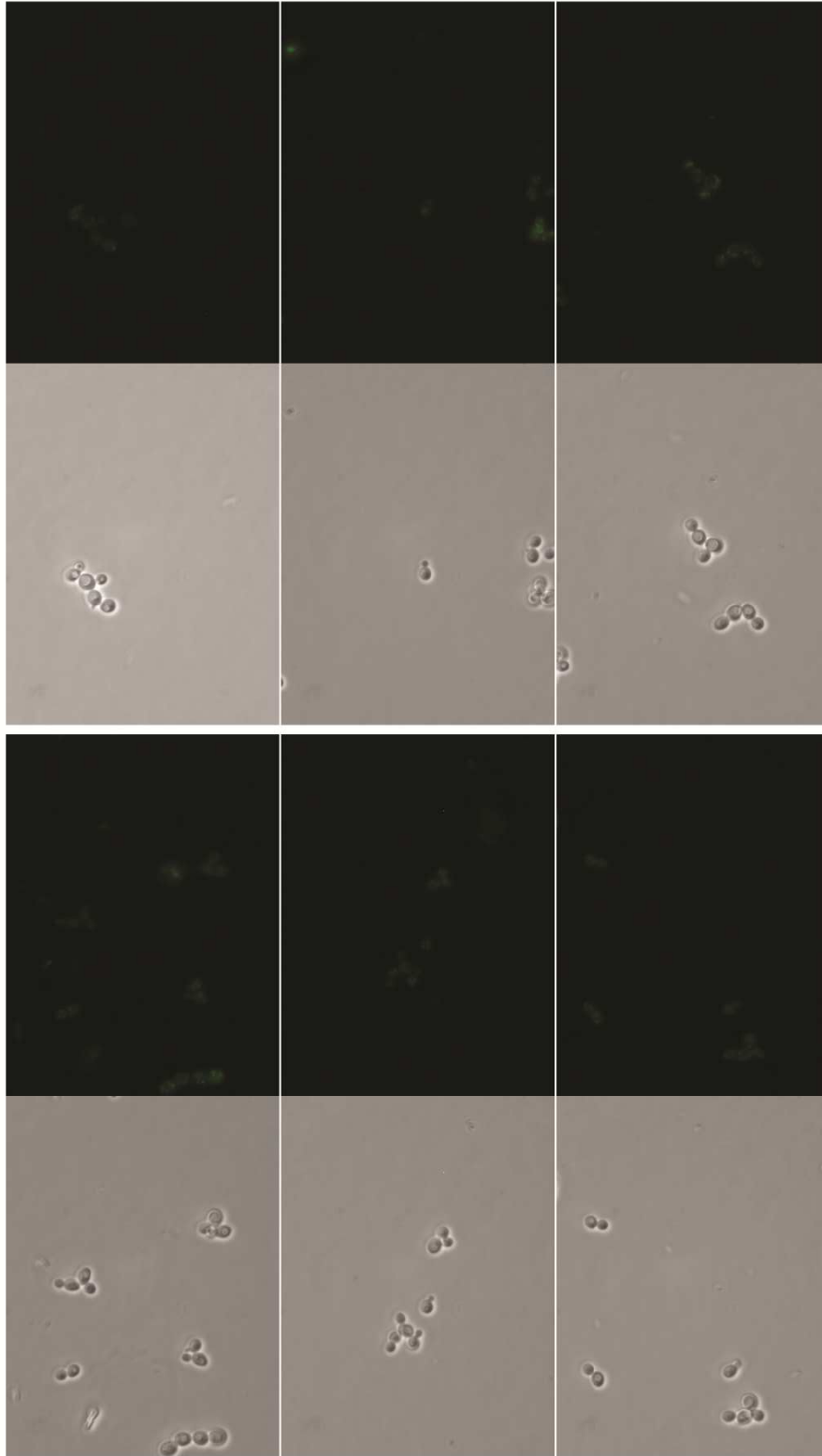


EGFP-Rer1, WT, HU, 180 min, 36°C

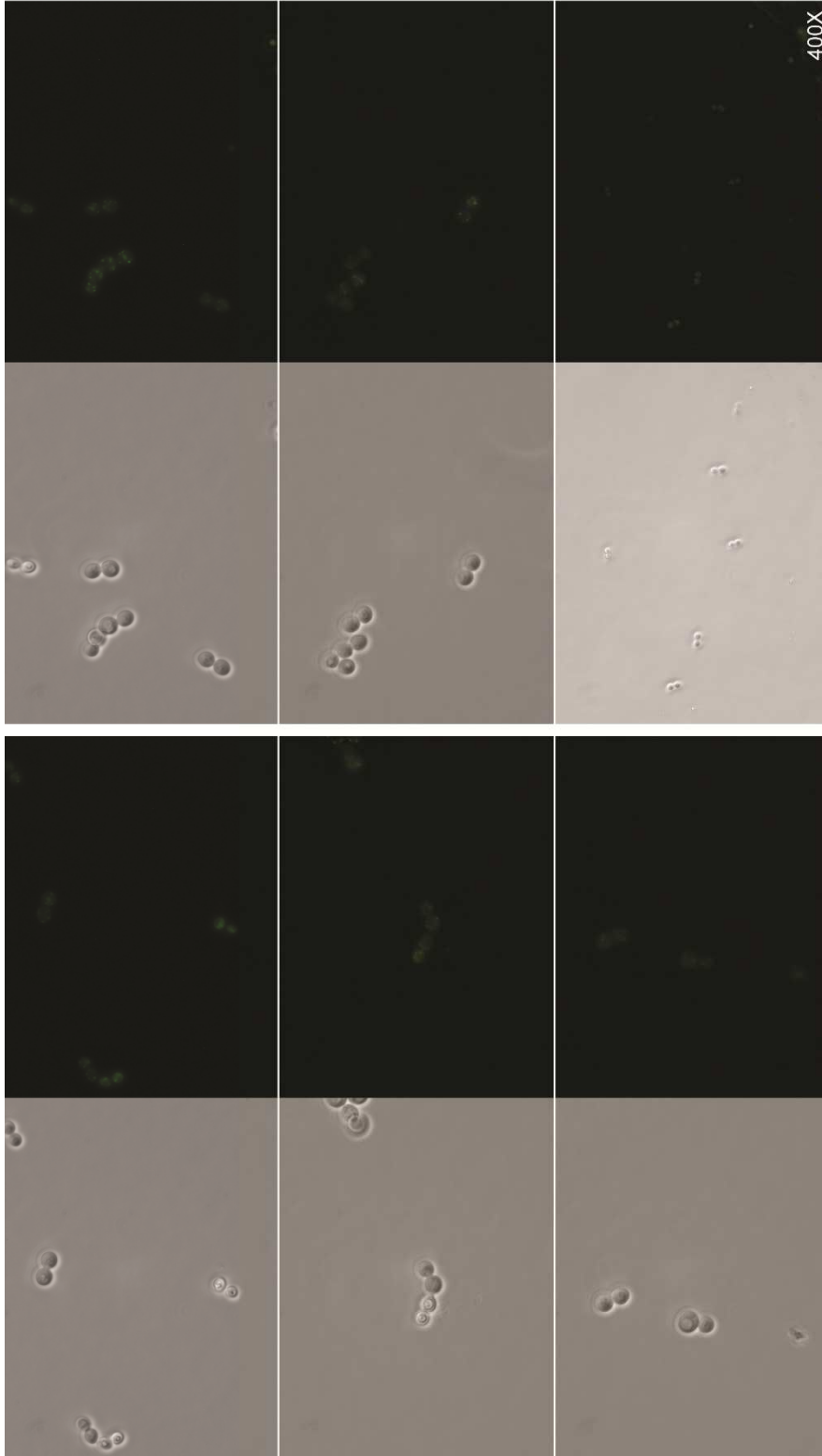




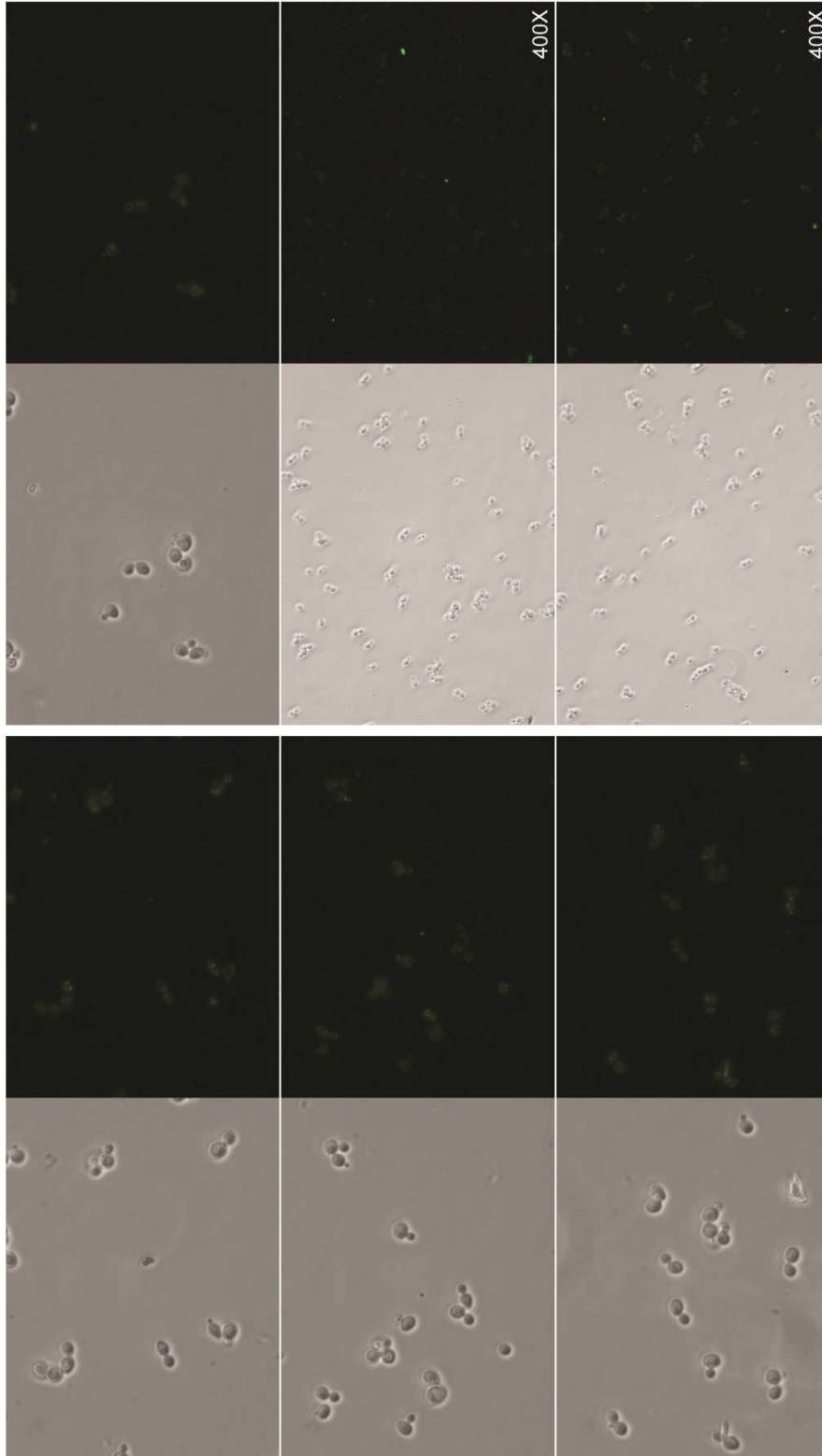
Sec7-EGFP, WT, 0 min, 23°C



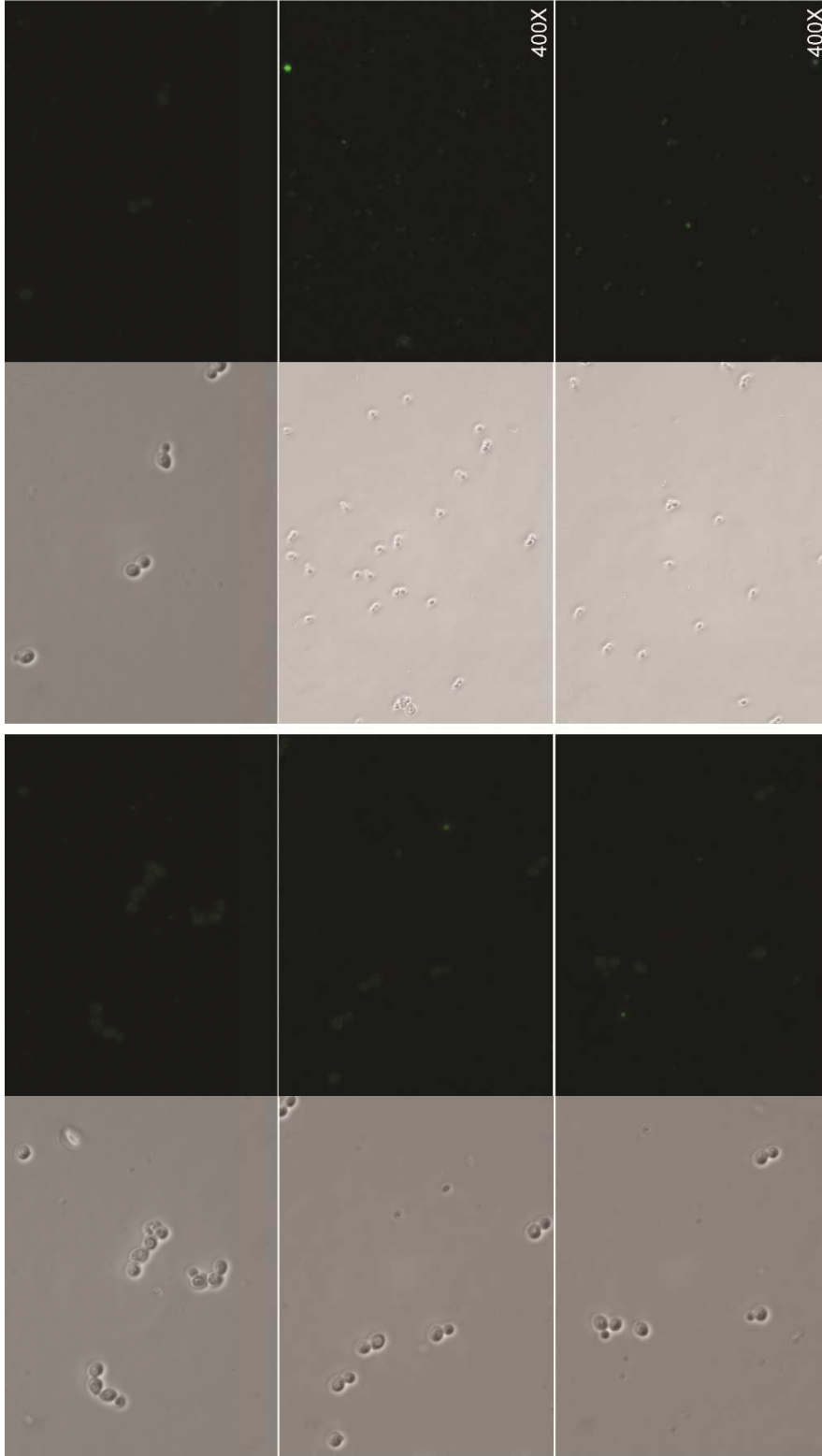
Sec7-EGFP; *cdc13-1*, 0 min, 23°C



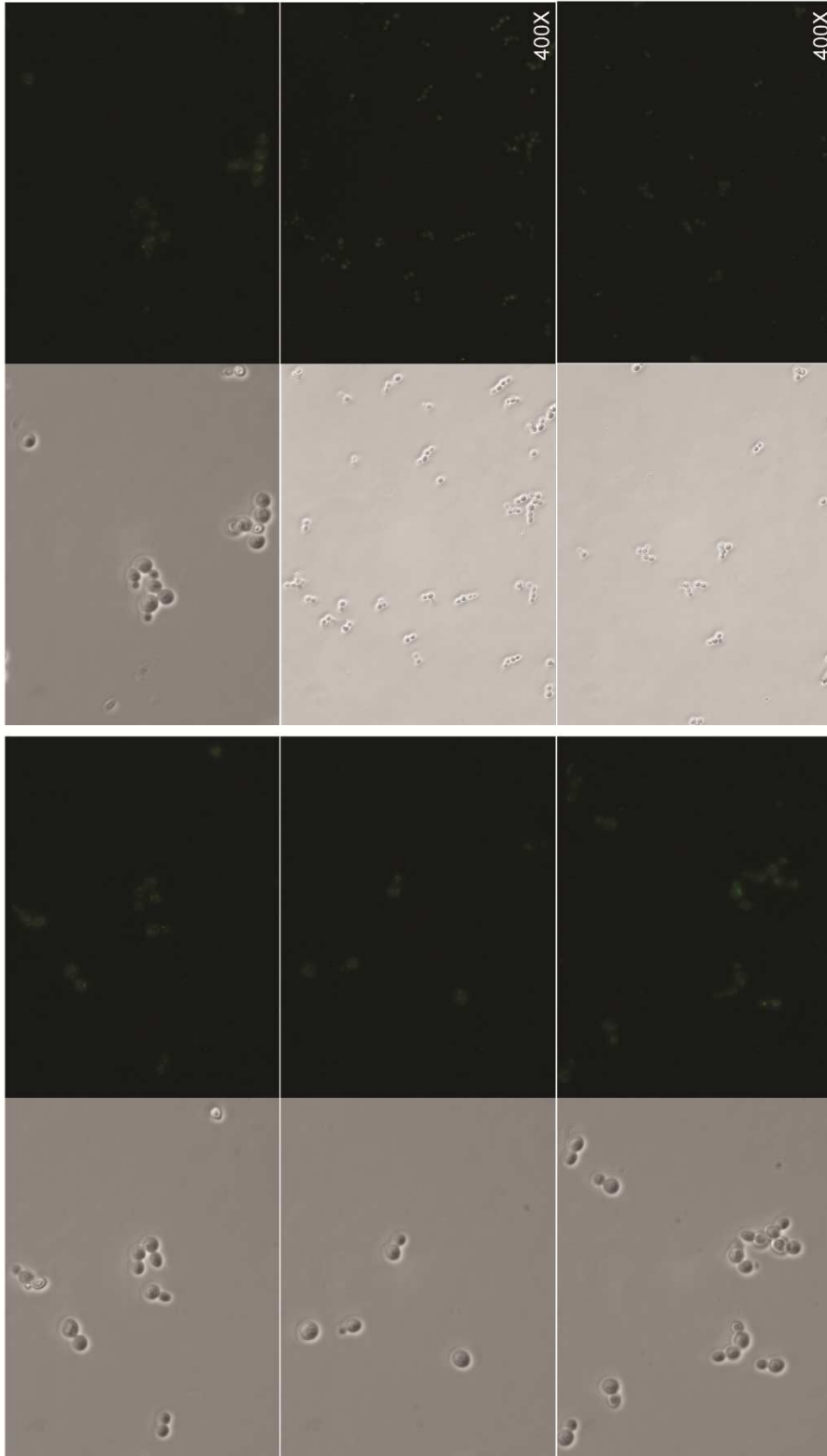
Sec7-EGFP, *cdc13-1*, 180 min, 36°C



Sec7-EGFP, WT, water 180 min, 36°C



Sec7-EGFP, WT, MMS 180 min, 36°C



Sec7-EGFP, WT, HU 180 min, 36°C

References

- Custom Primers - OligoPerfect™ Designer.
- Adams A, Gottschling DE, Kaiser CA, Stearns T. 1997. *Methods in Yeast Genetics*. Cold Spring Harbor Laboratory Press, New York.
- Addinall SG, Downey M, Yu M, Zubko MK, Dewar J, Leake A, Hallinan J, Shaw O, James K, Wilkinson DJ et al. 2008. A genomewide suppressor and enhancer analysis of *cdc13-1* reveals varied cellular processes influencing telomere capping in *Saccharomyces cerevisiae*. *Genetics* **180**: 2251-2266.
- Addinall SG, Holstein EM, Lawless C, Yu M, Chapman K, Banks AP, Ngo HP, Maringele L, Taschuk M, Young A et al. 2011. Quantitative Fitness Analysis Shows That NMD Proteins and Many Other Protein Complexes Suppress or Enhance Distinct Telomere Cap Defects. *PLOS Genetics* **7**: e1001362.
- Agarwal R, Tang Z, Yu H, Cohen-Fix O. 2003. Two distinct pathways for inhibiting *pds1* ubiquitination in response to DNA damage. *The Journal of Biological Chemistry* **278**: 45027-45033.
- Ahn S, Joyner AL. 2005. In vivo analysis of quiescent adult neural stem cells responding to Sonic hedgehog. *Nature* **437**: 894-897.
- Allison LA. 2009. *Fundamental Molecular Biology*. Wiley.
- Amin NS, Nguyen MN, Oh S, Kolodner RD. 2001. *exo1*-Dependent mutator mutations: model system for studying functional interactions in mismatch repair. *Molecular and Cellular Biology* **21**: 5142-5155.
- An O, Dall'Olio GM, Mourikis TP, Ciccarelli FD. 2016. NCG 5.0: updates of a manually curated repository of cancer genes and associated properties from cancer mutational screenings. *Nucleic Acids Research* **44**: D992-999.
- Anderson JS, Parker RP. 1998. The 3' to 5' degradation of yeast mRNAs is a general mechanism for mRNA turnover that requires the SKI2 DEVH box protein and 3' to 5' exonucleases of the exosome complex. *The EMBO Journal* **17**: 1497-1506.
- Araki Y, Takahashi S, Kobayashi T, Kajihio H, Hoshino S, Katada T. 2001. Ski7p G protein interacts with the exosome and the Ski complex for 3'-to-5' mRNA decay in yeast. *The EMBO Journal* **20**: 4684-4693.
- Arnoult N, Van Beneden A, Decottignies A. 2012. Telomere length regulates TERRA levels through increased trimethylation of telomeric H3K9 and HP1alpha. *Nature Structural & Molecular Biology* **19**: 948-956.
- Aronson BD, Silveira LA. 2009. From genes to proteins to behavior: a laboratory project that enhances student understanding in cell and molecular biology. *CBE-Life Sciences Education* **8**: 291-308.
- Arora C, Kee K, Maleki S, Keeney S. 2004. Antiviral protein Ski8 is a direct partner of Spo11 in meiotic DNA break formation, independent of its cytoplasmic role in RNA metabolism. *Molecular Cell* **13**: 549-559.
- Arora R, Lee Y, Wischniewski H, Brun CM, Schwarz T, Azzalin CM. 2014. RNaseH1 regulates TERRA-telomeric DNA hybrids and telomere maintenance in ALT tumour cells. *Nature Communications* **5**: 5220.
- Arudchandran A, Cerritelli S, Narimatsu S, Itaya M, Shin DY, Shimada Y, Crouch RJ. 2000. The absence of ribonuclease H1 or H2 alters the sensitivity of *Saccharomyces cerevisiae* to hydroxyurea, caffeine and ethyl methanesulphonate: implications for roles of RNases H in DNA replication and repair. *Genes to Cells : Devoted to Molecular & Cellular Mechanisms* **5**: 789-802.

- Asai DJ, Koonce MP. 2001. The dynein heavy chain: structure, mechanics and evolution. *Trends in Cell Biology* **11**: 196-202.
- Askree SH, Yehuda T, Smolikov S, Gurevich R, Hawk J, Coker C, Krauskopf A, Kupiec M, McEachern MJ. 2004. A genome-wide screen for *Saccharomyces cerevisiae* deletion mutants that affect telomere length. *Proceedings of the National Academy of Sciences of the United States of America* **101**: 8658-8663.
- Azvolinsky A, Giresi PG, Lieb JD, Zakian VA. 2009. Highly transcribed RNA polymerase II genes are impediments to replication fork progression in *Saccharomyces cerevisiae*. *Molecular Cell* **34**: 722-734.
- Azzalin CM, Lingner J. 2015. Telomere functions grounding on TERRA firma. *Trends in Cell Biology* **25**: 29-36.
- Azzalin CM, Reichenbach P, Khoriant L, Giulotto E, Lingner J. 2007. Telomeric repeat containing RNA and RNA surveillance factors at mammalian chromosome ends. *Science* **318**: 798-801.
- Balestrini A, Ristic D, Dionne I, Liu XZ, Wyman C, Wellinger RJ, Petrini JH. 2013. The Ku heterodimer and the metabolism of single-ended DNA double-strand breaks. *Cell Reports* **3**: 2033-2045.
- Balk B, Dees M, Bender K, Luke B. 2014. The differential processing of telomeres in response to increased telomeric transcription and RNA-DNA hybrid accumulation. *RNA Biology* **11**: 95-100.
- Balk B, Maicher A, Dees M, Klermund J, Luke-Glaser S, Bender K, Luke B. 2013. Telomeric RNA-DNA hybrids affect telomere-length dynamics and senescence. *Nature Structural & Molecular Biology* **20**: 1199-1205.
- Balogun FO, Truman AW, Kron SJ. 2013. DNA resection proteins Sgs1 and Exo1 are required for G1 checkpoint activation in budding yeast. *DNA Repair* **12**: 751-760.
- Balordi F, Fishell G. 2007. Hedgehog signaling in the subventricular zone is required for both the maintenance of stem cells and the migration of newborn neurons. *The Journal of Neuroscience : The Official Journal of the Society for Neuroscience* **27**: 5936-5947.
- Barr FA, Egerer J. 2005. Golgi positioning: are we looking at the right MAP? *The Journal of Cell Biology* **168**: 993-998.
- Bartke N, Hannun YA. 2009. Bioactive sphingolipids: metabolism and function. *Journal of Lipid Research* **50 Suppl**: S91-96.
- Bashkirov VI, King JS, Bashkirova EV, Schmuckli-Maurer J, Heyer WD. 2000. DNA Repair protein Rad55 is a terminal substrate of the DNA damage checkpoints. *Molecular and Cellular Biology* **20**: 4393-4404.
- Beaudenon SL, Huacani MR, Wang G, McDonnell DP, Huibregtse JM. 1999. Rsp5 ubiquitin-protein ligase mediates DNA damage-induced degradation of the large subunit of RNA polymerase II in *Saccharomyces cerevisiae*. *Molecular and Cellular Biology* **19**: 6972-6979.
- Bekaert S, De Meyer T, Van Oostveldt P. 2005. Telomere attrition as ageing biomarker. *Anticancer Research* **25**: 3011-3021.
- Ben-Shitrit T, Yosef N, Shemesh K, Sharan R, Ruppin E, Kupiec M. 2012. Systematic identification of gene annotation errors in the widely used yeast mutation collections. *Nature Methods* **9**: 373-378.
- Berdasco M, Esteller M. 2010. Aberrant Epigenetic Landscape in Cancer: How Cellular Identity Goes Awry. *Developmental Cell* **19**: 698-711.
- Bertuch AA, Lundblad V. 2003. Which end: dissecting Ku's function at telomeres and double-strand breaks. *Genes & Development* **17**: 2347-2350.

- . 2004. EXO1 contributes to telomere maintenance in both telomerase-proficient and telomerase-deficient *Saccharomyces cerevisiae*. *Genetics* **166**: 1651-1659.
- Betz JL, Chang M, Washburn TM, Porter SE, Mueller CL, Jaehning JA. 2002. Phenotypic analysis of Paf1/RNA polymerase II complex mutations reveals connections to cell cycle regulation, protein synthesis, and lipid and nucleic acid metabolism. *Molecular Genetics and Genomics : MGG* **268**: 272-285.
- Birrell GW, Giaever G, Chu AM, Davis RW, Brown JM. 2001. A genome-wide screen in *Saccharomyces cerevisiae* for genes affecting UV radiation sensitivity. *Proceedings of the National Academy of Sciences of the United States of America* **98**: 12608-12613.
- Blankley RT, Lydall D. 2004. A domain of Rad9 specifically required for activation of Chk1 in budding yeast. *Journal of Cell Science* **117**: 601-608.
- Bonangelino CJ, Chavez EM, Bonifacino JS. 2002. Genomic screen for vacuolar protein sorting genes in *Saccharomyces cerevisiae*. *Molecular Biology of the Cell* **13**: 2486-2501.
- Bonetti D, Martina M, Clerici M, Lucchini G, Longhese MP. 2009. Multiple pathways regulate 3' overhang generation at *S. cerevisiae* telomeres. *Molecular Cell* **35**: 70-81.
- Booher RN, Deshaies RJ, Kirschner MW. 1993. Properties of *Saccharomyces cerevisiae* wee1 and its differential regulation of p34CDC28 in response to G1 and G2 cyclins. *The EMBO Journal* **12**: 3417-3426.
- Booth C, Griffith E, Brady G, Lydall D. 2001. Quantitative amplification of singlestranded DNA (QAOS) demonstrates that cdc13-1 mutants generate ssDNA in a telomere to centromere direction. *Nucleic Acids Research* **29**: 4414-4422.
- Botstein D, Chervitz SA, Cherry JM. 1997. Genetics - Yeast as a model organism. *Science* **277**: 1259-1260.
- Bowers K, Stevens TH. 2005. Protein transport from the late Golgi to the vacuole in the yeast *Saccharomyces cerevisiae*. *Biochimica et Biophysica Acta* **1744**: 438-454.
- Braun KA, Lao Y, He Z, Ingles CJ, Wold MS. 1997. Role of protein-protein interactions in the function of replication protein A (RPA): RPA modulates the activity of DNA polymerase alpha by multiple mechanisms. *Biochemistry* **36**: 8443-8454.
- Briscoe J, Therond PP. 2013. The mechanisms of Hedgehog signalling and its roles in development and disease. *Nature Reviews Molecular Cell Biology* **14**: 416-429.
- Broccoli D, Smogorzewska A, Chong L, deLange T. 1997. Human telomeres contain two distinct Myb-related proteins, TRF1 and TRF2. *Nature Genetics* **17**: 231-235.
- Brown JT, Bai X, Johnson AW. 2000. The yeast antiviral proteins Ski2p, Ski3p, and Ski8p exist as a complex in vivo. *RNA* **6**: 449-457.
- Brush GS, Morrow DM, Hieter P, Kelly TJ. 1996. The ATM homologue MEC1 is required for phosphorylation of replication protein A in yeast. *Proceedings of the National Academy of Sciences of the United States of America* **93**: 15075-15080.
- Bryan TM, Englezou A, Dalla-Pozza L, Dunham MA, Reddel RR. 1997. Evidence for an alternative mechanism for maintaining telomere length in human tumors and tumor-derived cell lines. *Nature Medicine* **3**: 1271-1274.
- Bryan TM, Englezou A, Gupta J, Bacchetti S, Reddel RR. 1995. Telomere elongation in immortal human cells without detectable telomerase activity. *The EMBO Journal* **14**: 4240-4248.

- Bryan TM, Reddel RR. 1997. Telomere dynamics and telomerase activity in in vitro immortalised human cells. *European Journal of Cancer* **33**: 767-773.
- Buschman MD, Rahajeng J, Field SJ. 2015. GOLPH3 links the Golgi, DNA damage, and cancer. *Cancer Research* **75**: 624-627.
- Cannavo E, Cejka P. 2014. Sae2 promotes dsDNA endonuclease activity within Mre11-Rad50-Xrs2 to resect DNA breaks. *Nature* **514**: 122-125.
- Carpenter AE, Sabatini DM. 2004. Systematic genome-wide screens of gene function. *Nature Reviews Genetics* **5**: 11-22.
- Carpten JD, Robbins CM, Villablanca A, Forsberg L, Presciuttini S, Bailey-Wilson J, Simonds WF, Gillanders EM, Kennedy AM, Chen JD et al. 2002. HRPT2, encoding parafibromin, is mutated in hyperparathyroidism-jaw tumor syndrome. *Nature Genetics* **32**: 676-680.
- Cerritelli SM, Crouch RJ. 2009. Ribonuclease H: the enzymes in eukaryotes. *The FEBS Journal* **276**: 1494-1505.
- Chan A, Boule JB, Zakian VA. 2008. Two pathways recruit telomerase to *Saccharomyces cerevisiae* telomeres. *PLOS Genetics* **4**: e1000236.
- Chan CS, Tye BK. 1983. A family of *Saccharomyces cerevisiae* repetitive autonomously replicating sequences that have very similar genomic environments. *Journal of Molecular Biology* **168**: 505-523.
- Chandra A, Hughes TR, Nugent CI, Lundblad V. 2001. Cdc13 both positively and negatively regulates telomere replication. *Genes & Development* **15**: 404-414.
- Chang M, French-Cornay D, Fan HY, Klein H, Denis CL, Jaehning JA. 1999. A complex containing RNA polymerase II, Paf1p, Cdc73p, Hpr1p, and Ccr4p plays a role in protein kinase C signaling. *Molecular and Cellular Biology* **19**: 1056-1067.
- Chapman JR, Taylor MR, Boulton SJ. 2012. Playing the end game: DNA double-strand break repair pathway choice. *Molecular Cell* **47**: 497-510.
- Chen FX, Woodfin AR, Gardini A, Rickels RA, Marshall SA, Smith ER, Shiekhattar R, Shilatifard A. 2015. PAF1, a Molecular Regulator of Promoter-Proximal Pausing by RNA Polymerase II. *Cell* **162**: 1003-1015.
- Chen QJ, Ijima A, Greider CW. 2001. Two survivor pathways that allow growth in the absence of telomerase are generated by distinct telomere recombination events. *Molecular and Cellular Biology* **21**: 1819-1827.
- Chen X, Ruggiero C, Li S. 2007. Yeast Rpb9 plays an important role in ubiquitylation and degradation of Rpb1 in response to UV-induced DNA damage. *Molecular and Cellular Biology* **27**: 4617-4625.
- Chen YX, Yamaguchi Y, Tsugeno Y, Yamamoto J, Yamada T, Nakamura M, Hisatake K, Handa H. 2009. DSIF, the Paf1 complex, and Tat-SF1 have nonredundant, cooperative roles in RNA polymerase II elongation. *Genes & Development* **23**: 2765-2777.
- Cherry JM, Hong EL, Amundsen C, Balakrishnan R, Binkley G, Chan ET, Christie KR, Costanzo MC, Dwight SS, Engel SR et al. 2012. *Saccharomyces* Genome Database: the genomics resource of budding yeast. *Nucleic Acids Research* **40**: D700-705.
- Chu X, Qin X, Xu H, Li L, Wang Z, Li F, Xie X, Zhou H, Shen Y, Long J. 2013. Structural insights into Paf1 complex assembly and histone binding. *Nucleic Acids Research* **41**: 10619-10629.
- Churikov D, Corda Y, Luciano P, Geli V. 2013. Cdc13 at a crossroads of telomerase action. *Frontiers in Oncology* **3**: 39.
- Clerici M, Mantiero D, Lucchini G, Longhese MP. 2006. The *Saccharomyces cerevisiae* Sae2 protein negatively regulates DNA damage checkpoint signalling. *EMBO Reports* **7**: 212-218.

- Cockell M, Palladino F, Laroche T, Kyrion G, Liu C, Lustig AJ, Gasser SM. 1995. The carboxy termini of Sir4 and Rap1 affect Sir3 localization: evidence for a multicomponent complex required for yeast telomeric silencing. *The Journal of Cell Biology* **129**: 909-924.
- Cohen-Fix O, Koshland D. 1997. The anaphase inhibitor of *Saccharomyces cerevisiae* Pds1p is a target of the DNA damage checkpoint pathway. *Proceedings of the National Academy of Sciences of the United States of America* **94**: 14361-14366.
- Cole GM, Schild D, Lovett ST, Mortimer RK. 1987. Regulation of RAD54- and RAD52-lacZ gene fusions in *Saccharomyces cerevisiae* in response to DNA damage. *Molecular and Cellular Biology* **7**: 1078-1084.
- Cole GM, Schild D, Mortimer RK. 1989. Two DNA Repair and recombination genes in *Saccharomyces cerevisiae*, RAD52 and RAD54, are induced during meiosis. *Molecular and Cellular Biology* **9**: 3101-3104.
- Collins SR, Miller KM, Maas NL, Roguev A, Fillingham J, Chu CS, Schuldiner M, Gebbia M, Recht J, Shales M et al. 2007. Functional dissection of protein complexes involved in yeast chromosome biology using a genetic interaction map. *Nature* **446**: 806-810.
- Craven RJ, Petes TD. 2000. Involvement of the checkpoint protein Mec1p in silencing of gene expression at telomeres in *Saccharomyces cerevisiae*. *Molecular and Cellular Biology* **20**: 2378-2384.
- Cristofari G, Sikora K, Lingner J. 2007. Telomerase unplugged. *Acs Chem Biol* **2**: 155-158.
- Crisucci EM, Arndt KM. 2011. The Roles of the Paf1 Complex and Associated Histone Modifications in Regulating Gene Expression. *Genetics Research International* **2011**: 707641.
- Cusanelli E, Romero CA, Chartrand P. 2013. Telomeric noncoding RNA TERRA is induced by telomere shortening to nucleate telomerase molecules at short telomeres. *Molecular Cell* **51**: 780-791.
- D'Aquino KE, Monje-Casas F, Paulson J, Reiser V, Charles GM, Lai L, Shokat KM, Amon A. 2005. The protein kinase Kin4 inhibits exit from mitosis in response to spindle position defects. *Molecular Cell* **19**: 223-234.
- De Gois S, Slama P, Pietrancosta N, Erdozain AM, Louis F, Bouvrais-Veret C, Daviet L, Giros B. 2015. Ctr9, a protein in the transcription complex Paf1, regulates dopamine transporter activity at the plasma membrane. *The Journal of Biological Chemistry* **290**: 17848-17862.
- de la Torre-Ruiz MA, Green CM, Lowndes NF. 1998. RAD9 and RAD24 define two additive, interacting branches of the DNA damage checkpoint pathway in budding yeast normally required for Rad53 modification and activation. *The EMBO Journal* **17**: 2687-2698.
- de Lange T. 2002. Protection of mammalian telomeres. *Oncogene* **21**: 532-540.
- . 2005. Shelterin: the protein complex that shapes and safeguards human telomeres. *Genes & Development* **19**: 2100-2110.
- Debrauwere H, Loeillet S, Lin W, Lopes J, Nicolas A. 2001. Links between replication and recombination in *Saccharomyces cerevisiae*: a hypersensitive requirement for homologous recombination in the absence of Rad27 activity. *Proceedings of the National Academy of Sciences of the United States of America* **98**: 8263-8269.
- Dewar JM, Lydall D. 2010. Pif1- and Exo1-dependent nucleases coordinate checkpoint activation following telomere uncapping. *The EMBO Journal* **29**: 4020-4034.
- Dickson MA, Hahn WC, Ino Y, Ronfard V, Wu JY, Weinberg RA, Louis DN, Li FP, Rheinwald JG. 2000. Human keratinocytes that express hTERT and also

- bypass a p16(INK4a)-enforced mechanism that limits life span become immortal yet retain normal growth and differentiation characteristics. *Molecular and Cellular Biology* **20**: 1436-1447.
- Dickson RC, Lester RL. 1999. Yeast sphingolipids. *Biochimica et Biophysica Acta* **1426**: 347-357.
- Dilley RL, Greenberg RA. 2015. ALternative Telomere Maintenance and Cancer. *Trends in Cancer* **1**: 145-156.
- Dippold HC, Ng MM, Farber-Katz SE, Lee SK, Kerr ML, Peterman MC, Sim R, Wiharto PA, Galbraith KA, Madhavarapu S et al. 2009. GOLPH3 bridges phosphatidylinositol-4-phosphate and actomyosin to stretch and shape the Golgi to promote budding. *Cell* **139**: 337-351.
- Donate LE, Blasco MA. 2011. Telomeres in cancer and ageing. *Philosophical transactions of the Royal Society of London. Series B, Biological sciences* **366**: 76-84.
- Dudley AM, Janse DM, Tanay A, Shamir R, Church GM. 2005. A global view of pleiotropy and phenotypically derived gene function in yeast. *Molecular Systems Biology* **1**: 2005 0001.
- Duong MT, Sahin E. 2013. RAP1: Protector of Telomeres, Defender against Obesity. *Cell Reports* **3**: 1757-1758.
- Emili A. 1998. MEC1-dependent phosphorylation of Rad9p in response to DNA damage. *Molecular Cell* **2**: 183-189.
- Eshel D, Urrestarazu LA, Vissers S, Jauniaux JC, van Vliet-Reedijk JC, Planta RJ, Gibbons IR. 1993. Cytoplasmic dynein is required for normal nuclear segregation in yeast. *Proceedings of the National Academy of Sciences of the United States of America* **90**: 11172-11176.
- Esteller M. 2007. Cancer epigenomics: DNA methylomes and histone-modification maps. *Nature Reviews Genetics* **8**: 286-298.
- Fabre A, Martinez-Vinson C, Goulet O, Badens C. 2013. Syndromic diarrhea/Trichohepatoenteric syndrome. *Orphanet Journal of Rare Diseases* **8**: 5.
- Farber-Katz SE, Dippold HC, Buschman MD, Peterman MC, Xing M, Noakes CJ, Tat J, Ng MM, Rahajeng J, Cowan DM et al. 2014. DNA damage triggers Golgi dispersal via DNA-PK and GOLPH3. *Cell* **156**: 413-427.
- Feldmann H, Winnacker EL. 1993. A putative homologue of the human autoantigen Ku from *Saccharomyces cerevisiae*. *The Journal of Biological Chemistry* **268**: 12895-12900.
- Fell GL, Munson AM, Croston MA, Rosenwald AG. 2011. Identification of yeast genes involved in k homeostasis: loss of membrane traffic genes affects k uptake. *G3* **1**: 43-56.
- Ferreira PC, Ness F, Edwards SR, Cox BS, Tuite MF. 2001. The elimination of the yeast [PSI⁺] prion by guanidine hydrochloride is the result of Hsp104 inactivation. *Molecular Microbiology* **40**: 1357-1369.
- Fourel G, Revardel E, Koering CE, Gilson E. 1999. Cohabitation of insulators and silencing elements in yeast subtelomeric regions. *The EMBO Journal* **18**: 2522- 2537.
- Frank CJ, Hyde M, Greider CW. 2006. Regulation of telomere elongation by the cyclin-dependent kinase CDK1. *Molecular Cell* **24**: 423-432.
- Frederick RL, Shaw JM. 2007. Moving mitochondria: establishing distribution of an essential organelle. *Traffic* **8**: 1668-1675.
- Friedel AM, Pike BL, Gasser SM. 2009. ATR/Mec1: coordinating fork stability and repair. *Current Opinion in Cell Biology* **21**: 237-244.
- Gallardo F, Chartrand P. 2008. Telomerase biogenesis. *RNA Biology* **5**: 212-215.

- Gallardo F, Laterreur N, Cusanelli E, Ouenzar F, Querido E, Wellinger RJ, Chartrand P. 2011. Live Cell Imaging of Telomerase RNA Dynamics Reveals Cell Cycle-Dependent Clustering of Telomerase at Elongating Telomeres. *Molecular Cell* **44**: 819-827.
- Gan W, Guan Z, Liu J, Gui T, Shen K, Manley JL, Li X. 2011. R-loop-mediated genomic instability is caused by impairment of replication fork progression. *Genes & Development* **25**: 2041-2056.
- Gao H, Cervantes RB, Mandell EK, Otero JH, Lundblad V. 2007. RPA-like proteins mediate yeast telomere function. *Nature Structural & Molecular Biology* **14**: 208-214.
- Garcia V, Phelps SE, Gray S, Neale MJ. 2011. Bidirectional resection of DNA doublestrand breaks by Mre11 and Exo1. *Nature* **479**: 241-244.
- Garneau NL, Wilusz J, Wilusz CJ. 2007. The highways and byways of mRNA decay. *Nature Reviews Molecular Cell Biology* **8**: 113-126.
- Garvik B, Carson M, Hartwell L. 1995. Single-stranded DNA arising at telomeres in *cdc13* mutants may constitute a specific signal for the RAD9 checkpoint. *Molecular and Cellular Biology* **15**: 6128-6138.
- Gasparyan HJ, Xu L, Petreaca RC, Rex AE, Small VY, Bhogal NS, Julius JA, Warsi TH, Bachant J, Aparicio OM et al. 2009. Yeast telomere capping protein Stn1 overrides DNA replication control through the S phase checkpoint. *Proceedings of the National Academy of Sciences of the United States of America* **106**: 2206-2211.
- Gaytan BD, Loguinov AV, Penate X, Lerot JM, Chavez S, Denslow ND, Vulpe CD. 2013. A genome-wide screen identifies yeast genes required for tolerance to technical toxaphene, an organochlorinated pesticide mixture. *PLOS One* **8**: e81253.
- Giannattasio M, Sommariva E, Vercillo R, Lippi-Boncambi F, Liberi G, Foiani M, Plevani P, Muzi-Falconi M. 2002. A dominant-negative MEC3 mutant uncovers new functions for the Rad17 complex and Tel1. *Proceedings of the National Academy of Sciences of the United States of America* **99**: 12997-13002.
- Giraud-Panis MJ, Teixeira MT, Geli V, Gilson E. 2010. CST meets shelterin to keep telomeres in check. *Molecular Cell* **39**: 665-676.
- Glick BS. 2002. Can the Golgi form de novo? *Nature Reviews Molecular Cell Biology* **3**: 615-619.
- Goffeau A, Barrell BG, Bussey H, Davis RW, Dujon B, Feldmann H, Galibert F, Hoheisel JD, Jacq C, Johnston M et al. 1996. Life with 6000 genes. *Science* **274**: 563-567.
- Goldstein AL, McCusker JH. 1999. Three new dominant drug resistance cassettes for gene disruption in *Saccharomyces cerevisiae*. *Yeast* **15**: 1541-1553.
- Gomez EB, Espinosa JM, Forsburg SL. 2005. *Schizosaccharomyces pombe* *mst2+* encodes a MYST family histone acetyltransferase that negatively regulates telomere silencing. *Molecular and Cellular Biology* **25**: 8887-8903.
- Gonzalez-Perez A, Perez-Llamas C, Deu-Pons J, Tamborero D, Schroeder MP, Jene-Sanz A, Santos A, Lopez-Bigas N. 2013. IntOGen-mutations identifies cancer drivers across tumor types. *Nature Methods* **10**: 1081-1082.
- Gothwal SK, Patel NJ, Colletti MM, Sasanuma H, Shinohara M, Hochwagen A, Shinohara A. 2015. The Double-Strand Break Landscape of Meiotic Chromosomes Is Shaped by the Paf1 Transcription Elongation Complex in *Saccharomyces cerevisiae*. *Genetics* **202**: 497-512.
- Gottschling DE, Aparicio OM, Billington BL, Zakian VA. 1990. Position Effect at *Saccharomyces-Cerevisiae* Telomeres - Reversible Repression of Pol- α Transcription. *Cell* **63**: 751-762.

- Grach AA. 2011. Alternative telomere-lengthening mechanisms. *Cytology and Genetics* **45**: 121-130.
- Grandin N, Damon C, Charbonneau M. 2000. Cdc13 cooperates with the yeast Ku proteins and Stn1 to regulate telomerase recruitment. *Molecular and Cellular Biology* **20**: 8397-8408.
- Gravel S, Chapman JR, Magill C, Jackson SP. 2008. DNA helicases Sgs1 and BLM promote DNA double-strand break resection. *Genes & Development* **22**: 2767-2772.
- Griffith JD, Comeau L, Rosenfield S, Stansel RM, Bianchi A, Moss H, de Lange T. 1999. Mammalian telomeres end in a large duplex loop. *Cell* **97**: 503-514.
- Hadjiiladis N, Sletten E. 2009. *Metal Complex - DNA Interactions*. Wiley.
- Hanahan D, Weinberg RA. 2011. Hallmarks of Cancer: The Next Generation. *Cell* **144**: 646-674.
- Hang LE, Liu X, Cheung I, Yang Y, Zhao X. 2011. SUMOylation regulates telomere length homeostasis by targeting Cdc13. *Nature Structural & Molecular Biology* **18**: 920-926.
- Harley CB, Futcher AB, Greider CW. 1990. Telomeres shorten during ageing of human fibroblasts. *Nature* **345**: 458-460.
- Harrison JC, Haber JE. 2006. Surviving the breakup: the DNA damage checkpoint. *Annual Review of Genetics* **40**: 209-235.
- Haruki H, Nishikawa J, Laemmli UK. 2008. The anchor-away technique: rapid, conditional establishment of yeast mutant phenotypes. *Molecular Cell* **31**: 925-932.
- Hass EP, Zappulla DC. 2015. The Ku subunit of telomerase binds Sir4 to recruit telomerase to lengthen telomeres in *S. cerevisiae*. *eLife* **4**: e07750.
- Hayflick L, Moorhead PS. 1961. The serial cultivation of human diploid cell strains. *Experimental Cell Research* **25**: 585-621.
- Hedges SB. 2002. The origin and evolution of model organisms. *Nature Reviews Genetics* **3**: 838-849.
- Hemann MT, Strong MA, Hao LY, Greider CW. 2001. The shortest telomere, not average telomere length, is critical for cell viability and chromosome stability. *Cell* **107**: 67-77.
- Henry NL, Bushnell DA, Kornberg RD. 1996. A yeast transcriptional stimulatory protein similar to human PC4. *The Journal of Biological Chemistry* **271**: 21842-21847.
- Herrero J, Muffato M, Beal K, Fitzgerald S, Gordon L, Pignatelli M, Vilella AJ, Searle SM, Amode R, Brent S et al. 2016. Ensembl comparative genomics resources. *Database : The Journal of Biological Databases and Curation* **2016**.
- Herskowitz I. 1988. Life cycle of the budding yeast *Saccharomyces cerevisiae*. *Microbiological Reviews* **52**: 536-553.
- . 1989. A regulatory hierarchy for cell specialization in yeast. *Nature* **342**: 749-757.
- Holstein EM, Clark KR, Lydall D. 2014. Interplay between nonsense-mediated mRNA decay and DNA damage response pathways reveals that Stn1 and Ten1 are the key CST telomere-cap components. *Cell Reports* **7**: 1259-1269.
- Holtzman DA, Yang S, Drubin DG. 1993. Synthetic-lethal interactions identify two novel genes, SLA1 and SLA2, that control membrane cytoskeleton assembly in *Saccharomyces cerevisiae*. *The Journal of Cell Biology* **122**: 635-644.
- Hoppe GJ, Tanny JC, Rudner AD, Gerber SA, Danaie S, Gygi SP, Moazed D. 2002. Steps in assembly of silent chromatin in yeast: Sir3-independent binding of a Sir2/Sir4 complex to silencers and role for Sir2-dependent deacetylation. *Molecular and Cellular Biology* **22**: 4167-4180.

- Huangfu D, Anderson KV. 2006. Signaling from Smo to Ci/Gli: conservation and divergence of Hedgehog pathways from *Drosophila* to vertebrates. *Development* **133**: 3-14.
- Huibregtse JM, Yang JC, Beaudenon SL. 1997. The large subunit of RNA polymerase II is a substrate of the Rsp5 ubiquitin-protein ligase. *Proceedings of the National Academy of Sciences of the United States of America* **94**: 3656-3661.
- Hurley PJ, Bunz F. 2007. ATM and ATR: components of an integrated circuit. *Cell Cycle* **6**: 414-417.
- Iglesias N, Redon S, Pfeiffer V, Dees M, Lingner J, Luke B. 2011. Subtelomeric repetitive elements determine TERRA regulation by Rap1/Rif and Rap1/Sir complexes in yeast. *EMBO Reports* **12**: 587-593.
- Ikeda A, Muneoka T, Murakami S, Hirota A, Yabuki Y, Karashima T, Nakazono K, Tsuruno M, Pichler H, Shirahige K et al. 2015. Sphingolipids regulate telomere clustering by affecting the transcription of genes involved in telomere homeostasis. *Journal of Cell Science* **128**: 2454-2467.
- Indiviglio SM, Bertuch AA. 2009. Ku's essential role in keeping telomeres intact. *Proceedings of the National Academy of Sciences of the United States of America* **106**: 12217-12218.
- Ingham PW, Nakano Y, Seger C. 2011. Mechanisms and functions of Hedgehog signalling across the metazoa. *Nature Reviews Genetics* **12**: 393-406.
- Jackson MA, Hu MI, Perrier ND, Waguespack SG. 2015. CDC73-Related Disorders. in *GeneReviews(R)* (eds. RA Pagon, MP Adam, HH Ardinger, SE Wallace, A Amemiya, LJH Bean, TD Bird, CR Dolan, CT Fong, RJH Smith, et al.), Seattle (WA).
- Jager D, Philippsen P. 1989. Many yeast chromosomes lack the telomere-specific Y' sequence. *Molecular and Cellular Biology* **9**: 5754-5757.
- Janke C, Magiera MM, Rathfelder N, Taxis C, Reber S, Maekawa H, Moreno-Borchart A, Doenges G, Schwob E, Schiebel E et al. 2004. A versatile toolbox for PCR-based tagging of yeast genes: new fluorescent proteins, more markers and promoter substitution cassettes. *Yeast* **21**: 947-962.
- Jazayeri A, Falck J, Lukas C, Bartek J, Smith GC, Lukas J, Jackson SP. 2006. ATM and cell cycle-dependent regulation of ATR in response to DNA double-strand breaks. *Nature Cell Biology* **8**: 37-45.
- Jeong HS, Backlund PS, Chen HC, Karavanov AA, Crouch RJ. 2004. RNase H2 of *Saccharomyces cerevisiae* is a complex of three proteins. *Nucleic Acids Research* **32**: 407-414.
- Jia X, Weinert T, Lydall D. 2004. Mec1 and Rad53 inhibit formation of singlestranded DNA at telomeres of *Saccharomyces cerevisiae* cdc13-1 mutants. *Genetics* **166**: 753-764.
- Johnson ES, Ma PC, Ota IM, Varshavsky A. 1995. A proteolytic pathway that recognizes ubiquitin as a degradation signal. *The Journal of Biological Chemistry* **270**: 17442-17456.
- Jones PA, Baylin SB. 2007. The epigenomics of cancer. *Cell* **128**: 683-692.
- Kachroo AH, Laurent JM, Yellman CM, Meyer AG, Wilke CO, Marcotte EM. 2015. Evolution. Systematic humanization of yeast genes reveals conserved functions and genetic modularity. *Science* **348**: 921-925.
- Karran P. 2000. DNA double strand break repair in mammalian cells. *Current Opinion in Genetics & Development* **10**: 144-150.
- Kato R, Ogawa H. 1994. An essential gene, ESR1, is required for mitotic cell growth, DNA Repair and meiotic recombination in *Saccharomyces cerevisiae*. *Nucleic Acids Research* **22**: 3104-3112.

- Kent J. 2016. UCSC In-Silico PCR.
- Kim J, Guermah M, Roeder RG. 2010. The Human PAF1 Complex Acts in Chromatin Transcription Elongation Both Independently and Cooperatively with SII/TFIIS. *Cell* **140**: 491-503.
- Kiyono T, Foster SA, Koop JI, McDougall JK, Galloway DA, Klingelutz AJ. 1998. Both Rb/p16INK4a inactivation and telomerase activity are required to immortalize human epithelial cells. *Nature* **396**: 84-88.
- Klermund J, Bender K, Luke B. 2014. High nutrient levels and TORC1 activity reduce cell viability following prolonged telomere dysfunction and cell cycle arrest. *Cell Reports* **9**: 324-335.
- Kowalik KM, Shimada Y, Flury V, Stadler MB, Batki J, Buhler M. 2015. The Paf1 complex represses small-RNA-mediated epigenetic gene silencing. *Nature* **520**: 248-252.
- Krejci L, Altmannova V, Spirek M, Zhao X. 2012. Homologous recombination and its regulation. *Nucleic Acids Research* **40**: 5795-5818.
- Krogan NJ, Dover J, Wood A, Schneider J, Heidt J, Boateng MA, Dean K, Ryan OW, Golshani A, Johnston M et al. 2003a. The Paf1 complex is required for histone H3 methylation by COMPASS and Dot1p: linking transcriptional elongation to histone methylation. *Molecular Cell* **11**: 721-729.
- Krogan NJ, Keogh MC, Datta N, Sawa C, Ryan OW, Ding H, Haw RA, Pootoolal J, Tong A, Canadien V et al. 2003b. A Snf2 family ATPase complex required for recruitment of the histone H2A variant Htz1. *Molecular Cell* **12**: 1565-1576.
- Kueng S, Oppikofer M, Gasser SM. 2013. SIR proteins and the assembly of silent chromatin in budding yeast. *Annual Review of Genetics* **47**: 275-306.
- Larabee RN, Krogan NJ, Xiao T, Shibata Y, Hughes TR, Greenblatt JF, Strahl BD 2005. BUR kinase selectively regulates H3 K4 trimethylation and H2B ubiquitylation through recruitment of the PAF elongation complex. *Current Biology* **15**: 1487-1493.
- Larrivee M, Wellinger RJ. 2006. Telomerase- and capping-independent yeast survivors with alternate telomere states. *Nature Cell Biology* **8**: 741-747.
- Le S, Moore JK, Haber JE, Greider CW. 1999. RAD50 and RAD51 define two pathways that collaborate to maintain telomeres in the absence of telomerase. *Genetics* **152**: 143-152.
- Lee BI, Wilson DM, 3rd. 1999. The RAD2 domain of human exonuclease 1 exhibits 5' to 3' exonuclease and flap structure-specific endonuclease activities. *The Journal of Biological Chemistry* **274**: 37763-37769.
- Lee CY, Horn HF, Stewart CL, Burke B, Bolcun-Filas E, Schimenti JC, Dresser ME, Pezza RJ. 2015. Mechanism and regulation of rapid telomere prophase movements in mouse meiotic chromosomes. *Cell Reports* **11**: 551-563.
- Lee J, Mandell EK, Tucey TM, Morris DK, Lundblad V. 2008. The Est3 protein associates with yeast telomerase through an OB-fold domain. *Nature Structural & Molecular Biology* **15**: 990-997.
- Leehy KA, Lee JR, Song X, Renfrew KB, Shippen DE. 2013. MERISTEM DISORGANIZATION1 encodes TEN1, an essential telomere protein that modulates telomerase processivity in Arabidopsis. *The Plant Cell* **25**: 1343-1354.
- Lendvay TS, Morris DK, Sah J, Balasubramanian B, Lundblad V. 1996. Senescence mutants of *Saccharomyces cerevisiae* with a defect in telomere replication identify three additional EST genes. *Genetics* **144**: 1399-1412.
- Lewis LK, Karthikeyan G, Westmoreland JW, Resnick MA. 2002. Differential suppression of DNA Repair deficiencies of Yeast rad50, mre11 and xrs2

- mutants by EXO1 and TLC1 (the RNA component of telomerase). *Genetics* **160**: 49-62.
- Li BB, Oestreich S, de Lange T. 2000. Identification of human Rap1: Implications for telomere evolution. *Cell* **101**: 471-483.
- Liebman SW, Derkatch IL. 1999. The yeast [PSI⁺] prion: making sense of nonsense. *The Journal of Biological Chemistry* **274**: 1181-1184.
- Lill R, Muhlenhoff U. 2008. Maturation of iron-sulfur proteins in eukaryotes: mechanisms, connected processes, and diseases. *Annual Review of Biochemistry* **77**: 669-700.
- Lin JJ, Zakian VA. 1996. The *Saccharomyces* CDC13 protein is a single-strand TG(1-3) telomeric DNA-binding protein in vitro that affects telomere behaviour in vivo. *Proceedings of the National Academy of Sciences of the United States of America* **93**: 13760-13765.
- Lisby M, Barlow JH, Burgess RC, Rothstein R. 2004. Choreography of the DNA damage response: spatiotemporal relationships among checkpoint and repair proteins. *Cell* **118**: 699-713.
- Liu CC, Gopalakrishnan V, Poon LF, Yan T, Li S. 2014. Cdk1 regulates the temporal recruitment of telomerase and Cdc13-Stn1-Ten1 complex for telomere replication. *Molecular and Cellular Biology* **34**: 57-70.
- Llorente B, Symington LS. 2004. The Mre11 nuclease is not required for 5' to 3' resection at multiple HO-induced double-strand breaks. *Molecular and Cellular Biology* **24**: 9682-9694.
- Longhese MP, Foiani M, Muzi-Falconi M, Lucchini G, Plevani P. 1998. DNA damage checkpoint in budding yeast. *The EMBO Journal* **17**: 5525-5528.
- Longtine MS, McKenzie A, Demarini DJ, Shah NG, Wach A, Brachat A, Philippsen P, Pringle JR. 1998. Additional modules for versatile and economical PCR-based gene deletion and modification in *Saccharomyces cerevisiae*. *Yeast* **14**: 953-961.
- Lopes J, Ribeyre C, Nicolas A. 2006. Complex minisatellite rearrangements generated in the total or partial absence of Rad27/hFEN1 activity occur in a single generation and are Rad51 and Rad52 dependent. *Molecular and Cellular Biology* **26**: 6675-6689.
- Lopez-Otin C, Blasco MA, Partridge L, Serrano M, Kroemer G. 2013. The hallmarks of aging. *Cell* **153**: 1194-1217.
- Louis EJ. 2016. Historical Evolution of Laboratory Strains of *Saccharomyces cerevisiae*. *Cold Spring Harbor Protocols* **2016**: pdb top077750.
- Lu CY, Tsai CH, Brill SJ, Teng SC. 2010. Sumoylation of the BLM ortholog, Sgs1, promotes telomere-telomere recombination in budding yeast. *Nucleic Acids Research* **38**: 488-498.
- Lue NF. 2010. Plasticity of telomere maintenance mechanisms in yeast. *Trends in Biochemical Sciences* **35**: 8-17.
- Luke B, Panza A, Redon S, Iglesias N, Li Z, Lingner J. 2008. The Rat1p 5' to 3' exonuclease degrades telomeric repeat-containing RNA and promotes telomere elongation in *Saccharomyces cerevisiae*. *Molecular Cell* **32**: 465-477.
- Lundblad V, Blackburn EH. 1993. An alternative pathway for yeast telomere maintenance rescues est1- senescence. *Cell* **73**: 347-360.
- Lydall D. 2003. Hiding at the ends of yeast chromosomes: telomeres, nucleases and checkpoint pathways. *Journal of Cell Science* **116**: 4057-4065.
- Ma JL, Lee SJ, Duong JK, Stern DF. 2006. Activation of the checkpoint kinase Rad53 by the phosphatidylinositol kinase-like kinase Mec1. *The Journal of Biological Chemistry* **281**: 3954-3963.

- Ma Y, Wang X, Wu Y, Sun B, Lv H, Rong F, Zheng X. 2014. Overexpression of GOLPH3 protein is associated with worse prognosis in patients with epithelial ovarian cancer. *Tumour biology : the journal of the International Society for Oncodevelopmental Biology and Medicine* **35**: 11845-11849.
- MacDonald BT, Tamai K, He X. 2009. Wnt/beta-catenin signaling: components, mechanisms, and diseases. *Developmental Cell* **17**: 9-26.
- Maicher A, Kastner L, Dees M, Luke B. 2012. Deregulated telomere transcription causes replication-dependent telomere shortening and promotes cellular senescence. *Nucleic Acids Research* **40**: 6649-6659.
- Majka J, Binz SK, Wold MS, Burgers PM. 2006. Replication protein A directs loading of the DNA damage checkpoint clamp to 5'-DNA junctions. *The Journal of Biological Chemistry* **281**: 27855-27861.
- Majka J, Burgers PM. 2003. Yeast Rad17/Mec3/Ddc1: a sliding clamp for the DNA damage checkpoint. *Proceedings of the National Academy of Sciences of the United States of America* **100**: 2249-2254.
- Marcomini I, Gasser SM. 2015. Nuclear organization in DNA end processing: Telomeres vs double-strand breaks. *DNA Repair* **32**: 134-140.
- Marechal A, Zou L. 2015. RPA-coated single-stranded DNA as a platform for posttranslational modifications in the DNA damage response. *Cell research* **25**: 9- 23.
- Maringele L, Lydall D. 2002. EXO1-dependent single-stranded DNA at telomeres activates subsets of DNA damage and spindle checkpoint pathways in budding yeast yku70 Delta mutants. *Genes & Development* **16**: 1919-1933.
- . 2004. EXO1 plays a role in generating type I and type II survivors in budding yeast. *Genetics* **166**: 1641-1649.
- Martin SG, Laroche T, Suka N, Grunstein M, Gasser SM. 1999. Relocalization of telomeric Ku and SIR proteins in response to DNA strand breaks in yeast. *Cell* **97**: 621-633.
- Marton HA, Desiderio S. 2008. The Paf1 complex promotes displacement of histones upon rapid induction of transcription by RNA polymerase II. *BMC Molecular Biology* **9**: 4.
- Matsuura-Tokita K, Takeuchi M, Ichihara A, Mikuriya K, Nakano A. 2006. Live imaging of yeast Golgi cisternal maturation. *Nature* **441**: 1007-1010.
- Mazouzi A, Velimezi G, Loizou JI. 2014. DNA replication stress: causes, resolution and disease. *Experimental Cell Research* **329**: 85-93.
- Mimitou EP, Symington LS. 2008. Sae2, Exo1 and Sgs1 collaborate in DNA doublestrand break processing. *Nature* **455**: 770-774.
- Min TH, Kriebel M, Hou S, Pera EM. 2011. The dual regulator Sufu integrates Hedgehog and Wnt signals in the early Xenopus embryo. *Developmental biology* **358**: 262-276.
- Mitchell P, Tollervey D. 2003. An NMD pathway in yeast involving accelerated deadenylation and exosome-mediated 3'-->5' degradation. *Molecular Cell* **11**: 1405-1413.
- Moravec M, Wischnewski H, Bah A, Hu Y, Liu N, Lafranchi L, King MC, Azzalin CM. 2016. TERRA promotes telomerase-mediated telomere elongation in *Schizosaccharomyces pombe*. *EMBO Reports* **17**: 999-1012.
- Mordes DA, Nam EA, Cortez D. 2008. Dpb11 activates the Mec1-Ddc2 complex. *Proceedings of the National Academy of Sciences of the United States of America* **105**: 18730-18734.
- Moretti P, Freeman K, Coodly L, Shore D. 1994. Evidence That a Complex of Sir Proteins Interacts with the Silencer and Telomere Binding-Protein Rap1. *Genes & Development* **8**: 2257-2269.

- Morrow DM, Morrow M, Tagle DA, Shiloh Y, Collins FS, Hieter P. 1995. Tel1, an *Saccharomyces-Cerevisiae* Homolog of the Human Gene Mutated in Ataxia-Telangiectasia, Is Functionally Related to the Yeast Checkpoint Gene Mec1. *Cell* **82**: 831-840.
- Mortensen UH, Lisby M, Rothstein R. 2009. Rad52. *Current Biology* **19**: R676-R677.
- Mosimann C, Hausmann G, Basler K. 2006. Parafibromin/Hyrax activates Wnt/Wg target gene transcription by direct association with beta-catenin/Armadillo. *Cell* **125**: 327-341.
- Mozdy AD, Podell ER, Cech TR. 2008. Multiple yeast genes, including Paf1 complex genes, affect telomere length via telomerase RNA abundance. *Molecular and Cellular Biology* **28**: 4152-4161.
- Mueller CL, Jaehning JA. 2002. Ctr9, Rtf1, and Leo1 are components of the Paf1/RNA polymerase II complex. *Molecular and Cellular Biology* **22**: 1971-1980.
- Mueller CL, Porter SE, Hoffman MG, Jaehning JA. 2004. The Paf1 complex has functions independent of actively transcribing RNA polymerase II. *Molecular Cell* **14**: 447-456.
- Muller HJ. 1938. The remaking of chromosomes. *Collecting Net* **13**: 181-198.
- Nagaike T, Logan C, Hotta I, Rozenblatt-Rosen O, Meyerson M, Manley JL. 2011. Transcriptional activators enhance polyadenylation of mRNA precursors. *Molecular Cell* **41**: 409-418.
- Naito T, Matsuura A, Ishikawa F. 1998. Circular chromosome formation in a fission yeast mutant defective in two ATM homologues. *Nature Genetics* **20**: 203-206.
- Nakada D, Matsumoto K, Sugimoto K. 2003. ATM-related Tel1 associates with double-strand breaks through an Xrs2-dependent mechanism. *Genes & Development* **17**: 1957-1962.
- Nakamura H, Miura K, Fukuda Y, Shibuya I, Ohta A, Takagi M. 2000. Phosphatidylserine synthesis required for the maximal tryptophan transport activity in *Saccharomyces cerevisiae*. *Bioscience, Biotechnology, and Biochemistry* **64**: 167-172.
- Negrini S, Gorgoulis VG, Halazonetis TD. 2010. Genomic instability - an evolving hallmark of cancer. *Nature Reviews Molecular Cell Biology* **11**: 220-228.
- Nespoli A, Vercillo R, di Nola L, Diani L, Giannattasio M, Plevani P, Muzi-Falconi M. 2006. Alk1 and Alk2 are two new cell cycle-regulated haspin-like proteins in budding yeast. *Cell Cycle* **5**: 1464-1471.
- Ngo GH, Balakrishnan L, Dubarry M, Campbell JL, Lydall D. 2014. The 9-1-1 checkpoint clamp stimulates DNA resection by Dna2-Sgs1 and Exo1. *Nucleic Acids Research* **42**: 10516-10528.
- Ngo GH, Lydall D. 2015. The 9-1-1 checkpoint clamp coordinates resection at DNA double strand breaks. *Nucleic Acids Research* **43**: 5017-5032.
- Nordick K, Hoffman MG, Betz JL, Jaehning JA. 2008. Direct interactions between the Paf1 complex and a cleavage and polyadenylation factor are revealed by dissociation of Paf1 from RNA polymerase II. *Eukaryotic Cell* **7**: 1158-1167.
- Nugent CI, Bosco G, Ross LO, Evans SK, Salinger AP, Moore JK, Haber JE, Lundblad V. 1998. Telomere maintenance is dependent on activities required for end repair of double-strand breaks. *Current Biology* **8**: 657-660.
- Nugent CI, Hughes TR, Lue NF, Lundblad V. 1996. Cdc13p: A single-strand telomeric DNA binding protein with a dual role in yeast telomere maintenance. *Science* **274**: 249-252.
- Nussleinvolhard C, Wieschaus E. 1980. Mutations Affecting Segment Number and Polarity in *Drosophila*. *Nature* **287**: 795-801.

- Olovnikov AM. 1973. A theory of marginotomy. The incomplete copying of template margin in enzymic synthesis of polynucleotides and biological significance of the phenomenon. *Journal of Theoretical Biology* **41**: 181-190.
- Paciotti V, Clerici M, Lucchini G, Longhese MP. 2000. The checkpoint protein Ddc2, functionally related to *S. pombe* Rad26, interacts with Mec1 and is regulated by Mec1-dependent phosphorylation in budding yeast. *Genes & Development* **14**: 2046-2059.
- Palm W, de Lange T. 2008. How Shelterin Protects Mammalian Telomeres. *Annual Review of Genetics* **42**: 301-334.
- Pan X, Lei B, Zhou N, Feng B, Yao W, Zhao X, Yu Y, Lu H. 2012. Identification of novel genes involved in DNA damage response by screening a genome-wide *Schizosaccharomyces pombe* deletion library. *BMC Genomics* **13**: 662.
- Panday A, Xiao L, Grove A. 2015. Yeast high mobility group protein HMO1 stabilizes chromatin and is evicted during repair of DNA double strand breaks. *Nucleic Acids Research* **43**: 5759-5770.
- Parenteau J, Wellinger RJ. 1999. Accumulation of single-stranded DNA and destabilization of telomeric repeats in yeast mutant strains carrying a deletion of RAD27. *Molecular and Cellular Biology* **19**: 4143-4152.
- Penheiter KL, Washburn TM, Porter SE, Hoffman MG, Jaehning JA. 2005. A posttranscriptional role for the yeast Paf1-RNA polymerase II complex is revealed by identification of primary targets. *Molecular Cell* **20**: 213-223.
- Peterson SE, Stellwagen AE, Diede SJ, Singer MS, Haimberger ZW, Johnson CO, Tzoneva M, Gottschling DE. 2001. The function of a stem-loop in telomerase RNA is linked to the DNA Repair protein Ku. *Nature Genetics* **27**: 64-67.
- Petreaca RC, Chiu HC, Eckelhoefer HA, Chuang C, Xu L, Nugent CI. 2006. Chromosome end protection plasticity revealed by Stn1p and Ten1p bypass of Cdc13p. *Nature Cell Biology* **8**: 748-755.
- Pfeiffer V, Lingner J. 2012. TERRA promotes telomere shortening through exonuclease 1-mediated resection of chromosome ends. *PLOS Genetics* **8**: e1002747.
- Pickart CM, Eddins MJ. 2004. Ubiquitin: structures, functions, mechanisms. *Biochimica et Biophysica Acta* **1695**: 55-72.
- Poli J, Gerhold CB, Tosi A, Hustedt N, Seeber A, Sack R, Herzog F, Pasero P, Shimada K, Hopfner KP et al. 2016. Mec1, INO80, and the PAF1 complex cooperate to limit transcription replication conflicts through RNAPII removal during replication stress. *Genes & Development* **30**: 337-354.
- Pon JR, Marra MA. 2015. Driver and passenger mutations in cancer. *Annual Review of Pathology* **10**: 25-50.
- Porro A, Feuerhahn S, Lingner J. 2014. TERRA-reinforced association of LSD1 with MRE11 promotes processing of uncapped telomeres. *Cell Reports* **6**: 765-776.
- Porro A, Feuerhahn S, Reichenbach P, Lingner J. 2010. Molecular dissection of telomeric repeat-containing RNA biogenesis unveils the presence of distinct and multiple regulatory pathways. *Molecular and Cellular Biology* **30**: 4808-4817.
- Poruchynsky MS, Komlodi-Pasztor E, Trostel S, Wilkerson J, Regairaz M, Pommier Y, Zhang X, Kumar Maity T, Robey R, Burotto M et al. 2015. Microtubuletargeting agents augment the toxicity of DNA-damaging agents by disrupting intracellular trafficking of DNA Repair proteins. *Proceedings of the National Academy of Sciences of the United States of America* **112**: 1571-1576.
- Price CM, Boltz KA, Chaiken MF, Stewart JA, Beilstein MA, Shippen DE. 2010. Evolution of CST function in telomere maintenance. *Cell Cycle* **9**: 3157-3165.

- Qi HY, Zakian VA. 2000. The *Saccharomyces* telomere-binding protein Cdc13p interacts with both the catalytic subunit of DNA polymerase alpha and the telomerase-associated Est1 protein. *Genes & Development* **14**: 1777-1788.
- Qian W, Wang J, Jin NN, Fu XH, Lin YC, Lin JJ, Zhou JQ. 2009a. Ten1p promotes the telomeric DNA-binding activity of Cdc13p: implication for its function in telomere length regulation. *Cell research* **19**: 849-863.
- Qian W, Wang JY, Jin NN, Fu XH, Lin YC, Lin JJ, Zhou JQ. 2009b. Ten1p promotes the telomeric DNA-binding activity of Cdc13p: implication for its function in telomere length regulation. *Cell research* **19**: 849-863.
- Raab M, Gentili M, de Belly H, Thiam HR, Vargas P, Jimenez AJ, Lautenschlaeger F, Voituriez R, Lennon-Dumenil AM, Manel N et al. 2016. ESCRT III repairs nuclear envelope ruptures during cell migration to limit DNA damage and cell death. *Science* **352**: 359-362.
- Reddi AR, Culotta VC. 2013. SOD1 integrates signals from oxygen and glucose to repress respiration. *Cell* **152**: 224-235.
- Redon S, Reichenbach P, Lingner J. 2010. The non-coding RNA TERRA is a natural ligand and direct inhibitor of human telomerase. *Nucleic Acids Research* **38**: 5797-5806.
- Rice C, Skordalakes E. 2016. Structure and function of the telomeric CST complex. *Computational and Structural Biotechnology Journal* **14**: 161-167.
- Riethman H. 2008. Human telomere structure and biology. *Annual Review of Genomics and Human Genetics* **9**: 1-19.
- Rine J, Herskowitz I. 1987. Four genes responsible for a position effect on expression from HML and HMR in *Saccharomyces cerevisiae*. *Genetics* **116**: 9-22.
- Ritchie KB, Petes TD. 2000. The Mre11p/Rad50p/Xrs2p complex and the Tel1p function in a single pathway for telomere maintenance in yeast. *Genetics* **155**: 475-479.
- Rog O, Smolnikov S, Krauskopf A, Kupiec M. 2005. The yeast VPS genes affect telomere length regulation. *Current Genetics* **47**: 18-28.
- Romano GH, Harari Y, Yehuda T, Podhorzer A, Rubinstein L, Shamir R, Gottlieb A, Silberberg Y, Pe'er D, Ruppin E et al. 2013. Environmental stresses disrupt telomere length homeostasis. *PLOS Genetics* **9**: e1003721.
- Rosonina E, Willis IM, Manley JL. 2009. Sub1 functions in osmoregulation and in transcription by both RNA polymerases II and III. *Molecular and Cellular Biology* **29**: 2308-2321.
- Rossi ML, Bambara RA. 2006. Reconstituted Okazaki fragment processing indicates two pathways of primer removal. *The Journal of Biological Chemistry* **281**: 26051-26061.
- Ruddon RW. 2007. *Cancer Biology*. Oxford University Press, USA.
- Sadeghi L, Prasad P, Ekwall K, Cohen A, Svensson JP. 2015. The Paf1 complex factors Leo1 and Paf1 promote local histone turnover to modulate chromatin states in fission yeast. *EMBO Reports* **16**: 1673-1687.
- Saffran WA, Greenberg RB, Thaler-Scheer MS, Jones MM. 1994. Single strand and double strand DNA damage-induced reciprocal recombination in yeast. Dependence on nucleotide excision repair and RAD1 recombination. *Nucleic Acids Research* **22**: 2823-2829.
- Saiardi A, Caffrey JJ, Snyder SH, Shears SB. 2000. The inositol hexakisphosphate kinase family. Catalytic flexibility and function in yeast vacuole biogenesis. *The Journal of Biological Chemistry* **275**: 24686-24692.
- Saiardi A, Resnick AC, Snowman AM, Wendland B, Snyder SH. 2005. Inositol pyrophosphates regulate cell death and telomere length through

- phosphoinositide 3-kinase-related protein kinases. *Proceedings of the National Academy of Sciences of the United States of America* **102**: 1911-1914.
- Salk JJ, Fox EJ, Loeb LA. 2010. Mutational Heterogeneity in Human Cancers: Origin and Consequences. *Annual Review of Pathology* **5**: 51-75.
- Sanchez Y, Bachant J, Wang H, Hu FH, Liu D, Tetzlaff M, Elledge SJ. 1999. Control of the DNA damage checkpoint by Chk1 and Rad53 protein kinases through distinct mechanisms. *Science* **286**: 1166-1171.
- Schmidt O, Teis D. 2012. The ESCRT machinery. *Current Biology* **22**: R116-120.
- Schmitz KR, Liu J, Li S, Setty TG, Wood CS, Burd CG, Ferguson KM. 2008. Golgi localization of glycosyltransferases requires a Vps74p oligomer. *Developmental Cell* **14**: 523-534.
- Schneider CA, Rasband WS, Eliceiri KW. 2012. NIH Image to ImageJ: 25 years of image analysis. *Nature Methods* **9**: 671-675.
- Schramke V, Luciano P, Brevet V, Guillot S, Corda Y, Longhese MP, Gilson E, Geli V. 2004. RPA regulates telomerase action by providing Est1p access to chromosome ends. *Nature Genetics* **36**: 46-54.
- Schuh AL, Audhya A. 2014. The ESCRT machinery: from the plasma membrane to endosomes and back again. *Critical Reviews in Biochemistry and Molecular Biology* **49**: 242-261.
- Schwartz MF, Duong JK, Sun Z, Morrow JS, Pradhan D, Stern DF. 2002. Rad9 phosphorylation sites couple Rad53 to the *Saccharomyces cerevisiae* DNA damage checkpoint. *Molecular Cell* **9**: 1055-1065.
- Scott KL, Kabbarah O, Liang MC, Ivanova E, Anagnostou V, Wu J, Dhakal S, Wu M, Chen S, Feinberg T et al. 2009. GOLPH3 modulates mTOR signalling and rapamycin sensitivity in cancer. *Nature* **459**: 1085-1090.
- Shahbazian MD, Grunstein M. 2007. Functions of site-specific histone acetylation and deacetylation. *Annual Review of Biochemistry* **76**: 75-100.
- Shampay J, Blackburn EH. 1988. Generation of telomere-length heterogeneity in *Saccharomyces cerevisiae*. *Proceedings of the National Academy of Sciences of the United States of America* **85**: 534-538.
- Sharp DJ, Rogers GC, Scholey JM. 2000. Roles of motor proteins in building microtubule-based structures: a basic principle of cellular design. *Biochimica et Biophysica Acta* **1496**: 128-141.
- Shay JW, Wright WE. 2011. Role of telomeres and telomerase in cancer. *Seminars in Cancer Biology* **21**: 349-353.
- Sheldon KE, Mauger DM, Arndt KM. 2005. A Requirement for the *Saccharomyces cerevisiae* Paf1 complex in snoRNA 3' end formation. *Molecular Cell* **20**: 225-236.
- Shen M, Schmitt S, Buac D, Dou QP. 2013. Targeting the ubiquitin-proteasome system for cancer therapy. *Expert Opinion on Therapeutic Targets* **17**: 1091-1108.
- Shental-Bechor D, Levy Y. 2008. Effect of glycosylation on protein folding: a close look at thermodynamic stabilization. *Proceedings of the National Academy of Sciences of the United States of America* **105**: 8256- 8261.
- Shiotani B, Zou L. 2009. Single-stranded DNA orchestrates an ATM-to-ATR switch at DNA breaks. *Molecular Cell* **33**: 547-558.
- Shukla S, Acharya S, Rajput D, Vagha S, Grover S. 2010. Telomere--the twilight to immortality. *The Journal of the Association of Physicians of India* **58**: 553-560.
- Siede W, Friedberg AS, Friedberg EC. 1993. RAD9-dependent G1 arrest defines a second checkpoint for damaged DNA in the cell cycle of *Saccharomyces cerevisiae*. *Proceedings of the National Academy of Sciences of the United States of America* **90**: 7985-7989.

- Signon L, Malkova A, Naylor ML, Klein H, Haber JE. 2001. Genetic requirements for RAD51- and RAD54-independent break-induced replication repair of a chromosomal double-strand break. *Molecular and Cellular Biology* **21**: 2048-2056.
- Sikorski TW, Ficarro SB, Holik J, Kim T, Rando OJ, Marto JA, Buratowski S. 2011. Sub1 and RPA associate with RNA polymerase II at different stages of transcription. *Molecular Cell* **44**: 397-409.
- Singer MS, Gottschling DE. 1994. TLC1: template RNA component of *Saccharomyces cerevisiae* telomerase. *Science* **266**: 404-409.
- Sinha H, David L, Pascon RC, Clauder-Munster S, Krishnakumar S, Nguyen M, Shi G, Dean J, Davis RW, Oefner PJ et al. 2008. Sequential elimination of major effect contributors identifies additional quantitative trait loci conditioning high temperature growth in yeast. *Genetics* **180**: 1661-1670.
- Skourti-Stathaki K, Proudfoot NJ. 2014. A double-edged sword: R loops as threats to genome integrity and powerful regulators of gene expression. *Genes & Development* **28**: 1384-1396.
- Smogorzewska A, de Lange T. 2004. Regulation of telomerase by telomeric proteins. *Annual Review of Biochemistry* **73**: 177-208.
- Smolka MB, Chen SH, Maddox PS, Enserink JM, Albuquerque CP, Wei XX, Desai A, Kolodner RD, Zhou H. 2006. An FHA domain-mediated protein interaction network of Rad53 reveals its role in polarized cell growth. *The Journal of Cell Biology* **175**: 743-753.
- Smoyer CJ, Jaspersen SL. 2014. Breaking down the wall: the nuclear envelope during mitosis. *Current Opinion in Cell Biology* **26**: 1-9.
- Somesh BP, Reid J, Liu WF, Sogaard TM, Erdjument-Bromage H, Tempst P, Svejstrup JQ. 2005. Multiple mechanisms confining RNA polymerase II ubiquitylation to polymerases undergoing transcriptional arrest. *Cell* **121**: 913-923.
- Song YH, Duan R, Ryu HY, Ahn SH. 2014. The yeast ESCRT complexes are involved in the regulation of transcription elongation. *Genes & Genomics* **36**: 335-343.
- Sopko R, Huang D, Preston N, Chua G, Papp B, Kafadar K, Snyder M, Oliver SG, Cyert M, Hughes TR et al. 2006. Mapping pathways and phenotypes by systematic gene overexpression. *Molecular Cell* **21**: 319-330.
- Sousa M, Duarte AM, Fernandes TR, Chaves SR, Pacheco A, Leao C, Corte-Real M, Sousa MJ. 2013. Genome-wide identification of genes involved in the positive and negative regulation of acetic acid-induced programmed cell death in *Saccharomyces cerevisiae*. *BMC Genomics* **14**: 838.
- Squazzo SL, Costa PJ, Lindstrom DL, Kumer KE, Simic R, Jennings JL, Link AJ, Arndt KM, Hartzog GA. 2002. The Paf1 complex physically and functionally associates with transcription elongation factors in vivo. *The EMBO Journal* **21**: 1764-1774.
- Stansel RM, de Lange T, Griffith JD. 2001. T-loop assembly in vitro involves binding of TRF2 near the 3' telomeric overhang. *The EMBO Journal* **20**: 5532-5540.
- Stehling O, Sheftel AD, Lill R. 2009. Chapter 12 Controlled expression of iron-sulfur cluster assembly components for respiratory chain complexes in mammalian cells. *Methods in Enzymology* **456**: 209-231.
- Stewart SA, Weinberg RA. 2006. Telomeres: cancer to human aging. *Annual review of cell and developmental biology* **22**: 531-557.
- Strahl-Bolsinger S, Hecht A, Luo K, Grunstein M. 1997. SIR2 and SIR4 interactions differ in core and extended telomeric heterochromatin in yeast. *Genes & Development* **11**: 83-93.

- Strahl T, Thorner J. 2007. Synthesis and function of membrane phosphoinositides in budding yeast, *Saccharomyces cerevisiae*. *Biochimica et Biophysica Acta* **1771**: 353-404.
- Sun H, Bennett RJ, Maizels N. 1999. The *Saccharomyces cerevisiae* Sgs1 helicase efficiently unwinds G-G paired DNAs. *Nucleic Acids Research* **27**: 1978-1984.
- Sweeney FD, Yang F, Chi A, Shabanowitz J, Hunt DF, Durocher D. 2005. *Saccharomyces cerevisiae* Rad9 acts as a Mec1 adaptor to allow Rad53 activation. *Current Biology* **15**: 1364-1375.
- Symington LS. 1998. Homologous recombination is required for the viability of rad27 mutants. *Nucleic Acids Research* **26**: 5589-5595.
- . 2002. Role of RAD52 epistasis group genes in homologous recombination and double-strand break repair. *Microbiology and Molecular Biology Reviews* **66**: 630-670.
- Taggart AK, Zakian VA. 2003. Telomerase: what are the Est proteins doing? *Current Opinion in Cell Biology* **15**: 275-280.
- Taggart AKP, Teng SC, Zakian VA. 2002. Est1p as a cell cycle-regulated activator of telomere-bound telomerase. *Science* **297**: 1023-1026.
- Taipale J, Beachy PA. 2001. The Hedgehog and Wnt signalling pathways in cancer. *Nature* **411**: 349-354.
- Takahashi A, Tsutsumi R, Kikuchi I, Obuse C, Saito Y, Seidi A, Karisch R, Fernandez M, Cho T, Ohnishi N et al. 2011a. SHP2 tyrosine phosphatase converts parafibromin/Cdc73 from a tumor suppressor to an oncogenic driver. *Molecular Cell* **43**: 45-56.
- Takahashi YH, Schulze JM, Jackson J, Hentrich T, Seidel C, Jaspersen SL, Kobor MS, Shilatifard A. 2011b. Dot1 and histone H3K79 methylation in natural telomeric and HM silencing. *Molecular Cell* **42**: 118-126.
- Takata H, Kanoh Y, Gunge N, Shirahige K, Matsuura A. 2004. Reciprocal association of the budding yeast ATM-related proteins Tel1 and Mec1 with telomeres in vivo. *Molecular Cell* **14**: 515-522.
- Tamakawa R, Fleisig H, Wong JMY. 2013. Telomeres, Telomerase, and DNA Damage Response in Cancer Therapy. in *Advances in DNA Repair in Cancer Therapy*, pp. 229-279.
- Tani M, Kuge O. 2014. Involvement of Sac1 phosphoinositide phosphatase in the metabolism of phosphatidylserine in the yeast *Saccharomyces cerevisiae*. *Yeast* **31**: 145-158.
- Teixeira MT, Arneric M, Sperisen P, Lingner J. 2004. Telomere length homeostasis is achieved via a switch between telomerase- extendible and –nonextendible states. *Cell* **117**: 323-335.
- Teng SC, Zakian VA. 1999. Telomere-telomere recombination is an efficient bypass pathway for telomere maintenance in *Saccharomyces cerevisiae*. *Molecular and Cellular Biology* **19**: 8083-8093.
- Teo H, Perisic O, Gonzalez B, Williams RL. 2004. ESCRT-II, an endosome-associated complex required for protein sorting: crystal structure and interactions with ESCRT-III and membranes. *Developmental Cell* **7**: 559-569.
- Teo SH, Jackson SP. 2001. Telomerase subunit overexpression suppresses telomere-specific checkpoint activation in the yeast yku80 mutant. *EMBO Reports* **2**: 197-202.
- Tham WH, Zakian VA. 2002. Transcriptional silencing at *Saccharomyces* telomeres: implications for other organisms. *Oncogene* **21**: 512-521.

- Thomas M, White RL, Davis RW. 1976. Hybridization of RNA to double-stranded DNA: formation of R-loops. *Proceedings of the National Academy of Sciences of the United States of America* **73**: 2294-2298.
- Tishkoff DX, Boerger AL, Bertrand P, Filosi N, Gaida GM, Kane MF, Kolodner RD. 1997. Identification and characterization of *Saccharomyces cerevisiae* EXO1, a gene encoding an exonuclease that interacts with MSH2. *Proceedings of the National Academy of Sciences of the United States of America* **94**: 7487-7492.
- Tkach JM, Yimit A, Lee AY, Riffle M, Costanzo M, Jaschob D, Hendry JA, Ou J, Moffat J, Boone C et al. 2012. Dissecting DNA damage response pathways by analysing protein localization and abundance changes during DNA replication stress. *Nature Cell Biology* **14**: 966-976.
- Toh EA, Guerry P, Wickner RB. 1978. Chromosomal superkiller mutants of *Saccharomyces cerevisiae*. *Journal of Bacteriology* **136**: 1002-1007.
- Tomson BN, Arndt KM. 2013. The many roles of the conserved eukaryotic Paf1 complex in regulating transcription, histone modifications, and disease states. *Biochimica et Biophysica Acta* **1829**: 116-126.
- Tong AHY, Evangelista M, Parsons AB, Xu H, Bader GD, Page N, Robinson M, Raghibizadeh S, Hogue CWV, Bussey H et al. 2001. Systematic genetic analysis with ordered arrays of yeast deletion mutants. *Science* **294**: 2364-2368.
- Tran PT, Erdeniz N, Symington LS, Liskay RM. 2004. EXO1-A multi-tasking eukaryotic nuclease. *DNA Repair* **3**: 1549-1559.
- True HL, Berlin I, Lindquist SL. 2004. Epigenetic regulation of translation reveals hidden genetic variation to produce complex traits. *Nature* **431**: 184-187.
- Trujillo KM, Sung P. 2001. DNA structure-specific nuclease activities in the *Saccharomyces cerevisiae* Rad50*Mre11 complex. *The Journal of Biological Chemistry* **276**: 35458-35464.
- Tsai YL, Tseng SF, Chang SH, Lin CC, Teng SC. 2002. Involvement of replicative polymerases, Tel1p, Mec1p, Cdc13p, and the Ku complex in telomere-telomere recombination. *Molecular and Cellular Biology* **22**: 5679-5687.
- Tseng HM, Tomkinson AE. 2004. Processing and joining of DNA ends coordinated by interactions among Dnl4/Lif1, Pol4, and FEN-1. *The Journal of Biological Chemistry* **279**: 47580-47588.
- Tsubouchi H, Ogawa H. 2000. Exo1 roles for repair of DNA double-strand breaks and meiotic crossing over in *Saccharomyces cerevisiae*. *Molecular Biology of the Cell* **11**: 2221-2233.
- Ungar L, Harari Y, Toren A, Kupiec M. 2011. Tor complex 1 controls telomere length by affecting the level of Ku. *Current Biology* **21**: 2115-2120.
- Uptain SM, Lindquist S. 2002. Prions as protein-based genetic elements. *Annual Review of Microbiology* **56**: 703-741.
- Usui T, Foster SS, Petrini JH. 2009. Maintenance of the DNA-damage checkpoint requires DNA-damage-induced mediator protein oligomerization. *Molecular Cell* **33**: 147-159.
- van Hoof A, Frischmeyer PA, Dietz HC, Parker R. 2002. Exosome-mediated recognition and degradation of mRNAs lacking a termination codon. *Science* **295**: 2262-2264.
- van Hoof A, Wagner EJ. 2011. A brief survey of mRNA surveillance. *Trends in Biochemical Sciences* **36**: 585-592.
- Vancura A, O'Connor A, Patterson SD, Mirza U, Chait BT, Kuret J. 1993. Isolation and properties of YCK2, a *Saccharomyces cerevisiae* homolog of casein kinase-1. *Archives of Biochemistry and Biophysics* **305**: 47-53.

- Vancura A, Sessler A, Leichus B, Kuret J. 1994. A prenylation motif is required for plasma membrane localization and biochemical function of casein kinase I in budding yeast. *The Journal of Biological Chemistry* **269**: 19271-19278.
- Vega LR, Phillips JA, Thornton BR, Benanti JA, Onigbanjo MT, Toczyski DP, Zakian VA. 2007. Sensitivity of yeast strains with long G-tails to levels of telomerebound telomerase. *PLoS Genetics* **3**: e105.
- Verdelli C, Forno I, Vaira V, Corbetta S. 2015. Epigenetic alterations in human parathyroid tumors. *Endocrine* **49**: 324-332.
- Verissimo F, Pepperkok R. 2013. Imaging ER-to-Golgi transport: towards a systems view. *Journal of Cell Science* **126**: 5091-5100.
- Vialard JE, Gilbert CS, Green CM, Lowndes NF. 1998. The budding yeast Rad9 checkpoint protein is subjected to Mec1/Tel1-dependent hyperphosphorylation and interacts with Rad53 after DNA damage. *The EMBO Journal* **17**: 5679-5688.
- Wade PA, Werel W, Fentzke RC, Thompson NE, Leykam JF, Burgess RR, Jaehning JA, Burton ZF. 1996. A novel collection of accessory factors associated with yeast RNA polymerase II. *Protein Expression and Purification* **8**: 85-90.
- Walker JR, Corpina RA, Goldberg J. 2001. Structure of the Ku heterodimer bound to DNA and its implications for double-strand break repair. *Nature* **412**: 607-614.
- Walker JR, Zhu XD. 2012. Post-translational modifications of TRF1 and TRF2 and their roles in telomere maintenance. *Mechanisms of Ageing and Development* **133**: 421-434.
- Wang YB, Ghosh G, Hendrickson EA. 2009. Ku86 represses lethal telomere deletion events in human somatic cells. *Proceedings of the National Academy of Sciences of the United States of America* **106**: 12430-12435.
- Watt PM, Hickson ID, Borts RH, Louis EJ. 1996. SGS1, a homologue of the Bloom's and Werner's syndrome genes, is required for maintenance of genome stability in *Saccharomyces cerevisiae*. *Genetics* **144**: 935-945.
- Webb CJ, Wu Y, Zakian VA. 2013. DNA Repair at telomeres: keeping the ends intact. *Cold Spring Harbor Perspectives in Biology* **5**: a012666.
- Weinert TA, Hartwell LH. 1993. Cell Cycle arrest of cdc mutants and specificity of the RAD9 checkpoint. *Genetics* **134**: 63-80.
- Weisman R, Cohen A, Gasser SM. 2014. TORC2-a new player in genome stability. *EMBO Molecular Medicine* **6**: 995-1002.
- Wellinger RJ, Zakian VA. 2012. Everything You Ever Wanted to Know About *Saccharomyces cerevisiae* Telomeres: Beginning to End. *Genetics* **191**: 1073-1105.
- Wera S, Bergsma JC, Thevelein JM. 2001. Phosphoinositides in yeast: genetically tractable signalling. *FEMS Yeast Research* **1**: 9-13.
- Wilson MA, Meaux S, Parker R, van Hoof A. 2005. Genetic interactions between [PSI⁺] and nonstop mRNA decay affect phenotypic variation. *Proceedings of the National Academy of Sciences of the United States of America* **102**: 10244-10249.
- Wilson S, Warr N, Taylor DL, Watts FZ. 1999. The role of *Schizosaccharomyces pombe* Rad32, the Mre11 homologue, and other DNA damage response proteins in non-homologous end joining and telomere length maintenance. *Nucleic Acids Research* **27**: 2655-2661.
- Wood CS, Hung CS, Huoh YS, Mousley CJ, Stefan CJ, Bankaitis V, Ferguson KM, Burd CG. 2012. Local control of phosphatidylinositol 4-phosphate signaling in the Golgi apparatus by Vps74 and Sac1 phosphoinositide phosphatase. *Molecular Biology of the Cell* **23**: 2527-2536.

- Wood JG, Sinclair DA. 2002. TPE or not TPE? It's no longer a question. *Trends in Pharmacological Sciences* **23**: 1-4.
- Wotton D, Shore D. 1997. Novel Rap1p-interacting factor, Rif2p, cooperates with Rif1p to regulate telomere length in *Saccharomyces cerevisiae*. *Genes & Development* **11**: 748-760.
- Wu Y, Zakian VA. 2011. The telomeric Cdc13 protein interacts directly with the telomerase subunit Est1 to bring it to telomeric DNA ends in vitro. *Proceedings of the National Academy of Sciences of the United States of America* **108**: 20362-20369.
- Xu C, Ng DT. 2015. Glycosylation-directed quality control of protein folding. *Nature Reviews Molecular Cell Biology* **16**: 742-752.
- Xue Y, Ren J, Gao X, Jin C, Wen L, Yao X. 2008. GPS 2.0, a tool to predict kinasespecific phosphorylation sites in hierarchy. *Molecular & Cellular Proteomics : MCP* **7**: 1598-1608.
- Yang X, Mao F, Lv X, Zhang Z, Fu L, Lu Y, Wu W, Zhou Z, Zhang L, Zhao Y. 2013. *Drosophila* Vps36 regulates Smo trafficking in Hedgehog signaling. *Journal of Cell Science* **126**: 4230-4238.
- Ye JZ, Donigian JR, van Overbeek M, Loayza D, Luo Y, Krutchinsky AN, Chait BT, de Lange T. 2004a. TIN2 binds TRF1 and TRF2 simultaneously and stabilizes the TRF2 complex on telomeres. *The Journal of Biological Chemistry* **279**: 47264-47271.
- Ye JZS, Hockemeyer D, Krutchinsky AN, Loayza D, Hooper SM, Chait BT, de Lange T. 2004b. POT1-interacting protein PIP1: a telomere length regulator that recruits POT1 to the TIN2/TRF1 complex. *Genes & Development* **18**: 1649-1654.
- York SJ, Armbruster BN, Greenwell P, Petes TD, York JD. 2005. Inositol diphosphate signaling regulates telomere length. *The Journal of Biological Chemistry* **280**: 4264-4269.
- Yu M, Yang W, Ni T, Tang Z, Nakadai T, Zhu J, Roeder RG. 2015. RNA polymerase II-associated factor 1 regulates the release and phosphorylation of paused RNA polymerase II. *Science* **350**: 1383-1386.
- Zhang C. 2014. Essential functions of iron-requiring proteins in DNA replication, repair and cell cycle control. *Protein & Cell* **5**: 750-760.
- Zhang LJ, Wang KB, Liu LS, Chen LZ, Peng BG, Liang LJ, Li Z, Xue L, Li W, Xia JT. 2014. Overexpression of GOLPH3 is associated with poor prognosis and clinical progression in pancreatic ductal adenocarcinoma. *BMC Cancer* **14**: 571.
- Zhang X, Ding Z, Mo J, Sang B, Shi Q, Hu J, Xie S, Zhan W, Lu D, Yang M et al. 2015. GOLPH3 promotes glioblastoma cell migration and invasion via the mTOR-YB1 pathway in vitro. *Molecular Carcinogenesis* **54**: 1252-1263.
- Zhang X, Paull TT. 2005. The Mre11/Rad50/Xrs2 complex and non-homologous endjoining of incompatible ends in *S. cerevisiae*. *DNA Repair* **4**: 1281-1294.
- Zhao X, Muller EG, Rothstein R. 1998. A suppressor of two essential checkpoint genes identifies a novel protein that negatively affects dNTP pools. *Molecular Cell* **2**: 329-340.
- Zhou BB, Elledge SJ. 2000. The DNA damage response: putting checkpoints in perspective. *Nature* **408**: 433-439.
- Zhu B, Mandal SS, Pham AD, Zheng Y, Erdjument-Bromage H, Batra SK, Tempst P, Reinberg D. 2005. The human PAF complex coordinates transcription with events downstream of RNA synthesis. *Genes & Development* **19**: 1668-1673.
- Zhu XF, Gustafsson CM. 2009. Distinct Differences in Chromatin Structure at Subtelomeric X and Y ' Elements in Budding Yeast. *PLOS One* **4**: e6363.

- Zhu Z, Chung WH, Shim EY, Lee SE, Ira G. 2008. Sgs1 helicase and two nucleases Dna2 and Exo1 resect DNA double-strand break ends. *Cell* **134**: 981-994.
- Zou L, Elledge SJ. 2003. Sensing DNA damage through ATRIP recognition of RPA-ssDNA complexes. *Science* **300**: 1542-1548.
- Zubko MK, Guillard S, Lydall D. 2004. Exo1 and Rad24 differentially regulate generation of ssDNA at telomeres of *Saccharomyces cerevisiae* cdc13-1 mutants. *Genetics* **168**: 103-115.
- Zubko MK, Lydall D. 2006. Linear chromosome maintenance in the absence of essential telomere-capping proteins. *Nature Cell Biology* **8**: 734-740.
- Zvereva MI, Shcherbakova DM, Dontsova OA. 2010. Telomerase: structure, functions, and activity regulation. *Biochemistry Biokhimiia* **75**: 1563-1583.